Max-Planck-Institut
für Plasmaphysik

Annual Report 2002

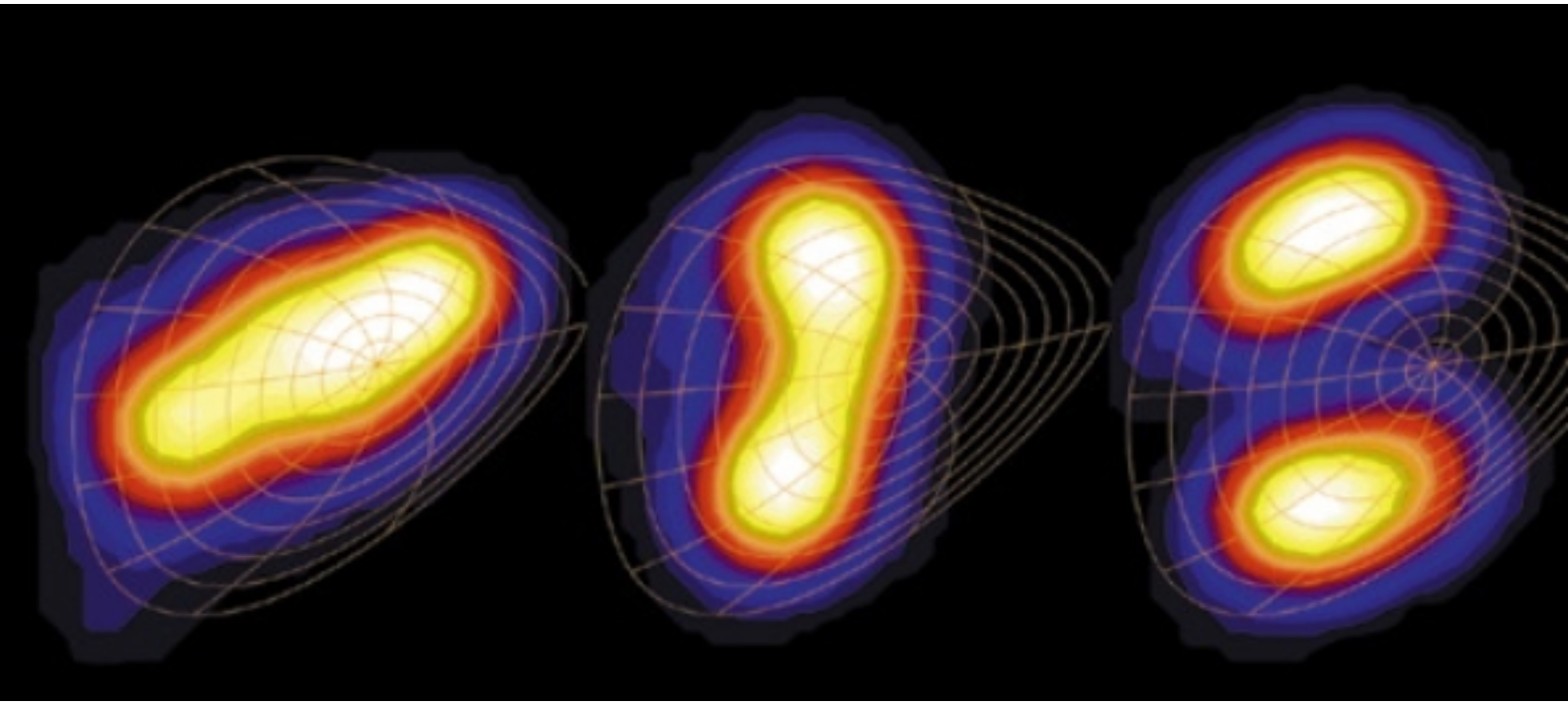

Foreword

At the Max-Planck-Institut für Plasmaphysik (IPP) we investigate the basic physics associated with the construction and operation of a future fusion power plant. This task involves research on the two most advanced types of fusion devices, the tokamak and the stellarator, as well as on plasma-surface interactions and materials. The work on the ASDEX Upgrade tokamak is directed towards the next step in fusion research, the International Tokamak Experimental Reactor (ITER). Although operation of the WENDELSTEIN 7-AS "advanced stellarator" was discontinued in July 2002, construction of its successor WENDELSTEIN 7-X at the Greifswald Branch of IPP proceeds apace. With this experiment we hope to demonstrate that the stellarator is a viable option for the step following ITER.

The ASDEX Upgrade tokamak programme is strongly motivated by possible ITER operating scenarios. In particular, the investigation of reactor-relevant plasma edge and bulk physics with a reactor-compatible divertor configuration plays a major role. In the last year it has been demonstrated – in close collaboration with theory – that heat and particle transport in the basic ITER operating scenario, i.e. in the high-confinement H-mode with edge-localised modes, is governed by "profile stiffness". Power and particle exhaust in the ELMy H-mode could be achieved in a benign way by establishing small "type II" ELMs. Stability was improved by using the new capability to shape the poloidal plasma cross-section. Combination of these factors has led to a new operating scenario with tolerable ELMs, good confinement and superior stability properties.

Although numerous other institutes already work on ASDEX Upgrade, IPP has recently increased its efforts to open up the experiment to more European fusion scientists. A new organisational structure has been established to facilitate the participation of the EURATOM Associations. An international ASDEX Upgrade Programme Committee with equal representation of IPP and other Associations has been set up to determine the ASDEX Upgrade experimental programme in consensus with the European fusion community. In line with this development, facilities for remote participation are also being improved and expanded.

In the last three years the Joint European Torus experiment (JET) in Culham, UK has been run under the auspices of the European Fusion Development Agreement (EFDA). IPP physicists continue to make major contributions to the preparation, execution and analysis of the JET experimental programme. In 2002, IPP physicists supported the JET programme with more than 1500 days of on-site participation.

A similarly large effort has gone into the analysis of the data at IPP. The results of these investigations are now appearing regularly as full journal articles. In preparation for the 2003 experimental programme, IPP has made more than 40 proposals for new experiments, many in collaboration with colleagues from the other fusion Associations.

The realisation of ITER gained considerable momentum in 2002 due to three site proposals from France, Spain and Japan (giving with Canada a total of four). Moreover, in early 2003 both the United States and China announced their commitment to ITER and have since joined the negotiations. IPP has continued its support. One area is the contribution to ITPA, the International Tokamak Physics Activity, which aims at establishing the physics basis for burning plasma experiments. Here, the input mainly comes from the ASDEX Upgrade experiments, which contribute key physics elements. In preparation for ITER construction, IPP has an on-going interest in contributing to R&D for diagnostics and heating systems. In the latter area, an RF source for the ITER NNBI system is now being developed under an EFDA task agreement, thus documenting strong EU support for this activity.

IPP continues to develop the low-shear line of stellarators, the aim of which is to produce a viable concept for a fusion power plant. On WENDELSTEIN 7-AS the use of modular coils has been pioneered and the island divertor successfully tested. With the latter, densities as high as 4×10^{20} m^{-3} were achieved in 2002; the maximal ß-values of 3.4% are still heating power-limited.

Divertor operation has also shown that volume losses in the divertor region allow power fluxes on the target plates to be reduced, leading to mostly "detached" conditions. The high-density H-mode was further explored. It exhibits the energy confinement properties of the conventional H-mode but does not have ELM´s – the detrimental H-mode MHD instability located at the plasma edge – and, most surprisingly, it has basically L-mode impurity confinement.

This regime therefore combines all the necessary properties for steady state plasma operation. It will be left to WENDELSTEIN 7-X to explore its extension towards lower collisionalities. WENDELSTEIN 7-AS, as a partially optimised device, has also demonstrated within its limits the design principles of WENDELSTEIN 7-X: The Shafranov shift is reduced by about a factor of two; the bootstrap current agrees with the calculated values; the neo-classical electron root develops as expected; energetic particles are better confined in a "linked mirror" configuration. Moreover, the remaining stellarator MHD effects – thermal pressure-driven instabilities located at resonances and fast particle-driven Global Alfven waves – are self-stabilised and disappear toward high ß, also as expected theoretically.

The situation with regard to the manufacturing of the WENDELSTEIN 7-X superconductor has improved. Several superconducting winding packages have been fabricated and the first coils are currently under completion. Production of the coil support structure, the plasma vessel, the outer vessel and the ports is continuing. The first power supply units for the coils and the heating systems have been installed and tested.

Foreword

The facilities at CEA/Saclay are ready for the low temperature tests of the superconducting coils. Jointly with CRPP Lausanne and European industry, the Forschungszentrum Karlsruhe has successfully completed the development of a continuously operating gyrotron with an output power of one MW. The final detailed planning for the assembly of WENDELSTEIN 7-X is now being completed.

However, due to various factors (delays in coil production by the manufacturers and their sub-contractors, the insolvency of the main contractor for the coils and an underestimate of the time required for assembly) the projected start of operation of WENDELSTEIN 7-X is now 2010.

This Annual Report describes the many achievements at IPP in 2002 in various fields of basic research related to fusion science. It is also an opportunity for me on behalf of the Directors and the Scientific Board to praise all members of the staff for their contributions to this success and to thank them for their motivation and dedication throughout the year.

Alexander M. Bradshaw

ASDEX Upgrade

Head of Project: Dr. Otto Gruber

1 Overview

1.1 Scientific Aims and Operation

The design of the tokamak fusion experiment ASDEX Upgrade combines the successful divertor concept of ASDEX with the requirements of a next step fusion reactor, in particular the need for an elongated plasma shape and poloidal magnetic field coils outside the toroidal magnetic field coils. As a result, ASDEX Upgrade is close to ITER in its magnetic geometry and in particular the relative length of both divertor legs compared with the plasma dimension. The installed heating power of up to 28 MW ensures that the energy fluxes through the plasma boundary are equivalent to those in ITER. The scientific programme gives priority to the preparation of the design, physics basis and discharge scenarios of ITER. It consists the study of

- confinement and performance of the ITER base-line scenario, the ELMy H-mode near operational limits, including ELM mitigation,
- investigation of scenarios and physics of advanced tokamak plasma concepts with both internal transport barriers and improved H-mode scenarios leading to enhanced performance, long hybrid and possibly steady-state operation,
- magnetohydrodynamic (MHD) stability and active stabilisation of β limiting instabilities as well as avoidance and mitigation of disruptions,
- edge and divertor physics in high power, high confinement regimes, with the aim of optimising power exhaust and particle control (ash removal),
- testing of alternative first wall materials, especially tungsten.

The similarity of ASDEX Upgrade to ITER makes it particularly suited to testing control strategies for shape, plasma performance and MHD modes. Additionally, the similarity in cross-section to other divertor tokamaks is important in determining size scales for core and edge physics. This collaborative work, including extrapolation to ITER parameters, was enhanced in the JET operation under EFDA during the last years. Furthermore, the ASDEX Upgrade programme is embedded in a framework of national (see section on University contributions to IPP programme) and international collaborations (see section on International Co-operation).

The ASDEX Upgrade Programme Committee is open to the Associations to take more responsibility for the ASDEX Upgrade programme. This body defines the Task Forces responsible for the different elements of the ASDEX Upgrade programme, nominates the Task Force leaders and approves the experimental programme. At present, it comprises 10 members from the Associations and 9 from IPP. Furthermore, the bodies that work out the programme proposals, are now open for external participants and remote participation in these meetings is possible. With this structure, we aim at a compromise between the increased international participation and the flexibility that has so far been typical for the ASDEX Upgrade programme.

The operation in 2002 was based on the hardware upgrades from 2001, namely the more tangential injection of 93 keV neutral beams, which should provide 250 kA off-axis current drive (CD), the divertor IIb structure, which is adapted to maintain good divertor properties at high triangular plasma shapes, and a more reactor-compatible tungsten coverage of the low field side (LFS) heat shield, based on the positive experience with tungsten plasma facing components so far. The new high-field-side (HFS) pellet launcher, which allows injection velocities of up to 800 m/s, was used for both deep fuelling and controlling the frequency of type I ELMs. In the shut-down from August to October the heat shield tiles on the high field side limiter were replaced by larger tungsten coated tiles being capable of higher heat loads. Additionally, the upper passive stabiliser against vertical plasma movements and the HFS baffle at the lower divertor entrance were covered by tungsten so that the total tungsten covered surface is presently about 15 m^2. The ICRH antennas were equipped with new straps.

During the 2002 experimental campaigns, ASDEX Upgrade operated routinely with NBI heating powers up to 15 MW, which allowed studies of the influence of heat deposition on energy and particle transport, of MHD stability and of fast particle effects. Minority heating with the ICRH system (with up to 6 MW coupled) was used for central heating at high densities, and to study the influence of deep particle refuelling and toroidal rotation by substituting NI. The ECRH system with a coupled power of 1.6 MW allowed pure electron heating and current drive, electron transport studies and feedback stabilisation of neo-classical tearing modes (NTM). Provisions for current drive and for active control of current profiles in advanced scenarios were available with more perpendicular or tangential NI and ECRF using steerable mirrors. Stationary H-mode discharges not only on the transport and MHD time scales but also on the current diffusion time with 10 s flat-top have been run for the first time with the reactive power compensation installed last year. This allows steady state investigations for more than five current diffusion times, a unique feature for tokamks with ITER plasma geometry.

The physics programme of 2002 was based on the conclusions and findings of the last years, ITER requirements and tokamak concept improvement (see section 1.2). High shaping capability with elongations κ

≤1.8 and triangularities δ up to 0.45 at the separatrix allowed study of the influence of plasma shape on performance and operational limits. Provisions for δ = 0.55 operation are in progress. Major points of our experimental programme have been the investigation of the particle transport in conventional and advanced H-modes, electron transport, exploration of high performance plasmas with respect to confinement and maximised plasma pressure, stability and transport in the H-mode edge and the combination with tolerable ELMs and wall interaction physics. In the advanced scenarios characterized by a high fraction of bootstrap current and external current drive, emphasis was placed on performance enhancement and the extension of both internal transport barriers (ITBs) and improved H-mode scenarios.

1.2 Summary of Main Results

Both ion and electron temperature ($T_{i,e}$) profiles in conventional L- and H- mode on ASDEX Upgrade are generally stiff and limited by a critical temperature gradient length $L_T=T/\nabla T$ normalized to the major radius R as given by ion temperature gradient (ITG) and trapped electron (TEM) driven turbulence. Accordingly, the core and edge temperatures are proportional to each other and the plasma energy is proportional to the pedestal pressure for fixed density profiles. Electron cyclotron heating and modulation experiments revealed a reduced electron temperature profile stiffness, as predicted by TEM turbulence, under dominant electron heating conditions. Density profiles are not stiff, and confinement improves with density peaking. The influence of the heat deposition profile on the particle transport, namely density profile peaking with off-axis deposition and profile broadening with central deposition, first established with neutral injection, was further substantiated. The explanation is based on a link between particle fluxes and heat fluxes: off-axis deposition leads to a low central heat flux and consequently a reduced central particle out-flux. This was further confirmed by comparing the effect of on- and off-axis wave heating without any core particle refuelling. Drift wave instabilities including dissipative effects from collisions seem to explain these phenomena. A corresponding impurity transport behaviour was observed for tungsten and for injected Silicon impurities.

At high densities with reduced edge temperatures small type II ELMs can provide good confinement combined with low divertor power loading. The operational regime of these type II ELMs was established at $q_{95}>3.5$ and closeness to magnetic double null configuration. Another way to mitigate ELMs may be active type I ELM control by means of hydrogen or impurity injection. Using small hydrogen pellets we demonstrated controlled ELM triggering by each pellet injected in ELM free phases at a frequency of 20 Hz.

A main focus has again been the stationary advanced H-mode scenarios combining the beneficial elements of high β_N >3.5, improved confinement ($H_{98\text{-}P}$ ≈1.3), high density operation close to the Greenwald density and tolerable type II ELMs for many current redistribution times at highly shaped plasma configurations, near double null. This integrated scenario has many elements in common with the "improved H-mode", achieving ASDEX Upgrade records in the tripple product but at lower densities. In both advanced scenarios with weak central magnetic shear the temperature profiles are governed by ITG / TEM turbulence, while the confinement is improved via peaked density profiles. Both H-mode scenarios have been merged showing both $ß_N$ and H factors to increase with triangularity and to be nearly independent of the edge q_{95}≈3.2 -> 4.2. NTMs are avoided by density profile control with NBI and core ICRH. The total non inductively driven current exceeds 50% of the plasma current making this advanced H-mode a serious candidate for a long stationary integrated reactor scenario with "hybrid" current drive consisting of non-inductive and a small amount of inductive drive. In the experiments with ion ITBs an optimised heating scenario in the current ramp-up was developed which allows reproducible ITB formation and has led to broad internal barriers with ASDEX Upgrade records in the central ion temperature of more than 20 keV, β_N = 3.9 and $H_{89\text{-}P}$ ≈3.1 values. However, the duration of these ITBs is terminated by the transition to an H-mode edge barrier with type I ELMs.

The marginal stability limit in terms of β for (3,2) and (2,1) neo-classical tearing modes, limiting the operational regime of conventional and advanced scenarios with positive magnetic shear, was investigated in ramp-down phases of the heating power. There, the mode disappearance allows a much more precise determination of the stability limit without the influence of seed island size. Correspondingly the plasma pressure at the mode offset is smaller than at the mode onset, but is still proportional to the normalized gyroradius. Using ECCD at the island position (10% of the total heating power) replacing the missing bootstrap current in the magnetic islands not only complete NTM stabilisation was demonstrated, but also the β was enhanced compared with the pre-NTM phase. Disruption avoidance and mitigation (via strong Neon and Argon puffs) techniques have been further developed and can be used in real-time.

Finally, the plasma operation with a tungsten coverage of large wall areas shows tungsten concentrations below 10^{-5}. In discharges with improved core confinement and density peaking, a tailored central RF heating was used to control the impurity content accompanied by only a modest reduction of energy confinement and electron density peaking. In parallel the carbon migration and the mechanism for the build up of carbon layers below the divertor structure was investigated.

1.3 ASDEX Upgrade Technical Enhancements and Programme in 2003

In 2002 the operation of ASDEX Upgrade in close connection with the JET programme and in co-operation with the EU Associations will continue. Core physics studies will emphasize the improvement of plasma performance (energy and particle transport, MHD-stability and β-limits, mode stabilization using ECCD) in both "conventional" H-mode and "advanced" tokamak scenarios. Main elements will be pressure and density profiles as well as impurity control using tailored heat deposition from ICRF, ECRF and NBI. Current profile control and sustainment in advanced mode operation with non-inductively driven currents in addition to the internally

driven bootstrap current can be done in a flexible way. The tungsten coverage will be extended in the next step towards the upper divertor targets and the low field side divertor entrance regions. A new fast control and data acquisition system is under development. An upgrading of the ECRF power to 4 MW at tuneable frequencies between 104 and 140 GHz is underway. To reach the ultimate ideal MHD limits in addition to profile control, the introduction of a stabilizing wall close to the plasma in combination with active feedback coils working on the resistive time scale of the wall are under consideration.

Sections 2- 5 are concerned with operation of tungsten coated walls and W transport, progress in the internal ion transport barrier scenario, off-axis neutral beam current drive experiments, and type II ELM operation and edge stability. In section 6 the ASDEX Upgrade technical and heating systems are described. Section 7 deals with core and edge performance and MHD stability, and disruption forces. Scrape-off layer, wall interaction and divertor physics issues are described in section 8.

2 Tungsten Programme

The ASDEX Upgrade tungsten programme addresses the questions, how a tungsten first wall influences plasma

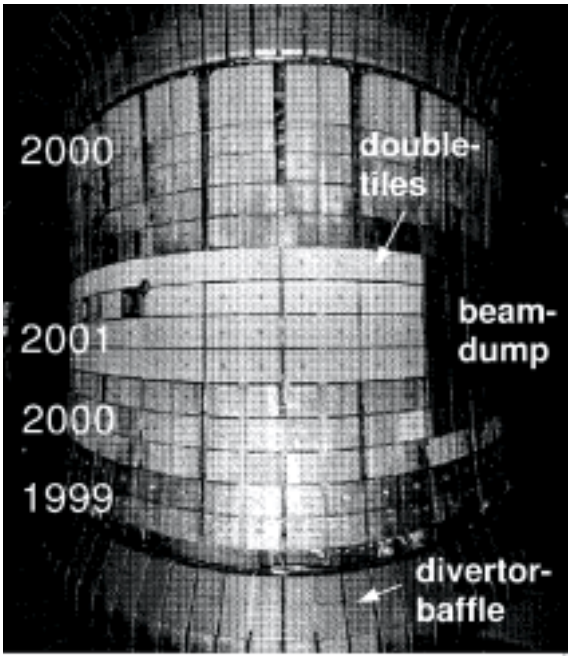

Figure 1: The central column of ASDEX Upgrade with the tungsten-coated tiles. The four rows in the equatorial plane are used as a limiter during plasma start up and in dedicated limiter discharges. The numbers give the year of installation.

operation and performance and whether the amount of migrating carbon can be reduced. To this end, the central column has been coated with tungsten in a step by step approach, reaching almost full coverage, except the regions of the beam dumps for the 2001/2002 campaign. For this purpose, the limiter region was equipped with newly designed double tiles (shown in Fig. 1) which reduced the number of leading edges and prevented misalignment through independent movement of the substructure.
As in the previous year, the tiles were coated commercially by plasma arc deposition to a thickness of $1.0\,\mu m$. No significant difference in plasma behaviour was observed during the flattop phase of the discharges compared to the earlier results. Typically, the W-concentration C_w was far below 10^{-5} and no influence of the large W-area on the discharges was found. Therefore, in 2002 the work was concentrated on the investigation of the startup behaviour at a W-limiter and the erosion pattern at the central column (see Project PFMC) as well as on detailed analyses of the transport and accumulation properties of W.

2.1 Startup Behaviour with W-limiter and evolution of C-concentration

The start-up is investigated in 'standard H-Modes' for the different phases of the W-programme, starting with a complete graphite central column. Besides the material of the tiles itself, the status of the wall conditioning turns outto be an even more important parameter. Fig. 2 shows the behaviour of several parameters in 'standard H-Modes' versus discharge number.

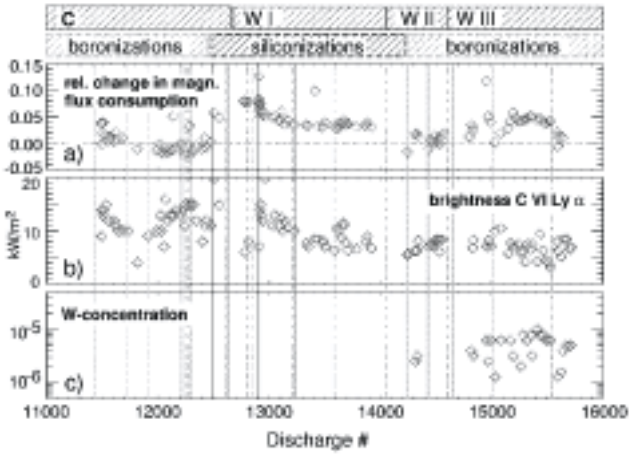

Figure 2: Behaviour of ohmic transformer current, C VI radiation and W concentrations during phases of different wall conditioning in 'standard H-mode discharges'. Boronizations/siliconizations are represented by solid vertical lines and vents by dashed lines.

It clearly indicates, that the increase of the flux consumption of the ohmic transformer with W-limiter is below 5% and is even weaker than after siliconization. From post mortem surface analyses (see Project PFMC), it can be discounted that deposited layers (boron from boronization, carbon from deposition) mask the effect of W, because at least half the W area is found to be erosion dominated. The plasma current ramp is not hampered in any way, as can also be concluded from the radiation measurements, which were highest with siliconized graphite walls. The boronizations lead to a strong reduction of the radiation, independent of the material of the tiles, which lasts only for a few shots, and after these, the radiation increases typically on the time scale of 100 discharges. A long term decrease in the CVI brightness I_{CVI} measured during the high density flattop of the discharges

is visible, especially since the regular application of the siliconization. During the last two campaigns no siliconization was applied. Nevertheless, I_{CVI} is at the lower end of the observed range right from the start, pointing to some carbon reduction due to the increased area of W-coating. The tungsten concentration is evaluated at its maximum during the start-up limiter phase (t=0.6s). It decays quickly after the evolution of the X-point in the plasma. After boronization, a clear reduction of C_w by a factor of 5 is observed, but the W-concentration recovers faster than the total radiation and the radiation from oxygen. This leads to the conclusions that the boron layer is quickly eroded at the positions of strong plasma wall interaction and that W contributes only a minor part to the radiation during the startup. Spectroscopic measurements of the W influx, as well as Langmuir probe measurements at the central column, point to the fact, that the erosion is dominated by the current ramp up and ramp down phase, when the central column is used as a limiter, consistent with the observed increased W-concentration during this discharge phase.

2.2 W-Transport and Suppression of Accumulation

Under steady state conditions in the source free region, the normalized impurity density gradient is

$$\frac{d\ell nn_I^{eq}}{dr} = \frac{d\ell nn_D}{dr}\frac{Z_I}{Z_D}\frac{D_{neo}}{D_{neo}+D_{an}}(1-H\eta_D) \quad (1)$$

Here, it is assumed that the diffusion coefficient consists of an anomalous and a neo-classical part $D = D_{an} + D_{neo}$ and that the convective contribution is purely neo-classical with $v = v_{neo}$, where only collisions of impurity and main ions are considered. Z_I, Z_D are the charges of the impurity ions and the background ions and H $\approx$0.2 - 0.5 represents the so-called impurity screening, which depends on the collisional regime.

$\eta_D = \left(\frac{d\ell nn_D}{dr}\right)/\left(\frac{d\ell nT_D}{dr}\right)$ is the ratio of the normalized temperature gradient to the normalized density gradient of the background ions. From these equations one can easily see that a necessary ingredient for neoclassical impurity accumulation is a density gradient (density peaking) of the main ions. This gradient is amplified by Z_I / Z_D, and it is diminished through the anomalous diffusion and the term in parenthesis. This term appears to be critical because it may vary from small positive numbers to small negative numbers: typically the normalized temperature gradient is significantly larger than the density gradient in the confinement region and hence the product $H\eta_D$ is of the order of one.

Accumulation becomes evident not only from the W-concentration measurements but also from the radiation profile. Figure 3 shows the behaviour of the line integrated plasma radiation for an ensemble of plasma discharges with low to high auxiliary heating power (P_{aux}=3-14 MW) comprising all discharge scenarios run at ASDEX Upgrade with sufficiently long steady state conditions. The total main chamber radiation is low and usually amounts to 25%-40% of the heating power.

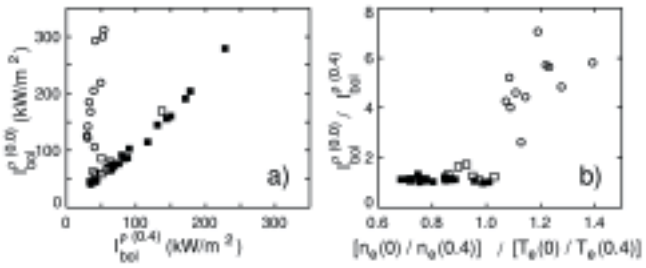

Figure 3: Behaviour of the plasma radiation in a set of plasma discharges comprising all discharge scenarios with sufficiently long steady state conditions. Filled symbols: discharges with central wave heating. Circles: discharges without sawteeth or fishbones. a) Total line integrated radiation $I_{bol}^{\rho(0.0)}$ (central bolometer channel) versus $I_{bol}^{\rho(0.4)}$ (bolometer channel with normalized tangential radius =0.4) b) Central radiation peaking versus the ratio of density peaking over temperature peaking ($\approx \eta_D^{centr}$).

The features of the dataset are the following:

- In discharges without accumulation the radiation is strongly dominated by edge radiation because the line integrated radiation is almost equal for the bolometer channels with different normalized tangential radii.
- In phases with accumulation the enhanced radiation is only visible on central channels (ρ_{tang} <0.2). No increase of the total radiation is observed.
- Central wave heating (ICRH or ECRH) prevents centrally peaked radiation profiles.
- Density peaking alone is not sufficient for accumulation, but the ratio of the normalised gradients η_D in eq. 1 is an important ordering parameter. For this dataset, this is linked to the loss or the absence of sawteeth or fishbones.

Typical conditions for such centrally peaked radiation profiles are low to intermediate heating power without central wave heating, where the anomalous diffusion is low. In these cases, the central radiation is increased by all impurity species existent in the plasma as seen by spectroscopic measurements. The very small affected volume explains that for similar influxes, strongly different central impurity contents may be observed. Finally, this effectively overrides any correlation between influx and central impurity density in discharges with accumulation.

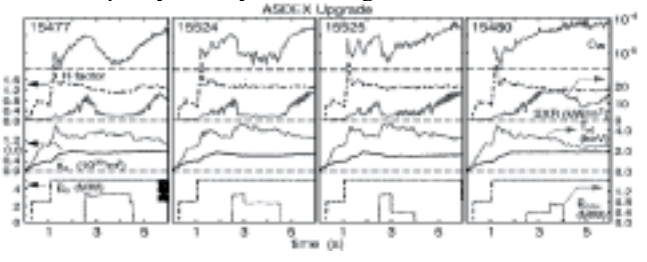

Figure 4: ECRH power scan in similar improved H-Mode discharges I_p=1 MA, B_t=-2.5 T, _=0.35, P_{NBI} =5 MW) demonstrating the control of the central c_w

The above considerations clearly point to the tool which may be used to quench accumulation: An increase of D_{an} at the critical position decreases $\frac{d\ell nn_D}{dr}, \frac{D_{neo}}{D_{neo}+D_{an}}$ and increases $H\eta_D$. Since the affected volume is very small,

the central accumulation can be suppressed very efficiently by central heating *without* strongly degrading the total confinement.

In a series of discharges with very good confinement ($H_{ITER-H98_y} \approx 1.3$) the central ECRH-power was varied from zero (reference discharge) up to 1.2 MW (3 gyrotrons), see Fig. 4. For the highest ECRH power applied (1.2 MW) a very strong reduction of c_w by more than a factor of 30 and the onset of sawteeth is observed, but at the same time the energy confinement is also degraded. Using 0.4 MW of ECRH, the confinement is not affected, but also the c_W is not decreased. The most successful results where achieved when starting with 3 gyrotrons and reducing the power after 0.5 s (e.g. # 15524). In these cases, both effects (the reduction of c_w and the good confinement) are maintained. In all cases the discharges return to their initial behaviour after switching off ECRH.

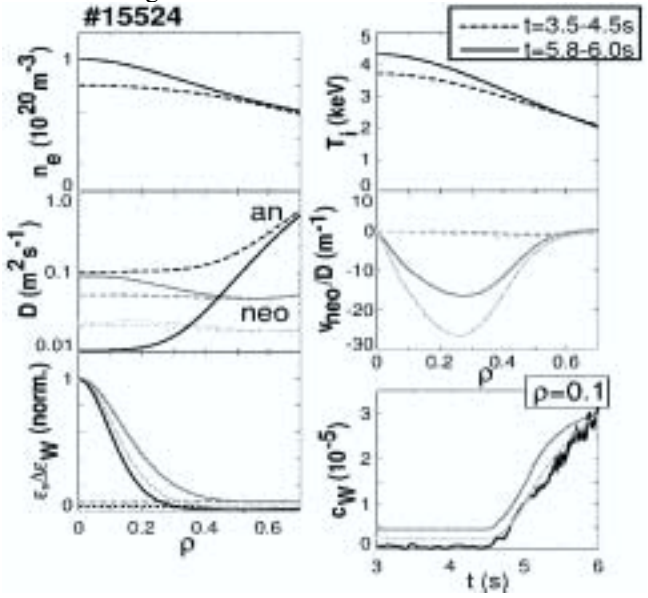

Figure 5: Measured profiles of n_e, T_i, neoclassical transport coefficients of tungsten with (dark grey) and without (light grey) inclusion of additional impurities, used D_{an}, calculated tungsten radiation and measured total radiation for two time slices. In the lower right corner, time traces of measured and simulated central tungsten concentration are shown.

In Fig. 5 the result of impurity transport simulations for the above shown discharge #15524 are presented. Dashed lines give radial profiles for a time slice during the ECRH phase (t=3.5-4.5s) and solid lines are used for t=5.8-6.0s, which is at the end of the second pure NBI-heating phase. Neoclassical impurity transport coefficients were calculated numerically with NEOART, which can include the effect of impurity-impurity collisions for an arbitrary number of species. The transport simulation was started with flat impurity concentrations and the impurity densities at the edge are kept constant during the simulation. In one case (light grey) only W was taken into account, while in the second case (dark grey) additional impurities were considered with 'typical' concentrations of 5% He, 1% C, 0.5% O, 0.02% Fe at the edge. n_e, T_e and T_i profiles were taken from measurements and n_D followed from the given electron density, the impurity ion distributions and quasi neutrality. C, O, Fe and W are in the plateau regime with W at the Pfirsch-Schluter limit, while D and He are in the banana regime. The anomalous diffusion coefficient was assumed to be equal for all impurity species and to decay from edge to centre, where the central value was chosen to be $D_{an}(0)=0.1m^2/s$ during ECRH and below neoclassical values during pure NBI heating. These choices are based on previous determinations of impurity transport coefficients between sawtooth crashes in sawtoothing H-mode discharges.

The increased central diffusion coefficient with the additional central power flux from ECRH is interpreted to be a consequence of profile stiffness. Analysis of the local heat diffusivities with ASTRA yields an increase of central χ_i and χ_e. For ρ =0.3 both values change from $\approx 0.2m^2/s$ with ECRH off to $\approx 0.7m^2/s$ with ECRH on. The evolution of the main ion density can be understood by a higher anomalous diffusion being connected to the higher χ in the ECRH phase. The increase of D_{an} counteracts the neoclassical inward drift due to the Ware pinch. Tungsten has a much higher collisionality and the Ware pinch, which is included in the simulations was found to yield a negligible contribution to its drift velocity.

For W, the calculated values of v/D are small in the ECRH phase, mainly due to the rather flat density profile and partly due to the increased D_{an}. In the pure NBI-phase, the density peaking increases, while D_{an} becomes small and v/D reaches large negative (inward pinch) values inside ρ =0.5. In the case with inclusion of all impurities, the inward pinch is smaller and the v/D-profile is broader. The simulated W profile evolves the strongest peaking of all impurities as expected from eq.(1). The calculated peaking of W is smaller than the experimental one deduced from the unfolded total radiation. Similarly, the high central tungsten concentrations at the end of the discharge can only be simulated when setting the edge concentrations to 2-5 times the measured values depending on the inclusion of other impurities in the simulation. Perfect agreement can be achieved with a v/D profile that reaches a minimum value of -50 m^{-1}. Thus, the main features of the impurity flattening with ECRH and the strong peaking without ECRH are well described by the simulation and calculated v/D values agree with the measurement within a factor of 2. For t=5.8-6s, the T_i gradient is increased and the related outwardly directed drift velocity is $\approx$ 50% above the value during the ECRH phase. Thus, the central radiation is still not large enough to change the temperature screening.

3 Ion ITB and new ITB scenarios

Ion temperature transport barriers are generated through neutral beam heating in the current ramp. Compared with previous campaigns on ASDEX Upgrade, significant progress has been made mainly through a change in discharge scenario, heating the plasma later in the current ramp and (often) with significantly more power. A comparison between the two scenarios is given in Fig. 6. The dotted curves in this figure refer to the old early beam timing, whereas the full curve given shows the new scenario. It can be seen that performance in terms of stored energy is the same at the same heating power. However, the new scenario will be shown to allow for a larger applied heating power and thus, a better performance. Below we

will discuss some physics analysis based on the old scenario as well as the performance of the new scenario.

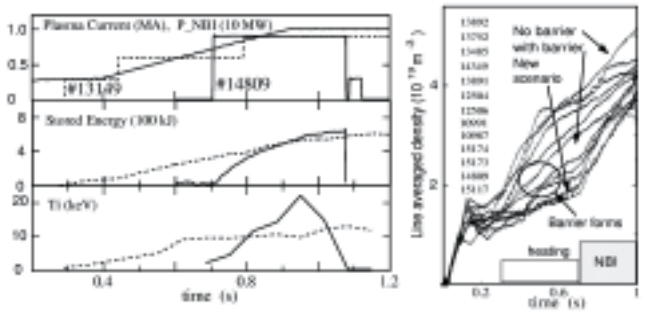

Figure 6: Comparison between the old and new scenarios, right: density evolution of the different scenarios.

3.1 Physics studies of the old scenario

In the old scenario no reproducible barrier formation was obtained. Therefore, at the start of the 2000/2001 campaign an investigation was initiated to determine under what conditions barriers form. To this extent a number of discharges in which a barrier was formed were compared with similar discharges in which no formation was observed. Correlations with global plasma parameters just before the barrier formation were investigated.

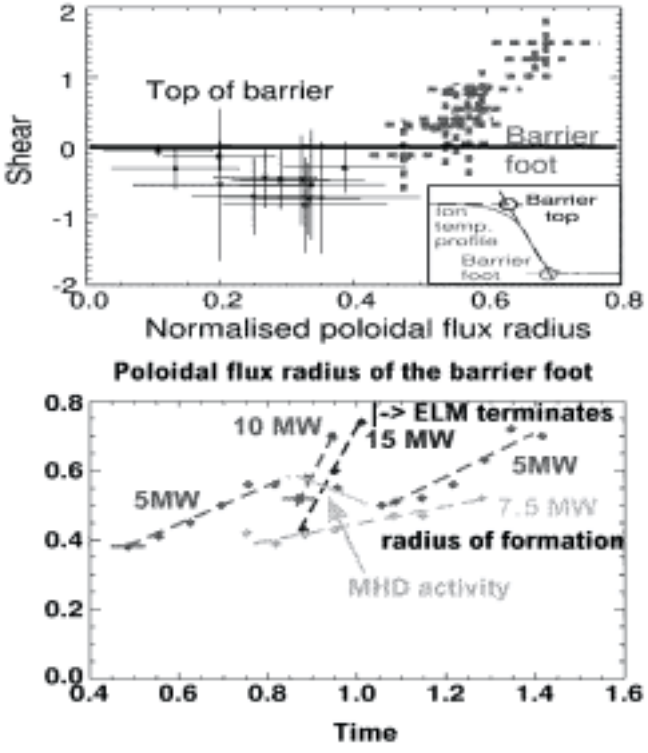

Figure 7: Top a): Shear at the top and foot of a strong ion transport barrier, Bottom b): propagation of the barrier in the old and new scenario

It was found that density plays an important role in the formation criterion (see Fig. 6). The plasmas in which a barrier was formed all had lower densities compared with the cases without a barrier. Also it was found that barrier formation in the earlier campaign occurred only shortly after boronization, again pointing to low density as a necessary condition. No clear correlation with other global parameters has been found. In terms of local parameters, it is found that the low density is also correlated with a larger density gradient length. However, often $R/L_n \approx 6-9$ and the influence on the stability of ion temperature gradient modes is therefore weak.

Unfortunately, no measurements of the current profile in the 2001/2002 campaign are available, due to diagnostic problems. Investigations of the barrier position against the q-profile are, therefore only available for the previous campaign in which barriers were generated with 5 or 7.5 MW of neutral beam heating early in the current ramp up. Fig. 7 reports the findings of the barrier position at the time point when a strong barrier is present. It can be seen that the barrier foot is always in the region of positive shear and the barrier top is always in the region of negative shear. The barrier therefore extends over the region of zero shear and has roughly its strongest gradient at this position. The occurrence at zero shear is a puzzle for theoretical explanation, since this condition is not necessarily the most stable. However, a possible explanation could be the large distance between the rational surfaces at the zero shear position.

The barrier position when it is formed lies further inward as also shown in Fig. 7. As a function of time it propagates outward, with a timescale that is relatively long in the old scenario (5 and 7.5 MW), but very fast in the case of higher heating power. In the latter case the propagation seems inconsistent with a resistive time scale.

3.2 Performance of the new scenario

The finding that density plays a role in the formation (not necessarily sustained), was one of the reasons for delaying the neutral beam heating in the current ramp. The beams provide a density source and therefore it might be more advantageous to have a current ramp without beams, until a favourable q-profile has been established and then switch on all the NBI power at once. It can be seen in Fig. 6 that the density is indeed kept at a lower value and that the sudden switch on of the beams leads to a more ready formation of the ion transport barrier, i.e. a much steeper increase in the central ion temperature with time.

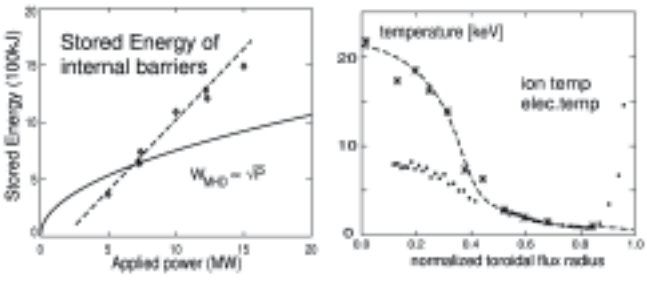

Figure 8: left: Stored energy of barrier discharges as a function of applied heating power, right: Temperature profile of a discharge with 10 MW NBI heating and 1.6 MW counter ECCD

The new scenario, in contrast to the old, generates reproducible barriers and has more freedom in applied heating power. Also, in this scenario it was possible to generate barriers in lower single null configurations, with high triangularity. The timing of the beams can be varied

between 0.6 and 0.9s however, this yields weaker barriers at both ends. Powers up to 17.5 MW have been applied. However, at 17.5 MW the β rise in the plasma is so fast that the control coils cannot keep the plasma at its position, leading to a vertical instability. This limitation at present sets the limit to the applied power.

Fig. 8 shows that for the internal transport barriers the stored energy increases almost linearly with the applied power. Therefore, in terms of normalised parameters, the performance (confinement as well as β_N) goes up with heating power. At a toroidal field of 2.9 T, plasma current of 1 MA and an NBI heating power of 15 MW, a record stored energy of 1.5 MJ was reached with an ion temperature in excess of 20 keV. This plasma has a normalised pressure $\beta_N = 3.2$. At this toroidal field the plasma position control does not allow more heating power. Record values in normalised plasma parameters are therefore obtained at lower magnetic field (2 T) and lower plasma current (0.8 MA). This is shown in Fig. 9. At these values a normalised pressure $\beta_N = 4.$ and $H_{89} = 3.3$ are reached. However, the barrier in these discharges is weaker with a maximum temperature of 16 keV.

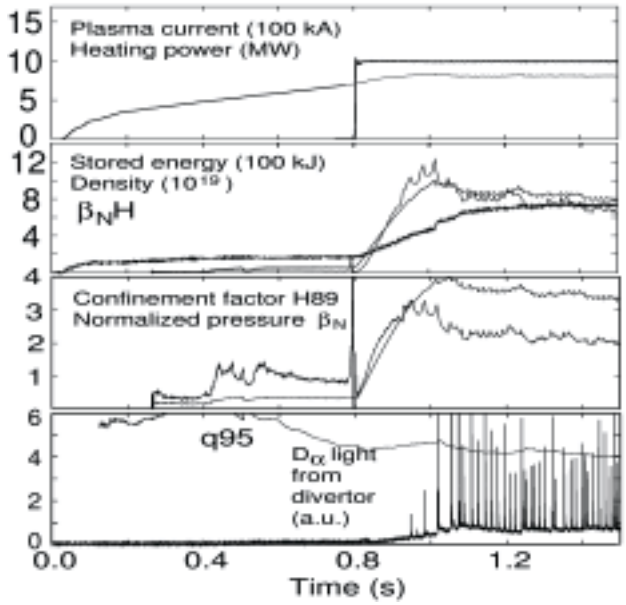

Figure 9: Time trances of the record β_N shot

The progress in normalised parameters is large since the old scenario reached $H_{89} = 2$ and $\beta_N = 1.7$. The increase in normalised pressure is especially striking since the values in the old scenario are limited by the external kink. The reason for the strong difference remains unclear, but it is possible that the q-profiles in the new scenario are less inverted and provide better stability. At 2.7 T with 10 MW heating power a (3,1) resistive mode has been observed as far as $\rho = 0.25$, indicating that the q-profile is reversed, but the record discharges with their lower current and magnetic field, might have a more flat q-profile. Current profile measurements are necessary to clarify this point.

In the new scenario the ELMs terminate the internal barrier. The high triangularity, high power, low density discharges have a very large first ELM that perturbed the plasma over a large radius reaching into the barrier region. This leads to a collapse of the barrier.

Experiments with a variation in the power deposition of the neutral beams have been undertaken. At 7.5 MW, which is close to the threshold, no strong barrier forms if one uses 2 on-axis sources and one off-axis neutral beam source, in contrast to the case with 3 on axis sources. At 10 MW (4 sources) the switch of one source makes a negligible difference. In discharges with reversed current and magnetic field, in which the power deposition is largely off-axis, no barrier could be obtained even at heating powers of 15 MW. It is concluded that a minimum amount of central heating is necessary to generate an ion transport barrier.

3.3 Electron heating in ion barriers

Various experiments with ECRH pre-heating and ECCD counter current drive have been undertaken. The electron temperature can be raised by counter current drive without destroying the ion barrier. Although the electron temperature is significantly raised (from 5 keV to 8.5), no clear barrier structures can be observed in the electron temperature profile. Of course, the EC wave power is only 1.6 MW against 10 MW beam power. Off-axis ECRH pre-heating is expected to slow down the current diffusion and therefore generate more reversed shear discharges. This could influence position and strength of the barrier. It is found experimentally, that the pre-heating did not have a favourable influence. The barrier did not form at the switch on of the beams, but formed at a later time point, at roughly the same radial position and was somewhat less strong. The implication of this result is unclear. It is possible that the current profile is changed and is only favourable at a later time point in the discharge. Also, these experiments were performed with 7.5 MW, which is close to the threshold, and more neutral beam heating power might change the picture.

4 Neutral beam current drive experiments

The first experiments with the changed neutral beam injection geometry have shown less effect on the measured q profile than expected from code calculations (ASTRA). As a consequence an experiment has been created to maximise the effect on the current profile with the new injection geometry. The most important time traces of this experiment are shown in Fig. 10 .

Of special importance is the fact that most plasma parameters are constant over the time the neutral beam injection is switched from on-axis deposition to off-axis deposition. The beam deposition and all plasma parameters are kept constant for 2s (t=1.3s-3.3s on-axis, t=3.3s-5.3s off-axis). This time duration is long enough for building up stationary profiles in temperature, density and current according to the ASTRA modelling of this discharge. For this experiment also MSE measurements are taken but unfortunately the diagnostic was not calibrated and no equilibrium can be reconstructed with MSE measurements and no q or current profile can be inferred. Furthermore, the MSE angles plotted in Fig. 11 are offset corrected to the angles calculated by ASTRA at t=2.8s. This calculation gives a neutral beam driven current of I_{NBI} =61kA centrally peaked for the first 2s interval and I_{NBI} =192kA off-axis at

$\rho_{tor} \approx 0.5$ peaked from t=3.3s to t=5.3s. The ASTRA calculated MSE angles indicate the slow change in the q profile in the second interval due to current diffusion.

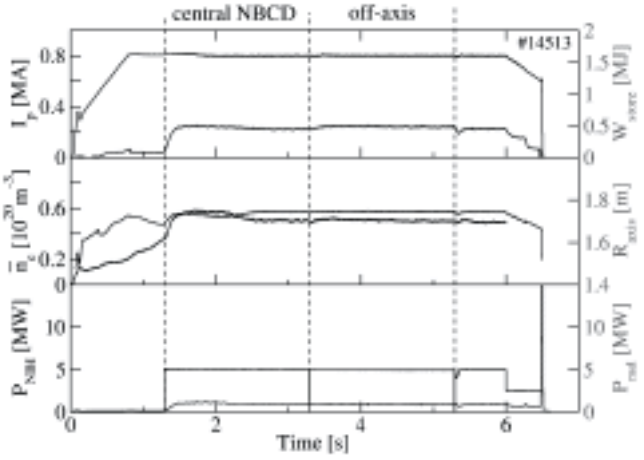

Figure 10: Time traces of a co NBCD discharge. In the middle the line averaged electron density and the R co-ordinate of the magnetic axis are represented.

The measured MSE angles follow the calculated angles reasonably well, before turning on the off-axis depositing beam sources but they do not changed after turning off the off-axis sources. This is in clear contradiction to the modelling. After turning off the off-axis current source the modelled MSE angles decrease to their former values on the current diffusion time scale. The values at the end of the decay reach the measured values at the beam switching time which again shows that the measured MSE angles do not predict any driven current by the off-axis neutral beam deposition.

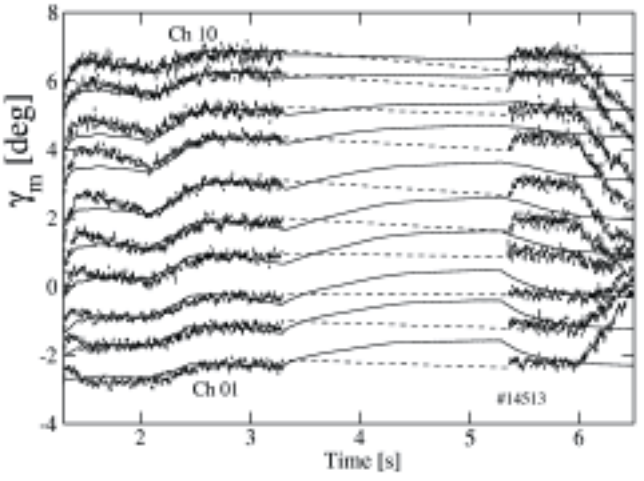

Figure 11: MSE polarisation angles. From t=3.3s to t=5.3s no data is available. The noisy time traces are the measurement. ASTRA calculations are shown as solid lines.

This is underlined by the MHD activity in this discharge which shows sawteeth and fishbones at the q=1 surface before the beam deposition is changed. With off-axis injection the sawtooth oscillation is stopped but a continuous (1,1) mode starts at the same radial location as the sawtooth precursors were before. This shows that the position of the q=1 surface does not change. The frequency and position of this (1,1) mode is stable for the whole 2s interval. After switching back to the central depositing neutral beam sources the sawteeth reappear in less than 10ms, which is too fast to be a result of a current diffusion process over a large spatial range. The constant q=1 surface determined by the MHD activity is in full agreement with interpretation of the MSE angles but again in contradiction to the modelling.

The experiments shown so far indicate that no neutral beam current is driven. However, this is a contradiction to the fact that the slope of the current in the ohmic transformer changes with a change in the beam deposition. In Fig. 12 two discharges are presented, one with weak on axis current drive and one with larger off axis current drive but otherwise the same parameters. The difference in slope of the ohmic transformer current presented in Fig. 12 can be used to infer the total current driven by the off-axis neutral beam injection, if all other current sources are given. Using the bootstrap current from the ASTRA calculation, the off-axis driven current is approximated to I_{NBI} =250kA which agrees reasonably well with the I_{NBI} =300kA calculated by ASTRA. This shows that the predicted current is driven.

The experiments discussed here do not lead to an unequivocal conclusion. The current driven by the neutral beam injectors can be found in the ohmic transformer current but the predicted influence of this current on the total current profile is not confirmed by the MSE measurement or by MHD activity. This leads to speculation that a fast transport may transfer the off-axis deposited fast particles to the plasma centre so that the neutral beam driven current just replaces ohmic current. But up to now no such transport events could be observed.

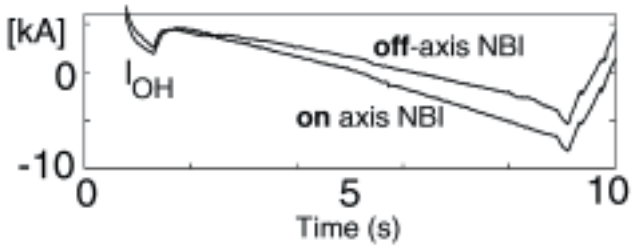

Figure 12: Comparison of the currents in the ohmic transformer on between two very similar discharges at low density and I_p =0.8 MA. The currents have been adjusted to each other at t=2.5s because of a different startup phase.

5 Type II ELMs and Edge Stability

The reference scenario for ITER inductive operation with Q≈10 is the ELMy H-mode. Besides sufficient confinement (H-mode confinement of $H_{H98-P} = 1$) and stability margin (in terms of beta normalised $\beta_N \approx 2$) at low $q_{95} \approx 3$, operation at a density close to the Greenwald density n_{GW} for optimised heat and particle exhaust and ELMs (edge localised modes) producing tolerable peak heat loads at the divertor targets are needed in an integrated scenario. Type I ELMs are normally connected with the best performing H-modes but result in pulsed heat flows to the divertor target plates, which could cause high erosion and severely reduce the lifetime of the divertor in ITER FEAT to unacceptable levels.

5.1 Tolerable type II ELMs close to the Greenwald density

Small irregular high-frequency type II ELMs are actively being studied as a solution to the reactor divertor power load problem. These type II ELMs, partly mixed with type I ELMs, were originally found in discharges with $q_{95} > 4.2$ and $<\delta> > 0.4$, close to a double null configuration and at high densities close to the Greenwald limit. As they preserve high edge pressures, the confinement is almost as good as with type I ELMs and significantly higher than for type III ELMs, providing $\tau_E/\tau_{H98\text{-}P} \approx 1$. In recent conventional H-mode experiments steady-state type II ELM phases could be established, limited only by the length of the current flattop phase. The type II ELM features are as described earlier: The ELM amplitude of the D_α signal decreases, and ELM frequencies between 0.5 and 1 kHz are observed. Even in the case of non-conclusive D_α traces, magnetic precursors and target plate thermography allow a clear identification. The thermography data of the divertor target plates show that the peak power load is strongly reduced with type II ELMs, especially at the inner target. The power flux on the plates is quasi-stationary and slightly above the value in between ELMs in purely type I ELM phases.

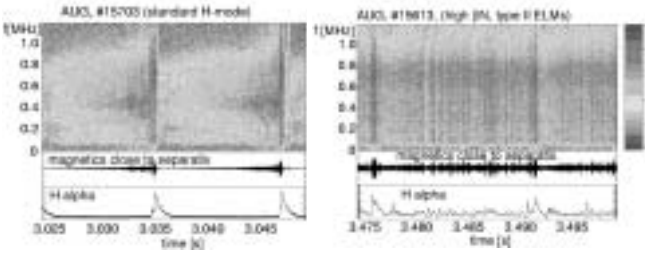

Figure 13: Magnetic precursors for type I (left) and II (right) ELMs measured by magnetic pick-up coils on the low field side with a high frequency response up to 1 MHz and sampling rate of 2.5 MHz, together with time traces of magnetic and D_α signals.

Magnetic measurements close to the separatrix and reflectometry show that single type II ELMs, best observed in mixed type I and II phases, are characterised by a precursor of broadband MHD fluctuations in the frequency range between 15 and 30 kHz. Correlation analyses of poloidal and toroidal arrays of magnetic pick-up coils give mode numbers $m \geq 14$, $n \approx 3\text{-}4$, which corresponds to localisation at the plasma edge. In pure type II ELM phases the precursors unify to a wide frequency band. New features have been detected using magnetic coils on the low field side with a high frequency response up to 1 MHz and sampled at 2.5 MHz (Fig. 13). While type I ELMs exhibit a high frequency precursor around 400 kHz with a local $m \approx 10\text{-}15$ at the outer midplane 1-2 ms before the actual ELM, type II ELMs show a broadband fluctuation around 700-800 kHz.

5.1.1 Integrated high performance scenario with tolerable type II ELM activity

In highly shaped plasma configurations with $<\delta> = 0.42$, near double null, high-β_N H-mode discharges with $\beta_N > 3.5$ and good confinement $H_{H98\text{-}P} \approx 1.3$ have been obtained in steady state at $q_{95} \approx 3.6$, with $\beta_N H_{89\text{-}P}$ reaching up to 8.0 for 40 energy confinement times and many current redistribution times. In these discharges line averaged densities of 80%-90% of the Greenwald density are achieved while maintaining the good confinement. At the highest densities and close to double null configurations a strong reduction of the ELM activity to type II ELMs is observed as in conventional H-modes, providing a strong reduction of the peak heat load on the divertor which becomes steady in the range of 6 MW/m^2, despite the high input power used ($\geq$10 MW) in our example. During the NBI heating phase, the ELMs are reduced significantly in size as the density increases and the plasma configuration is moved up, closer to a double null configuration. This movement to a double null configuration is made deliberately. Infrared data shows that initially type I ELMs are observed on the outer target with a peak heat flux of up to 18 MW/m^2. The type I ELM activity drops and finally the maximum heat flux on the divertor has become fully steady, in the range of 6 MW/m^2, and only type II ELMs remain. For the inner target plate, high peak loads are observed during type I ELMs, however, the heat flow reduces to nearly zero during the close to double null configuration phase. During the transition and in the type II phase the time averaged heat flux to the outer divertor does not change and is 2.5 MW out of 10 MW heating power, while about 1.3 MW go to the upper outer divertor. This ELM behaviour is very similar to what is observed for type II ELMs in standard H-mode discharges at medium heating powers of 5 MW. Here type II ELMs are achieved despite the high heating powers of $\geq$10 MW well in excess (factor 5) of the H-mode power threshold and the high gas fuelling rates.

5.1.2 Operational regime of type II ELMs

The operational space and the edge parameter regime for the occurrence of type II ELMs are the same for conventional and advanced H-modes: a combination of closeness to double null and high densities. The closeness of the two separatrice Δx is stringent and has to be kept below 1 – 2 cm in the torus midplane as is seen in Fig. 14b. Triangularity or q_{95} are not the decisive parameters, indeed they can vary over a broad range (see Fig. 14a). In experiments on ASDEX Upgrade with its reactor relevant PF coils being outside the TF magnet and distant from the plasma, the close to double null condition is difficult to separate from high triangularity. The accessible operational space in triangularity and closeness to double null is shown as the shaded area in Fig. 14b. The operation window in q_{95} has been extended towards $q_{95} \geq 3.5$ (Fig. 14a) being closer to the ITER reference value.

The second condition means a sufficiently high edge pedestal density is required to get type II ELMs: above 50% of the Greenwald density, which is connected with line averaged densities above 85% of Greenwald density. For one given magnetic configuration, the requirement of increasing density to change from type I to type II ELMs can of course be framed as a collisionality limit at the pedestal and has led to the concern that, with the low edge collisionality required for high core confinement in ITER, type II ELMs might then be inaccessible. However, this condition on collisionality is connected with the driven

edge bootstrap current and the edge magnetic shear. Type II ELMs have been observed over a range of collisionalities ($\nu^* \approx 1$–2), depending on magnetic configuration and input power (or alternatively the plasma β).

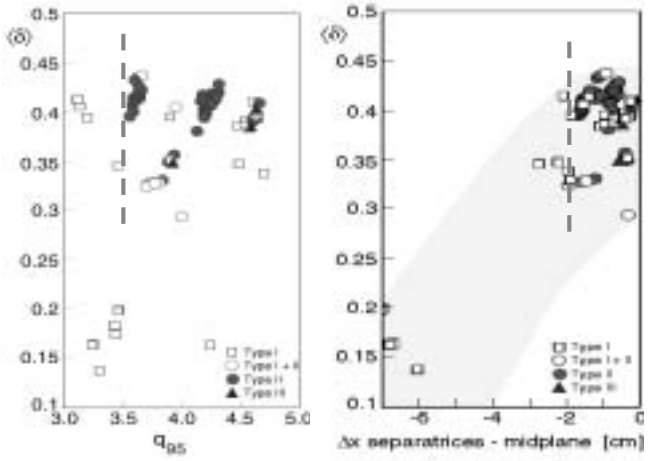

Figure 14: Operational regime of type I, II and III ELMs in both conventional and advanced scenarios in terms of triangularity δ, q_{95} and the separation Δx of the two separatrices in the torus midplane.

5.1.3 Stability of type II ELMs

The fundamental mechanism behind the ELM phenomenon is not known. Several possible explanations have been given. The model presented by Connor for Type I ELMs is used here as a working model. In this model, the type I ELMs are triggered by coupled peeling-ballooning mode MHD instabilities. After an ELM crash, the plasma edge pressure gradient starts recovering until it reaches the high-n ballooning mode boundary. Then, on a slower (resistive) time scale, the edge bootstrap current builds up. The bootstrap current destabilizes the peeling-ballooning mode and causes an ELM crash.

To investigate the significance of the closeness to the double null, two plasmas (#15863 and #15865) are analysed with almost identical density and temperature profiles, triangularity δ=0.42 and safety factor q_{95}=4.2. The only operational difference between the two is that one (#15863) is shifted upwards by a few mm and is thus closer to double null. These shots are chosen because one of them (#15865) has mixed type I and type II ELMs and the other one (#15863) pure type II ELMs.

The double null configuration is found to have a stabilizing effect on the low-n peeling-ballooning modes. The second X-point creates a strong magnetic shear in its vicinity (just like the first X-point). Fig. 15a shows the growth rates for the n=3 mode as a function of the maximum pressure gradient in the pedestal region for the different configurations. The calculation for a pure double null configuration is also shown for comparison. The growth rate decreases as the configuration approaches double null. However, as the mode number increases, the growth rate increases in both plasmas. The higher the mode number, the smaller the pressure gradient required to destabilize it. On the other hand, the mode width decreases with the increasing mode number. Consequently, the higher modes can directly affect only a very narrow part of the plasma.

The double null configuration also has the effect of making the low- to intermediate-n peeling-ballooning mode strongly localized at the edge. The localization is prevalent irrespective of the mode number. Even a small shift of the plasma towards the upper X-point can lead to a significant change in the eigenfunction width. This is shown for an intermediate-n mode (n=8) in Fig. 15b. The vertical position of the type I and type II ELMy plasmas differ only by a few millimetres at the midplane. On the top of the plasma, the type II ELMy plasma is 8 cm closer to the second X-point.

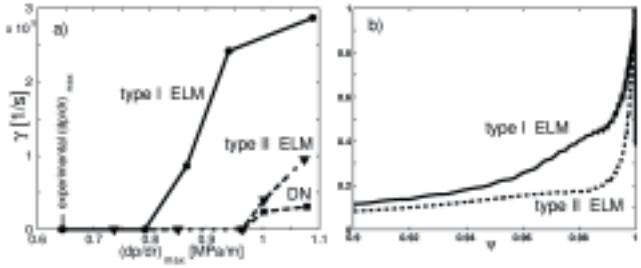

Figure 15: a) The n=3 peeling-ballooning mode growth rate as a function of the edge pressure gradient for plasmas with type I (#15865) ELMs, type II (#15863) ELMs and for a double null configuration. b)The n=8 peeling-ballooning mode radial envelope (the normalised sum of Fourier components of the $\vec{\xi} \cdot \nabla\psi / |\nabla\psi|$) for type I (#15865) and type II (#15863) ELMy plasmas. The pedestal top is at ψ=0.94. Note that both modes are narrower than the pedestal.

5.2 Conclusions

Type II ELMs have recently been observed in a wider range of plasma conditions. In particular, integration of type II ELMs with high performance, 'hybrid' regimes has led to an attractive candidate for operation in a fusion reactor. The understanding of the fundamental mechanisms responsible for type II ELMs has been advanced. The peeling-ballooning mode model is able to explain qualitatively many of the features observed in type II ELM plasmas. The calculated eigenfunction of unstable modes is narrower in such plasmas and is thus correlated with the observed smaller ELM amplitude.

The primary remaining uncertainty with type II ELM operation for a reactor is the present constraint that they are found only at relatively high edge collisionality. Experiments to study increased collisionality are a near-term priority of the ASDEX Upgrade experimental programme.

6 Technical Systems

In 2002, the experiment was in operation for 63 days performing 1304 shots in total. Only 34 days were dedicated to physics, as the commissioning of the new thyristor group 6 required 24 days and 252 shots. Calibration of diagnostics and servicing consumed a further 5 days. There was one unscheduled opening in mid March for repairing a loose microwave shutter which touched the plasma boundary. The summer opening from early August to late September was mainly dedicated to improving the inner heat shield and the inner target of the upper divertor. All new turbo molecular pumps (TMPs) are now in

operation. The hydrogen pumping capability of the cryopump (CP) was improved. With the NI-2 modification towards a more tangential injection angle, beam heating has gained additional potential for modifying the heat and particle flux. The availability of ICRH at high power levels could be increased. For the new ECRH system mounting of the wave-guides has almost reached the access port.
In the following, the improvements of the vacuum vessel, the torus pumping-system and the power supply are described.

Figure 16: Tungsten coated inner heat shield and upper PSL

Vacuum vessel: The new tile design with doubled length, tested in 2001 on two rows only, now covers the whole heat shield. The tiles vary poloidally in length to maintain a small constant gap of a few millimetres between adjacent rows. The tungsten-coated area was further increased. Now the whole heat shield, the upper PSL (Fig. 16) and the inner baffle of the lower divertor are W-covered. To withstand vertical disruptions up to higher plasma currents on the upper divertor, the support structure of its inner target plate was reinforced. Additionally, the water feeding pipes got an electrical break, to avoid halo currents flowing along them. Next year the outer target plate will be hardened too.

Turbo molecular pumping system: The pumping system has now been completely renewed. With the 14 new TMPs the working range with relevant pumping speed is extended up to 10^{-1} mbar. The rotor (Fig. 17) of the new TMPs is very robust against pressure shocks. This is advantageous with respect to the pressure bursts during regeneration of the cryopump. Together with the TMPs, the pressure gauges (Pfeiffer Digiline) were also renewed. The new multi-range gauges could be housed inside the iron shielding of the TMPs. The resulting reduction of the magnetic field no longer required us to switch off the gauges during a plasma discharge. Additionally, for the data transfer of the TMP sensors and actuators a serial bus system was established.

Figure 17: Robust rotor of the new TMPs

Cryo supply and cryopump: Since early 2002 the new liquefier TCF 50 has been in operation and provides the specified liquefaction rate. The operation cycle of the TCF 50 with and without LN2 pre-cooling is now automatically controlled by the status of the gas recovery and the 5000 l LHe storage vessel. During hydrogen-operation of the experiment, the helium (He) cryostat of the CP supply circuit is now routinely pumped down to 0.3 bars (Fig. 18). This reduces the cryopanel temperature from 4.2 K at ambient pressure down to 3.2 K. Consequently the nominal deuterium pumping speed of 100 Nm^3/s is even for hydrogen pumping maintained down to a vessel pressure of 10^{-7} mbar, whereas it would drop at ambient conditions already below 10^{-4} mbar.

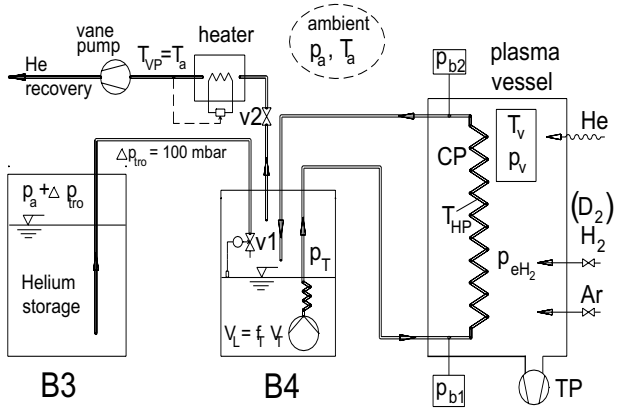

Figure 18: He circuit for extended CP hydrogen operation

Power Supply: The thyristor group No. 6, a modular 135 MVA converter equipped with neutral thyristors, was successfully commissioned. This group now extends the pulse duration for strongly shaped plasmas considerably. The technical design for paralleling the EZ3 and EZ4 variable frequency networks was finalised. Torsion oscillations became a mechanical problem for the couplings of the EZ3 and EZ4 flywheel generator shafts. They are excited during non-quiescent plasma discharges due to the

low natural frequencies of the shaft lines (24 resp. 26 Hz). In order to protect the generators from mechanical damage, torque sensors were installed which initialise "soft landing" of a plasma discharge above the allowable torsion stress. Meanwhile a new concept could be established for damping the torsion oscillations actively via a thyristor fed independent load circuit. Tests with 36 MJ energy storage units, each consisting of four paralleled compact flywheel generators were successfully performed in co-operation with RWE Piller and Rostock University. Numerical simulations have additionally verified this concept. A stepwise extension of the existing networks by 36 MJ units will thus be prepared.
(In collaboration with Universities Karlsruhe and Rostock.)

6.1 Data Acquisition (DAQ)

Development for real-time DAQ systems based on PCI/compactPCI hardware and Solaris and LINUX operating systems has been carried on.
A Thomson scattering DAQ system with 1GHz sampling rate measures background, stray light and a laser reference signal. Between laser shots the data is read out into the Sun's memory where immediate analysis is made to feedback the amplitude of the signals in order to adapt the gain factors of the input channels. Also in real-time, single channels will be evaluated to achieve density and temperature values to be fed back into the plasma performance control algorithms. Final analysis will allow us to discriminate the approximately 50 nsec broad stray light pulses from the fluctuating background and to estimate the involved errors based on the found signal to noise ratio.
An implementation of the MSE diagnostic based on a LINUX PC and fast PCI-ADCs is under development by the XDV group of the Rechenzentrum Garching. Real-time analysis of the measured data will allow feedback with control algorithms for the current profile as soon as the new plasma control system is ready to co-operate with the diagnostics.
The new real-time diagnostics will be time controlled by the new AUG timing system, which is under development by the AUG control group. Dedicated time to digital converters (TDCs) as PCI devices couple the individual diagnostics to this central timing system. A Solaris driver for these TDC devices has been developed to allow exact timing of the multiple Thomson scattering diagnostic computers.

6.2 Remote Data Access and Remote Collaboration Efforts

The philosophy for remote collaboration on ASDEX Upgrade data requires users to apply for a personal account in the AUG computer systems and to become an associated member of the AUG team. A wide palette of tools for remote collaboration is available: internal www services, remote data access, remote computer access, video conferences for broadcast lectures, meetings and remote presentations, etc.. Security is maintained by the IPP's firewall and the usage of secure protocols for data traffic across this border.
MDSplus access to AUG data was implemented by providing an MDSplus interface to the AUG data access library and by setting-up an MDSplus server allowing read access from outside the Garching campus.
A SOLARIS and LINUX version of the AUG data access routines is available for users who want to access AUG data via the AFS global file system. This path, besides read access, also provides write access to the AUG data.
Two seminar rooms at AUG have been equipped with H.323 videoconference systems. In the big seminar room a Tandberg 6000, together with a fully featured audio and multi camera video system provides high quality conferencing facilities. With a single microphone, standard PC loudspeakers and a Tandberg 880 VC system featuring echo cancelling and a remote controllable wide angle camera, the smaller "E4" seminar room is designed for smaller meetings of up to 15 people.

6.3 Neutral Beam Heating

The Neutral Beam Injection system has been reliably operated during the last year, with high availability at the design values: 2.5 MW / beam (D^0), altogether 20 MW, 60 kV on NI-1 and 93 kV on NI-2. NBI heating was requested for most of the Tokamak discharges. Extended pulse length discharges have been heated with 5 MW for 10 s and individual beams have been switched on for up to 8 s. The summer shut-down was used for regular maintenance of the systems and for solving minor technical problems.

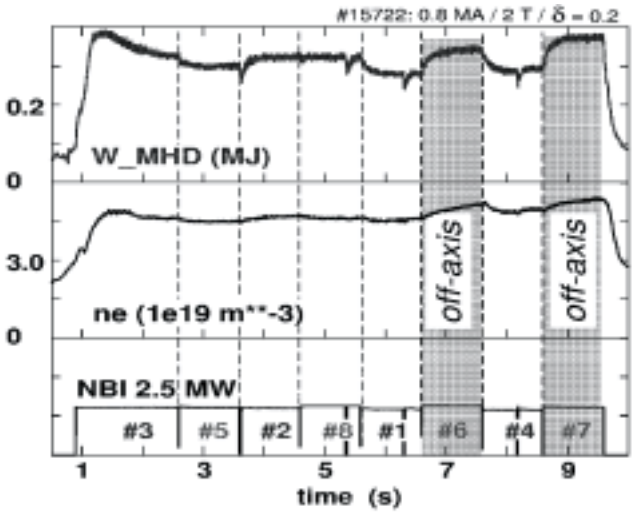

Figure 19: Stored energy, line averaged density and beam power of a shot heated with all eight beams successively.

With the modified geometry of NI-2 (see Annual Report 2001) the flexibility of NBI heating has proven to be significantly increased. Fig. 19 shows a plasma heated successively with all eight beams. Even though the heating power was kept roughly constant (2.4-2.5 MW), the plasma stored energy and the density varied by 30% and 20% respectively. The increase in density during tangential off-axis heating (beams #6 and #7) is essentially due to density peaking as shown in Fig. 20, thus confirming the strong link between local heat and particle fluxes as discussed in detail elsewhere in this report. In addition to this density

profile control capability, central MHD can be controlled by an appropriate choice of beam sources as well: Tangential off-axis beams tend to suppress sawteeth and fishbones, which are both known to trigger neoclassical tearing modes. All these features of the new tangential off-axis beams turned out to be important ingredients for the further development of advanced scenarios like the improved H-mode or high β_N plasmas. However, discharges with internal transport barriers for the ions, require maximum on-axis heating for barrier formation. The different beam geometries have made the NBI system a valuable tool to tailor discharge scenarios according to the various physics needs.

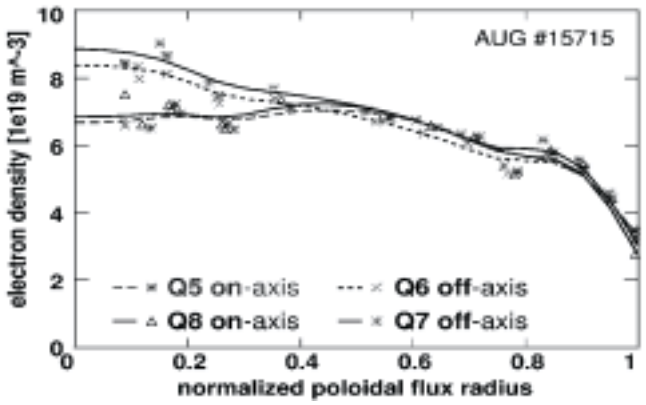

Figure 20: Comparison of n_e profiles with on-axis and off-axis heating in one shot.

6.4 Ion Cyclotron Resonance Heating

High power operation became possible and more reliable since renewed tubes (see last reports) re-established the generator output power to 4 x 2 MW. A heating power of 6 MW could be launched into the plasma for more than 3 seconds. This is the design power value aimed at for the system. The maximum heating power achieved was 7.2 MW, 90 % of the full maximum generator power. A well conditioned system and additionally about 10 conditioning shots with plasma and increasing power were required to achieve these values. This is one of the best technical results ever reached with ICRH systems and unique since it was done in the presence of substantial ELMs. The applied procedures allow reliable ICRH application with powers up to 5 MW and pulse lengths of 5 s routinely launched into the plasma and used for various experimental programs.

The ferrite matching system has been further delayed due to mechanical accuracy problems at the long ferrite loaded striplines. It is expected that this can be solved and that the system can be delivered in the second quarter of 2003.

One antenna pair was equipped with new antenna straps. They have larger radii which require larger fabrication effort but reduce the electric fields in the antenna. remarkably. Test bed measurements and first experimental experience indicate an improved voltage strength.

The RF probe for antenna breakdown studies was installed and operated near the plasma boundary. The interesting results of these experiments will be reported in 2003 in a doctoral thesis.

6.5 Electron Cyclotron Resonance Heating

The existing ECRH system at f = 140 GHz with an installed power of 4 x 0.5 MW for 2 s was routinely used in the experiments. It is designed to provide very localised heating or current drive even under conditions of off-axis deposition by poloidal beam deflection. This feature was experimentally confirmed studying the transient temperature response following power switch-on or switch-off, or modulated power deposition.

The new system under construction (see Fig. 21) will provide 4 x 1 MW for 10 s at several frequencies in the range 105 to 140 GHz. The first two gyrotrons will be a 2-frequency gyrotron, using a single disk diamond window resonant at both frequencies, and a step tuneable gyrotron which will be equipped with a broadband Brewster angle window or a narrowband, but tuneable, double disk window. These gyrotrons will work with collector voltage depression leading not only to an enhanced efficiency close to 50%, but also to a much more efficient use of the existing 70 kV power supplies. Both gyrotrons are expected to arrive during 2003.

A broadband matching optics unit (MOU) feeds the power into the transmission lines of 87 mm i.d. waveguides with corrugated walls designed for broadband transmission. In order to generate different frequencies the gyrotron has to be operated at different cavity modes. This means that with a fixed internal quasi optical mode converter, the output beam leaves the gyrotron at a slightly different direction. Therefore the MOU comprises a different set of 2 mirrors for each frequency to redirect the beam onto the transmission line axis.

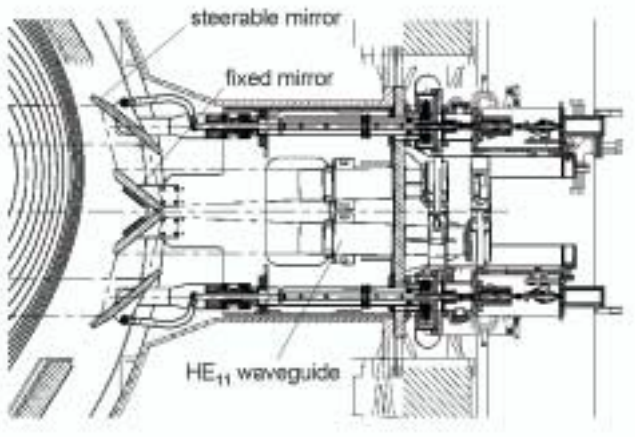

Figure 21: Launcher concept for the new ECRH system. The beam is launched from an open-ended waveguide via a fixed focusing mirror and a fast steerable plane mirror.

At the torus we will have a tuneable double disk window since this can transmit an arbitrary polarisation. The launcher mirrors are designed for a fast feedback controlled poloidal beam steering which allows controlled power deposition on a wanted flux surface even under conditions of a changing magnetic field distribution. The design value

for this mirror scan is 10° / 100 ms. Toroidal beam steering will be slow. The uncooled mirrors will be made of graphite with a conducting copper layer to minimise disruption forces. A drawing of the launcher set-up is shown in Fig. 21. By poloidal beam steering nearly every point in a cross-section can be heated. The steerable mirror assembly can be rotated such that the mirror faces the vacuum chamber wall when plasma pulses without ECRH are performed.

7 Core Plasma Physics

7.1 Stationary advanced scenarios at ASDEX Upgrade

Recent experiments have achieved advanced scenarios with high β_N (>3) and confinement enhancement over ITER98(y,2) scaling, H^{H98y2} = 1.1-1.5, for several seconds in plasmas approaching stationary conditions. In ELMy H-modes, with low shear in the centre and q_0 close to 1, the core confinement and stability is improved due to the absence of sawteeth. Fishbones are the dominant MHD activity in these advanced discharges maintaining q on axis near 1. This improved H-mode can be obtained with q_{95} in the range 3.3-4.5. Off axis heating with tangential NBI sources leads to the creation and sustainment of the required q-profile, especially at the lowest values of q_{95} (Fig. 22). Here, the use of the off axis NBI injection has widened the operation space of the improved H-modes (low q_{95}, and more peaked density profiles at high density).

The off axis heating leads to a strong peaking of the density profile, which is beneficial in obtaining improved confinement. However, the off axis heating leads to a strong peaking of the density profile and impurity accumulation in the core. This can be explained due to the reduction of the turbulent transport in the core as a result of the reduced central heating (stiff temperature profiles). Too strong density peaking and impurity accumulation can be avoided by adding central heating from ICRH or ECRH, providing an additional tool to control this scenario.

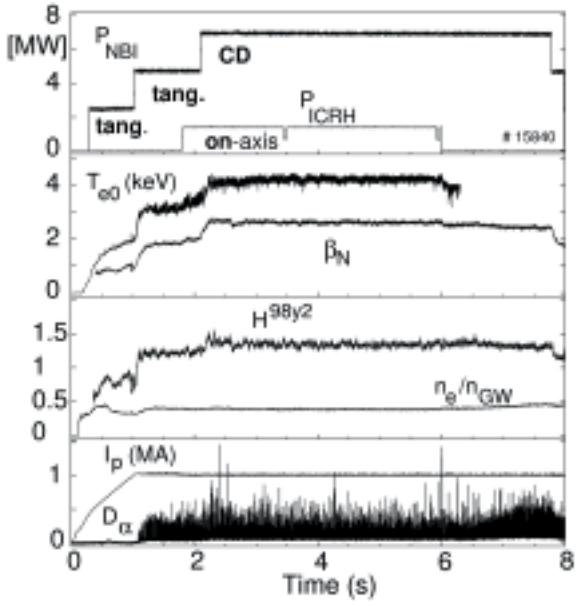

Figure 22: Typical improved H-mode scenario, $\delta = 0.17, q_{95} = 3.3$.

High density, up to 80%-90% of the Greenwald density limit is possible using a combination of NBI and gas fuelling in a highly shaped plasma configuration with δ = 0.43. Even at these densities the confinement is significantly improved over the ITER reference scenario, while β_N reaches values of 3.5 in steady state.

7.2 Density Peaking

In the years 2000 and 2001, a strong relation between the shape of the density profile and the heat flux profile has been observed on ASDEX Upgrade. In 2002, these studies could be extended to purely ICR heated plasmas, comparing on- and off-axis heating. Fig. 23 summarises the effects on the density profile: pure NBI heating leads to the development of peaked density profiles by slow spontaneous density peaking. Substituting the NBI with central ICRH and keeping all other control parameters the same, the density profile is almost flat.

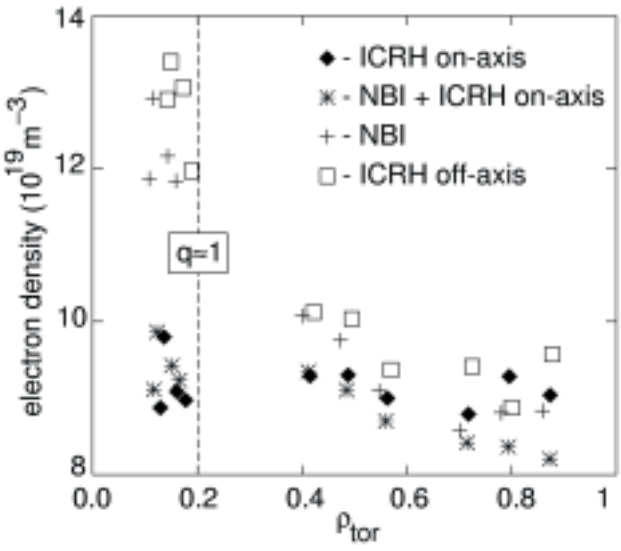

Figure 23: Electron density profiles for different heating scenarios (zero suppressed): $I_p = 1MA, q_{95} \approx 4.3, \delta = 0.32$.

This is not only due to the missing fuelling of the NBI, since the case with 50% of NBI and 50% of central ICRH also leads to flat density profiles. In contrast, off-axis ICRH again leads to peaked density profiles. A similar, though less pronounced behaviour is observed when comparing on- and off-axis NBI. Such behaviour can be understood by a relation between particle and energy transport. The basic observation is, that due to the stiffness of the temperature profiles the heat flux profile determines the heat conductivity profile or in other words a more central heat deposition increases the central turbulence level. If particle transport is related to these turbulences, it should be increased as well and the density profiles will flatten. The first attempts to model the data showed good agreement using $D \approx 0.12 \cdot \chi$ and $v_{in} \approx 1.5 \cdot v_{Ware}$. More recently it turned out, that the neoclassical ion conductivity $\chi_{i,neo}$ contributes significantly to the energy transport for these well confined high density H-modes. Since $\chi_{i,neo}$ is not due to turbulence it makes sense to define an effective

turbulent $\chi_{eff}^{turb} = 0.5(\chi_e + \chi_i - \chi_{i,neo})$. Then one obtains $D \approx 0.2 \cdot \chi_{eff}^{turb}$ using only the Ware pinch. This refined model also holds for scenarios where $\chi_{i,neo}$ is negligible.

As already shown in 2001, the experiments with peaked density profiles also revealed serious drawbacks of peaked density profiles, which are an early onset of neoclassical tearing modes due to a stronger weight of the density gradient length for the bootstrap current and the tendency to accumulate heavy impurities. Further studies in 2002, using Silicon laser-blow-off, showed that central heating not only flattens the main ion density profile but also reduces impurity accumulation, mainly due to a reduced neoclassical pinch (which depends on the main ion density peaking) and additionally due to an increase of the impurity ion diffusivity.

7.3 Core MHD and its modification by local current drive

Neoclassical tearing modes were a major concern theoretically, as well as experimentally during last year's programme. During power ramp down experiments the marginal β_p^{marg} for the (3,2) NTM, as well as for the first time for the (2,1) NTM has been analysed. This scheme is of special importance, as the marginal β_p^{marg} is independent from the conditions of the seeding process by a seed island. For both the (3,2) and the (2,1) NTM, a linear dependence of β_p^{marg} on the poloidal ion gyro radius ρ_{pi}^* has been measured (see Fig. 24 for the (3,2) NTM). The collisionality dependence for the (2,1) NTM is much more pronounced. The importance of a more refined analysis for the driving bootstrap current has been realized and included (separation between $n_e dT_e / dr$ and $T_e dn_e / dr$).

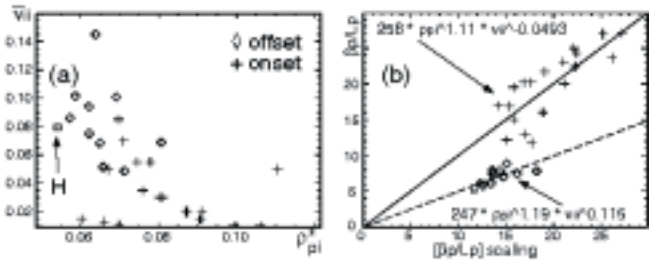

Figure 24: Scaling of the onset β_p^{onset} (a) and the marginal β_p^{marg} at the stabilisation (b) during the power rampdown.

Besides this analysis of NTM behaviour, efforts have been put into actively controlling the stability of NTMs. Recently a complete stabilisation of the (2,1) NTM with local current drive by ECCD has been successfully shown. A similar scheme to the (3,2) NTM stabilisation at reduced background NBI heating power has been used. In the case of the (3,2) NTM with increased NBI power, β_N could be raised significantly above the onset value without a reappearance of the mode while the confinement recovers.

The externally driven current has not only been used for the direct stabilisation of NTMs by replacing the reduced bootstrap current within the island, but also by driving current outside the island's separatrix. This external current could trigger an ideal (4,3) mode (see Fig. 25) leading to a forced FIR-NTM phase. The FIR-NTM regime was reported last year. The additional mode leads to an averaged reduced (3,2) amplitude and an improvement in confinement.

Another approach has been used by changing the size of the seed islands for NTMs. Local co- and counter current drive as well as heating, again by the ECRH system, in the vicinity of the q=1 surface has been used to modify the size and the repetition rate of sawteeth.

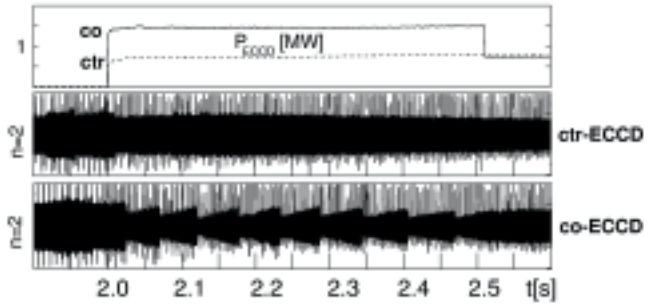

Figure 25: At 10 MW constant NBI power, co- or counter ECCD is used to lower or increase the magnetic shear at the q=4/3 surface. In the co-ECCD case a clear transition to the FIR-NTM regime can be observed.

It can be seen that co-ECCD leads to an increase in the sawtooth period when deposited just outside the sawtooth inversion radius. With 0.8 MW of ECRH/ECCD and a background heating of 5 MW NBI, it is possible to completely stabilise the sawteeth. For central deposition, a reduction in sawtooth period occurs. Similar behaviour is observed with pure ECRH, which is consistent with a local decrease of resistivity due to ECRH that also generates co-current. Conversely, for ctr-ECCD, central deposition stabilises the sawteeth, clearly demonstrating the importance of the local current generated by ECCD. These findings (summarized in Fig. 26) are consistent with the hypothesis that a decrease in current density gradient at the q=1 surface tends to stabilise sawteeth. Note that, contrary to stabilisation of sawteeth by fast particles, the amplitude does not increase here. This method has already been used to create sawtooth-free discharges for impurity transport investigations; future studies will also study the effect of sawtooth tailoring on NTM onset by affecting the seed island size.

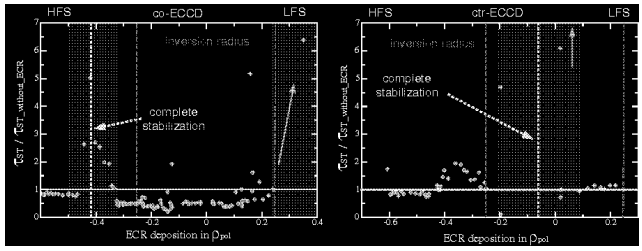

Figure 26: Sawtooth repetition period as a function of the ECCD deposition(negative values of rho indicate deposition on the HFS). Complete stabilisation can be achieved by co-ECCD outside the inversion radius or central ctr-ECCD.

7.4 Electron heat transport with ECRH

The stiff behaviour of temperature profiles in conventional scenarios is believed to be caused by anomalous transport driven by turbulence with a threshold in $\nabla T/T$ (see previous annual reports). This assumption was confirmed in 2002 by experiments where we varied the electron heat flux in the confinement region by one order of magnitude while keeping the heat flux at the plasma edge constant. For this purpose, we deposited the ECRH power at two radial ($\rho \approx 0.35$ and $\rho \approx 0.65$) locations with respective intensities P_{ECH1} and P_{ECH2} varied, while keeping $P_{ECH1} + P_{ECH2}$ constant at about 1.3 MW. The discharges were run in $q_{95} = 4.4$ and low density to reduce the electron-ion energy transfer and provide good conditions to study the electron heat transport. In addition, a ±10% partial power modulation allows us to analyse transient transport χ_e^{HP} . The steady-state temperature profiles indeed show that a variation of ∇T_e and $\nabla T_e / T_e$ can be achieved. The results of power balance and transient transport ρ ≈ 0.5 are shown in Fig. 27. The lines are deduced from a model based on the existence of a critical $\nabla T_e / T_e$. The same model included in transport simulations yields the lines drawn in Fig. 27, which agree very well with the experimental data over the whole radius. The same type of experiments carried out at $q_{95} = 9.9$ strongly suggest a q dependence of electron heat transport. Further analysis suggests that the TEM driven turbulence may be responsible for the anomalous electron heat transport in theses L-Mode discharges at low density with high electron temperature.

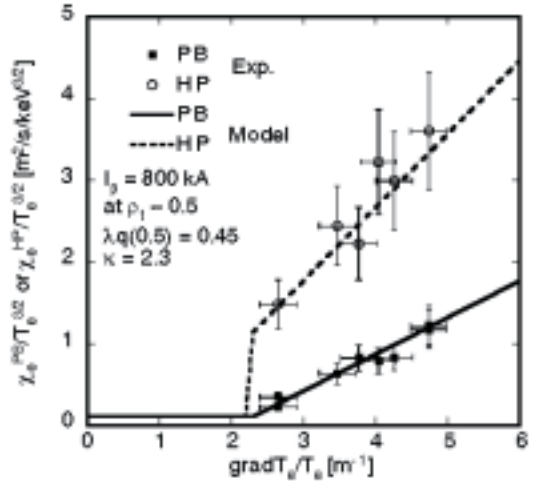

Figure 27: Results from power balance and heat pulse analysis at ρ = 0.5. The lines are given by the model.

7.5 Edge profile constraints

Radial profiles of the edge electron temperature and density were measured with the high resolution edge Thomson scattering system. The raw Thomson data is regularised with a Bayesian filer of 2 mm spatial width and fitted with modified tanh functions to enable the calculation of gradients. A close coupling of the temperature and density profile gradient lengths, $\eta_e = (\nabla T_e / T_e) / (\nabla n_e / n_e) \approx 2$ is observed over the edge transport barrier region, for $T_e > 10$ eV to the pedestal top for a wide range of discharge parameters. The observed resilience of the relative profile shapes indicates the influence of drift wave turbulence on the profiles over the edge transport barrier region.

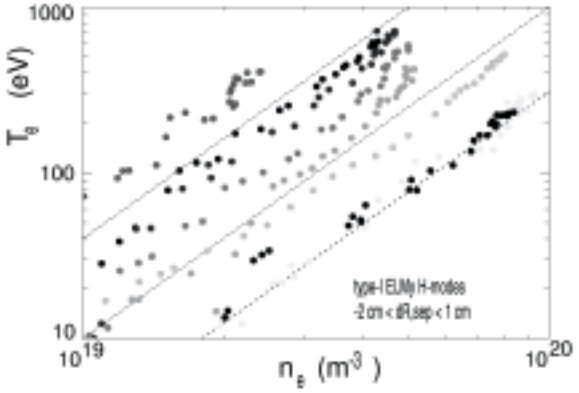

Figure 28: T_e vs. n_e for 8 discharges. The data points cover the radial range –2 < dRsep < 1 cm mapped to the outer midplane. The straight lines indicate the slope corresponding to $\eta_e = 2$ in the logarithmic plot.

7.6 Edge rotation velocity profiles from Doppler reflectometry

One of the topics of great interest in the study of the H-mode edge pedestal is the behaviour of the E x B velocity profile and the rate of shearing in the velocity. Using Doppler reflectometer channels with tilted O and X-mode launch antennas in the 50 to 75GHz microwave band, new experimental measurements of the edge perpendicular (i.e. close to poloidal) velocity $v_\perp$ profile evolution have been obtained with high temporal and radial resolution during the L-mode to H-mode transition. With co-injected NBI, the Doppler measured $v_\perp$ matches the plasma fluid velocity (from Charge Exchange Recombination Spectroscopy) in the core region, however it dramatically reverses sign across the H-mode pedestal region with a peak coinciding with the steep plasma pressure gradient. With counter-injected NBI (i.e. reversed B_t and I_p) the $v_\perp$ profile also reverses across the pedestal confirming that the E x B velocity is dominated by the diamagnetic drift velocity component in this region. Temporal measurements show the magnitude of the E x B peak increasing as the H-mode forms, i.e. the shearing in the edge velocity rises in concert with the strength of the H-mode barrier.

7.7 Type III ELMs

The availability of simultaneous low field side (LFS) and high field side (HFS) density profile measurements using reflectometry, with high temporal and spatial resolution, is unique to ASDEX Upgrade. This diagnostic capability has been extensively exploited in the study of ELM dynamics, especially for characterizing and contrasting the low-field and high-field side ELM behaviour. The reflectometer measurements reveal that particle losses (relative to the total pedestal particle content) and the ELM affected region are smaller on the HFS, and that there is a substantial delay

in the onset of the ELM perturbation in the density profile between the HFS and LFS. It was also found that for low density type-III ELMs the particle losses are purely convective, compared to type-I ELMs where both convective and conductive losses are seen. Notably, at low plasma triangularity, the behaviour of type-I and type-III ELMs (i.e. the occurrence of the ELM, the pedestal crash, and the outward movement of the edge profile) are very similar. For type-I ELMs preliminary measurements indicate that the perturbation onset time delay between HFS and LFS is commensurate with the ion sound speed, which is suggestive of a ballooning character for the ELM. Further measurements are in-hand for type-III ELMs, where the HFS to LFS connection length was changed by varying q_{95}. The presence, or not, of a similar time delay will help to establish whether type-III ELMs are also resistive ballooning in character.

7.8 ELM frequency control by continuous small pellet injection

Pellet refuelling experiments demonstrated that pellets reliably trigger ELMs when injected during type-I ELMy H-mode phases.

A major step of this investigation was to find out the minimum pellet mass required for reliable ELM triggering. Results of this mass scan are presented in Fig.29, displaying data for prompt and total pellet induced energy losses. The reduction of total energy losses with pellet mass is evident. In the case of a big pellet, a burst of ELMs is observed during the post-pellet density decay phase. It consists the prompt pellet triggered ELM and several ELMs longer and stronger than corresponding intrinsic ELMs. They result in a transient reduction of the plasma energy of a total amount,

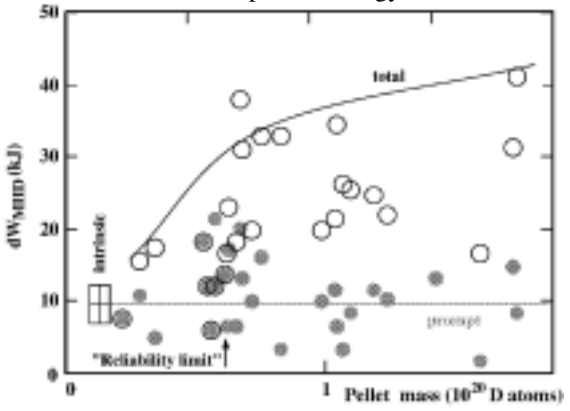

Figure 29: Pellet mass scan data. Total (black circles) and prompt (grey dots) pellet induced energy losses versus applied pellet mass. The squared box represents the standard deviation of intrinsic ELMs induced energy and particle losses, the solid arrow the pellet size chosen for controlling sequences.

eventually significantly surpassing the instant loss. Consequently, total pellet induced energy losses exceeding the value of the prompt losses must be avoided by reducing the pellet mass. It has also become clear that the optimal pellet size may be below the minimum available.

The belief that still smaller pellets are suitable for ELM triggering and thus provide further relief on the fuelling flux constraint is feasible. This observation was supported by the fact that ELM obviously starts at less than 0.2 ms after the onset of pellet ablation. At this moment, pellets have just crossed the pedestal region and smaller ones lost there only about ($\approx 10^{19} D$) by ablation. At its best, pellet induced energy losses equal the energy amount expelled during an intrinsic ELM, and the pellet mass almost equals plasma particle losses due to an intrinsic ELM. This is indicated by the square in the plot, representing a dataset derived for corresponding intrinsic ELMs. The solid arrow indicates the typical pellet size, which was applied in the ELM control sequences.

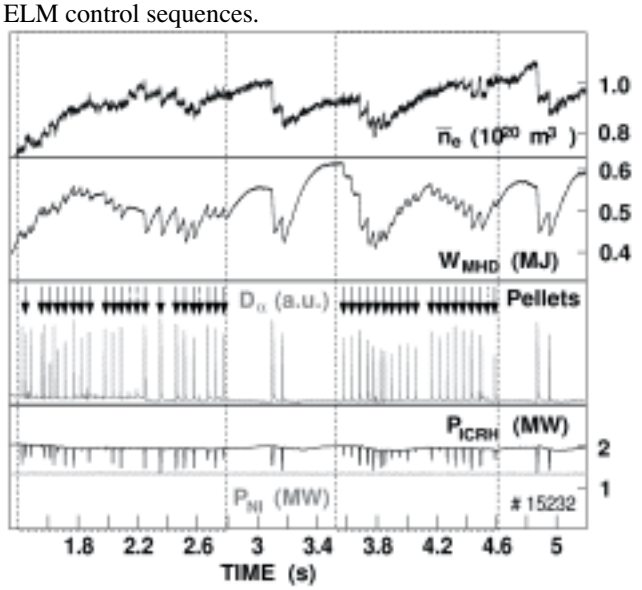

Figure 30: Periods selected for pellet forced ELM control are marked by vertical dashed lines.

In the next step we concentrated on optimising the pellet injection system for the desired ELM control. In order to limit the pellet induced density rise, imposed by the minimum pellet size technically required to deliver a reliable sequence, an upper limit of about 20 Hz had to be set for the pellet repetition rate. Suitable injection conditions were established so that long periods were obtained, where essentially every pellet triggered an ELM and no ELMs occurred without pellet trigger. Moreover, it was demonstrated in discharge #15232 shown in Fig. 30 that pellet forced ELM control can be, if desired, repeatedly switched on and off at any time. Control sequences are marked in Fig. 30 by vertical dashed lines; pellet launch detection (corrected by the pellet flight time) is indicated by small solid arrows. Pellet triggered ELMs showed (especially after about 300 ms when the control approach establishes a regular self-consistent situation) a reduction in maximum particle and energy losses of at least a factor of 2 with respect to their intrinsic counterparts.

It turned out that higher forces acting on the pellets in the looping shaped track resulted in somewhat enhanced transfer mass losses, providing the additional advantage of further pellet size reduction. Also, significant reduction of this delay time can be obtained. Improvements of the hardware during the 2002 shutdown now allow us to operate at pellet velocities up to 1000 m/s and >20 Hz instead of 600 m/s as before.

7.9 ELM-free stationary H-mode

Edge Localised Modes (ELMs) can present a significant peak power load to the divertor and it is not yet clear whether large type I ELMs can be tolerated in ITER or a reactor. Therefore stationary regimes with small or no ELMs are intensively studied.

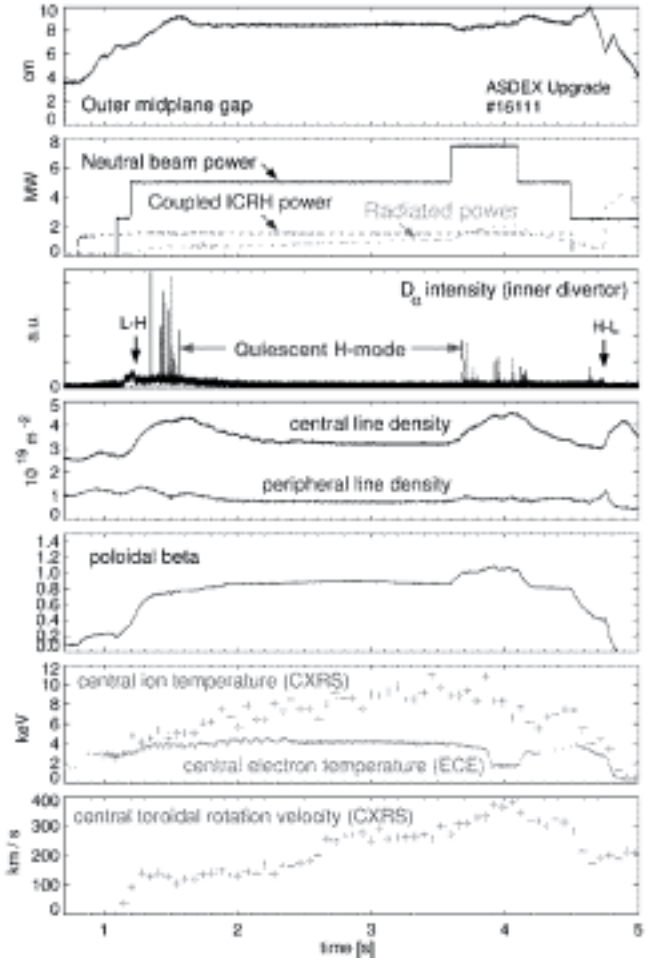

Figure 31: Time traces of a stationary ELM-free H-mode discharge.

Recently, the ``Quiescent H-mode'' (QH) regime has been successfully obtained, the second tokamak after DIII-D where it had been originally discovered. This type of stationary ELM-free plasmas occurs with neutral beam injection opposite to the plasma current (counter-injection) and sufficiently large gap between the plasma boundary and limiting surfaces in the plasma chamber. The divertor strike points are positioned for good pumping with cryopump on and no external gas puff is applied after the start-up phase of the discharge to keep the plasma density as low as possible. The resulting discharge behaviour is demonstrated by the time traces in Fig. 31. After ICRH and NBI heating power is applied and H-mode is reached, a brief ELMy phase occurs. As soon as a configuration with high wall clearance is reached, the ELMs disappear. In this QH phase, the central and peripheral line densities drop to stationary values below those in the ELMy phase. Only a moderate increase of the radiated power is observed. The β_p increases by about 10% compared to the ELMy H-mode phase along with a corresponding increase of the edge pedestal pressure.

The central and pedestal ion temperatures are very high, reaching about 9 keV and 1.2 keV, respectively. Neutral particle analyser measurements show that the density of fast particles in the plasma periphery in stationary QH-mode is well above that of ELMy phases.

The quiescent H-mode regime is accompanied by pronounced MHD behaviour. There are no sawteeth, but strong m=1,n=1 fishbone activity. In addition, the ``Edge Harmonic Oscillation'' (EHO) is seen in magnetic, ECE, reflectometry and Soft X-ray measurements with a fundamental in the frequency range of 10 ... 15 kHz and 11 harmonics clearly recognisable. A modulation of the outer divertor D_α signal with the EHO frequency is observed, indicating that the EHO is correlated with particle and or heat losses across the edge barrier region. A new finding is a magnetic oscillation in the frequency range above 350 kHz, dubbed the ``High Frequency Oscillation'' (HFO, Fig. 32), which is amplitude modulated in phase with the EHO. The figure insert shows one EHO cycle. Often the HFO occurs in bursts , during which the HFO frequency drops by a few 10 kHz. The bursts are correlated with oscillations of the divertor D_α signal, such that the maximum HFO amplitude corresponds to the end of the rise and the begin of the decay phase of the D_α intensity. This behaviour might suggest a fishbone-like mechanism as the origin of the HFO; however, the nature of the observed MHD mode is not known as yet.

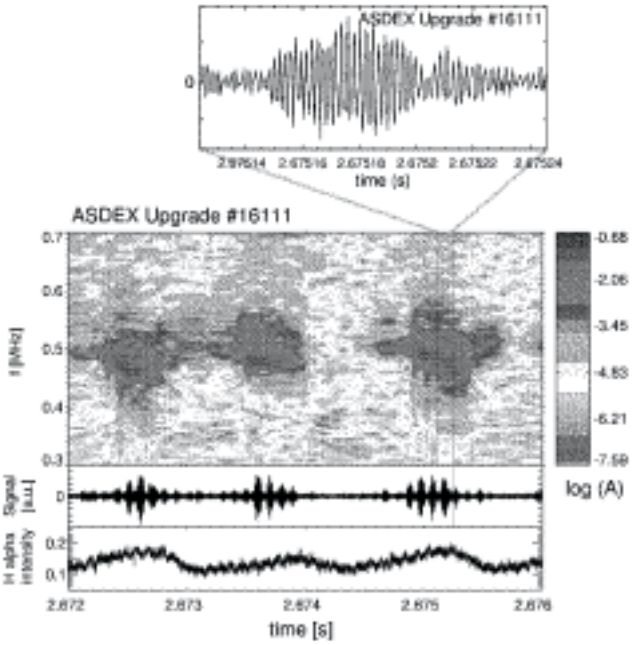

Figure 32: The spectrogram shows the ``High frequency oscillation'' which is amplitude-modulated with the EHO frequency (insert shows one EHO cycle) and occurs in bursts, which are correlated with the rise and fall of the divertor D_α signal.

7.10 Hydrocarbons

During the last year, a new improved spectroscopic system was established in the divertor. With this system the dependence of photon efficiency of CD molecules on the local plasma parameter could be measured. Puffing a constant flux of CD_4 molecules during a discharge and

simultaneously moving the strike point position, allows us to investigate the D/XB coefficients in a single discharge for different plasma conditions. Both L- and H-mode scenarios were used.
In order to analyse the contribution of higher hydrocarbons to the CD band emission and a possible isotope effect, C_2H_6 and CH_4 puffs were also done.

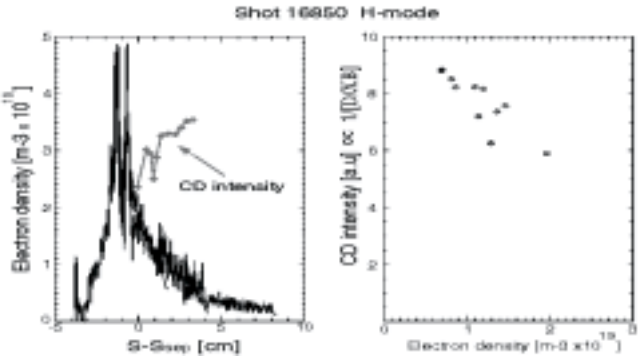

Figure 33: Reconstructed density profile during a strike point scan in the outer divertor and the CD molecular band emission profile as a function of the distance from the separatrix and the CD intensity vs. the electron density.

During the discharge the puffed particles flux was kept constant, therefore the decrease of the CD intensity indicates an increase of the D/XB coefficient as a function of the local electron density (see Fig. 33).

7.11 On the toroidal asymmetry of the forces on the vessel after disruption

Large radial vessel displacements (up to 6 mm) have been observed up to now, only on JET. The toroidally asymmetric vessel movement is accompanied by an n=1 tilt of the whole plasma seen in the magnetic reconstruction of the plasma position. This peculiarity and its relevance in the design of the ITER vessel has motivated a careful analysis of the mechanical forces on ASDEX Upgrade.
It is equipped with several diagnostics, which indirectly measure the mechanical forces on different components. The vacuum vessel is suspended by eight rods fixed to an external supporting structure. The rods are 45° apart and each of the rods is equipped with a strain gauge. The vessel is also equipped with displacement gauges, which measure its radial and vertical movement at the equatorial plane at four toroidal positions, 90° apart.
The amplitude of the forces measured at the rods can reach values above 300 kN at plasma currents of 0.8-1 MA; in slow VDEs downwards, with growth rates of the order of 100 ms, the negative force reached 500 kN. The max and min forces do not simply scale with I_p^2 or $I_p \cdot B_t$; as a *rule of thumb*, we derive that $|F_z| =< 250$ kN/(MA Tesla). The toroidal asymmetries of the vertical forces, as measured at the rods, are typically less than 20 % and on average about 10 %. The vertical displacement of the vessel, measured at the vessel mid plane has a time behaviour similar to that measured by the strain gauges at the suspension rods. The maximum vertical displacement is about 0.7 mm, in both positive and negative vertical directions. The largest net radial displacements observed in the shot period analysed are of the order of 0.2 mm and therefore significantly small.
The vessel was intentionally laterally displaced by applying a known force to establish the correspondence between applied force and radial displacement; this was found to be approximately linear and amounted to 0.014 mm/kN for a statically applied force. The largest radial displacement observed during disruptions is of 0.24 mm and corresponds to a statically applied radial force of 17 kN; but since the forces during disruptions act for a fraction of the oscillation period of the vessel, the shortly applied force could be up to one order of magnitude larger. It is interesting to point out that the discharges with the largest radial displacement are disruptions following VDE as in JET.
The relation between asymmetries of halo currents and vessel displacements has not yet been clarified.

8 SCRAPE-OFF LAYER AND DIVERTOR PHYSICS

8.1 Filamentary transport in the scrape-off layer wing

Density profiles in H-mode discharges always show a wing in the cold SOL which cannot be explained by transport due to small scale electrostatic turbulence. A possible explanation is the occurrence of filamentary transport driven by ballooning/peeling or drift mode instabilities in the edge plasma on a centimetre cross field scale length. In fact, burst-like transport events were clearly observed in the far scrape-off layer and even in the limiter shadow by Langmuir probes. Such events were clearly seen during ELMs as expected, but also in-between ELMs, especially during the last few milliseconds before the next ELM. The latter frequently seemed to be correlated with ELM precursors observed simultaneously on several other edge diagnostics. Fig. 34 shows such events during and in-between ELMs as measured by a multipin Langmuir probe deep in the shadow of the low field side poloidal limiters. Though such transient events have been identified in various discharge scenarios, a statistical analysis and an assessment of their contribution to the total radial fluxes has not yet been done.
It has been argued that some of these events, if large enough, should also be detectable with the high-resolution edge Thomson laser scattering diagnostic and might be partly responsible for the large scatter seen on edge plasma profiles from this diagnostic. However, distinction from trivial noise peaks turned out to be difficult. Meanwhile, an improved version of the Vertical Thomson Scattering (VTS), based on a new fast digitizer system has become operational. It allows us to investigate fast events with a time delay of only 500 ns between the six consecutive laser pulses and with significantly increased signal to noise ratio. As a consequence, the number of apparent 'events' has reduced drastically, but still, a few physically relevant pulses per discharge could be clearly identified by spatial and temporal correlation analysis between neighbouring channels. Again, an assessment of the contribution of these large events to radial fluxes still requires some assumptions on the event statistics and the determination of the efficiency of the applied event detection algorithm.

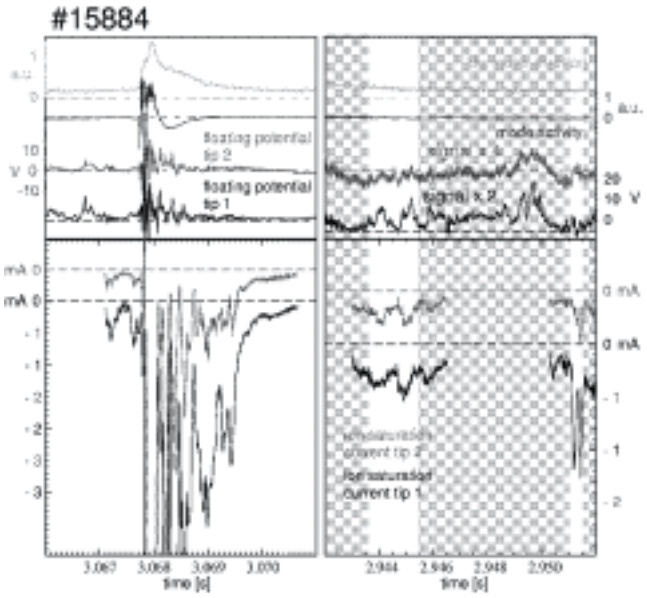

Figure 34: Transport events observed by a Langmuir probe in the shadow of a low field side poloidal limiter (4cm behind the limiter front). Left hand side: floating potential and current measurement during an ELM; right hand side: transport events in-between ELMs.

8.2 Investigation of carbon sources in the main chamber

30 new lines of sight have been installed in the vacuum vessel for spectroscopic measurements of the impurity influx from the outer guard limiters. In conjunction with the lines of sight that span over the inner heat shield it is now possible to make a quantitative comparison of impurity fluxes from inner heat shield and outer guard limiters.

Detailed analysis was done for H- and L-mode discharges. The line-of-sight integrated measurements were spatially resolved by analysing the B-field splitting (Zeeman, Pasch-Back) of the spectral lines supported by camera pictures in the light of carbon. The inner heat shield showed erosion that accounted for about 50-90% of the main chamber influx, depending on the plasma position. The number of ions per square meter entering the plasma from the outer limiter were about 3 times larger than from the heat shield, but the about 8 times larger area of the heat shield makes the heat shield the dominant source for the total carbon influx. The other part of the influx from the low field side is entering the plasma in-between the guard limiters. The origin of that part cannot be determined. If this contribution is said to be eroded from the closest carbon source, i.e. the limiters, the limiter source doubles and reaches the mentioned 10-50%.

Impurity transport from the divertor might also contribute to the carbon influx at the lower part of the heat shield, as the carbon emission along the heat shield shows a maximum there. However, when the plasma is moved toward the heat shield the influx at the heat shield is increasing considerably. This demonstrates, that a big part of the in flowing carbon at the heat shield gets eroded from it. 85% of the heat shield consists of tungsten coated tiles, but deposited carbon was found to be abundant on the surface of these tiles. This carbon is eroded and makes the heat shield an important impurity source.

8.3 Plasma position determination by reflectometry

Microwave reflectometry has been proposed as an alternative/back-up approach to the usual magnetic systems in long pulse operation on ITER for plasma position and shape control. In preparation of such applications, proof of principle experiments have been made on ASDEX Upgrade using existing low and high field side reflectometer channels. The position of equi-density lines near to and inside the separatrix has been determined with high temporal and spatial resolution. Because of rapid parallel transport, the density can be assumed to be constant on flux surfaces in this hot edge region. Ohmic (L-mode) density limit shots as well as ELMy H-mode discharges with strong density variations and pre-programmed plasma displacements have been investigated.

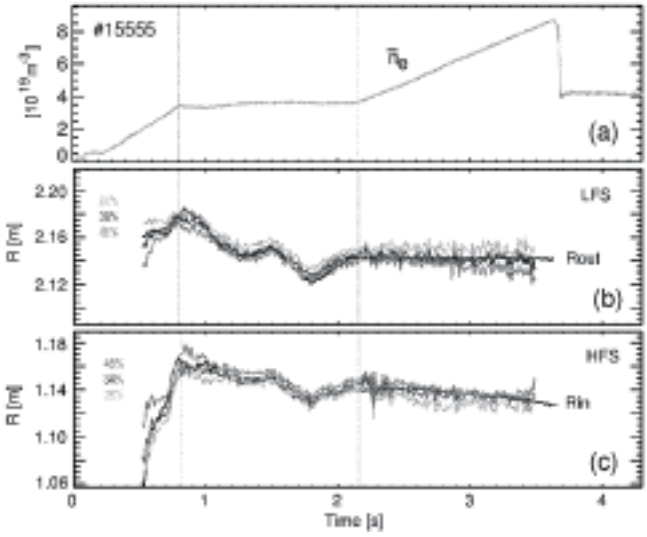

Figure 35: Temporal evolution of: (a) line average density from interferometry; (b) position of the magnetic separatrix at the low field side (Rout) inferred from the magnetic diagnostics and position of layers with constant fractions of the line averaged density from reflectometry; (c) same as (b), but data taken from high field side (Rin). The best match between the data from reflectometry and from the magnetics is obtained for a 38% scaling on the LFS and for 34% on the HFS .

In order to derive a magnetic separatrix position from these density contours in case of strong density variations, a scaling law of the separatrix density with line averaged density, measured in parallel, has to be assumed or determined experimentally. Comparing the temporal evolution of the high and low field side positions of constant density layers with the magnetically determined separatrix position at both sides reveals an increase of the separatrix density that scales approximately linearly with the increase of the line average density. In turn, tracking of normalized, instead of absolute densities, should provide a good measure for the local separatrix position. In fact, following this prescription, plasma displacements can be followed with sufficient accuracy in discharge phases with strongly varying line averaged density as shown in Fig. 35 for a density limit shot #15555. Different fractions of the line averaged density were used to find the scaling factor

that leads to agreement between the estimation of the separatrix position from reflectometry and the magnetic data. The best match found occurs around 38% where the total verified RMS deviation was ~ 0.6 cm.
Good results were also obtained for standard H-Mode shots, with type I ELMs, e.g. shot #14829. In this case the scaling factor that leads to the best agreement with the position of the magnetic separatrix at low field (Rout) and high field (Rin) sides, inferred from the magnetic diagnostics, is 42% with a total RMS deviation of 0.85 cm.

8.4 Interaction of radio frequency electric fields with the scrape-off layer plasma

A radio frequency (RF) probe, which was developed for studies of high voltage breakdown phenomena in ion cyclotron RF antennas was used also to study the mutual influence of the scrape-off layer plasma with the radio frequency field. The probe is an open end of the coaxial resonator with a high RF voltage (10-50 kV). The probe has been operated on the mid plane manipulator of ASDEX Upgrade at a radial position about 3.5 cm behind the ICRF antenna limiter. Measurements of the RF voltage, phase between the RF voltage and current are possible as well as the measurements of the DC current flowing between the coaxial RF conductors. The measurements during AUG discharges with H-mode and type-I ELMs indicate a drastic increase of the RF power coupled to the plasma during type I ELMs and ELM precursors. Furthermore, measurements of the RF power transmission by a pick-up RF probe and the measurement of the DC (rectified) current indicate that a large fraction of the power is dissipated locally in the region of the probe head. The increase of the coupled power is associated with an increase of the plasma density during type I ELMs and ELM-like events. The transient signal of the coupled power as well as the rectified current signal have a burst structure during ELMs. The RF probe was used as a monitor of the plasma density in the limiter shadow which is sensitive enough to reliably resolve the precursors of type I ELMs and minor intermittent events. Work on a detailed description of the mutual influence of the intermittent SOL plasma and the RF power is in progress.

8.5 Modelling of tungsten migration

The investigations on the use of tungsten as a plasma facing material at the central column of ASDEX Upgrade (see Sect. 2) have been supplemented by modelling computations for the scrape-off layer transport of tungsten using the 2D Monte-Carlo impurity transport code DIVIMP. The required background plasmas were provided by B2/EIRENE. Since the area of direct interaction of plasma ions and walls in the code is restricted to the divertor, DIVIMP had to be extended to accommodate the tungsten source at the central column during the flat-top phase of the discharge. This was done by extrapolating the plasma parameters from the computational mesh to the wall for the calculation of the sputtered tungsten flux. This method is flexible enough to describe the measured influx patterns of eroded tungsten.
The ramp-up and ramp-down phases which, as seen experimentally, dominate the whole tungsten erosion have been investigated using a special limiter case, the results of which indicate a rather local re-deposition of the eroded tungsten on the central column.
Accordingly the migration patterns derived from the modelling of the flat-top should correspond to the measured distribution of deposited tungsten(see project PFMC).
The modelled deposition pattern shows good qualitative agreement with the measurement. Fig. 36 shows the modelled poloidal distribution of the tungsten deposition for the first phase of the tungsten coated central column 1999 for which a deposition measurement for a full poloidal circumference exists.
In particular the strong deposition on the inner baffle and the inner strike point region as well as the pronounced decay of the deposited tungsten towards the top central column above the coated area can be well reproduced with the code.

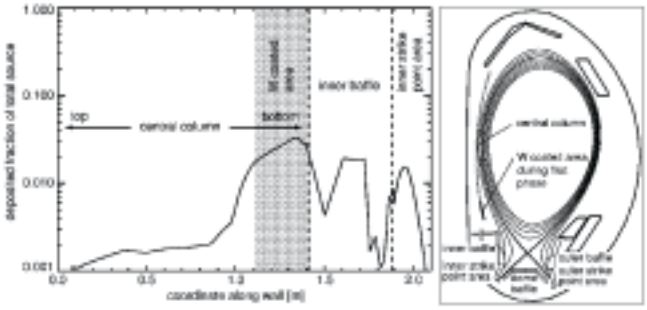

Figure 36: Modelled deposition of tungsten along a contour of the wall starting on the top central column and ending at the inner strike point.

8.6 Divertor asymmetries

In-out asymmetries of divertor power load and temperature have been investigated by means of thermography and shunt measurements of thermoelectric currents. The installation of the new high time resolution 2D-thermograpy system for the upper divertor allowed measurements in upper single null (SN) configuration as well as a shot-to-shot change of the toroidal field direction for fixed plasma current direction. These measurements complement data obtained in lower SN Div II configuration, where toroidal field and current can only be reversed together due to the target plate tilting. The picture obtained from the analysis of the thermoelectric currents, which basically measure the temperature difference between the divertor, is quite simple and robust: If the ion ∇B drift points towards a divertor (upper or lower), the outer divertor is hotter than the inner divertor. For standard field and current directions (ion ∇B drift downward), the outer lower divertor is the hotter one in lower SN configuration and the upper inner divertor is hotter in upper SN. The non-aligned targets in the upper divertor allowed us to demonstrate the in-out reversal of the divertor temperature with change of the B direction, supporting drifts as the dominating cause of the asymmetries. If a DN configuration is approached, thermo currents in the inner divertors vanish due to a lack of input power (ballooning-like nature of transport), in full DN currents flow from the hot lower outer to the colder upper outer divertor (standard field and current).

The situation in view of the thermography is different, probably due to the combined effects of drifts, the balloning like nature of transport favouring the outer plasma side and the influence of fast ions. Most of the averaged power flows to the outer divertor in lower and upper SN discharges for both directions of the ion ∇B drift. The ELM power deposition behaves differently in lower and upper SN configurations. Whereas in lower SN the ELM power deposition is to the inner target plate, it favours the outer plate for higher SN.

8.7 Determination of the 2D radiation distribution in the divertor

Valuable information about the behaviour of the divertor plasma is available, if the spatial distribution is not only known for the total radiation, but individually for the main species contributing to it, e.g. hydrogen and bright impurity lines. In order to get reliable 2-D emissivity distributions from a mathematical reconstruction of the data of a CCD-camera viewing the divertor tangentially, some experimental and related mathematical improvements of this technique have been introduced. As all the reconstruction techniques performed so far, which make use of only one tangential CCD-camera, have the problem of missing vertical resolution in the low-lying strike-point regions, two additional 1D-arrays of chords have been installed in divertor IIb, which view exactly these regions poloidally, and thus improve the reconstruction process significantly. This poloidal system provides, in addition to supporting the 2D-reconstruction, the time-resolved emission profiles of two lines for each discharge. Fig. 37, which compares the reconstruction results (CIII-data for #14375) obtained with and without including the poloidal data, clearly demonstrates the importance of these improvements for reliable 2D-profiles.

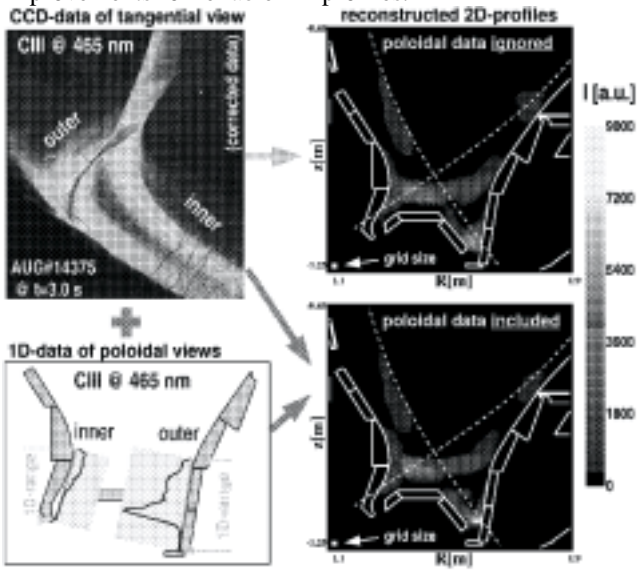

Figure 37: 2D-reconstruction with and without including profile information from poloidal views

Taking the pre-processed CCD-data (calibration and corrections for lens distortion) of the tangential view (upper left) as input, the 2D-profile in the *upper* row was reconstructed without the information from the poloidal views, whereas the 2D-profile in the *lower* row was obtained by including the poloidal data sketched in the lower left corner. The main improvements brought about by adding the additional z-resolved data are clearly visible: The CIII-emission in the vicinity of the outer strike-point is much more localized and the maximum value is considerably higher. The same behaviour is seen, only less pronounced, for CIII between X-point and roof-baffle in the inner divertor.

8.8 Parasitic plasma below the divertor structure

Using Langmuir probes, a parasitic plasma was found below the divertor roof baffle. Typical data of a standard H-mode discharge show an electron density up to 10^{18} m^{-3} and an electron temperature up to 15 eV. An unexpectedly high variation of the electron density of almost three orders of magnitude during the same shot is observed. During divertor detachment an electron temperature of 5 eV was measured.

Since the position of the probe is not connected with the divertor plasma along magnetic field lines, the electrons found at the probe must have been created locally underneath the divertor structure. Since in this region the connection to mechanical structures along magnetic field lines is only a few meters, the typical plasma loss time is of the order of 100 microseconds, and the plasma must be produced very efficiently on those field lines intersecting the probe. To get an idea of the origin of the parasitic plasma, the dependence of its density on various divertor quantities was investigated. Despite a density variation over three orders of magnitude, a good fit was obtained using only two input signals, the radiation power in the outer divertor corner and the neutral gas flux below the divertor, $n_{e,div} \approx \text{const} \cdot P_{rad,div}^{2.7} \cdot \Gamma_0^{0.7}$. This result supports the assumption that the plasma below the divertor baffle structure is created by energetic photons emitted from the highly radiating divertor plasma above it .

The existence of a plasma below the divertor has direct consequences for the deposition of C_xH_y species. On their way to the pumps hydrocarbon molecules interact with the parasitic plasma, which may result in a high deposition on adjacent structures with short spatial decay lengths as observed in ASDEX Upgrade and JET.

8.9 Quartz micro balance monitors

Three quartz micro balance monitors where routinely operated below the divertor IIb. These instruments offer the measurement of deposited layers on a shot to shot basis. A quasi-continuous growth of the layers during an experimental campaign was observed. For identification of the mechanisms involved in the formation of a-C:H layers underneath the divertor, the increase per shot was compared with global plasma parameters and other possibly relevant diagnostic signals in the same discharge. For this comparison, the signals have been averaged or integrated over the divertor phase of the respective shot only.

Taking all discharges in the data base, representing a wide range of shot scenarios, no simple correlation of the layer growth with any of these quantities could be found. Obviously, the instantaneous layer growth depends on a combination of various parameters in a rather complex

manner. However, restricting the data base to shots with rather similar plasma shape, a correlation with the neutral flux Γ_0 below the divertor was found, despite different heating scenarios, core densities etc. With further scenario restrictions, this correlation becomes even more obvious.

9 International Co-operation

9.1 DOE - ASDEX Upgrade Activities

The collaboration in this Agreement continued in 2002. It was very productive and beneficial to both sides. The primary area of collaboration concerns Advanced Tokamak physics issues and divertor physics. The activities ranged from sharing data, carrying out theoretical studies and computations, to joint work on demonstrating new advanced mode operations (such as QH mode and EDA mode). While the number of personnel exchanges between ASDEX Upgrade and the U.S. institutions have decreased compared with last year, the interaction between the U.S. and ASDEX Upgrade scientists has increased substantially through the International Tokamak Physics Activity (ITPA), through joint work on JET and through a joint workshop with the IEA Large Tokamak Agreement. About six scientists from each side were involved directly in personnel exchanges this year between the U.S. (DIII-D, C-MOD, ORNL, and PPPL) and ASDEX Upgrade in experiments, theory and modelling. Some of the collaborative work is carried out off-site, at home laboratories, in data analysis and modelling work. The collaboration with South Korea is slowly being integrated into the existing collaborations and the basis will expand substantially, if the South Korean long-pulse and superconducting Tokamak KSTAR starts operating. There were five personnel exchanges and two joint workshops from South Korea to U.S. Labs. Results from these exchanges have been presented at various international meetings and published in journals.

The ASDEX Upgrade programme is aimed at establishing and expanding the physics basis for ITER-FEAT and at Tokamak concept improvement. The U.S. Fusion programme aims, amongst other goals, at increased understanding of Tokamak physics. Both of these goals have many common research interests. For example, both ASDEX Upgrade and DIII-D have been at the forefront of research on feedback stabilization of 'Neoclassical Tearing' modes using Electron Cyclotron Heating (ECH) system and on development of reactor-relevant advanced hybrid scenarios. A joint effort on ELM modelling was started. Here, the emphasis lies on generating consistent edge stability analyses for both machines using the same numerical tools. With the help of two GA scientists who visited IPP in June 2002, the quiescent H-mode (QH mode), previously found in the DIII-D Tokamak has been established in ASDEX Upgrade (see Sec. 7.9). Also, preparations for similar experiments to be executed in 2003 were made in the area of hybrid scenarios for prolonged burn in ITER, ITB scenarios and resistive wall modes. ASDEX Upgrade and C-Mod share close interest on high-Z wall materials, wall recycling and impurity transport, whereas DIII-D will stay with graphite walls. All three Tokamaks are keenly interested in plasma fuelling, particle transport and density limits. The main heating and CD methods are based on NBI, ICRH and ECRH at ASDEX Upgrade and DIII-D, while Alcator C-Mod relies on ICRH and LHCD. RWM stabilization was pioneered at DIII-D and is also being considered for ASDEX Upgrade. NSTX with its low aspect ratio complements these investigations in many fields and looks for off-axis FWCD and RWM stabilisation. This collaboration serves the interests of both the EURATOM/IPP and the U.S. programmes. At KBSI the buildings for KSTAR were completed and assembling starts in May 2003. Prototype coil tests of both external and internal PF coils have started.

The 17th meeting of the IEA Executive Committee was held at Lyon, France on October 15, 2002 during the IAEA Fusion Energy Conference. The collaboration is expected to continue in 2003 with enhanced interaction through multilateral arrangements such as the ITPA and other IEA Tokamak agreements. As indicated above, the value of collaborations is being enhanced through co-ordinated research among the major world Tokamaks. A slightly higher level of activity in direct exchanges is expected, resulting from the participation of Korean scientists.

9.2 CEA Cadarache

ICRF ion heating with mode conversion performed in collaboration with EURATOM Associate CEA/Cadarache.

A new ICRF heating scenario with the potential to provide bulk ion heating, was developed and analysed in collaboration with CEA/Cadarache. It relies on the non-linear damping on an ion species of the Ion Bernstein Wave at its 3/2 cyclotron harmonic. The IBW itself is not launched directly. Rather, the fast magnetosonic wave, which is more easily launched is used and in a two ion species (hydrogen and deuterium), the Ion Bernstein Wave is created at the plasma centre by Mode Conversion. The series of discharges performed last year during a transition from pure hydrogen to deuterium plasmas were analysed in more detail. The scan in isotopic ratio changes the position RMC of the mode conversion layer. The closeness of this mode conversion layer to the location of the ion resonance at the 3/2 deuterium cyclotron harmonic determines how the heating power is divided between electrons and ions (deuterium in this case). Power deposition on electrons has been measured by power modulation, and the location of the maximum of the damping varies accordingly with the position of the MC layer. Indications for direct ion heating have been deduced from the energy spectrum of neutral deuterium escaping from the plasma and from observed modifications of the power fraction deposited on electrons. This data indicates that ion heating takes place when the MC layer lies close to the 3/2 D cyclotron harmonic layer and confirm the effectiveness of a non-linear damping mechanism involving an IBW for bulk ion heating.

9.3 University of Cork

The collaboration with the University of Cork concerning MHD equilibrium identification using magnetic measurements was continued. The "CLISTE" interpretative equilibrium package and the FP real-time reconstruction now include information from magnetic probes, MSE diagnostics and kinetic data. The q-profiles from both codes agree within error bars over most of the plasma radius, but

there are significant deviations over the innermost 15% of the radius. This deviation indicates an over-regularisation of the inner q-profile in the FP database and work is in progress to improve the database generation procedure to rectify this. The CLISTE code has been further extended to fit the current hole-like equilibria with q on axis taking values of several hundred by expressing the source profiles in terms of a spatial co-ordinate and by introducing the technique of successive over-relaxation to the convergence process. The second part of the collaboration deals with a detailed investigation of the internal transport barriers. The position of the barrier against the minimum q-position, shearing versus growth rates, propagation of the barrier and strength of the barrier are currently being investigated.

9.4 Centro de Fusão Nuclear

The collaboration with CFN on the measurement of density profiles and fluctuations using fast swept microwave reflectometers has proceeded along the lines of well defined tasks covering various physics topics, as well as hardware, software and control developments. 2002 has seen the regular implementation (upon user request) of "burst mode" averaging of the group delay to reduce statistical distortions in the density profile. Burst mode averaging is proving to be particularly useful for studies of the H-mode density pedestal behaviour. To extend the profile coverage to higher densities (up to $1.5 \cdot 10^{20} m^{-3}$) much effort has been spent on improving the W-band channel (75 - 110GHz), including converting to heterodyne detection, complemented with modelling studies using ray-tracing codes for antenna optimization.

The proposed use of reflectometers in ITER for plasma position and shape control was also successfully demonstrated on ASDEX Upgrade by tracking edge density layers during bulk plasma movements. For shape control, tracking layers with a fixed density ratio to the line averaged density were found to give good estimates of the separatrix position. Substantial progress has also been made in the understanding of the density and pressure profile behaviour during ELM events. The density profile collapses and rebuilds with different time scales inside and outside the separatrix position. The reflectometers have also been crucial to the investigation of energy quench, particularly the evolution of the density profile, just prior to a disruption.

9.5 TEKES

The collaboration between TEKES and IPP aims at describing kinetic effects using Monte Carlo techniques and the study of MHD instabilities. Last year the collaboration was also extended to include experimental proposals on ASDEX Upgrade. These include an interest in the heat load on the divertor plates through the loss of fast ions and the difference in behaviour of reversed field configurations. Furthermore, comparisons of orbit loss models for the L-H transition have been compared with competing calculations based on B2 Eirene simulations.

9.6 Institut fur Physik TU Wien

In order to develop a new electron density and temperature diagnostic based on fast He beam emission spectroscopy, the IAP has performed various proof-of-principle experiments at ASDEX Upgrade. Measured HeI emission profiles showed fair agreement with simulated ones for given plasma density, temperature and impurity distributions, utilising a collisional-radiative model and atomic collision data provided by the ADAS group. The experiments made use of on-site spectroscopy systems and a "doped"diagnostic He beam produced by adding a small amount of helium gas into a standard deuterium heating beam ion source. Out of eleven HeI lines considered seven showed sufficient intensity, and the 667.8 nm HeI singlet and 587.6 nm triplet lines proved most suitable for reconstruction of plasma temperature and density profiles.

9.7 National Institute of Laser, Plasma and Radiation Physics

The co-operation with the Institute of Atomic Physics, MEC EURATOM Association, Romania, has been continued with the interpretation and control of helical perturbations in Tokamak, as the main area of study. Our activity was focalised on to directions: Improvement of equilibrium calculations for stability analysis of modes in the separatrix vicinity, in order to determine the influence of the plasma triangularity on the tearing mode stability parameter DELTA for the ASDEX Upgrade Tokamak and elaboration of plasma models for feedback control of helical perturbations.

9.8 Fast camera system for pellet observation

To detect the spatial distribution and time evolution of the visible radiation emitted during pellet ablation in ASDEX Upgrade plasmas, a fast observation system was developed and put into operation. The set up consists of two fast, trigger-able digital cameras and an optical imaging system. With the help of two image guides both a tangential and a vertical view of the inboard pellet injection are imaged onto each camera with good spatial resolution. Both the exposure time of the images and the delay of the cameras can be as short as 1μ s.

The results showed that light intensity emitted by the smallest pellets available is high enough to detect images with μ s long exposure time. The observation from two different directions with long exposure time (typically 10 ms) allows us to reconstruct the 3D pellet trajectory and to measure the penetration depth. The pellet cloud size and shape can be determined by examining the snapshot images. The first experiments measured the penetration depth of pellets with 1000 m/s velocity and the pellet cloud distribution. In order to improve the code calculations of pellet-plasma interaction, experimental investigation of the evolution of the pellet cloud has begun.

10 Scientific Staff

Experimental Plasma Physics Division E1: N. Berger, U. Brendel, A. Carlson, A. Cierpka, T. Eich, H.U. Fahrbach, J.C. Fuchs, O. Gehre, A. Geier, J. Gernhardt, L. Giannone, O. Gruber, G. Haas, T. Härtl, A. Herrmann, J. Hobrik, L. Horton, K. Iraschko, M. Kaufmann, B. Kleinschwärzer, H. Kollotzek, P.T. Lang, P. Leitenstern, A. Lorenz, A. Manini, K. Mank, K.F. Mast, D. Meisel, D. Merkl, V. Mertens, H.W. Muller, P. Muller, Y.-S. Na, J. Neuhauser, E. Oberlander, G. Prausner, G. Reichert, V. Rohde, W. Sandmann, M. Sator, G. Schall, H.-B. Schilling, P. Schotz, G. Schramm, K.-H. Schuhbeck, S. Schweizer, J. Schweinzer, H.-P. Schweiß, U. Seidel, O. Sigalov, C. Sihler, A. Sips, J. Stober, B. Streibl, A. Tanga, W. Treutterer, M. Troppmann, T. Vierle, S. Vorbrugg, M. Wolf, R.C. Wolf, E. Posthumus-Wolfrum.

Tokamak Physics Division: C. Angioni, M. Apostoliceanu, G. Becker, A. Bergmann, R. Bilato, K. Borrass, M. Brambilla, D. Coster, S. Gunter, V. Igochine, F. Jenko, O. Kardaun, A. Kendl, J. Kim, R. Kochergov, P. Lauber, P. Martin, P. Merkel, Y. Nishimura, G. Pautasso, A.G. Peeters, G. Pereverzev, S. Pinches, E. Poli, S. Riondato, T. Schmidt-Dannert, W. Schneider, E. Schwarz, B. Scott, D. Strintzi, E. Strumberger, G. Tardini, C. Tichmann, Q. Yu, H.-P. Zehrfeld.

Experimental Plasma Physics Division E2: C. Aubanel, H. Bauer, K. Behler, H. Blank, A. Buhler, G.D. Conway, R. Drube, K. Engelhardt, A. Gude, H. Hohenocker, M. Jakobi, A. Keller, S. Klenge, B. Kurzan, A. Lohs, M. Maraschek, H. Meister, R. Merkel, A. Muck, M.G. Munoz, H. Murmann, G. Neu, M.-G. Pacco-Duchs, G. Raupp, J. Schirmer, W. Suttrop, K.-H. Steuer, H. Urano, D. Wagner, D. Zasche, T. Zehetbauer, H. Zohm.

Experimental Plasma Physics Division E4: K. Behringer, R. Dux, W. Engelhardt, J. Fink, J. Gafert, B. Heger, A. Kallenbach, C. Maggi, R. Neu, D. Nishijima, T. Putterich, R. Pugno, S.-W. Yoon.

Technology Division: W. Becker, F. Braun, H. Faugel, P. Franzen, D. Hartmann, B. Heinemann, M. Kick, K. Kirov, W. Kraus, F. Leuterer, F. Meo, F. Monaco, M. Munich, J.-M. Noterdaeme, S. Obermayer, F. Probst, R. Riedl, F. Ryter, W. Schärich, E. Speth, A. Stäbler, F. Wesner, R. Wilhelm, E. Wursching.

Plasma Diagnostics (Berlin): D. Hildebrandt, M. Laux, W. Schneider, U. Wenzel.
Garching Computer Centre: P. Heimann, J. Maier, H. Reuter, M. Zilker.
Materials Research: M. Balden, H. Bolt, H. Greuner, H. Maier, M.Y. Ye.

Surface Physics Division: X. Gong, K. Krieger, M. Mayer, J. Roth. Central

Technical Services: H. Eixenberger, T. Franke, F. Gresser, E. Grois, M. Huart, C. Jacob, C.-P. Käsemann-Wilke, K. Klaster, M. Kluger, J. Perchermeier, G. Raitmeir, I. Schoenewolf, F. Stobbe, H. Tittes, F. Zeus.

University of Cork, Ireland: M. Foley, P. McCarthy, E. Quigley.

IPF University of Stuttgart: G. Dodel, G. Gantenbein, E. Holzhauer, W. Kasparek, P. Lindner, U. Schumacher.

Centro de Fusao Nuclear, IST Lisbon, Portugal: J. Borreicho, R. Coelho, L. Cupido, L. Farinha, L. Fattorini, S. Hacquin, M.-E. Manso, I. Nunes, T. Ribeiro, F. Salzedas, J. Santos, F. Serra, A. Silva, P. Varela.

TEKES (HUT and VTT), Finland: O. Dumbrjas, T. Kiviniemi, T. Kurki-Suonio, S. Saarelma.

CNR Padua, Italy: T. Bolzonella, R. Lorenzini.

IFP, CNR Milano, Italy: C. Capuano, A. Jacchia, P. Mantica,

University of Augsburg: U. Fantz, S. Meir, P. Starke, D. Wunderlich.

IAP, Vienna, Austria: H. Falter, E. Galutschek.

FZ Julich, Germany: A. Savtchkov.

Guests: R. Kamendje, Universität Graz, Austria;
M. Tsalas, NCSR Demokritos, Athens, Greece;
S. Kalvin, G. Kocsis, KFKI, Budapest, Hungary;
C.V. Atanasiu, G. Miron, Inst. of Atomic Physics, Romania;
H. Summers, University of Strathclyde, Glasgow, Scotland;
S. Egorov, V. Rozhansky, Semchenkov, S. Voskoboynikov, Technical University, Plasma Physics Department, St. Petersburg, CIS;
S. Lebedev, IOFFE, St. Petersburg, CIS;
A. Komarov, A. Kozachok, Kharkov Institute, Kharkov, Ukraine;
S. Sesnic, USA;
H. Weitzner, N.Y. University, USA;
X. Zhang, Academia Sinica, Hefei, China.

JET Co-operation

Head of Project: Prof. Dr. Michael Kaufmann

1 Introduction

The JET tokamak is exploited under the framework of the European Fusion Development Agreement. The facility is operated by the UKAEA under contract with the European Commission while the physics exploitation of JET is carried out by task forces from the Euratom Fusion Associates.

In 2002, three experimental campaigns (C5-C7) of 108 experimental days were planned. In the event only 68.5 days were executed due to machine failures. In addition, the available neutral beam power was lower than foreseen and thus experiments requiring high input power had to be delayed to 2003. In order to make up for some of the shortfall in experimental time, Campaign C7 was extended into Jan/Feb 2003.

The contributions of IPP scientists to the JET programme have been as part of the larger JET work programme, in collaboration with colleagues from the other Associates[1]. Below are described some of the areas where IPP physicists have made major contributions to the execution and analysis of specific experiments on JET.

1.1 Task Force S1

Participation of IPP in JET TF-S1 work concentrated on the study of the H-mode pedestal with plasma shapes optimized for edge diagnostics, on ion temperature modulation for transport analysis and on pellet injection, of which we describe the first topic in some detail.

Specialised plasma shapes („Diagnostics optimised configurations“, DOC) have been developed for best diagnostics of the gradient region in the H-mode edge. A significant improvement of the effective radial resolution of the edge LIDAR diagnostics is achieved by X-point positioning such that a tangential sightline is obtained in the H-mode barrier region (DOC-U). It is found that this arrangement allows the resolution of the edge pressure gradient at plasma currents of up to about 2 MA.

A variant of this configuration with downshifted strike points (DOC-L) is used to obtain best possible resolution of the power deposition width in between and during type I ELMs by IR-thermography and probe measurements. Here, best spatial resolution of 7 mm for the outside target and 5 mm for the insde target in poloidal direction was achieved by a simultaneous coverage of nearly all target tile in the JET MKII SRP divertor. This optmised positioning of the strike zones is accompanied by very fast data acquisition speed of up to 22 µs of the IR-system, thus adressing the temporal evolution of ELM power depsoition on the divertor target. A picture presenting the covered area of the divertor target is given in figure 1.

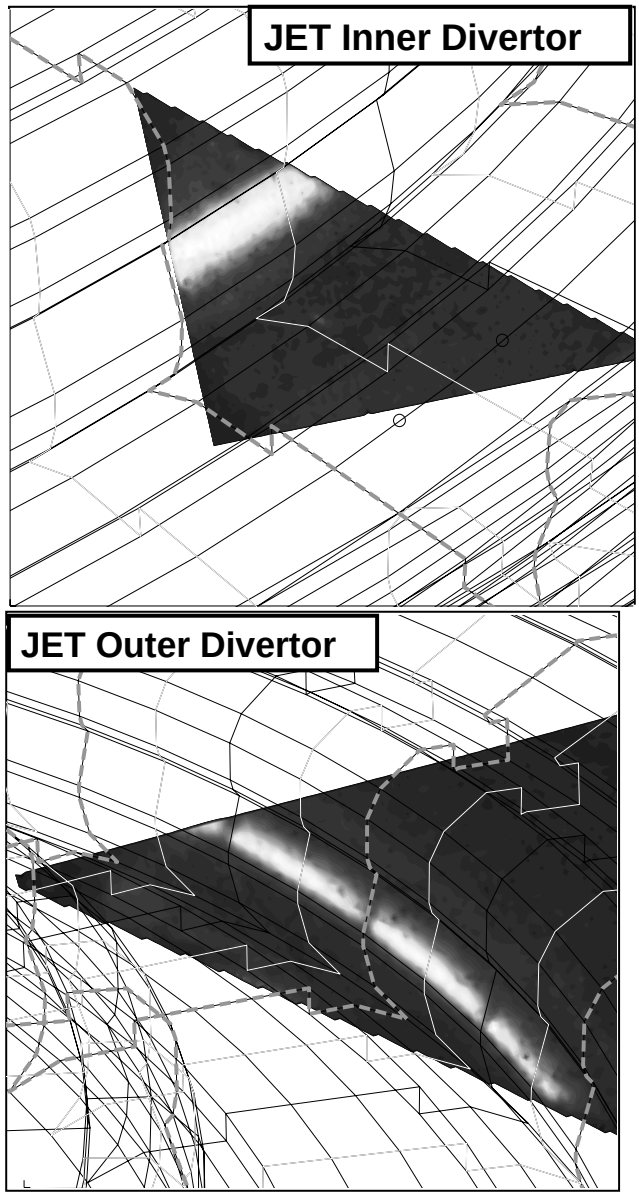

Figure 1: Area covered by the JET thermographic camera.

[1] See Annex to J. Pamela et al., „Overview of Recent JET Results and Future Perspectives“, Fusion Energy 2000 (Proc. 18th Int. Conf. Sorrento, 2000), IAEA, Vienna (2001).

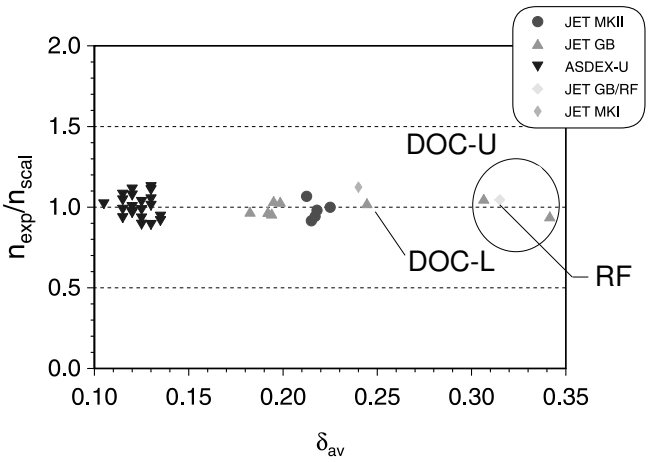

Figure 2: Critical density, normalised to the Borrass, Lingertat, Schneider scaling, versus average triangularity.

Finally, a high triangularity variant („HT3“) with LIDAR compatible X-point geometry has been developed. A multi-dimensional scan of experimental parameters (density, plasma current, heating power and edge safety factor) in these three configurations has begun to study the parameter dependencies of the edge pedestal parameters, of main chamber ELM losses and power deposition on the target. This work is carried out as the combination of several experimental proposal from different laboratories.

First work has been started to analyse the stability of the plasma edge against ballooning and medium-n kink modes. For the first time at JET, direct measurements of the edge gradients are now available, thus imposing experimental restrictions on the pressure gradient and the edge bootstrap current used in the underlying equilibria.

The important question of the amount of stiffness of the ion temperature profiles and its compatibility with ‘non-parametric’ transport models has been addressed on JET. To clarify this point, experiments have been performed in which the ion temperature was modulated using modulated ICRH He3 minority heating. The experiments allowed the observation of a propagating heat wave in the ions, which has a clear phase delay between centre and edge meaning that the ion transport is not infinitely stiff. Analyses on the agreement with transport models are underway.

Studies with pellet fuelling of JET plasmas aiming at high-density plasmas with good confinement by more central particle deposition were continued. The aim was to improve the refuelling performance using the new high-field side pellet-track. Unfortunately the finalization of the new set up faced major technical difficulties resolved by support from IPP only by the end of the year. Experiments are now scheduled early in 2003.

Toroidal field B_t and major radius R are the two parameters which are significantly increased when going from present tokamaks to ITER. Due to a strong covariance between R and triangularity δ in the existing JET and ASDEX Upgrade databases, it is difficult to distinguish between the two. Therefore, since there is no way to change R in either JET or ASDEX Upgrade, a careful assessment of the δ-dependence is required to determine the R-dependence of the density limit. A series of successful high triangularity JET gas scans have been performed in 2002 using the DOC configuration. They confirm the absence of any δ-dependence as predicted by models (figure 2). A high triangularity radio frequency heated scan also fits into this picture. Scans at even higher triangularity are planned for 2003.

1.2 Task Force S2

Several scientists from IPP contributed to the programs of S2 at JET. The main contributions were in areas of operation support, scientific coordination of experiments and data analysis. The main topics of this scientific work in S2 concentrated on: (i) Turbulence suppression in ITB discharges, (ii) profile resilience in ITB’s, (iii) impurity transport in ITB discharges and suppression of central impurity accumulation, (iv) the modelling of current profile control with neutral beams and (v) similarity experiments on improved H-modes between JET and ASDEX Upgrade.

1.2.1 Turbulence suppression in ITB Discharges

The aim of the experiments was to investigate modification of turbulence levels and characteristics with varying velocity shear in low, moderate and strongly reversed shear discharges. Previous studies showed that low frequency ($f < 50$kHz) core turbulence in JET is suppressed/reduced during both dominant ion heated (NBI) ion-ITB discharges and pure electron heated (LHCD) electron-ITB discharges. In both ion and electron dominated ITB discharges the radial extend of the turbulence suppression coincides with regions of reduced thermal conductivity. The results experimentally confirm the respective roles of velocity and magnetic shearing in turbulence suppression in advanced scenario discharges and give further insight into the interplay between velocity shear and magnetic shear.

1.2.2 Profile Resilience and ITBs

In ITB plasmas the temperature profiles are observed to deviate from critical gradient lengths in L- and H-modes. Nevertheless the ion temperature gradient inside the transport barrier seems not solely to be determined by the neoclassical ion conductivity, but rather on the value of the magnetic shear and velocity shear. A comparison of a weakly reversed shear and a strongly reversed shear discharge in JET, shows that initially for the weak shear case the ion temperature profiles slowly deviate from the stiff profiles, while for the strongly reversed case they depart immediately from the stiff regime with the application of the heating power. However once the ITB is formed in both cases, the values of the shear at the ITB location is very similar and close to zero. More detailed analysis and transport simulations are required to explain the differences observed.

1.2.3 Impurity transport in ITB discharges and suppression of central impurity accumulation

Impurity behaviour in scenarios with internal transport barrier is of special concern since neo-classical convection might cause strong inwardly directed drift velocities, which

are not suppressed by anomalous diffusion or MHD phenomena (sawteeth, fishbones etc.). In particular, the behaviour of metallic impurities in JET discharges with an internal transport barrier has been studied by using the intrinsic nickel impurity sources in the JET tokamak. Previously, it was found that impurities accumulate in discharges with deep shear reversal and a strong barrier. The strength of the impurity peaking increases with the impurity charge. New experiments have concentrated on weakly reversed or zero shear discharges (the so called "optimised shear plasmas"). Initial results, combined with the analysis of older shots, show no significant differences in the impurity accumulation between the two types of q-profiles. In parallel to the impurity transport studies, experiments were started to documents the evolution of the impurities with various different central heating schemes. This is a preparation for the control of the central impurity accumulation in advanced scenarios.

1.2.4 Modelling of current profile control with neutral beams

For real-time current profile control at ASDEX Upgrade, it is planned to use neutral beam injection as an actuator for the control of the current density at three radial positions and poloidal beta. In a similar way, the current profile control could be obtained in JET, using the NB power from six sources at 80 keV. For control, the current density profile at five radial positions and poloidal beta are selected. An analysis method used for the system identification at ASDEX Upgrade has been applied to ASTRA simulations of JET discharges. From the identified system model, a controller will be developed and tested in experiments at JET in 2003.

1.2.5 Similarity experiments on improved H-modes between JET and ASDEX Upgrade

The aim of the experiments at JET is to establish this regime at 1.4MA/1.7T (q_{95}=4). The emphasis is on similarity of non-dimensional parameters (for example: ρ^* and q-profile) with the scenario in ASDEX Upgrade. Two plasma shapes are to be used; a low triangularity shape (δ=0.20) and a higher triangularity shape (δ=0.45). In addition experiments at 2.8MA/3.4T are planned, lower ρ^* which is important for a better extrapolation to ITER. Extensive preparations were made for these experiments in 2002. Due to machine problems at JET, these experiments will now be done at the beginning of 2003.

1.3 Task Force E

Major topics of IPP contributions to JET exhaust physics were the development of thermography evaluation software, the study of steady state and ELM target powerload and characterisation of the edge plasma in diagnostic optimized configurations (DOC).

Very steep profiles of the target power flux are observed under low density H-mode conditions. Since the profile width approaches the instrumental spatial resolution of the thermography system, a deconvolution procedure had to be developed to resolve the gradients of the power flux densities on the targets. Broadening of the power load profiles with increasing density is observed as well as a slight narrowing with power. Strongly enhanced power fluxes are measured during ELMs. The width of the power profile does not increase during regular type-I ELMs on the outer target. The characterisation of power deposition on the inner target was found to be much more complex due to the influence of detachment physics and fast ion losses. Furthermore, different features of ELM energy release have been parametrised, namely the wetted area, the deposited energy, the movement of the power deposition maxima and finally the characteristic power deposition time. This work has led to a first unified picture of type-I ELMs from JET and ASDEX Upgrade supporting an extrapolation to ITER.

DOC discharges have been analysed with the Edge2d-Nimbus code package to obtain a physics-based regularization of experimental edge profile measurements, which suffer from large scattering and deficiencies of the magnetic reconstruction necessary for profile mapping. Transport coeficients around the edge transport barrier (ETB) are obtained from this analysis, including estimates of the barrier widths for a H-mode gas scan. A typical ETB width for 12 MW, 2 MA H-modes is 2.5 cm, with 1.5 cm inside the separatrix. The width increases for lower plasma current.

1.4 Task Force FT

The IPP is strongly involved in the determination of wall erosion and redeposition of eroded material. These investigations are of crucial importance for the prediction of the tritium inventory in ITER.

A set of long term samples (LTS), consisting of 400 nm Al and 270 nm Cu layers on carbon, was installed at JET in August 1999 and was removed in September 2001 after about 5750 pulse numbers, corresponding to 4200 plasma pulses in divertor configuration with a total discharge time of 62000 s. The LTS were installed at the inner vessel wall. After removal, the Al and Cu layers were completely eroded, showing clearly that the inner wall is a net erosion area and continuous source of carbon.

Two cavity samples were installed in the inner divertor close to the louvres and below the septum. These areas can be reached only by neutral particles, and it is assumed that deposited hydrocarbon layers are formed by hydrocarbon radicals. The cavity samples allow the determination of the sticking coefficient of hydrocarbon radicals. The thicknesses of deposited layers were analyzed with ion beam analysis techniques and profilometry. The inner divertor sample showed deposited layers with thicknesses up to 50 μm at the outer side and 15 μm inside the cavity. The layers consist mainly of D and C, with D/C $\approx$ 1. Additionally some H and O were detected, while the amount of metals (Be, Ni,...) was very low. The layers are mainly formed by hydrocarbon species with high sticking coefficient (surface loss probability $\beta \approx 0.9$). Possible species are C_2D_x radicals. The incident flux of low sticking species like CD_3 (with $\beta \approx 10^{-3}$) is comparable to the incident flux of high sticking species, but due to the low sticking their contribution to layer formation is negligible. The septum cavity showed a maximum deposited layer

thickness of 9 μm inside the cavity, the layer composition was identical to the inner divertor sample. The layer is formed mainly by particles with sticking coefficient s = 1. Particles with $\beta \approx 0.9$ and $\beta \approx 10^{-3}$ are also present, but their contribution to layer formation is small. The high sticking particles are originating likely from the inner strike point.

1.5 Task Force H

A number of ICRF scenarios that were developed by TF-H in 2001 laid the seed for interesting experiments done, also by other task forces, in 2002.

The mode conversion scenario, whereby the fast wave is launched and is mode-converted to an Ion Bernstein wave provides a localised source of power to the electrons. This was used extensively in JET, in particular by the task force Transport, to investigate electron transport effects.

The minority current drive scenario used to influence the stability of the sawteeth, was used extensively by TF-M to trigger the appearance of neoclassical tearing modes.

Very enthusiastic proposals were obtained for the use of the scenario whereby third harmonic heating of 4He injected at 110 keV with NBI can be accelerated to MeV energies. This scenario provides a method to obtain 4He ions with properties similar to alpha particles and opens up a route to investigate alpha particle issues.

Under conditions where the electron absoprtion is low and the IBW generated in the plasma can damp on ions, preliminary evidence was obtained of ion heating together with a possible evidence of induced shear flow.

The rotation induced in the absence of strong toroidal momentum input (heating with ICRF) was further investigated, and compared with present theories.

Some progress was made on coupling ICRF to ELMy plasmas, though improvements based on electronic measures will have to wait for 2003 and further improvements based on 3 dB couplers for two existing antenna arrays and on the new JET-EP antenna will have to await the installation of those systems in 2004-2005.

Further progress was achieved in the coupling of LH, in particular to ITB plasmas. Up to 3.4 MW was coupled to ITB plasmas together with 15 MW of combined NI and ICRF power, allowing also real time control of the discharge for the duration of the pulse (7.5 s). Full current drive was obtained for discharges of 1.8 MA.

1.6 Task Force M

The contributions from task force M were mainly concentrated on the behaviour of NTMs and the MHD at the plasma edge during ELMy H-mode discharges. Especially the NTM experiments suffered from the lack of NBI heating power and were to a large extent shifted to later campaigns in 2003. The programme that was performed in 2002 will be shortly summarized here.

The influence of rotating error fields, induced by the internal error field coils at frequencies of several kHz, on (3/2)-NTMs was studied. Some minor variation in the rotation profile could be observed. These results have as yet given no final answer about the coupling of external fluctuating error fields to NTMs and the coupling to the plasma rotation itself. The analysis of the (3/2)-NTMs showed more clearly that the so called FIR-NTM regime is also present at JET discharges and the required mode coupling between (3/2)-NTMs, a (1/1) mode and (4/3) modes is observed.

The continuing analysis and characterisation of edge MHD during various scenarios in discharges from task force S1 and S2 has been another task. Special interest has been the behaviour of EDA comparison shots with Alcator C-MOD and ASDEX Upgrade. Similar MHD events could be observed for all 3 machines.

The experiments proposed to look at the proximity to resistive wall mode (RWM) stability by using the saddle coil system on JET to look for evidence of error field amplification were also cancelled due to the early machine shutdown. These experiments have now been combined into the 2003 experimental programme.

The tailoring of the stability of sawteeth by ICCD has been another field where IPP members contributed to the JET programme, this time in support of task force H. Different heating and current drive scenarios were developed in order to investigate their influence on the sawtooth period.
In general, IPP staff have contributed to the continuous manning of the CATS system, the supplying of an MHD expert to the control room in support of the experimental programme of the other Task Forces and the logging of interesting MHD events in JET discharges.

2 Scientific Staff

S. Bäumel, R. Bilato, X. Bonnin, K. Borrass, G.D. Conway, D.P. Coster, R. Dux, T. Eich, J. Fink, P. Franzen, J.C. Fuchs, J. Gafert, A. Geier, S. Gunter, G. Haas, D. Hartmann, B. Heinemann, A. Herrmann, J. Hobirk, L.D. Horton, A. Kallenbach, K. Kirov, W. Kraus, P.T. Lang, M. Laux, F. Leuterer, M. Maraschek, K.F. Mast, M. Mayer, K. McCormick, F. Meo, A. Muck, Y-S. Na, R. Neu, J-M. Noterdaeme, A. Peeters, G. Pereverzev, S.D. Pinches, R. Pugno, F. Ryter, J. Schweinzer, A.C.C. Sips, E. Speth, A. Stäbler, J.K. Stober, W. Suttrop, J. Svensson, G. Tardini, H. Thomsen, D. Wagner, A. Werner, F. Wesner, R. Wolf, W. Zeidner, H. Zohm

ITER Co-operation Project

Head: Prof. Hartmut Zohm

1 Introductory Remarks

In 2002, the developments towards the realization of ITER have gained considerable momentum through the proposal of 3 more sites in France, Spain and Japan in addition to the existing Canadian proposal. Moreover, China and the US showed increasing interest in joining the activities. The ITPA (International Tokamak Physics Activity) has proven to be a bottom-up forum for physicists worldwide to establish the physics base for ITER and other burning plasma experiments. IPP contributes actively to this activity, mainly by providing input from the ASDEX Upgrade tokamak, which carries out a broad physics programme that is mainly directed towards the preparation of ITER (see respective section of this Annual Report). In future, also the stellarator community will contribute to the ITPA and IPP will actively participate in this contribution. Within the EU, preparations have been started for the negotiations about the share of different activities, namely diagnostics, heating, CODAC (COntrol and Data ACquisition) as well as staffing of the different teams. IPP has expressed a strong interest in the various fields, ranging from contributing activities such as participation in diagnostics design up to the interest in developing and procuring full parts of ITER such as the sources of the NNBI system. Moreover, building on its traditional strength in plasma physics, IPP aims at playing an important role in the EU accompanying physics programme during ITER construction with its facilities ASDEX Upgrade and W7-X, both of which will be available to the EU associations for experimental work.

2 Prediction of ITER Performance

The prediction of ITER performance in terms of confinement and L-H power threshold is mainly carried out in the framework of the ITPA activity, both through contribution of ASDEX Upgrade data into the various databases as well as analysis of these.

2.1 Confinement and Fusion Performance

New experimental data from ASDEX Upgrade have been contributed to the H-Mode confinement database. The dataset on confinement was focused on high-density points in steady-state phases and includes also variations of triangularity. It is therefore an important contribution to the ITPA database, which is weakly populated in this operational window.

The topic of probabilistic performance prediction to achieve $Q = P_{fus}/P_{aux}$ at least 10 in ITER, implying predominant alpha-particle heating, has been brought to a temporary conclusion by an article in Nuclear Fusion based on the development of a 1/2-D program. Special characteristics are (a) exposition of the probabilistic framework (‘distributional inference’) which differs from the Bayesian approach in that the specification of a prior `probability' is not needed; (b) a simple analytic formula for the alpha-particle heating power based on measured D-T cross-sections; (c) investigation of the plasma radiation, in particular the derivation of the cyclotron radiation; (d) analytical formulas for the variation of the plasma shape parameters (elongation, cross section and major radius) with flux-surface radius based on calculated PRETOR equilibria. A flat density profile and a typical temperature profile shape are applied throughout. The conclusion of the investigation is that the epistemic probability for reaching plasma conditions in ITER with Q at least 10 under standard (‘type-I’) ELMy H-mode at an output power of some 250 MW is fairly large (‘7/8’).

A comparison of ITER performance was made based on various methods: (a) 1/2-D analysis using SAS, see above; (b) dimensionless scaling analysis from JET and DIII-D similarity experiments; (c) performance predictions from four theory-based models (Multi-mode, Weiland, IFS-PPPL and GLF23). In the latter case, 1.5-D ASTRA and BALDUR codes have been employed, while inserting empirical predictions of the plasma pedestal temperature in ITER from publications using the ITPA pedestal database. From this investigation, the following is concluded: (a) a hypothetical reduction of helium fraction, say from 3.2% to 1.6%, markedly increases the operating window for achieving $Q > 10$; (b) ITER performance predictions by the various alternative methods are quite similar, for instance $5 < Q < 10$ when n_e/n_{Gr} varies between 0.5 and 1.0, while using $n_{ped} = 0.7\ n_e$ and $T_{ped} = c/(n_{ped}/n_{Gr})$ with $c \cong 1.7$ keV; (c) a pedestal temperature in the range of 3.6-5.5 keV is projected to be required for achieving $Q > 10$ at the reference operating point.

The interval estimation for the confinement-time prediction has been re-assessed using the DB3v10 ELMy confinement database. This led to a technical standard deviation of ±14%. Furthermore, an interaction-term scaling has been developed based on DB3v10, with additional time-slices from ASDEX Upgrade, JET and JT-60U, which describes more accurately than ITERH-98(y,2) the confinement time dependence near the Greenwald limit, depending on plasma shape and heating power, and which leads to some 15% - 20% more cautionary predictions for ITER than the point prediction by ITERH-98(y,2). A re-investigation of the L-mode database in ITPA framework has been started which yielded an interesting ratio between L-mode and H-mode thermal energy scaling depending on Larmor radius and in accordance to the perceived difference between Bohm (L-

mode) and gyro-Bohm (H-mode) transport. An extension of the L-mode database, especially with respect to hydrogen discharges, is needed to improve the scaling and to predict performance of ITER during hydrogen operation.

2.2 L-H Power Threshold

New ASDEX Upgrade data were added to the power threshold database. They were obtained during 2002 in divertor DIV-IIb and document the fact that the power threshold in this divertor version is about 20% lower than in DIV-II, reaching then the level obtained in DIV-I. This contribution was included in the analyses carried out by the ITPA Confinement Database and Modelling Topical Group.

3 Design of ITER Technical Systems

3.1 Diagnostics

The area of diagnostics remains a focus of IPP's ITER activities. Contributions are now given in the fields of bolometry, reflectometry, ECE, Thomson scattering, MSE and neutral pressure gauges. Concerning the latter, an ASDEX pressure gauge mock-up has recently passed a neutron irradiation test in the BR2 reactor at SCK.CEN in Mol, Belgium, under conditions as expected in the ITER divertor. The resistance of the insulators remained well above the value necessary for the gauge operation.
Together with CEA Cadarache, IPP plays a leading role in the present EU studies for the thermographic monitoring of in-vessel components. Also, a large dataset describing in detail the ASDEX Upgrade diagnostic systems and their performance has been contributed to the worldwide diagnostics database initiated and maintained by the ITPA diagnostics topical group.

3.2 Heating systems

A major field of support for ITER is the contribution to the R&D for heating systems, based on the experience gained on the IPP fusion experiments. Main contributions are given in the field of NNBI, ICRH and ECRH. For the latter, the contribution is a design study for the remotely steered launcher carried out by the IPP sub-association IPF Stuttgart. It is described in the respective part of this Annual Report.

3.2.1 ITER NNBI System

3.2.1.1 Development of an RF Negative Ion Source

In 2002 the development of a large-area RF source for negative hydrogen ions entered a new phase: it became the subject of an official EFDA task agreement, for which EURATOM preferential support was approved. The project is aiming at demonstrating ITER-relevant ion source parameters, i.e. a current density of 20 mA/cm^2 accelerated D^- ions from a PINI-size extraction area for pulse lengths of up to 1 hour. The corresponding development programme is scheduled to proceed along four activities in parallel: (i) raising the current density (at reduced pressure); (ii) extending the extraction grid area, (iii) extending the pulse length to 1 hour; (iv) implementing deuterium operation, which requires substantial neutron shielding of the test stand in building L6. The final results are expected by 2005.
As far as topic (i) is concerned, the investigations of Cs-free experiments (initiated in 2001) were continued. As reported previously, silver sputtered from the Faraday screen onto the internal surfaces of the source leads to a considerable reduction of the H^- fraction in the plasma. It turned out that, even after a first cleaning of the source, performance was still considerably lower than before the silver coating and a second time-consuming complete source cleaning was performed. This procedure led to a source with either no or very little caesium contamination from previous operations. This source has been used for the studies of the H^--yield in a caesium-free RF source. The large effect of the silver deposition on the H^--yield also showed, that investigating the effect of the plasma grid material was only meaningful when sputtering from the Faraday screen could be reduced sufficiently. It was therefore decided to prefer materials with a low sputtering yield like tungsten on the Faraday screen rather than using the same material as used for the plasma grid. Additionally the importance of a work function measurement in situ was demonstrated by the effect of silver. A tungsten-coated Faraday screen and the work function diagnostics have been ordered and will be available early 2003.

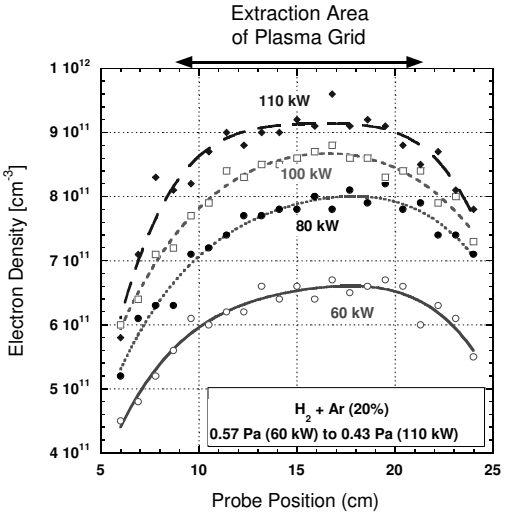

Figure 1: Electron density from Langmuir probe measurement as function of RF power for pulses with argon addition

Progress has also been made in some experimental areas. Langmuir probes allow deriving plasma parameters such as the electron temperature, electron density, plasma potential, and ion density. The measurements are complicated due to the magnetic filter field as this limits the free flux of charged particles to the probe and by the RF field, which introduces noise pickup. Fig. 1 shows electron density profiles in a distance of 45 mm parallel to the plasma grid. The density is constant to better than 10% above the extraction area falling off sharply outside the extraction area. This significant drop in density is either caused by the plasma supply from the driver mounted centrally above the extraction area or from losses to the screened area of the plasma grid, which is without the magnetic field of the electron deflection magnets. This will be investigated further under topic (ii), by using the 6.2 type source with

two drivers and by using a large area grid, which has a magnetic electron deflection field over the entire grid area. As can be seen, the electron density increases with increasing RF power.
In order to elucidate the processes in the source plasma, more emphasis is now being laid on improved diagnostics. Spectroscopic measurements of the source plasma have started in collaboration with Augsburg University. These measurements show a large potential giving access to plasma parameters like electron temperature, H_0 density, distribution function of vibrationally excited $H_2(v)$, and gas temperature. These data are being crosschecked with data from other diagnostics and will be used for modelling of the source plasma. A laser detachment system to measure the H^- concentration in the plasma has been ordered and installed in 2002 and is now under commissioning.

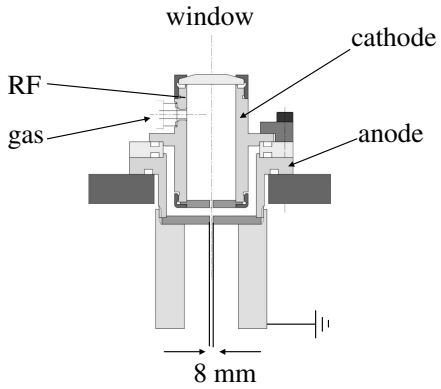

Figure 2: Schematic of the hollow cathode set-up

Experiments with a hollow cathode arrangement (Fig. 2) show that the ion density increases linearly with power in the frequency range of 1 – 10 MHz. From these data it can be extrapolated that a PINI size source would require approximately 30 kW of RF power. The electron temperature in the expansion region is of the order of a few eV and essentially independent of either power or location. The charm of the hollow cathode as an alternative driver concept is its clear separation between driver and expansion region. This could be beneficial for the required operation at lower pressures to reduce the electrode loading in the ITER neutral beam injector.
In preparing the activity (iii) the procurement of a high voltage power supply for c.w. operation is under way, and a cryo pumping system is being studied in collaboration with FZ Karlsruhe. It is envisaged to use a cryosorption pump similar to the type that is presently being tested for ITER. Concerning topic (iv) first considerations of a neutron shield have started.

3.2.1.2 Design Study for an alternative Residual Ion Dump

The scoping study on an alternative concept for the ITER residual ion removal system has been continued. The final concept (see Fig. 3) consists of magnetic deflection of the residual ions to in-line dump plates with an oblique incident angle (<14º). Previous studies have shown, that the preferred deflection to remote ion dumps is not possible due to the geometric restrictions of the ITER beam line.

The in-line target plates are hit only from one side and form a 0.5 m wide opening to the beam. The maximum power density deposited onto the target plates is well below 15 MW/m^2. In the calculations the ion grid optics was optimised to the open structure of the magnetic system, whereas the present reference grid optic design is aligned to the narrow exits of the four channels of the electrostatic system.

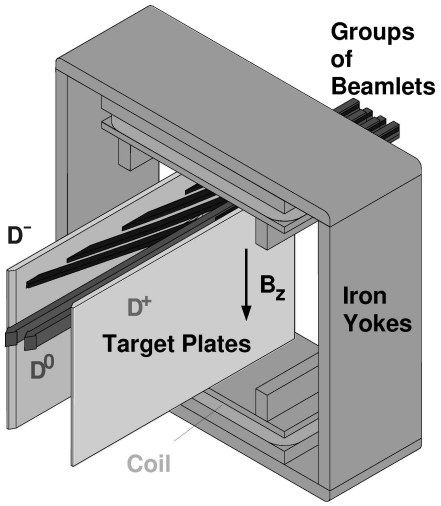

Figure 3: Schematic view of the residual ion dump design

The concept has several advantages over the reference design of an electrostatic deflection to in-line target plates:
a) an increased geometric beam line transmission and hence, an increased injected power (1.7 MW per beam line for a 3 mrad beam with the reference design parameters),
b) a wide operation window regarding beam alignment, perveance, transmission, divergence and steering, and
c) no accelerated secondary electrons.
On the other hand, a magnetic ion removal system creates an additional stray field that has to be compensated and the maximum power load is higher than in the case of an electrostatic system. But this can be handled by the better access to the target plates for the cooling (from the back instead from top). Furthermore, the presence of coils in a high-level neutron radiation field may cause additional problems.
If the magnetic ion removal system is chosen for ITER, a redesign of the grip optics and the whole beamline — especially the beam limiting components as the neutralizer and the duct — is essential in order to optimise the beam losses, the gas flows and the power densities at the high heat flux components of ion dump and calorimeter — and perhaps the deposition profile in the plasma.

3.2.2 Developments for the ITER ICRH System

The IPP ICRH group participates in the EFDA task on the technical specifications and industry contacts for the development of a fusion diacrode (tetrode) and of an ICRF steady-state generator in support of the principal association, CEA Cadarache. Part of this task is the specification of steady-state capable transmission lines. Key transmission line elements, such as ceramics and the cooling of the inner conductor, are being developed on a transmission line resonator built at IPP for W7-X.

Theoretical work was performed in support of the ITPA groups. A detailed quantitative study of the power absorption and predicted current drive, currently using Ehst-Karney parameterisation was done for three tokamaks: ASDEX Upgrade, DIII-D, and JET. The 2D full wave toroidal code TORIC is used to calculate the Fast Wave (FW) current drive efficiency weighted over the complete launched spectrum from the antenna. Preliminary work on FWCD simulations on ITER plasmas have shown that the current drive figure of merit (current drive efficiency multiplied by volume density) as a function of central temperature extrapolates linearly to ITER from the other three tokamaks. However, this was analysed for one value of the parallel index of refraction and further studies covering other launched $n_{//}$ need to be made.

3.3 Redeposition Studies with a Hot Liner

Dedicated studies on the redeposition of hydrocarbons were carried out in view of the importance of possible T-deposition in remote areas of the vacuum vessel due to this mechanism. In order to simulate the hydrocarbon redeposition pattern to be expected in the ITER divertor, a realistic set-up (called a "hot liner") was tested at the plasma generator PSI-2 in Berlin (some additional information is given in the section *Plasma diagnostic* of this report). The processes involved in layer formation were monitored using mass spectrometry, passive optical spectroscopy and a collector probe technique.

Carbon and hydrocarbon molecules were introduced into the plasma via erosion of a graphite target. A molybdenum box around the target was used to intensify the particle fluxes in the direction of a pumping duct where the hydrocarbon fluxes and the growing layers could be analysed. During plasma exposure the box walls were heated to temperatures above 230° C so preventing carbon deposition inside the box. A small, cooled holder facing the plasma beam was installed at the end of the duct. Some experiments were performed with a tantalum liner head at the duct entrance. The surface of the LN_2-cooled panel installed at the end of the duct was checked in situ for almost each run. A large amount of experimental data has been collected for this geometry. They can be summarized as follows:

No deposition is found at the duct walls which are maintained at 100° C, whereas very thin, (but quite detectable) films grow on the holder kept at 20° C. Measuring the erosion profiles along the duct gives a decay length of ~10 cm with no detectable erosion of prepared films installed at the duct ending. Cooling the duct below 50° C leads to film deposition but only at the duct entrance with no deposition on the cooled holder. In addition, a shadow pattern is observed indicating that the films are produced by very active particles with sticking coefficients close to unity. Heating the tantalum liner to about 700° C results in an increase in the deposition rates. One possible explanation is that the hot Ta-liner produces additional reactive hydrocarbon species via plasma-assisted pyrolysis. The growth of the deposit is measured when cooling the panel down to -180° C. However, such deposits are fully evaporated after warming the panel up to 30° C. The panel remains clean even after many cycles of cooling and warming.

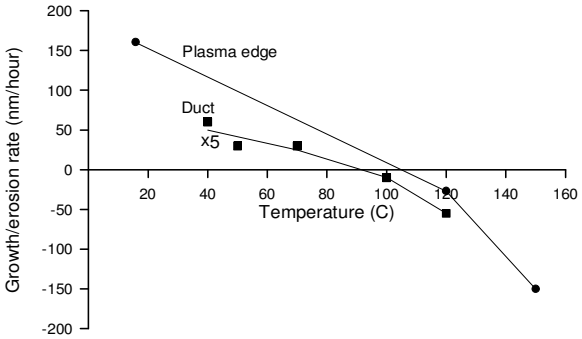

Figure 4: Growth rate vs. surface temperature for two different positions of the collector.

Finally, the growth rate of the hydrocarbon layers has been studied as a function of surface temperature for collectors arranged in the vicinity of the target (plasma edge) and about 30 cm further away in the duct region. As is to be seen from Figure 4 this rate can be positive (deposition dominated) or negative (erosion dominated). In case of zero growth rate there is a balance between erosion and deposition. This equilibrium is found for temperatures of about 100° C, almost independent on collector position.

These findings may open a route to controlling the location where tritriated hydrocarbons are deposited in ITER through controlling the wall temperature.

4 Staff

Performance predictions: O. Kardaun, F. Ryter, A. Stäbler, J. Stober, ITER International Team, ITPA database and modelling group

Diagnostics: G. Haas, A. Hermann, F. Mast

NNBI: M. Bandyopadhyay (IPR Gandhinagar, India), A. Encheva, H. Falter, P. Franzen, B. Heinemann, D. Holtum, W. Kraus, P. McNeely, R. Riedl, W. Schärich, J. Sielanko (University of Lublin, Poland), E. Speth, A. Tanga

ICRH: W. Becker, D. Birus, F. Braun, D. Hartmann, F. Meo, J.-M. Noterdaeme, J. Wendorf, F. Wesner

Redeposition studies: W. Bohmeyer, G. Fussmann, A.V. Markin (Institute of Physical Chemistry, RAS, Moscow), D. Naujoks, H.-D. Reiner

WENDELSTEIN 7-AS

Head: Dr. Rolf Jaenicke

1 Overview

The experiments on the Stellarator W7-AS ceased on July 31, 2002, according to schedule. The unprecedented and in its magnitude unexpected success of the island divertor determined the activities of W7-AS also in the last half year of operation. Thus, the physics base of the extremely promising High Density H-mode (HDH) was clarified further, with important questions remaining.

The favorable properties of the HDH-regime could be consolidated and even extended:

- ultra-high densities up to 4 10^{20} m^{-3} in quasi steady-state discharges
- very flat density profiles, which are responsible for the high upstream densities
- plasma partial detachment at the divertor targets
- a dramatic decrease in impurity confinement and thus no impurity accumulation
- radiation levels up to 90% of the absorbed power, largely at the edge
- passive density control even for neutral injection powers up to 2.8 MW
- energy confinement times of up to a factor of two above the ISS95 scaling

Like the conventional quiescent H-mode (H*) in W7-AS the HDH-mode shows:

- high energy confinement times τ_E
- absence of any ELM- or evident mode activity
- flat radial density profiles
- existence above a threshold density increasing with heating power (but higher than in H*)
- a negative radial *E*-field at the edge (but lower than in H*)

Most remarkable and in contrast to H* is the absence of impurity accumulation.

For better comparison, discharge scenarios were tailored whereby an H*-phase was transformed into an HDH-phase within the same discharge: Constant density H*-mode discharges, normally running to radiative collapse, could be further sustained by ramping the density up to a second plateau above the HDH-mode threshold, immediately before radiation collapse ensued. The radiation from the core was then drastically reduced ('self cleaning' of the discharge) leading to a quasi-steady-state.

It is interesting that the impurity transport in H* and HDH discharges is totally different, although differences in the profiles producing this different transport behavior are not clearly visible. The occurrence of impurity accumulation in spite of flat density profiles in H*-regimes can be modelled with significantly lower diffusivities at the edge and poorer compensation of the inwards pinch associated with the steep edge pressure profiles - but direct experimental evidence is still lacking.

An isotope effect between deuterium and hydrogen is documented, but due to present uncertainties in NBI deposition, it is not yet clear to what degree these differences reflect a difference in transport.

Distributions of near-target plasma parameters as well as neutral pressures in the sub-divertor chambers show a rather strong top/bottom asymmetry, and certain target regions which should be mutually shadowed by adjacent targets are, in attached scenarios, considerably exposed. A reversal of the B-field direction led to a complete inversion of the asymmetry thus indicating a prominent role of plasma drifts. This is supported by EMC3-EIRENE calculations which reproduced these results by introducing classical *ExB* drifts into the code.

In magnetic field configurations with smooth flux surfaces at the plasma boundary average β-values up to $<\beta> = 3.4$ % could be achieved at reduced toroidal field and maximum NBI heating power. In spite of a sophisticated search for different modes in these high-β discharges no indication of a stability ß-limit has been found. The maximum plasma ß is determined by the available heating power rather than by approaching an equilibrium- or stability-limit.

A key element of of the stellarator optimization anticipated in the W7-AS device, the reduced Shafranov shift compared with a classical stellarator along with an increased equilibrium ß-limit, has been verified by studies of its ß dependence in various configurations.

A comparison of the measured line integrated densities for steady state HDH-mode density limit discharges with those predicted from a scaling law derived for edge radiation dominated plasmas was done. Also the high beta discharges can be included.

Using the reduction of the recycling by the installation of the divertor, high (optimised) confinement conditions could be achieved, resulting in discharges with central ion temperatures of up to 1.7 keV at densities of about 6 10^{19} m^{-3}.

In high-β plasmas on W7-AS electron Bernstein waves are strongly absorbed even at higher cyclotron resonances. Therefore also the third- and fourth-harmonic OXB heating could be investigated with 140 GHz at 1.5 T and 1.1 T, respectively. Here both, the plasma energy and the plasma beta, could be significantly increased. This result is very promising for high density and high beta ECRH operation of W7-X.

On the whole, W7-AS has shown very promising results for W7-X in general and in particular for its island divertor.

2 Experimental and theoretical results

2.1 Divertor related studies

The island divertor together with NBI-heating allows access to a new high-density operating regime with improved confinement properties. This regime – the High Density H-mode (HDH) – is extant above a threshold density and characterised by flat density profiles, high energy- and low impurity-confinement times, and edge-localised radiation. Quasi-steady-state discharges with line-averaged densities $\bar{n}_e$ up to 4 10^{20} m^{-3}, edge radiation levels of up to 90%, and plasma partial detachment at the divertor targets can be simultaneously realised. Studies in 2002 were focused on extension of the database, including, in particular, relations to the conventional H-mode, first estimates of the impurity transport, isotope effects, more detailed characteristics of the near-target plasma, and high-density operational limit.

2.1.1 HDH-mode

The HDH-mode could be established in a variety of magnetic field configurations with the edge rotational transform $\iota_a \geq 1/2$ and is not restricted to typical island divertor configurations with large boundary islands. Common features with the conventional quiescent H-mode (H*) in W7-AS are high energy confinement times τ_E, existence above a threshold density increasing with heating power, flat density radial profiles, formation of a negative radial *E*-field at the edge, and absence of any ELM- or evident mode activity. Although the HDH-mode is reminiscent of the EDA-H-mode in Alcator C-Mod, no quasi-coherent mode such as seen in C-Mod is ever observed. Obvious differences between HDH- and H*-mode are higher threshold densities, lower radial *E*-fields and, most outstanding, the absence of impurity accumulation. Constant density H*-mode discharges, normally running to radiative collapse, could be further sustained by ramping up the density to a second plateau above the HDH-mode threshold immediately before radiatively collapsing. The radiation from the core was then drastically reduced ('self cleaning' of the discharge, Fig. 1), leading to a quasi-steady-state.

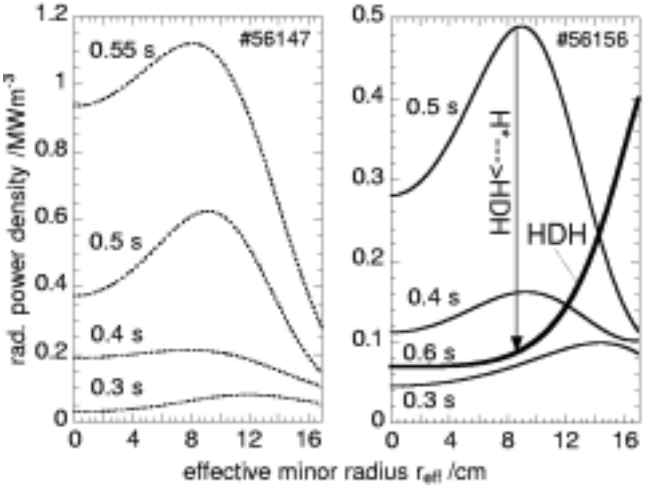

Figure 1: Comparison of quiescent H-mode (H*) and HDH-mode radiation profiles. NBI (Ho→H+) discharges with P_{NBI}^{abs} = 1.1 MW. Discharge #56147 (left) runs into the H*-mode with subsequent radiation collapse. Discharge #56156 (right) runs through the same cycle, but avoids radiation collapse by further increasing the density from the H*-mode level to above the HDH-mode threshold density.

Compared with lower-density Normal Confinement (NC) discharges, model calculations relate the strong reduction of the impurity confinement time by more than one order of magnitude in HDH scenarios to a reduction of the inward pinch velocity v_{in} in the core by factors 4-5 due to broadened n_e and, hence, pressure profiles. The spatio-temporal behaviour of the line radiation of laser-injected aluminium could be well simulated by assuming nearly unchanged diffusion coefficients (≈ 0.1 m^2s^{-1}) in the core and $v_{in} \sim dp/dr$ (*p* being the plasma pressure), Fig. 2. In the gradient region, large diffusivity (≈ 1 m^2s^{-1}) has to be assumed to balance the strong pinch and match the reduced confinement observed in HDH. Considering the collisionality regimes in the core - collisional impurities ($\nu^*>1$) and rather collisionless background ions ($\nu^*<1$) - classical temperature screening might be expected in both HDH and NC, but in the NC case this is strongly overcome by the inward driving forces of peaked n_e profiles being responsible for the different behaviour. The occurrence of impurity accumulation in spite of flat density profiles in H*-regimes is assumed to be due to significantly lower diffusivities at the edge, which is consistent with stronger radial *E*-fields, but there is not direct experimental evidence yet.

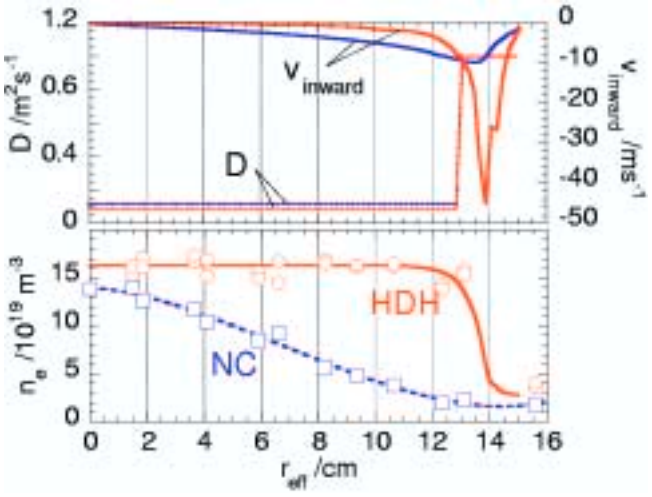

Figure 2: Impurity diffusion coefficients $D(r_{eff})$ (broken lines) and inward convective velocities $v_{in}(r_{eff})$ (solid lines) for the NC-type (blue, #55540) and the HDH-type (red, #55587) plasma derived from simulation of the line radiation of laser-injected aluminium, discharges with P_{NBI}^{abs} = 0.7 MW. Bottom: corresponding profiles of the electron density n_e. Electron temperature profiles were nearly parabolic and comparable in the two cases.

In deuterium discharges ($D^o \rightarrow D^+$ injection) the parameter changes associated with the NC→HDH transition evolve with increasing density more continuous than in hydrogen discharges, resulting in plasmas with even slightly higher energy- and low impurity-confinement times under certain conditions. Partial detachment on the divertor targets is observed at slightly higher density than in hydrogen, and the edge density and temperature are less decreased during detachment. Due to present uncertainties concerning details

of the NBI heating power profiles, it is, however, not yet clear to what degree the differences reflect a difference in transport.

2.1.2 Divertor regimes

Stable detachment could be established, but it was always partial in the sense that full detachment did not extend along the entire target. Along most of the wetted target area the energy and particle fluxes to the target were observed to drop by more than a factor of 10 which is indicative of full detachment, but in some small spots the plasma always remained attached (fluxes dropped only by a factor of about three to five). EMC3/EIRENE code simulations could qualitatively reproduce this inhomogeneity, Fig. 3. They indicate that it is due to inboard/outboard asymmetry of the temperature T_{es} at the upstream separatrix position. The target position with permanent attachment is magnetically connected to the outboard side of the configuration. This region shows strong flux surface compression, which favours local radial heat transport into the islands and - consistently with data from bolometry - leads to a lower level of carbon radiation, resulting in reduced local unloading of the plates.

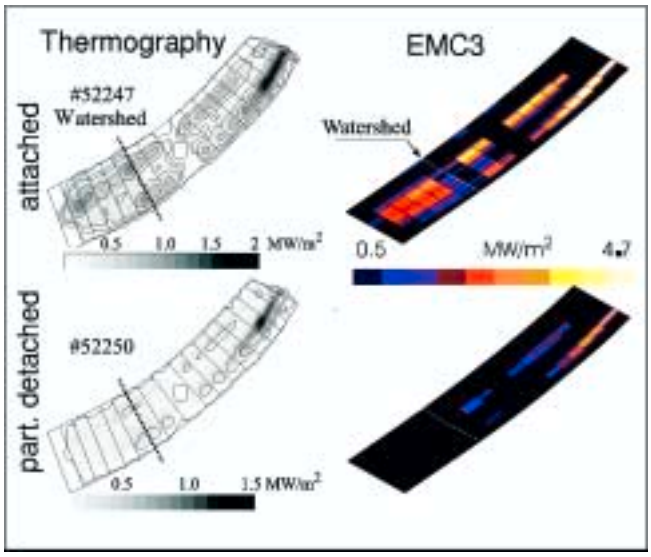

Figure 3: Power deposition contours on the W7-AS divertor plates from thermography and EMC3-EIRENE simulations for attached and partially detached conditions.

Line-of-sight integrated spectroscopic measurements parallel to the target surface in zones of complete detachment, with a spatial resolution of 3 mm perpendicular to the target, show the typical signature of an island divertor plasma: Measurements of the C II and III line radiation show that with the transition to detachment the radiation front moves away from the target surface towards the vicinity of the X-point. The intense carbon radiation results in a steep drop of the electron temperature towards the target down to values of < 3 eV (derived from Balmer continuum and Boltzmann plot) accompanied by a strong rise in electron density up to values of 5-8 10^{20} m^{-3} (from Stark broadening of Balmer lines). This density condensation is a consequence of pressure conservation. Across the last 10 mm towards the target plate the density abruptly dropps to values < 10^{20} m^{-3} (detection limit) which is consistent with the value of ~5 10^{19} m^{-3} derived from target-integrated Langmuir probes. This as well as the observed line intensity ratios of H_α/H_γ, the high level of hydrogenic line emission just within this region, the appearance of molecular lines such as the CH- and the BH-bands, and the sudden increase of the sub-divertor neutral pressure to values sufficient for efficient neutral pumping are all indications of complete detachment at the investigated location of the target.

Topological pre-conditions for the existence of stable partial detachment in W7-AS were studied by independently varying field line connection lengths L_c inside n/m = 5/9 boundary islands and minimum distances Δ_x between x-points and targets over large ranges. As is shown in Fig. 4, stable detachment exists above a critical Δ_x increasing with L_c, which indicates that sufficiently large values of the field line pitch Δ_x/L_c inside the islands are a necessary pre-condition. It is assumed that otherwise cross-field transport opens too strong a by-pass relatively to parallel transport in this geometry.

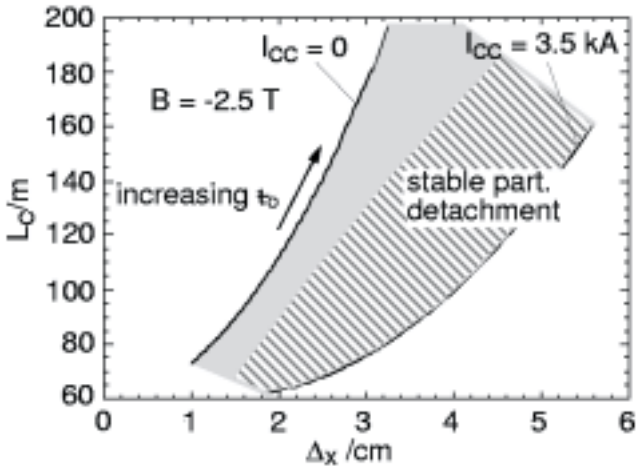

Figure 4: Field line connection lengths L_c (1 cm inside the island separatrix) and minimum distances Δ_x between x-points and targets, $\iota_a \approx 5/9$. The shaded and hatched ranges are accessible by proper adjustment of ι and control coil currents I_{cc} (technically limited to ≤ 3.5 kA). Stable partial detachment is restricted to the hatched range.

Distributions of near-target plasma parameters as well as neutral pressures in the sub-divertor chambers show a rather strong top/bottom asymmetry, and certain target regions, which should be mutually shadowed by adjacent targets, are, in attached scenarios, considerably exposed. A reversal of the B-field direction led to complete inversion of the asymmetry, thus indicating a prominent role of plasma drifts. This is supported by EMC3-EIRENE calculations which well reproduced the exposure of the geometrically shadowed regions by introducing classical ExB drifts into the code, providing a poloidal phase shift of the particle flow into the shadowed region. The E-field was calculated from equipotential surfaces obtained by integrating the parallel momentum equation for electrons from plate to plate.

2.1.3 Density limit

The introduction of divertor modules has allowed access to a high-density and high-power H-mode (HDH) regime where the radiation profiles with predominantly edge radiation reach a steady state. The density limit in stellarators has been treated theoretically using power balance considerations, and it has been recognised that radiation from the plasma edge or core can lead to a different power dependence for the density limit scaling law [Itoh, K. and Itoh, S.-I., J. Phys. Soc. Jpn., 57, 1269, 1988]. A scaling law more relevant to density limit shots in a stellarator with a radiating layer at the plasma edge, as in the HDH-mode, can be derived heuristically with assumptions concerning the power dependence of the impurity concentration:

$$\bar{n}_e[10^{20} m^{-3}] = 1.5\left(\frac{P_{NBI}[MW]}{V[m^3]}\right)^{0.4} B[T]^{0.32}\,\iota^{0.16}$$

A comparison of the measured line integrated densities for steady-state HDH-mode density limit discharges with those predicted from the scaling law derived for edge-radiation-dominated plasmas is shown in Fig. 5. Even the high beta discharges at magnetic fields less than 1.25 T that behave similarly to the HDH-mode and radiate at the edge follow the predicted scaling.

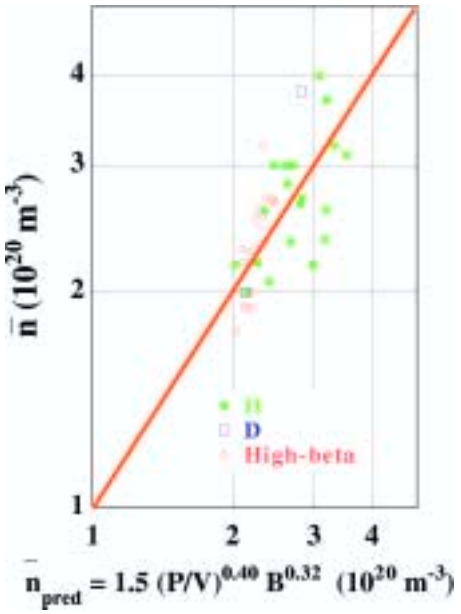

Figure 5: Power, plasma radius and magnetic field scans were carried out to obtain a comparison of the measured line-integrated densities in steady state HDH-mode density limit discharges with those predicted from the scaling law derived for edge-radiation-dominated plasmas.

2.2 Studies of the β-limit

In 2002 the high-β programme at W7-AS was continued, aiming at further optimization of the achievable β and at improved understanding of the β-limit physics in stellarators. A wide range of different magnetic configurations with B ≤ 1.25 T were investigated, including variations of the external rotational transform, the vertical field and the toroidal mirror term of the stellarator field. In addition, experiments with toroidal net-current drive were performed in order to investigate the interplay between current- and pressure-driven MHD instabilities close to the β-limit. The divertor control coils were used to compensate edge islands in order to obtain smooth magnetic surfaces at the edge and a maximum effective plasma radius. Besides configuration parameters, we also changed the plasma ion mass in order to optimize the energy confinement and/or the injected neutral beam power. However, the plasma performance deteriorated in the case of the D–>D as compared with the H–>H heating scenario. This is caused by increased bulk impurity radiation in the deuterium plasma, which has a particularly unfavourable effect in this parameter regime, where the densities are as high as 2-4·10^{20} m^{-3} and temperatures are below 0.5 keV. The effect of additional fourth-harmonic OXB heating with the 1.2 MW ECRH system at 140 GHz in high-β target plasmas could be demonstrated. However, a significant increase of the plasma β by OXB heating could not be achieved due to the power degradation of the confinement at the NBI heating power levels of up to 2.8 MW used for the target plasma.

In the case of "currentless" plasmas (bootstrap and Okhawa currents compensated by OH transformer) optimum performance was found in configurations with an external rotational transform (vacuum configuration) of $\iota_{ext} = 0.5$, where $\langle\beta\rangle = 3.4$ % could be achieved at a magnetic field of 0.9 T (Fig. 6).

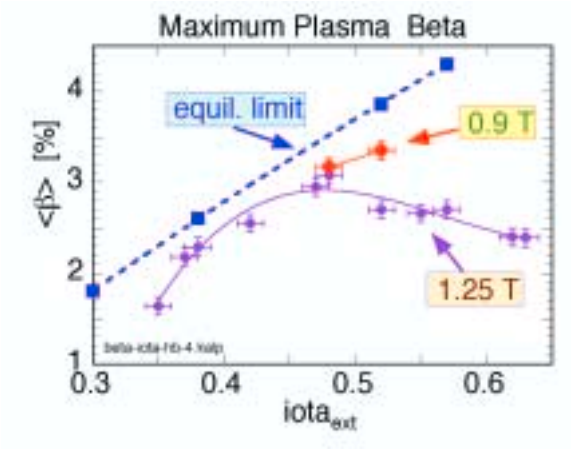

Figure 6: The deterioration of ⟨β⟩ at low iota is attributed to equilibrium limit effects. At high iota, residual edge islands may be present.

Under these conditions the maximum plasma β is determined by the available heating power rather than by approaching an equilibrium- or stability-limit. These discharges exhibit the favourable properties of the HDH-mode regime such as quasi-stationary behaviour, enhanced energy confinement, low impurity confinement times and very weak MHD activity. The confinement deteriorates progressively towards low iota. This can be attributed to the decrease of the equilibrium β-limit (critical Shafranov shift) associated with enhanced transport. On the other hand, if the rotational transform is raised above $\iota_{ext} = 0.53$, the global confinement likewise degrades to some extent, since the structure of the edge islands becomes more complicated, and therefore the control coils cannot completely restore the maximum plasma radius.

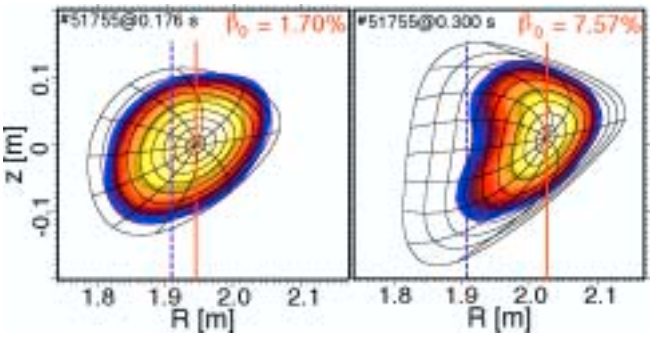

Figure 7: Comparison of X-ray tomograms for #51755 ($\iota_{ext} = 0.52$) at low and high β compared with flux surfaces calculated by NEMEC (dashed line: axis position of the vacuum configuration).

Tomographic reconstruction of X-ray emissivity distributions in the triangular plasma plane are in good agreement with flux surfaces calculated with the NEMEC code (Fig. 7). Hence, a key element of the stellarator optimization anticipated in the W7-AS device, the reduced Shafranov shift compared with a classical stellarator along with an increased equilibrium β-limit, was verified by studies of its β-dependence in various configurations.

Under optimum conditions the plasmas with highest β-values show only weak MHD activity, mostly coherent modes in the range 4..20 kHz. These low-frequency modes are usually attributed to pressure-driven modes around low-order rational surfaces. No indication of a stability β-limit has yet been found. During transition to high-β, in particular at lower densities, global Alfvén gap modes (AEs) with frequencies of up to ≈ 300 kHz can be excited. They disappear, however, with increasing density, where the fast ion content is reduced.

Results of further numerical stability studies, both of Alfvén instabilities and pressure-driven ideal modes, are roughly consistent with the observed MHD effects. A more detailed comparison of experimental data with theoretical predictions, which requires that realistic internal current distributions for the equilibrium reconstruction and resistive effects are taken into account, is under way.

The main objectives of the experiments with significant net currents in W7-AS were to study the effect of current induced rotational transform and shear on confinement and equilibrium in the high-β regime and to investigate the influence of rational surfaces and shear on low m/n pressure driven modes. Also, current driven MHD can be an important issue in hybrid systems such as the quasi-axisymmetric stellarator, where the bootstrap current contributes significantly to the rotational transform. We have applied OH-current ramps in co- and counter-directions up to 20 kA, similarly as in previous low-β studies, which aimed at the assessment of the stabilizing effect of the external rotational transform on tearing modes and disruptions.

At low external rotational transform the energy content increases significantly with increasing co-current. This is attributed to the increase of the equilibrium β-limit at higher total rotational transform and a change of the plasma volume. However, the plasma energy collapses in most cases due to the onset of strong tearing mode activity, particularly when $\iota = 1/2$ is formed in the gradient region (Fig. 8). Vice versa the maximum achievable β is reduced by currents in counter-direction. This is a similar equilibrium β effect as described in Fig. 6. No significant current driven MHD effects are seen in this case, presumably because of the involvement of more stable resonances with higher poloidal mode numbers m and/or the stabilizing effect of reversed shear configurations on the island growth.

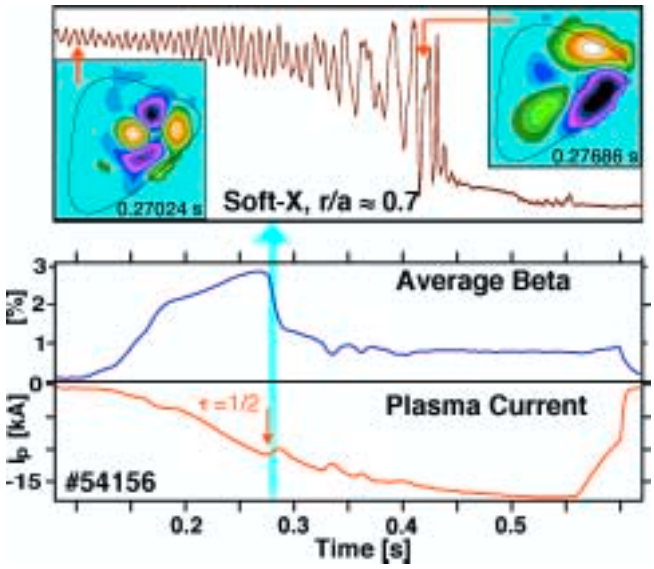

Figure 8: OH-current ramp up to -17 kA at $\iota_{ext} = 0.3$. The energy content rises with increasing ι. A thermal collapse induced by tearing modes occurs when $\iota = 1/2$ is formed in the gradient region.

2.3 Conventional H-mode

H-mode studies concentrated on the physics of the LH-transition, the parameter dependence of ELMs, and the operational boundaries between conventional H-mode and High Density H-mode (HDH).

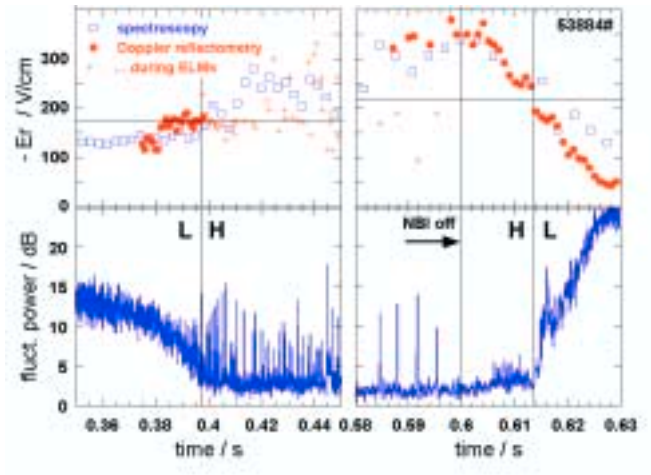

Figure 9: Plasma rotation (upper traces) and turbulence (lower traces) obtained from Doppler reflectometry at the L to H (left) and H to L transition (right). Probed density is $2 \cdot 10^{19}$ m^{-3} correspondingto 2 cm inside the 5/10 island separatrix. Spectroscopic data interpolated to the same radius are shown for comparison as open symbolss. The H-mode is initially characterized by grassy ELMs. Transition and back-transition occur at about the same rotation velocity of turbulence corresponding to $E_r \approx$ - 200 V/cm, i.e. $\Delta E_r \approx$ - 100 V/cm.

In the operational window with 5/10 island edge the LH- and HL-transitions were investigated in detail with respect to edge profile gradients, plasma rotation and turbulence (see Fig. 9). A maximum energy gain of $\Delta W/W = 56\%$ was achieved with a spontanous transition which evolves from a flat-top of the average density. The achieved H-mode characterized by grassy ELMs could be maintained for 200 ms with only a slight increase in radiation.
For the standard island divertor configuration (5/9 island edge) the operational boundaries between conventional quiescent H*-mode, HDH-mode and ELMy scenarios were explored with respect to heating power and density (Fig. 10). The quiescent H-mode was achieved with ECRH and NBI down to extremly low heating power.

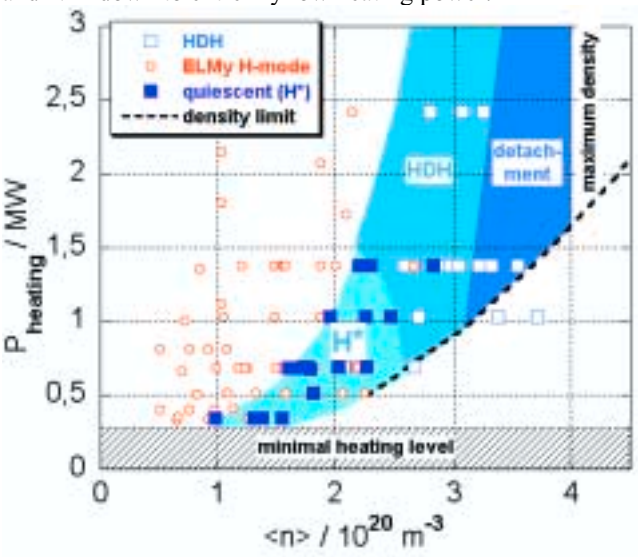

Figure 10: Operational ranges for different H-mode variants in W7-AS. Operational boundaries are included for orientation: minimum heating, maximum achieved density and the density limit.

2.4 "Optimised confinement" discharges with high ion temperatures with divertor

Prior to installing a divertor in W7-AS ion temperatures as high as 1.5 keV had been obtained in "optimised confinement" discharges (τ_E about twice as high as τ_E^{ISS95}) with combined heating of ECR (1-2 gyrotrons, 350-700 kW) and NBI (up to 850 kW of deposited power), at moderate central densities of about 5-6 10^{19} m^{-3} and at a rotational transform of $\iota = 1/3$ with a maximum plasma energy of 17 kJ. At $\iota = 1/2$ with about 300 kW of ECRH and less than 580 kW of absorbed NBI power slightly reduced ion temperatures of 1.3 keV and a plasma energy of 15 kJ could be achieved. Higher NBI heating powers at both ι - values resulted in non-steady-state conditions losing density control. In both cases intense conditioning of the machine and careful positioning the plasma, in order to avoid strong interactions with limiters or walls, had been essential to provide low recycling conditions.
By installing divertor elements into W7-AS the effective plasma radius was reduced from about 16.5 cm to about 15 cm. Despite this reduction and thus reduced plasma volume it was possible to keep the discharges stationary even with 4 NBI sources at both ι - values with about 1.3 MW absorbed power. Discharges with central ion temperatures of up to 1.7 keV at densities of about 6 10^{19} m^{-3} were performed with a maximum plasma energy of 22 kJ at $\iota = 1/3$ and with 19 kJ at $\iota = 1/2$. As in the case without divertor, the choice of the operating gas, hydrogen or deuterium, caused only minor differences. Furthermore, changes of the plasma configuration and position which had been fatal without divertor, were found to reduce the ion temperatures only moderately (10-15%). Thus it must be concluded that installation of the divertor was highly beneficial for achieving high (optimised) confinement conditions with high ion temperatures at moderate densities, mainly by considerably reducing the recycling in W7-AS, even if the discharges were run as limiter plasmas against the divertor target plates.

2.5 SOL and edge fluctuations

Inclination of fluctuation structures in the poloidal-radial plane had been demonstrated in earlier Langmuir probe measurements. Two possible reasons for such inclination were identified, which could be distinguished by observation, if the magnetic field was reversed. The lithium laser blow-off diagnostic, run in collaboration with FZ Julich and the Research Institute for Particle and Nuclear Physics, Budapest, was used to close the gap in the ealier observations and demonstrate that the observed inclination of the fluctuations is mainly due to the strong local magnetic shear of the W7-AS magnetic field configuration in conjunction with the high correlation of the edge fluctuations parallel to the magnetic field.
The first results from a poloidal array of 15 fast-swept Langmuir probes (see diagnostic development for W7-X) demonstrate the possibility of calculating the poloidal-temporal correlation functions and cross-spectra of simultaneously measured density, electron temperature, and potential fluctuations.
In order to complement the fast-swept Langmuir probes and better understand the probe theory necessary for their interpretation, emissive probes were used in several discharges for the first time in W7-AS. Measurements with these probes gave us important information on the amplitudes of and relative phases between floating potential and plasma potential fluctuations. The differences in potentials measured by emissive and non-emissive probes agree well with the expectations from probe theory.

2.5.1 Fast camera observations

A fast-framing CCD camera was used to observe part of the W7-AS divertor (see diagnostic development for W7-X). First results show that the H-alpha radiation during large edge-localized modes (type I ELMs) moves radially across the divertor tiles. The direction of this movement could be qualitatively explained by changes in the pressure profile due to the large particle loss during ELMs. During certain discharges, a radiative instability with intensity changes on time-scales of the order of 1 ms was observed. This phenomenon resembles MARFEs as observed in high-density tokamak discharges.

2.5.2 Fluctuations in the confinement region and during changes in the confinement regime

Density fluctuations in the confinement region of W7-AS were compared for different confinement states in measurements with the LOTUS CO_2 laser collective

scattering diagnostic, which was operated by Risø National Laboratory, Denmark, and CAT Science Bt., Budapest. Analysis of these data shows that the fluctuation level in different ranges of the wavenumber component perpendicular to the magnetic field can change in different ways at the transition between confinement regimes. In particular, a decrease of energy confinement time is not necessarily related to an increase of the fluctuation amplitude.

A search for experimental hints towards ETG turbulence was conducted using the LOTUS CO_2 scattering system, after numerical studies had shown that such turbulence could be expected in frequency and wavenumber ranges accessible with this diagnostic in W7-AS discharges with steep electron temperature gradients. So far, no features indicating the presence of ETG turbulence have been found in the spectra above the noise level. It will be tried to reduce the noise level in a further analysis, since the signal level expected from the theoretical analysis would indeed be rather low.

2.6 Electron Bernstein waves

2.6.1 Heating at high harmonic resonances

At W7-AS electron Bernstein waves (EBW) are strongly absorbed even at higher cyclotron resonances. Therefore, also the third and fourth-harmonic OXB heating was investigated with 140 GHz at 1.5 T and 1.1 T, respectively. Here both the plasma energy and the plasma beta could be significantly increased. Although central power deposition could not be achieved, a clear dependence on the magnetic field was found. The OXB conversion efficiency showed a strong dependence on the density gradient at the plasma edge, which increases with the peak density. The conversion efficiency could be determined from the ECRH stray radiation, which was measured far away from the ECRH launch antenna as shown in Fig. 11. When the peak density reached the cut-off density the reflection was nearly total, the stray radiation level was maximal, and the OXB conversion was minimal. With increasing density, the stray radiation level dropped to below 10% of the maximum value, which indicates that the conversion efficiency rose to above 90%. This result is very promising for high-density and high-β ECRH operation at W7-X.

2.6.2 EBW-current drive (EBCD)

The propagation of EBW's strongly depends on the magnetic configuration. Therefore the current drive efficiency was optimised by varying the magnetic mirror ratio. For the first-harmonic 70 GHz EBW's the highest current was found at standard mirror ratio for the co-direction and at increased mirror ratio for the counter-direction with respect to the magnetic field. The results could be confirmed by ray-tracing calculations, which clearly show the change of the sign of the parallel refractive index $N_{||}$ in the co- and counter-current case. With a detailed analysis of all plasma currents a normalised current drive efficiency of

could be estimated where I_{CD}, P_{HF} and R_o are driven current, HF power and major plasma radius. The dimensionless CD efficiency exceeds those of standard electron cyclotron CD by a factor of 2-3. This was confirmed by Fokker-Planck calculations. In comparison with standard ECCD, for EBCD the phase space interaction is far away from the trapped electrons and mainly supra-thermal electron are involved.

$$\zeta = \frac{e^2 I_{CD} n_e R_0}{\varepsilon_0^2 P_{HF} T_e} = 0.43 \pm 0.1 \quad \left(\frac{I_{CD}}{P_{HF}} \left[\frac{kA}{kW} \right], \frac{n_e R_o}{T_e} \left[\frac{10^{20}}{m^2 eV} \right] \right)$$

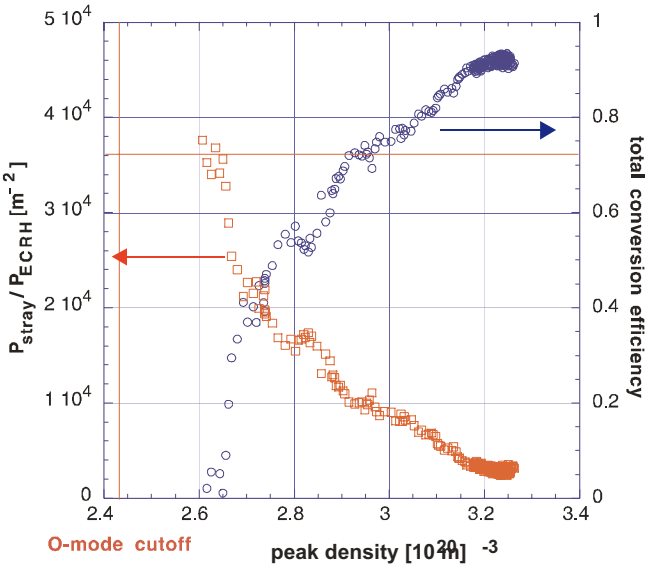

Figure 11: Relative stray radiation level (red squares) and total OXB conversion efficiency (blue circles) as functions of the peak density.

2.7 Tangential and perpendicular neutral beam injection

In 2002 NBI at W7-AS was fully operational with its final stage: two tangential co-injectors (2.8 MW heating power) and one radial injector. The co-injection was the "working horse" for the heating of W7-AS, especially for high beta and HDH discharges. On the scientific side a new attempt was made to measure the heating power in power modulation experiments with the ECE diagnostic. One channel of the ECE was connected directly to the NBI current signals. This minimizes the uncertainty of previous measurements using different ADC's. Modulation experiments were carried out also with deuterium injection for different plasma and heating scenarios.

The almost RADIal neutral beam injector RADI with two RF-sources provides nominal 550 kW power at an injection energy of 50 keV. Thus, energetic ions are created in the vicinity of a loss cone and lost without substantial slowing down. As the radial electric field E_r is determined by the ambipolar radial particle fluxes, the solution of the ambipolarity condition is modified by the driven fast ion orbit flux. The ion orbit losses drive therefore E_r more negative so that its value is increased. Such an increased E_r is expected to improve the global discharge confinement properties, both for the neoclassical and the anomalous transport.

Parameters scans were performed during discharges, where the impact of RADI was compared to tangential NBI heating and the change of E_r maximised with respect to global energy confinement. Maximum changes of E_r

obtained from passive BIV spectroscopy were ≈ - 200 V/cm. This is comparable to the amplitude of the ambipolar solution. The increase of the global energy content was up to 10%. However, this rather small value can be explained by the fact that the injection is not completely perpendicular so that the plasma is also directly heated.

2.8 Gasjet and pellet injection experiments

For W7-X, neoclassical transport calculations predict a strong particle outward transport, driven by the electron temperature gradient, so that flat or even hollow density profiles might result, with subsequent onset of instabilities and impurity accumulation. Thus central particle fuelling might be necessary. Therefore, two methods of deep particle fueling were tested on W7-AS.

With a new gasjet injector hydrogen gas is puffed at high pressure (up to 50 bar) through a small nozzle (0.1 mm diameter) into the plasma. Due to the large pressure difference, the gas is accelerated to supersonic velocities and penetrates deeply into the plasma as a supersonic gasjet. The effect of the gasjet was studied in ECRH heated plasmas and during the fast density increase after the start-up phase of high-β discharge. In the experiments, only a slight and transient density peaking could be monitored whereas the energy confinement was not improved. With deuterium ice pellet injection it was demonstrated that deep particle fuelling into ECRH discharges is feasible with pellet injection, even with enhanced pellet ablation due to the high ECRH power.

2.9 Theory

2.9.1 International collaboration in neoclassical theory

The benchmarking of various numerical tools for determining neoclassical transport coefficients was continued. First efforts were also made to describe the results using a fast semi-analytic approach appropriate for use in transport analysis as well as for predictive transport modelling. An example of numerical results and their semi-analytic representations is provided in Fig. 12 for the inward-shifted LHD, a configuration with a high degree of drift optimization (in collaboration with V. Tribaldos, CIEMAT; S. Murakami and A. Wakasa, NIFS; D.R. Mikkelsen and R.B. White, PPPL; W. Kernbichler and S. Kasilov, TU-Graz; D.A. Spong, ORNL).

2.9.2 Advanced δf Monte Carlo techniques

A new stellarator-specific δf Monte Carlo method (based on the Maxwellian as the inhomogeneity) for estimating the mono-energetic transport coefficients was implemented and tested. For the diagonal coefficients, i.e. the radial transport and parallel conductivity, good statistical properties are obtained, whereas estimation of the off-diagonals, i.e. the bootstrap current and the Ware pinch, is problematic due to the unfavourable weighting (due to ripple-trapped particles for the bootstrap coefficient). In the new advanced methods analytic estimates of the distribution function in next order are added to the inhomogeneity in order to improve the statistical convergence properties (collaboration with V. Tribaldos, CIEMAT, and S. Murakami, NIFS).

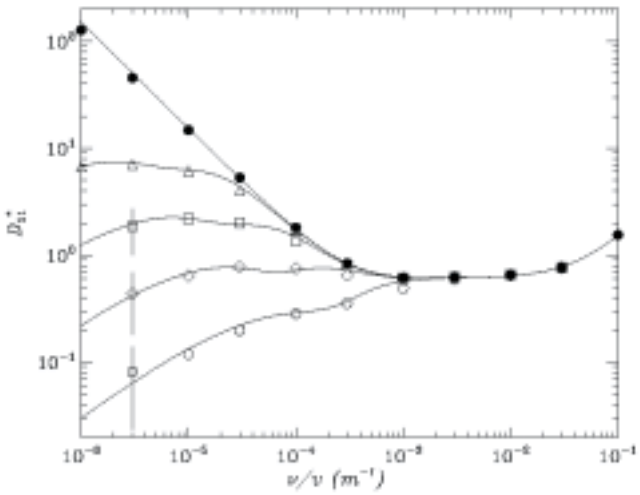

Figure 12: Normalized mono-energetic radial transport coefficients are plotted as a function of "collisionality" (ν/υ) for the inward-shifted LHD configuration. Numerical results from the Drift Kinetic Equation Solver (DKES) are shown as symbols, the semi-analytic descriptions of these results are given by the curves. Five different values of the radial electric field ($E/\upsilon B_0$) were considered.

2.9.3 Predictive transport code development

In addition to the particle and energy balance equations together with a diffusion equation for the ambipolar radial electric field, the current diffusion equation was implemented in the new predictive transport code. The interface to the databases of the neoclassical transport with the bootstrap current and the electrical conductivity taken into account was installed.

2.9.4 Hint code

A β-sequence was calculated to study first the influence of increasing β on the separatrix geometry of a W7-AS high-ι configuration at 5/9. Due to difficulties in handling coils close to the plasma the configuration did not include the correction coils used in the divertor experiments. The basic effect was an increase of the boundary island width with β leading to stronger identation of the separatrix. The x-points moved poloidally at the same time in accordance with the change in the magnetic coordinate due to the Shafranov shift. Additionally, on the basis of a last closed flux surface derived from the HINT results, the equilibria were recalculated with NEMEC, confirming the main effects on the bulk plasma. A benchmark with the PIES code developed at Princeton was started to increase the confidence in both codes and make further progress in their development (collaboration with T. Hayashi, NIFS, A. Reiman, PPPL, and M. Drevlack, ST)

2.9.5 W7-X version of TRANS library

A version of the TRANS library used at W7-AS for real-space to magnetic coordinate transformation has been developed, so that programs used for W7-AS can easily be used for diagnostic development for W7-X. This provides a preliminary tool until a more elaborate approach based on function parametrisation or neural network techniques becomes available.

2.9.6 EMC3-EIRENE modelling

The EMC3-EIRENE code was completely restructured by implementing the new "Finite Flux Tube" geometry and the new "Reversible Field Line Mapping" technique. This has extended the code applicability to general 3D magnetic edge structures, including open configurations of arbitrary stochasticity. Additionally to the previous benchmarks with the B2 code for a slab model, all equation terms sensitive to the field geometry were separately checked by benchmarking the code with an analytic model exhibiting strongly curved field lines. The accuracy of the RFLM technique for strongly stochastic fields was also checked by comparing the field line density distribution and the deposition profiles on the TEXTOR-DED limiter with the results of a direct field-line integration with the GOURDON code. As a first application to a 3D tokamak, the code has been implemented for TEXTOR-DED. First simulations including a fully self-consistent treatment of plasma mass, momentum, energy, and neutral gas equations with realistic boundary conditions at the limiter were successfully carried out for both the strongly stochastic 3D and the axisymmetric 2D cases (collaboration with M. Kobayashi and D. Reiter, IPP Julich).

2.9.7 High power neutral beam current drive

Contrary to tokamaks, where (anomalous) momentum transport must compensate the strong NBI momentum source, the friction with ripple-trapped particles in stellarators represents a significant momentum sink. The implementation of the full non-linear momentum balance in the bounce-averaged Fokker-Planck code, FPTM, allows one to treat the neutral beam current drive (NBCD) for high power at low collisionality. Furthermore, for better simulation of the NBCD experiments at W7-AS, it is necessary to improve the treatment of the electron Ohkawa current, which is presently available only in the collisional and the collisionless limits.

2.9.8 Electron Bernstein current drive

Electron Bernstein wave heating and current drive are implemented in quasi-linear formulation in the bounce-averaged Fokker-Planck code, FPTM. In addition to traditional ECCD with the anisotropy in the conductivity, the high $|N|_{||} \cong 1$ leads to a direct momentum source. For the fairly high collisionalities in the W7-AS experiments, bounce-averaging underestimates the EBCD efficiency (missing current diffusion into the trapped particle domain).

2.9.9 Kinetic stability analysis

The slowing-down distribution functions of the fast NBI ions for the quite different injection scenarios (tangential, new "radial", and diagnostic beams) are analysed with respect to the stability of ion Bernstein modes with harmonics up to the lower hybrid frequency (WTZ collaboration with E. Suvorov, IAP, Nizhny Novgorod).

2.9.10 Integrated data analysis

Realisation of integrated data analysis concepts was continued. Systematic combination of probability density functions of quantities to be measured was performed within the framework of Bayesian probability theory. The outcome shows gain of information. The major workload, however, is given by the development and exploration of statistical models representing distinct measurements. Here, progress for the Ruby Thomson scattering system and the ECE radiometer system has been achieved. First results for a joint evaluation of a statistical model with a function parametrisation of equilibrium calculations were derived. This approach represents the key issue for a combination of plasma bulk diagnostics measuring on different lines of sight. Concepts for diagnostics software developments for W7-X were also discussed within the second European workshop on data validation, which was held in autumn 2002 at Greifswald. Efforts on data consistency checks and data validation on W7-AS data were continued (cooperation with R. Fischer, S. Gori, Y. S. Yoon, and U. v. Toussaint, CIPS).

3 Diagnostic development

In view of the shutdown of W7-AS in July 2002 only minor modifications or completions of diagnostics were made. Some diagnostics were further developed with regard to the needs of W7-X.

3.1 Ruby Thomson scattering diagnostic

The diagnostic, whose set-up was described in the last annual report, was successfully in operation until the end of the last W7-AS campaign. It proved its suitability especially for high-density plasma operation (HDH-mode and high-ß discharges) where the maximum electron temperatures in the central region of the plasma are limited to a few hundred eV, which fits well to the spectral range of the detection system. A major topic in further diagnostic development remaining is the handling of the plasma radiation fraction of the signal, which greatly affects the data analysis.

3.2 Periodic multichannel Thomson scattering

In 2002, modification of the Nd-YAG Thomson scattering system for implementation of the island divertor was completed. The W7-AS detection system consists of 13 spatial channels, each equipped with its own polychromator. The basic design of the polychromators now consists of four spectral channels, in order to improve measurements at the very high densities obtained with the island divertor. Systematic modelling within the Bayesian probability theory is continued for reconstructing n_e und T_e profiles.

3.3 Multichannel Doppler reflectometry

A Doppler reflectometer which measures propagation velocity and amplitude of small scale turbulence (Lamda about 0.7 cm) with a temporal resolution of less than 10 µs at six radial positions simultaneously was developed in collaboration with IPF Stuttgart (for further details see contribution of IPF Stuttgart, chapter 1.3.1). In the final campaign of W7-AS the system was operated rountinely to study the interaction between turbulence and sheared flows, in particular in different confinement regimes. An example of a result obtained during an H-mode discharge is shown in Fig. 9.

3.4 Divertor thermography

At W7-AS two infrared cameras monitor simultaneously the power flux onto two opposite divertor modules via 50° endoscopes placed in re-entrance ports. A 3D finite-element code is used to derive the actual power flux from the measured temperature evolution at the target. In order to study power deposition during ELMs, the fast camera of the two infrared cameras was adapted for high-resolution measurements (in time $\delta t \approx 200$ µs, in space $\delta r \approx 4$ mm). Thus, temperature measurement were limited to the area of a single target tile, usually the most exposed one.

Fig. 13a shows the power flux onto the divertor target at the transition from an L-phase into an ELMy H-mode. Between ELMs, there is basically no power flux. Fig. 13b shows target plate deposition profiles for various conditions: L-phase, H*-phase and the flux between ELMs. All the energy of an ELM is deposited at about the same width.

Figure 13: Profiles of the power deposition onto the divertor target: a) at

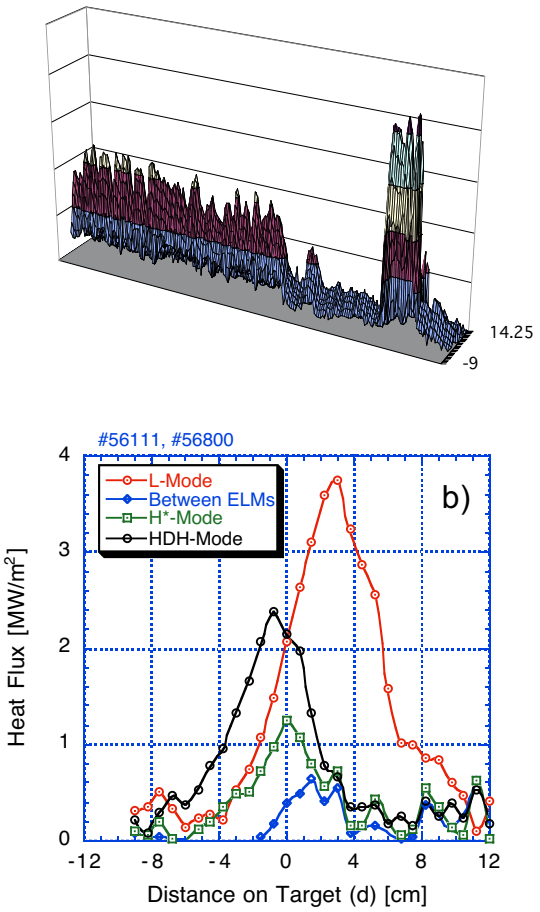

the transition from L- to ELMy H-mode, b) deposition profiles in different regimes.

3.5 Fabry-Perot spectrometer for CXRS

A high-speed spectroscopic system was installed on W7-AS to perform fast Charge Exchange Recombination Spectroscopy (CXRS) in a neutral beam. This system consists of a temperature-stabilised Fabry-Perot cell. The spectral dispersion is attained by imaging of the spectral light under a well-defined angle across the Fabry-Perot. A back-illuminated high-speed CCD camera system is used as detector. It allows a full transfer rate of up to 1 kHz. The spectral light from the interaction volume between the W7-AS plasma and the neutral beam is guided to the Fabry-Perot via six individual fibres of 1 mm diameter in a hexagonal arrangement. Thus, this set-up allows simultaneous CXRS measurement at six radial locations with a high spectral resolution of 0.2 Angstrom and high time resolution of 1 msec. The arrangement was used to measure the local ion temperature and the toroidal impurity rotation in W7-AS on the spectral lines of carbon VI and helium II.

4 Scientific Staff*

V. Afanasiev[11], T. Andreeva[17], C. Beidler, A. Bencze[7], M. Berta[7], A. Blagoev[2], T. Bindemann[17], R. Brakel, H. Braune, A. Dinklage, A. Dodhy, L. Empacher[6], V. Erckmann, Y. Feng, F. Gandini[8], G. Gantenbein[6], J. Geiger, L. Giannone, E. Harmeyer, H.J. Hartfuss, F. Herrnegger, C. Hidalgo[12], E. Holzhauer[6], J. Howard[1], K. Horvath[18], Y. Igitkhanov, K. Ida[9], S. Inagaki[9], R. Jaenicke, F. Karger, W. Kasparek[6], A. Kislyakov[11], J. Kisslinger, J. Knauer, M. Kobayashi[5], G. Y. Kolesnichenko[14], St. Koslovsky[11], A. Kreter[5], G. Kuehner, A. Kus, H. Laqua, J. Lingertat, R. Liu, J. Lyon[15], H. Maassberg, V. Marchenko[14], S. Marsen[19], N. Marushchenko, G. Michel, A. Mikkelsen[16], D. Monticello[16], S. Murakami[9], U. Neuner, M. Osakabe[9], M. Otte, E. Pasch, G. Petravich[7], E. Polunovsky[17], A. Reichert[19], A. Reiman[16], M. Rome[8], J. Sallander, F. Sardei, M. Schmidt[17], P.G. Schueller[6] K. Schwoerer[6], A. Shalashov[10], A. Sengupta[4], O. Shishkin[13], J. Volpe[18], M. Yoshinuma[9], F. Wagner, H. Wobig, H. Yamada[9], K. Yamazaki[9], L. Yao[3], M. Zarnstorff[16], D. Zimmermann

5 Technical Staff

G. Abele, P. Ahlrep, J. Ahmels, D. Assmus, T. Broszat, K. Ewert, H. Greve, U. Herbst, J. Hofner, F. Hollmann, J. Jonitz, P. Junghanns, B. Kursinski, K. Lehmann, U. Neumann, F. Noke, N. Paschkowski, F. Purps, T. Richert, H. Schmidt, T. Schulz, W. Schulz, H. Speer, M. Steffen, H. Volkenandt, G. Zangl, Do. Zimmermann, K. Zimmermann

*

1) Guest from Univ. of Australia, Canberra (Australia)
2) Guest from University of Sofia (Bulgaria)
3) Guest from SWIP, Chengdu (China)
4) Guest from University of Cork (Eire)
5) Guest from FZ Juelich (Germany)
6) Guest from IPF Stuttgart (Germany)
7) Guest from KFKI Research Inst., Budapest (Hungary)
8) Guest from University of Milan (Italy)
9) Guest from NIFS, Nagoya (Japan)
10) Guest from IAP Nizhny Novgorod (Russia)
11) Guest from IOFFE Institute, St. Petersburg (Russia)
12) Guest from CIEMAT, Madrid (Spain)
13) Guest from IPP Kharkov (Ukraine)
14) Guest from NUCRESI, Kyiv (Ukraine)
15) Guest from ORNL, Oak Ridge (USA)
16) Guest from PPPL, Princeton (USA)
17) Postdoc
18) Doctoral fellow
19) Graduand

WENDELSTEIN 7-X CONSTRUCTION

Head: Dr. Manfred Wanner

1 INTRODUCTION

The W7-X Construction project is responsible for the design, manufacture, and assembly of the W7-X stellarator, the heating systems, the power supplies, the cooling system, and the system control.

The main components of the stellarator are the superconducting magnet system to confine the plasma, the cryostat to insulate the cryogenic parts, the ports to observe and heat the plasma, and the plasma-facing components to control the energy and particle exhaust. Steady-state plasma heating is based on powerful ECR sources. In addition, the plasma temperature and density can be increased by pulses of ICR or NBI heating. The superconducting coils are energised with high current by dedicated supplies and kept at a temperature close to absolute zero by a helium refrigeration plant. Safe operation of the magnet system is ensured by fast detection of quenches and subsequent shut-down. The microwave sources and the NBI system are supplied with high voltage. A total input power of about 48 MW is required to operate the magnet system, supply the heating systems, and provide power for cryogenic refrigeration. Waste heat is removed by circulating water which is re-cooled by cooling towers. At a later stage NBI heating is to be upgraded to 20 MW to explore the high-density regimes and the _-limit of W7-X.

Production of most of the W7-X components made good progress in 2002. The power supplies for the control coils were installed and commissioned.

Nevertheless, the project faces a significant delay. Initially qualification of series production of the superconductor for the coils required more effort than planned. In 2002 the processes were improved, which increased the production capacity. In addition, several steps of the production of the non-planar and planar coils were not tested in time, which further delayed delivery of the coils. During summer, the contractor supplying the non-planar coils, Babcock Noell Nuclear, filed bankruptcy. Although the contract was successfully re-negotiated and the company is meanwhile producing again, there is further delay in delivery of the first coils. Although the coil manufacturer intends to speed up production the delay cannot be recovered. Prior to assembly all superconducting coils will be tested under operational conditions at the Low Temperature Laboratory of Commissariat à L'Énergie Atomique (CEA) in Saclay. The facilities are prepared and ready to receive coils. Several tests with the DEMO coil were performed to optimise the test procedure and find ways to advance the series tests.

Assembly of W7-X was detailed and assessed by a review board. Measures to accelerate assembly of W7-X are being assessed.

In summary, the consequence of the delayed delivery of the coils and the implications for assembly is a new date for commissioning W7-X and mapping the magnetic field at the beginning of 2010.

FZK is contributing the complete ECRH system for W7-X. After successful testing of a pre-prototype in 2001 and of the first prototype in summer 2002, which achieved a record performance of 0.9 MW for a pulse length of 180 s, development of a continuously working 140 GHz gyrotron by FZK, European Industry, and CRPP Lausanne was completed.

The University of Rostock and the University of Applied Sciences at Neubrandenburg are supporting the project with specific tasks. Co-operation was started with the D.V. Efremov Scientific Research Institute of Electrophysical Apparatus in St. Petersburg to perform structural analyses and characterise components at cryogenic temperatures. Forschungszentrum Julich, which already contributes to the project Diagnostics for W7-X, will take over engineering tasks within the W7-X Construction project.

Production of all W7-X components is quality-controlled by a quality management system which follows the standards of ISO 9001. The work flow is described in quality inspection and production plans, new processes are verified and approved before application, tests follow written procedures, and deviations are notified and handled through non-conformance reports. Fabrication at the contractors premises is witnessed by inspectors. Samples taken during manufacture are independently checked by IPP through regional laboratories.

2 BASIC MACHINE

2.1 Magnet System

The main components of the magnet system are the superconducting coils, the coil support structure, and the power supplies. All components of the magnet system are in an advanced state of fabrication. Babcock Noell Nuclear (BNN)/Ansaldo consortium made progress in the design and manufacture of the 50 non-planar coils. Tesla wound several planar coils and the main parts of the coil support structure were manufactured. The power supplies and the coil protection system are being fabricated and critical components were tested.

2.1.1 Superconductor

The superconducting cable is composed of 243 strands enclosed by an aluminium jacket. A total of 360 conductor lengths, typically 120 to 180 m long, are required to wind all superconducting coils. The conductor is being manufactured by the VAC/EM consortium. Difficulties experienced in the past during twisting of the strands, jacketing the cable, and verifying the specified properties of the conductor were overcome. In particular, the shortfalls of the helium leak test facility at EM were removed by installing a new vacuum test facility. By the end of December 2002, 206 conductor lengths were manufactured. The delivered lengths are sufficient for ten non-planar and eight planar coils.

IPP supervises all steps of conductor production by inspectors. A number of analyses and tests accompanied the quality tests of the manufacturers and helped to improve understanding of the flow dynamics within the conductor.

Integrity of the superconducting cable and the absence of impurities in the cooling channel are of fundamental importance for proper cooling of the coils. During cabling of the strands, slings and abrasion were occasionally observed. As a consequence the surface of the full length of each rope is checked for broken strands and loops and documented by a digital camera system. The cleanliness of the rope was also checked after extrusion of the Al jacket by washing samples through a filter. The size and amount of copper particles was in an acceptable range.

Works tests after conductor production showed that the gas flow through the cable-in-conduit conductor does not correlate with the void fraction as expected. Additional laboratory tests were therefore performed in a wide range of Reynolds numbers. Although the measured dependence of the pressure drop on throughput, temperature, pressure, and the gas used could be described by an ansatz, the dependence of the flow on the void fraction is still an open question. It was assumed that this phenomenon could be explained by a strong variation of the void fraction along the conductor. This was excluded, however, by measuring the void fraction of a series of samples taken from one length of conductor. The observed variations were below ±1%.

2.1.2 Superconducting coils

The non-planar coils are being wound on three winding lines at Ansaldo and two winding lines at BNN's subcontractor, ABB. Production of the winding packages at Ansaldo is supervised by an inspector. By end of 2002 three winding packages were ready for integration and several more were in different stages of winding (see Fig. 1).

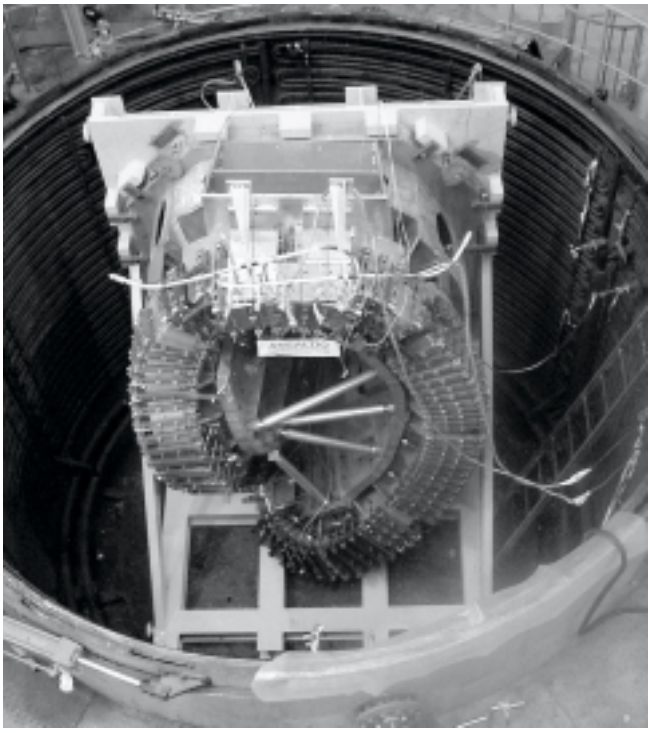

Figure 1: Non-planar winding package prior to vacuum impregnation (by courtesy of Ansaldo Superconduttori)

Control of the specified contour of the winding package requires precise measurement of approx. 1,000 co-ordinates on the surface, a best fit of the measured data to the CAD model, and transformation of the contour information to eight reference pins on each winding package. The co-ordinates of these pins represent the geometry of the winding package and are used during final machining of the coil casing and during assembly.

Some thirty half-shells for the coil casings were cast, heat treated, and machined by the Swedish subcontractor, Osterby Gjuteri AB. The cooling design of the cases was improved. The technique of spraying copper on the complicated surfaces of the cases was replaced because of the great effort in applying the copper and the difficulty in controlling and maintaining the required heat conductivity of the amorphous copper. In the new concept approx. 1/3 of the surface of the casing will be covered by strips of highly conductive sheet copper. The strips are welded to the casing and attached to the helium cooling pipes by soldering. The new concept also reduces eddy current heating of the coils in case of rapid shut-down of the magnet system.

Integration started at the production site of BNN at Zeitz and two coils were integrated and embedded in the casing

(see Fig. 2). The first non-planar coil is expected to be available for testing at Saclay in May 2003.

Design of the 20 planar coils at Tesla Engineering was basically completed and the first coil was already expected in 2002. Tesla experienced, however, a number of difficulties during production of the winding packages and casings, qualification of components, and testing.

Four winding packages were produced and one was integrated into the casing and embedded. Survey of the shape of the first winding packages revealed local deviations which were significantly larger than specified. The winding packages can be used, however, since the packages of one type of coil are sufficiently identical in shape.

The coil casings of the planar coils are manufactured from plate material. For each casing a U-shaped base part and a plane top plate are screwed together. The first coil was embedded and delivery is scheduled for May 2003.

Insulating the electric circuits of the winding package from the helium pipes requires special voltage breakers. These joints are made by two stainless-steel pipes connected by an insulating epoxy tube. The voltage breakers have to withstand a maximum voltage of 13 kV and allow different thermal contractions of the dissimilar materials during cool-down. Temperature cycle tests were performed with several voltage breakers at IPP to select the most reliable design. The design selected is already successfully in use at FZK and other laboratories and will now be used throughout the machine.

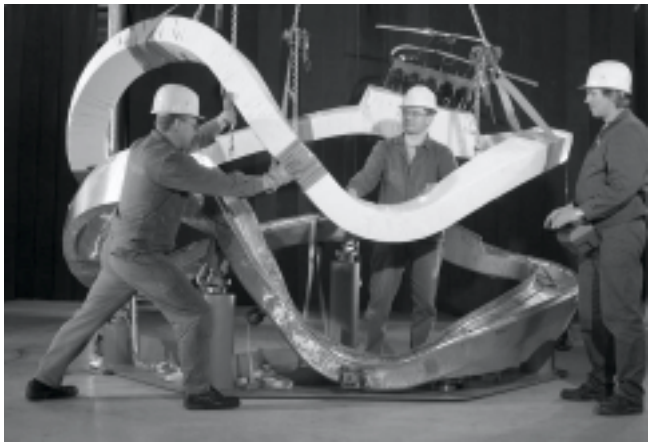

Figure 2: Non-planar winding package and lower half of the casing (by courtesy of BNN)

2.1.3 Coil support structure

The coil support structure is being manufactured by the Spanish contractor, Equipos Nucleares, S.A. and consists of ten identical sectors with a total weight of 72 t which are joined by screws to span a central pentagon. Ten supports carry the structure and provide the thermal barrier between the cold structure and the base plate. The coil support structure is made from steel plates and cast steel elements for the coil fixtures. Seven segments were pre-fabricated.

A detailed structural analysis of the magnet system by the Central Technical Services of IPP revealed that the screws which are to connect the coils with the coil support structure are overloaded during certain modes of operation. Measures to reinforce the magnet system and the coil connections are being investigated.

2.1.4 Magnet current supply

The five types of non-planar and two types of planar coils are powered by supplies which provide direct currents of up to 20 kA at voltages of less than 30 V. The Swiss contractor, ABB, selected the concept of twelve-pulse rectifiers to ensure that the currents are stabilised with an accuracy of $2x10^{-3}$.
Fast and reliable discharge of the superconducting magnets in case of a quench is realised by a fast circuit which short-circuits the coils and dumps the magnet energy to nickel resistors. These resistors feature a high heat capacity and a strong increase of the resistance with temperature. The switching voltages can thus be kept low. Production of the resistors was started and the breakers passed the works tests. The control concept was designed in detail and took into account the required detection of grounding defects in the electronic circuits.

2.1.5 Current leads

Fourteen current leads capable of carrying 20 kA connect the seven groups of superconducting coils with the power supplies. The concept is based on conventional current leads which are designed for lower than nominal current, and overloaded during nominal operation. In this way the heat conduction along the current leads and hence the cooling requirements are reduced during stand-by periods. The leads are fixed to the outer vessel and the coil support structure. The design keeps movements of the connected bus system within tolerable limits.

2.2 Cryostat

The cryostat provides the thermal protection of the magnet system and gives access to the plasma. Its main components are the plasma vessel, the outer vessel, the ports, and the thermal protection.
The German company, Deggendorfer Werft und Eisenbau GmbH, is responsible for manufacture of the plasma vessel and the outer vessel. The plasma vessel is composed of 20 segments for each half-module. Each half-module is again divided into two parts to allow stringing of the innermost coil during assembly. For each half-module 20 steel rings are precisely bent to the required shape and carefully welded to represent the changing cross-section of the plasma vessel. For local areas which cannot be approximated by bending steel sheets are fitted by hot pressing. The two parts of the first half-module were manufactured (see Fig. 3). The contours of the parts were measured by laser tracking and were well within the given narrow tolerances. Vacuum tightness of the welds will be checked by an integral helium leak test of the segments.

Precise cutting of the holes for the ports will be performed by the water jet technique.

Water pipes around the outside of the vessel allow its temperature to be controlled during plasma operation and for bake out. A process to attach thin-walled steel pipes to the vessel by welding has been qualified.

The outer vessel of W7-X is assembled from five lower and upper half-shells. Design of the vessel was continued and supported by structural analyses for the ports, manholes, domes, and feedthroughs. All upper and lower half-shells of the outer vessel were welded.

Figure 3: Half-module of the plasma vessel (by courtesy of Deggendorfer Werft und Eisenbau GmbH)

Manufacture of the 309 ports is performed by the Swiss company, Romabau. Production of bellows, flanges, and cooling pipes is ongoing. A large bellows with a cross-section of 500x1,000 mm_ successfully passed an endurance test of 1,000 full load cycles.
Efficient insulation of the cold magnet system requires careful protection against thermal radiation by high vacuum and multi-layers of reflecting metallic foils. Efficiency of the thermal protection is enhanced by metallic shields which cover all areas at ambient temperature. These shields are kept at temperatures between 40 K and 70 K by cold helium gas. A study was performed by industry to assess pre-fabrication and assembly of mats of multi-layer insulation. The thermal protection needs to consider rapid shut-down of the magnet system. In that case eddy currents are induced in the shields and the super-insulation. These currents and the resulting forces were modelled to dimension the fixtures for the thermal protection. Tendering activities were continued.

Routing of the cryogenic supply lines in the cryostat was continued and considered the restricted accessibility of the tubes during assembly for joining and leak testing. Modelling of the helium exhaust from the magnets during rapid shutdown was refined. In the worst case of a quench of all superconducting coils the total helium inventory of 500 kg would be released within a few seconds, resulting in maximum flow rates of up to 60 kg/s.

2.3 In-vessel Components

2.3.1 Divertor modelling

The behaviour of the neutral particles in the boundary layer of the W7-X plasma and recycling of impurities were modelled. The EMC3 (Edge Monte Carlo 3D) plasma transport code was adapted to the twisted surface of the W7-X plasma. Recent application of this code to the W7-AS divertor gave results, which were in good agreement with experimental data. In addition, a 3D plasma fluid model based on the W7-X geometry, where strong stochastic effects become important, is being developed by the plasma edge physics group of IPP.

2.3.2 Design of the plasma-facing components

Three different types of surfaces face the W7-X plasma: The divertor target plates are hit predominantly by hot particles from the plasma and have to withstand heat loads of up to 10 MW/m_. Baffles, which influence the fluxes and density of neutralised particles in front of the target plates and improve the pumping efficiency, need to be designed for heat loads of 0.5 MW/m_. The wall protection of the plasma vessel mostly interacts with neutral particles and radiation from the plasma boundary and receives heat loads of up to 0.2 MW/m_. To keep the reflux of impurities from the wall to the plasma at acceptable limits, all plasma-facing surfaces have to be covered with low-Z material. The neutralised particles are removed from the divertor by mechanical vacuum pumps outside the machine. Additional cryo-pumps are installed behind the divertor units to enhance the pumping capacity. Control coils allow one to modify the magnetic configuration and the interaction of the plasma edge with the target plates.

The ideal shape of the target plates has to follow the 3-dimensional boundary of the plasma and is approximated by a series of planes. Combinations of standardised plane target elements with a width of 55 mm and lengths between 270 and 500 mm achieve a nearly constant incidence angle of the particles. After assembly of the 8-13 target elements of the target modules the precise 3-dimensional shape of the plasma-facing surface is achieved by machining.

Each target plate is composed of a water-cooled metallic support and tiles from flat carbon fibre composite (CFC). Precipitation-hardened CuCrZr alloy is used for the support because of its good thermal conductivity and compatibility with the CFC.

The tiles are made from SEPCARB® NB31 because of its high tensile strength and good heat conductivity perpendicular to the tile surface. The same material has also been selected for ITER. A total amount of 700 kg of CFC material was ordered and is being manufactured by the French company, Snecma Propulsion Solide.

The baffles are composed of a water-cooled CuCrZr support and flat graphite tiles of typically 150x150 mm_ which are clamped by screws. The tiles are to be made from improved fine-grain graphite. Samples of this graphite were tested in the MARION test facility of Forschungszentrum Julich and successfully withstood transient heat pulses of 4 MW/m_ for 5.5 s and a maximum power density of 35 MW/m_ for 0.3 s. The same material was recently applied for the inner heat shield elements of ASDEX Upgrade.

The wall of the plasma vessel spans a total area of approx. 120 m_. Two concepts will be used to realise the protection of the plasma vessel: At critical areas where the distance between the plasma boundary and the wall is small the concept of clamped tiles as developed for the baffles will be applied.

The major part of the wall with an area of 70 m^2 will be protected by double-walled steel panels with integrated cooling loop. The panels are to be coated with boron carbide as low-Z material. The panel approach reduces the number of tiles and the carbon inventory and simplifies mounting within the plasma vessel. The complicated surface of the plasma vessel is approximated by cylinder segments of different radii, which further simplifies production. 190 panels with 19 different shapes are required to cover the wall of the plasma vessel.
The Materials Research Division continued studies on the characteristics of boron carbide coating up to 300 μm thick in ASDEX Upgrade and W7-AS (see Plasma-facing Materials and Components)

Design of all plasma-facing components and definition of the instrumentation required for operation and control were continued. The requirements of the diagnostics and the thermal loads from the heating systems were considered. Technical specifications for the plasma facing components were prepared and offers for the fabrication of the components were received. To realise the plasma-facing components within the allocated budget the target area needs to be reduced at the expense of a somewhat higher heat load during plasma operation. In addition, means to reduce the industrial supply by increased internal labour are under investigation.

2.3.3 Pumping

Vacuum pumps are required to evacuate the plasma vessel to a level of less than 10^{-8} mbar before plasma operation in order to control the density of auxiliary gases injected into the divertor chamber and pump out neutral particles. Additional cryo-pumps behind the divertor allow the pumping capacity to be increased during high-density plasma discharges, e.g. during injection of neutral beams or pellets. In such cases particle fluxes of $5x10^{21}$ s^{-1} have to be handled at pressures of about 10^{-3} mbar. For each divertor unit one segmented cryo-pump will be positioned behind the target plates. The cryo-pumps will be designed for a total capacity of 150,000 l/s for a duration of 2 hours.

2.3.4 Control coils

Ten copper coils will be installed in the plasma vessel behind the baffle plates to correct minor field errors, influence the extent and location of the magnetic islands, and allow the power deposition area to be swept across the target plates.

Each coil can be individually supplied with direct currents of up to 3 kA at voltages of up to 30 V, which can be modulated at frequencies of up to 20 Hz by dedicated power supplies. All ten power supplies were delivered and installed by the Spanish contractor, JEMA, and passed preliminary acceptance tests.

Design of the control coils was finished and the tendering documentation was prepared. The coils, with dimensions of 2x0.3 m_, will be wound by 8 turns of hollow copper conductor and cooled by water.

2.4 System Control

The W7-X experiment will be controlled by a master control system with local controllers for all subsystems such as magnets, cryogenics, heating units, diagnostics, and data acquisition. The local controllers will run automatically according to predefined routines and parameters, which will be set from the master control system as long as the units have to co-operate. In order to structure the experiment and all other activities in the system, all periods of operation will be divided into segments of variable duration. A "segment programme" defines the operational rules and parameters which determine the state and activity of each unit in use.

Programmable Logic Controllers (PLCs) will be used mainly to control those machine components and diagnostic systems which do not require short response times. A semi-automated control system for the gas supply of W7-X was completed. The standard control logic is implemented in a Siemens S7/400 PLC, safety interlocks are implemented on a PNOZplus device and the man-machine interface was programmed with WinCC. A WinCC server provides data access to any WinCC client connected to the experiment subnet. All clients have simultaneous and unrestricted access to inspect data, but operation of the system is restricted to one authorised station at a time. The gas control system allows one to run standard procedures such as evacuating pipes or mixing gases in automatic mode. For troubleshooting, each valve, mass flow controller etc. can be operated by manual action on the screen.

Segment processing and fast feedback control, which require data processing in real time, will be performed by PCs running the VxWorks real-time operating system. Special software and hardware are being developed for the segment control system. Software modules for sharing control data between computers and distributing messages

across a network were completed by means of layer 2 Ethernet, UDP or TCP. Prioritisation of data packets on the network is possible. Messages received are routed into different queues depending on the type of message and can be followed up in different tasks with different priority. The software for generating control objects based on information from a data base has still to be developed. A draft specification for an object editor which will be necessary to generate the data base information was prepared in co-operation with the XDV group. Emphasis was put on establishing methods and software tools to develop and document the software projects and control the version. SniFF+ was chosen as a multi-purpose tool offering, besides many other features, a suitable interface to the CVS version control system. The UML tool, Together®, was chosen to design, develop, and document object-oriented software.

A central trigger-time-event system (TTE) will serve to distribute the precise system time, triggers, and event messages. Local TTE-cards in the connected units respond to the central TTE system and have local trigger, time, and event-handling capabilities. A prototype for a local TTE card was developed in co-operation with the University of Rostock. Some cards were manufactured and tests performed with support from the Technical Services of IPP. The central TTE system with redundant GPS time receivers is now under development.

2.5 W7-X Assembly

Basically, the assembly of the basic machine can be divided into three main phases. During the first phase half-modules are assembled by stringing five non-planar and two planar coils across the plasma vessel and fixing them to a segment of the coil support structure. During the second phase the half-modules are joined to form a module of the magnet system. The sectors of the coil support structure are bolted, the plasma vessel segments are welded, and the electric bus and cooling lines are connected. All these activities are performed in the assembly hall on dedicated mounting devices. The mounting device to join half-modules was already erected in 2001; set-up of the mounting devices for the assembly of the coils starts in January 2003. Several auxiliary mounting tools were designed to handle and support the five non-planar and two planar coils and the plasma vessel during assembly.

After assembly of the half-modules each unit is moved into the torus hall and lifted into the insulated lower half of the outer vessel. After integration of supports, the outer vessel is closed and some fifty ports and the in-vessel components are installed. A special tool was designed to thread the ports with masses of several hundred kilograms into the correct position.

A review of the assembly of W7-X by experts of EFDA, TEXTOR, industry, and IPP showed that assembly of W7-X can be accelerated if the modules are sequentially mounted. This differs from the earlier concept, where W7-X was assembled by simultaneously moving the five modules radially to minimise the risk of unsymmetrical errors in the magnetic configuration.

In the new concept the W7-X modules are assembled in their final position on a fixed base frame. After assembly each module is joined with the preceding module. Achieving optimum symmetry of the magnetic configuration requires careful control of the positioning of the coils and adjustment of the sectors of the support system during all assembly steps by laser tracking. Assembly of the modules already in the final position allows one to install the supply lines and diagnostics earlier.

The ring-shaped base frame which carries the W7-X modules is supported by five steel foundation columns in the lower basement of the torus hall. The columns have been contracted out and are to be installed at the beginning of 2003.

The coils have to be electrically connected with each other and with the current leads by a system of superconducting bus lines. Interconnecting the coils of one module requires 25 helium-cooled bus lines which have to be routed bifilarly, supported by fixed and gliding bearings, and insulated against high voltage. The basic design of the bus system was finished and considered routing of some 1,100 m of conductor. Forschungszentrum Julich will design, manufacture, and assemble the complete bus system for W7-X.

Connection between the bus sectors is achieved by approx. 200 detachable low-resistance joints. The design of these joints is a modified version of that used for the inter-layer connections of the coils and aims at a resistance of 5 nΩ. Prototypes of such joints were prepared for tests at the D.V. Efremov Scientific Research Institute of Electrophysical Apparatus in St. Petersburg.

Design of some 20 km of cooling water pipes with diameters of up to 600 mm and vacuum-insulated helium pipes as well as positioning of some 750 valves were continued.

3 HEATING SYSTEMS

3.1 Electron Cyclotron Resonance Heating

The electron cyclotron resonance heating (ECRH) system is being developed and built by FZK as a joint project with IPP and IPF Stuttgart. The ‘Projekt Mikrowellenheizung fur W7-X‘ (PMW) co-ordinates all engineering and scientific activities in the laboratories and in industry. It is responsible for the realisation and installation of the ECRH system for W7-X.

ECRH is to be the main heating system during the first experimental phase and is capable of steady-state operation with 10 MW of heating power at a frequency of 140 GHz. Ten gyrotrons with 1 MW each will provide the required microwave power. The European R&D programme for the development of the W7-X gyrotrons, which was launched in 1998 as a joint effort of the French company, THALES Electron Devices (TED), and the FZK, IPP, IPF, and CRPP-Lausanne research laboratories was successfully terminated in 2002. The “Maquette“ pre-prototype

WENDELSTEIN 7-X Diagnostics

Head: Prof. Dr. Hans-Jurgen Hartfuß

1 Overview

Work of the project concentrated on the completion of the feasibility studies of the diagnostics proposed. However, in case of those diagnostics to be integrated into the vacuum vessel detailed design is being done and laboratory tests are underway. In addition new diagnostic systems are being developed and have successfully been tested in W7-AS (see reports below).

After thorough discussion those diagostics from the set of level-1 diagnostics -the set basic for machine and divertor operation and plasma characterization- have been selected which are indispensable for the start-up phase of W7-X. In the list of priorities it is called the level-0 diagnostics set. Detailed work of the project is concentrating on this particular selection, however, space requirements are considered and feasibility studies are carried out for the whole level-1 set of proposed diagnostics.

The project is divided into nine scientific subgroups, where details of the various systems are being discussed. All technical problems in the field of mechanics and electronics design are treated by a technical coordination group. This group coordinates the design work as well as space requirements in the experimental hall and the dedicated peripheral buildings

Problems connected with the long pulse operation of W7-X and which are common to a number of diagnostics have been identified. These are on one hand the thermal load of the plasma facing windows by broadband electromagnetic radiation from the plasma and their coating by particles, and on the other hand the load of windows and vacuum sealants and of all in-vessel diagnostic components by non-absorbed ECRH microwave stray radiation at 140 GHz. Since the quality of optical windows at the interfaces to the plasma vessel is of primary importance, two temporary working groups concentrating on these problems have been established.

The group "Plasma Facing Optical Components" is working on concepts for the construction of immersion flanges for optical observation which can stand the high heat flow and particle fluxes expected. The design of a prototype water cooled immersion flange equipped with a cooled movable window protection systems and the setting of a high heat flux vacuum test chamber has been started. The “ECRH Stray Radiation” working group is testing materials to be used inside the vacuum vessel, and is developing components resistant to high microwave radiation levels, as well as shielding and protection measures for in-vessel components. For investigations under realistic conditions a large test chamber is being constructed. It will be equipped with various diagnostics and will be operated together with a 140 GHz cw gyrotron generator at a sufficient power level to gene-rate inside the chamber the power flux densities expected in W7-X.

2 Reports of subgroups

The activities of the nine subgroups and the technical coordination group of the project are briefly summarized in the following chapters.

For more details see the homepage of the project under the address http://www.rzg.mpg.de/KRONO/

2.1 Fluctuations

The subgroup defines the turbulence diagnostics for W7-X. A number of research activities conducted at W7-AS help to identify problems and to find proper methods. In this context the aim of measuring simultaneously several fluctuating quantities with electric probes in the plasma edge has been further pursued. The first project was the improvement of fast swept Langmuir-probes in W7-AS: miniaturized differential amplifiers, mounted on a pneumatically operated reciprocating probe drive characterized by high common mode voltage input range of +/- 200 V, high bandwidth of now 15 MHz, and high common mode rejection of 55 dB at 1 MHz -specifications which are crucial for the intended purpose- were successfully tested with probe arrays. The improvement of the data analysis procedure is still subject of current work. In a second project, various types of emissive probes complementing the fast swept Langmuir probes have been tested in the edge of W7-AS plasmas. So far, the performance of plasma-heated LaB6 tips has been found to be inferior to that of a plasma-heated tungsten loop. Although interesting first results have been obtained a reliable operation requires further development.

In order to explore the possibilities of optically imaging fast phenomena, a fast framing CCD-camera, allowing to study fast radiation phenomena at the divertor plates in high spatial and temporal resolution, has been tested. Software for camera control was developed to enable remote control and fast data transfer from camera to hard disk in order to minimize the idle time.

2.2 Plasma edge

Standard edge and divertor diagnostics, spectroscopic, particle beam, and probe diagnostics are being developed. Activities were focused on the detailed design of a prototype pop-up Langmuir-probe array. It is planned to integrate pop-up probes developed on this basis into a top divertor target and into the opposite bottom target in order to obtain poloidal profiles of the near-target electron

density and temperature as well as of the ion saturation current (particle flux) and of the floating potential (plasma potential) at least at two toroidal positions per target. To avoid active cooling, the dome shaped probe tips made of CFC with a diameter of about 2 mm will be designed to be retractable behind the target surface with a stroke of about 6 mm. The envisaged exposition time is 100 ms every second. A prototype arrangement is now under construction. Extensive tests in particular of the pneumatic drive and the position control characteristics will be conducted after its completion.

2.3 Microwave diagnostics

The group develops the classical microwave diagnostics interferometry, ECE, reflectometry, and polarimetry. A 40-channel broadband radiometer covering the range 120 to 160 GHz has successfully been set into operation at W7-AS. It is designed in such a way that it can directly can be transferred to W7-X to cover the frequency range during standard operation at 2.5 T. While antennas and sightlines of the reflectometers proposed are being designed, the decision which kind of reflectometry systems will be used is shifted to a later phase to be able to react to recent progress in the development of microwave components.

A multi channel Doppler-reflectometer was put into operation at W7-AS measuring the poloidal propagation velocity of density structures at six radial positions. The radial propagation velocity is obtained from cross-correlation analysis. The velocity shear and its fluctuations can be measured directly from radially neighbouring channels. A dual antenna system with two poloidally separated spots allows to measure this quantity also via cross-correlation. This time-of-flight type reflectometry is complementary to Doppler-reflectometry as it is particularly suited for low propagation velocities, where the accuracy of Doppler reflectometry is intrinsically low.

A single channel CO2 interferometer was set up in the laboratory and first tests of vibration compensation by the aid of a second collinear He:Ne laser interferometer were successfully performed. The test interferometer will be used for vibration studies, the design of the transmission line and for component tests. Design studies were performed to incorporate reflecting mirrors into the first wall of W7-X. Protection methods during boronization are being developed to avoid coating. A procedure to find the optimum sightline orientation in the 3D stellarator geometry of W7-X has been developed in collaboration with the University of Helsinki. Systems with 4 and 8 channels were considered. In numerical studies including also noise, test density profiles could be reproduced with low errors. Tests both in the laboratory and at W7-AS are continued to optimize the polarimeter based on the Cotton-Mouton effect (linear birefringence) with the aim of developing a robust line integrated density measuring diagnostic for control purposes at W7-X.

2.4 Charge exchange diagnostics

The total set up considered consists of five neutral particle analyzers and a dedicated diagnostic neutral particle beam. For local measurements of the ion temperature using the neutral particle analyzers or by applying spectroscopic methods, a diagnostic neutral particle injector is indispensable. In close collaboration with the colleagues of FZ-Jülich and the Budker-Institute, Nowosibirsk, such a system called RUDI is being developed.

It will consist of an optimised single beam arrangement with minimised divergence (≈ 0.5 degrees) and diameter (≈15 cm in the beam waist). It will be possible to vary the acceleration voltage between 20 and 60 kV. The equivalent neutral beam current will be higher than 2.5 A, more than 70% of the neutrals being in the full energy beam component. As those parameters are rather ambitious, a long-term collaboration phase for the development and optimisation of RUDI at the Budker Institute will precede its operation on W7-X.

2.5 Spectroscopy

W7-X will be equipped with a large number of spectroscopic diagnostics, which will derive multiple information from optical measurements in the spectral region ranging from the visible to the soft X-ray.

The design for a set of four new VUV/XUV spectrometers has been developed, which will be used for impurity monitoring and impurity transport studies covering the entire wavelength range from 2.5 nm to 160 nm, divided into four subsections with some overlapping, thus achieving a complete coverage of prominent spectral lines from the relevant impurity elements. The numerical design of optimised new toroidal holographic diffraction gratings has been finalised, while the spectrometer geometries and detector properties are chosen to obtain a high efficiency at a good wavelength resolution. The list of technical specifications for the difffraction gratings , mechanics, detectors, and the vacuum system has been prepared for the forthcoming procurement of the systems. Viewing lines could be identified for the four systems which all meet in the plasma centre. The expected performance of the spectrometers is tested and optimised by means of ray tracing calculations. In order to investigate the possibilities for line identification as well as the expected levels of accuracy of the new systems, simulated spectra have been calculated using the impurity transport code STRAHL. Under typical plasma conditions the new spectrometers will allow to clearly identify practically all relevant impurity elements in the plasma.

The island divertor concept for the W7-X stellarator is very similar to the one tested in W7-AS. The installation of such a divertor in W7-AS for its last experimental campaign gave us therefore the unique opportunity to already put a number of new spectroscopic island divertor diagnostics to realistic test, well in advance to their later installation: (i) A low spectral resolution spectrometer equipped with a 2D CCD detector has been successfully tested imaging line and continuum emission, originating from the region between the target plate and the X-point, with a spatial resolution of about 3 mm in the direction perpendicular to the target surface. (ii) A pair of independently operable He-beam nozzles, installed in a narrow gap between two divertor tiles allowed us to investigate the principle suitability of a thermal He-beam diagnostic as a means to derive local T_e- and n_e-profiles perpendicular to the target plate of W7-X. (iii) This system was further complemented by a very high spectral resolution Echelle-type spectrometer with the same viewing geometry but with a somewhat lower spatial

resolution. This was found to be suitable for deriving electron densities from the Stark broadening of Balmer lines of hydrogen. (iv) A time resolved coherence imaging camera, called imaging MOSS spectrometer, has also been tested. It allowed to derive the ion temperature distribution across the entire W7-AS divertor surface in 2D, from the Doppler broadening of a He II line at 486 nm.

2.6 Thomson scattering

Work concentrated on space requirements of all proposed Thomson scattering systems with its large number of beam lines, mirrors, and all supporting structures at the machine and its periphery. The location of the laser hardware was fixed. The infrastructural needs were determined. The laser beam line for the plasma bulk system was designed using CAD tools, including radiation protection requirements. This beam line is compatible with other diagnostic equipment and subsidiary components of W7-X. One main demand was the application of standardised beam deflection mirrors for transferring the laser beam to the torus, considering the polarization requirements of the laser radiation at the measuring position. In additional studies at W7-AS, new fast data acquisition hardware components were tested with the existing Nd:YAG Thomson scattering diagnostic system. These tests proved the suitability of the bulk Thomson scattering system proposed for W7-X, which will include interference filter polychromators with discrete avalanche diode detectors.

2.7 Soft X-Ray and electromagnetic diagnostics

X-ray diagnostics proposed for W7-X consists of horizontal and vertical camera systems, a multi-camera, and a temperature camera. The design concentrates on defining space requirements for the various systems and the development of first concepts for their realization. Laboratory tests are being conducted with X-ray detectors, Peltier-cooling elements, vacuum feedthroughs, and choppers to block the radiation. Technical constraints are mainly determined by the first wall design of W7-X. Solutions have been found to incorporate the cameras into the vessel panelling

Saddle-coils, diamagnetic loops, Rogowski-coils, magnetic probes and Mirnov-coils have been designed and tested taking into account other in-vessel components, such as divertor substructures and the first wall as well as the whole mechanical assembly process. The expected signal levels of all coils for equilibrium reconstruction have been simulated using the NEMEC/DIAGNO code package. Saddle-coils have been found to exhibit the best performance with respect to energy measurements since their signals are insensitive to not-toroidal plasma currents. They are now being prepared for installation onto the first vessel module of W7-X. A test facility has been built to measure transfer functions of magnetic pick-up coils and the influence of conducting materials surrounding the coil in the frequency range of 10 Hz up to 5 MHz.

2.8 Heavy ion beam probe

In the field of measuring local electric fields with the heavy ion beam probe (HIBP), American institutes offered to collaborate and to contribute with hardware. The applicability of the 2 MeV accelerator successfully operated at TEXT-Upgrade in the context of European regulations is being investigated. First design of the probing and the detector beam lines has been conducted. Beam trajectories inside the machine are calculated to determine space erquirements and eventual collisions with in-vessel components.

2.9 Fusion product diagnostics

A number of fusion product diagnostics has been proposed in close collaboration with the Alfven Laboratory, Stockholm and the PTB Braunschweig. However, the level-0 set consists of six neutron detectors only, oriented symmetrically around the torus and in its centre. To define their dynamic range and the energy range of interest, neutron transport calculations are being conducted based on expected plasma parameters for given heating scenarios.

2.10 Technical coordination

Besides all the problems connected to the infrastructure indispensable for the large number of diagnostic systems, work mainly concentrated on CAD design of the diagnostics proposed. The work of including all diagnostics into the CAD-model was continued. These models serve to identify and find solutions for potential collisions with technical components of W7-X. This includes the positioning of diagnostic models in the small gap between the plasma vessel and the first wall and between the plasma vessel and the 70 K cooling shield. Furthermore prototypes of several diagnostics were developed. Modeling was started for the long term developments of periscopes, the diagnostic injector and the multi-channel interferometer. However, detailed design was made for the saddle-coils and the Rogowski-coils to be mounted onto the vacuum vessel. Work continued to find proper solution to integrate the large number of Mirnov-coils and the multi-camera X-ray diagnostic systems into the wall protection of the vacuum vessel. Work on the infrastructure systems for all diagnostics has been carried on. This includes vacuum requirements, power supplies, connection to data acquisition, as well as the adaptation of the grounding concept to each diagnostic. In addition the set-up of a vacuum test chamber for heat load experiments and the ECRH stray radiation test chamber has been initiated and designed respectively.

3 Scientific Staff*

Experimental Division 3: T. Bindemann[1], H. Ehmler, J. Geiger, H. Hartfuß, R. Jaenicke, S. Klose[1], J. Knauer, U. Neuner, M. Otte[1], E. Pasch, J. Sallander

Experimental Division 5: S. Bäumel[1], J. Baldzuhn, R. Burhenn, R. Konig, M. Endler, P. Grigull, M. Hirsch, R. Narayanan[1], K. McCormick, E. Sallander, H. Thomsen[1], A. Weller, A. Werner, D. Zhang

Plasma Diagnostics Division: D. Hildebrandt, M. Laux, U. Wenzel

FZ-Julich: W. Biel, G. Bertschinger, A. Kreter, P. Mertens, A. Pospieszczyk, B. Schweer

---

* [1] Postdoc

Stellarator Theory

Head: Prof. Jürgen Nührenberg

1. Introduction

In 2002, the work of the Stellarator Theory Division was concentrated on widening the scope of the theoretical work at the Greifswald Branch Institute /98, 269, 793, 241, 737/ and on further development of the stellarator concept, notably for quasi-axisymmetric /689/ and quasi-isodynamic configurations /689, 190, 320/.

2. Development of Stellarator Concept

The possibility to fulfill the condition of poloidal closure of the contours of the second adiabatic invariant for all reflected particles is studied for systems with poloidally closed contours of the magnetic field B on the magnetic surfaces through computational stellarator optimization in collaboration with the Kurchatov Institute. It was shown /190/ that by adjusting the geometry this is possible in a major fraction of the plasma volume. The most salient characteristic (as compared to previous quasi-isodynamic configurations) is a magnetic axis whose curvature vanishes in all cross-sections with an extremum of B on the magnetic axis and renders possible a 3D structure of B without transitional particles (see Fig. 1) and with unprecedentedly high collisionless α-particle confinement.

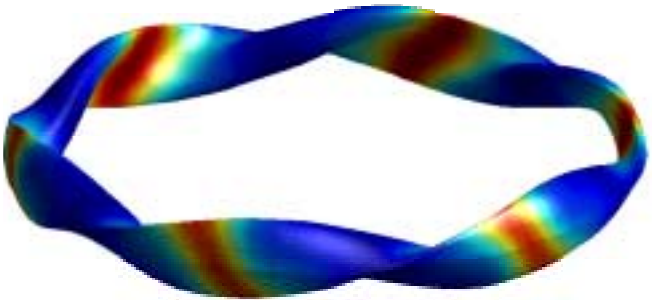

Figure 1: Boundary magnetic surface of the optimized configuration also showing the magnetic topography. The shading is related to the magnetic field strength $(B_{max}-B_{min})/B \approx 0.5$. The new characteristic feature of the configuration is the nearly vanishing curvature of the plasma column in the regions of the maxima of B occurring in the crescent-shaped cross-sections where the contours of B are poloidally closed, too.

3. MHD Theory of Stellarators

3. 1 Limiter free PIES Equilibria

In order to facilitate computation of free boundary equilibria at higher β using, in collaboration with PPPL, the PIES code, the auxiliary codes MORPH/VMORPH were written. They are designed to generate a coordinate system and initial field for arbitrary domain shape. Thus, an initial PIES computation can be reused when the plasma boundary moves too close to the previous computation domain. For W7-X, this effect is particularly strong at $\langle\beta\rangle \geq 3\%$ and was prohibitive to PIES computations at high pressure.
Figure 2 shows a calculation assisted with these codes. The upper half results from a preliminary PIES run with few modes, poloidal and toroidal mode numbers m=12 and n=10, respectively. The initial domain boundary is shown as dashed line. As the plasma gets very close to the boundary at some cross sections, a new domain (solid line, lower half) was chosen. A new PIES run was set up using the results from the preliminary one with MORPH. The Poincaré plot resulting from the final PIES run is shown in the lower half of the plot. The magnetic field was extended beyond the PIES computation domain using a Neumann problem solving code, EXTENDER_P, allowing for analysis of the 5/5 islands (see figure).
The calculations confirm earlier investigations using the MFBE procedure, showing that the last closed flux surface at finite pressure does not extend beyond the separatrix of the vacuum field.

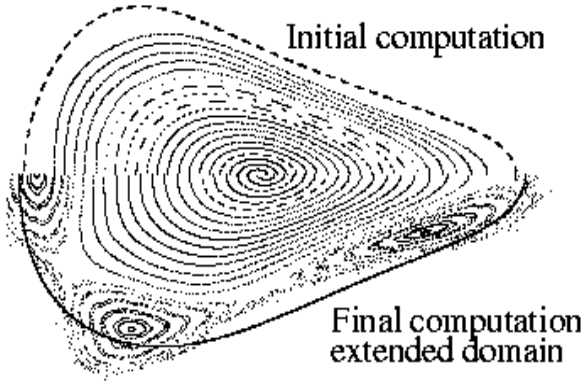

Figure 2: Computation of $\langle\beta\rangle = 3\%$ free boundary equilibrium with domain adaption.

3. 2 Ideal MHD Stability

In 2002, besides a generalization of the 3D global ideal MHD stability code CAS3D to general walls, work has included a number of application studies /369, 829/, among them investigations connected to the W7-AS high-β campaign /306, 806, 807, 813/ (see Fig. 3). With the present version of the code *physical* growth rates may now be given also for a finite adiabatic index, so that, knowing their growth times and mode structures, the potential risks of ideal MHD instabilities may be assessed more definitely.

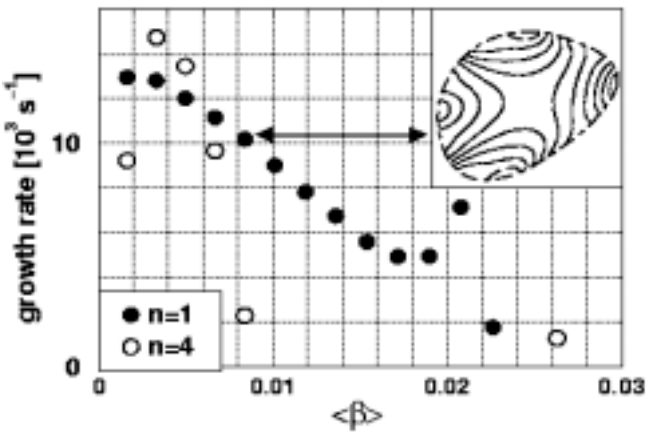

Figure 3: β-scan of free-boundary ideal MHD perturbations in W7-AS #51755: Instability is found for n = 4 (○) at low β and for n = 1 (●) at low to intermediate β. The growth time of the essentially (2,-1) perturbation at <β> = 0.008 (insert for the normal displacement contours) is ~ 100 μs.

3.3 MHD-Stability with Kinetic Effects

Fast particles in a magnetic fusion device have the potential to destabilize modes from the stable part of the MHD spectrum. During the last years the experimental as well as the theoretical investigation of this process has made progress. A kinetic energy integral [1)] from the solution of a drift kinetic equation in three dimensional geometry assuming zero radial orbit width has been used for a numerical approach to calculate the growth rate numerically (CAS3D-K) /574/. The code extends the 3D ideal MHD stability code CAS3D [2)]. The particle orbits have been integrated along field lines using a Fourier transform and a technique [3)], in which particle drifts are approximated as bounce averaged drifts. The code keeps track of all possible orbits in this approximation and retains all geometrical features of the magnetic configuration. In collaboration with the Institute for Nuclear Research Kiev the code has been benchmarked against analytical results [4)] for a large aspect ratio three dimensional heliotron device with satisfactory agreement of both results, see figure 4.

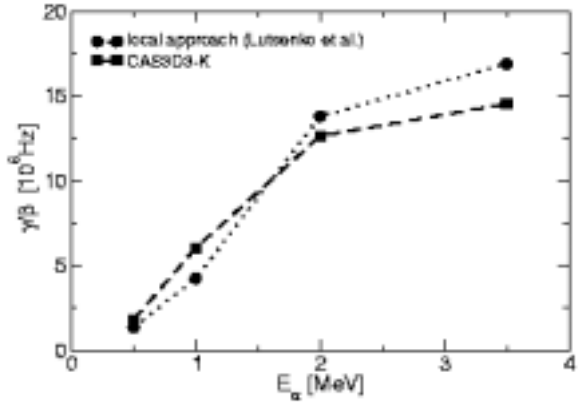

Figure 4: Benchmark of growth rate and frequency shift for a heliotron device with A=20, N_P=20 and a slowing down distribution of α-particles

[1)] A. Könies, Phys. Plasmas 7 (2000) 1139
[2)] C. Nührenberg, Phys. Plasmas 6 (1998) 137 and C. Nührenberg, Plasma Phys. Control. Fusion 41 (1999) 1055
[3)] R. Marchand, W. M. Tang and G. Rewoldt, Phys. Fluids 23 (1980) 1164
[4)]V. V. Lutsenko, private communication

However, there remain questions how a sufficient resolution for the pitch angle integration in the velocity space can be achieved when the particle drifts away from the field line are included. This is especially true for reflected particles. Further benchmarks of the code are desirable to improve the confidence in the results.
To allow easier comparison between experimentally determined modes frequencies and the theoretical Alfvén continua a 3D-MHD continuum code (CONTI) has been written.

4. ITG & Drift Wave Theory of Stellarators

4.1 Linear ITG Instabilities

ITG driven instabilities are likely to be one main mechanism to drive turbulence leading to anomalous transport in magnetically confined plasmas.
In collaboration with T. Rafiq (Chalmers University, Sweden) a ballooning study of ITG modes (using a two fluid model) in W7-X has been performed. It showed that depending on the ballooning parameters both localized and extended modes can be found /229/.
The studies of linear ITG instabilities which have been done so far /269/ will be extended to include electromagnetic perturbations. To explore the parameter space extensive studies with a gyrokinetic local dispersion relation have been done down to the Debye scale in a slab geometry.
An eigenvalue code for global ITG modes in general geometry based on the Braginskii equations has been developed and is currently being tested.
In collaboration with CRPP, the EUTERPE code -- a global 3dim. linear gyrokinetic PIC code [5)] -- has been ported to the REGATTA machine and is now used to study ITG modes in W7-X and related configurations.

4.2 Global non-linear particle-in-cell simulation of ITG turbulence for a cylindrical finite β equilibrium

Turbulence investigations in the geometry of a straight cylinder as a first simplified model of the W7-X stellarator have been started /98/. The gyrokinetic global non-linear particle-in-cell code TORB (CRPP/IPP) was further modified by implementing a finite-beta equilibrium leading to a magnetic well. Considering the results of linear global gyrokinetic calculations, this modification appears to be an important next step on the way to the description of W7-X. This modification leads to a significant decrease of the growth of ITG-modes compared to the case of an homogeneous magnetic field [6)].
First calculations showed a decrease of the turbulent heat transport due to the magnetic well. Particle and energy conservation obtained with an optimized initial distribution of the marker particles in phase space, are retained. In figure 5 are shown normalized energy contributions (top) and heat fluxes (bottom) as the result of non-linear PIC simulations for different plasma conditions.

[5)] G. Jost et al., Phys. Plasmas **8**, 3321 (2001)
[6)] R. Hatzky et al. Eur. Conf. Abstr. 22C, 1804 (1998)

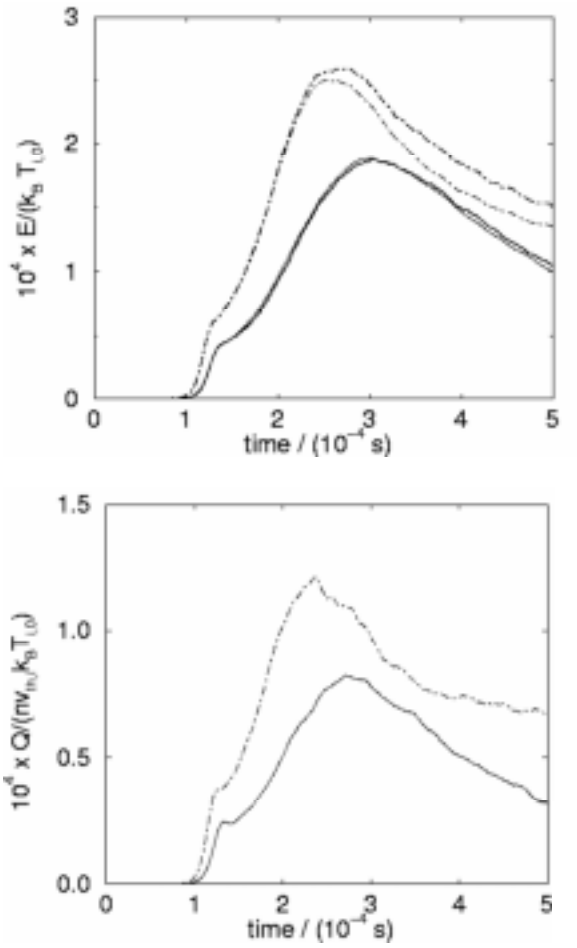

Figure 5: Dot-dashed lines: β=0, solid lines: β=5%; Top: electrostatic mode energies $E_{mode}/T_{i,0}$ (thin lines), the negative deviations from the initial kinetic energy $-\Delta E_{kin}/T_{i,0}$ (with thick lines), $T_{i,0}$=5 keV. The total energies are perfectly conserved, if the differences $(E_{mode}-|\Delta E_{kin}|)/T_{i,0}$ are zero. Plasma parameter: $T_{i,0}$=5keV

4.3 Drift Wave Turbulence in Stellarators

With the objective of investigating turbulence in the boundary plasma of stellarators the DALF-TI code was adopted and modified in collaboration with B. Scott.

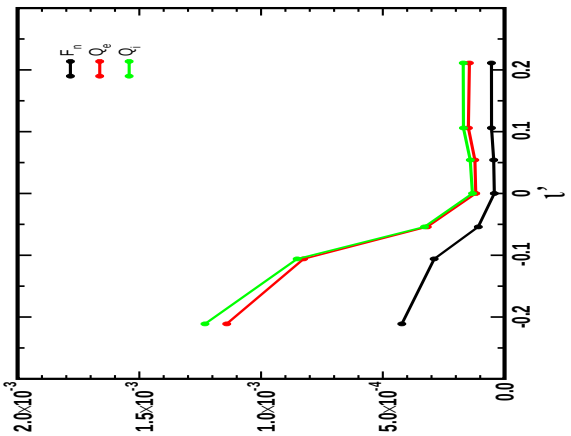

Figure 6: Particle and electron/ion heat flux F_n, Q_e, Q_i for different shear at ι_0=0.28

VMEC calculated equilibria transformed to magnetic (Boozer) coordinates can now be used. As a first application and in order to separate the influences of the rotational transform and the shear on turbulence simulations for a family of consistent tokamak configurations (circular, β=0, A=3.3) with different ι profiles ($\iota_0 \approx 0.3 \ldots 0.9$ and $\iota'_0 \approx -0.2 \ldots 0.2$, at the center of the flux tube) were performed. Changing the shear from tokamak- to stellarator-like leads to a strong decrease in the fluxes. Increasing ι but leaving the shear fixed has a similar effect.

5. Plasma Edge Theory

The physics model within the 3D SOL transport code BoRiS was further extended to solve in addition to the transport equations for the plasma (electron and ion heat equation, parallel momentum and continuity equation) also a fluid model for the neutral transport, analogous to fluid models used already quite successfully in tokomak edge codes like B2 or UEDGE. In implementing the new equations, several tests and benchmarks were performed in different geometries from simple slabs to full 3D setups /246, 722/. As a prerequisite for modelling of the full W7-X, magnetic coordinates and the metric information have to be generated for the complete plasma domain. For this, a generalized algorithm was developed based on solving a set of ordinary differential equations along the field-lines to optimize the numerical accuracy.

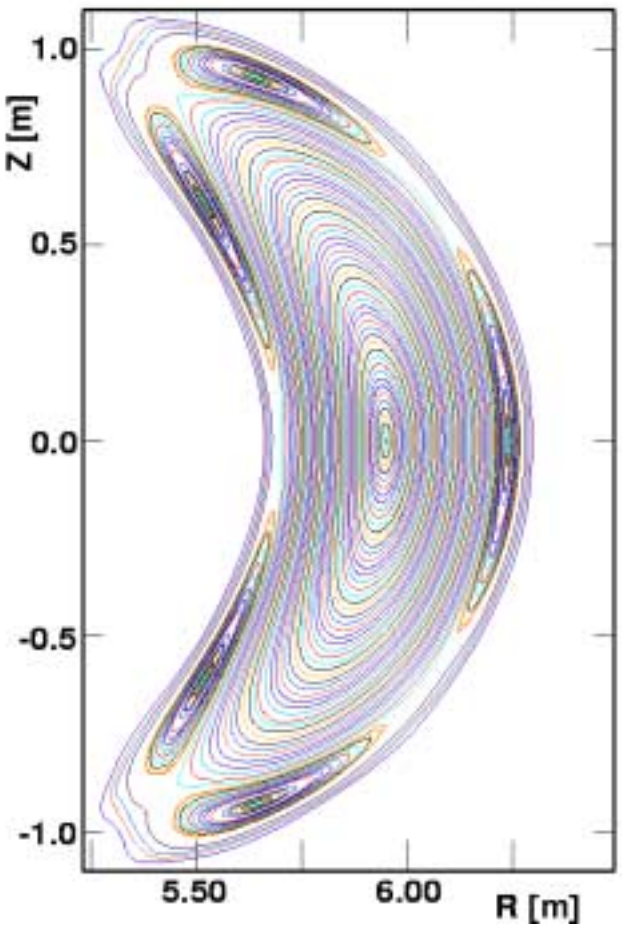

Figure 7: Flux surface geometry for W7-X vacuum field

A comparison with VMEC results shows quite good agreement in the core where both codes should be valid. In the edge region close to the separatrix the new algorithm

allows now also an accurate calculation without the problems of the Fourier approximation within VMEC.

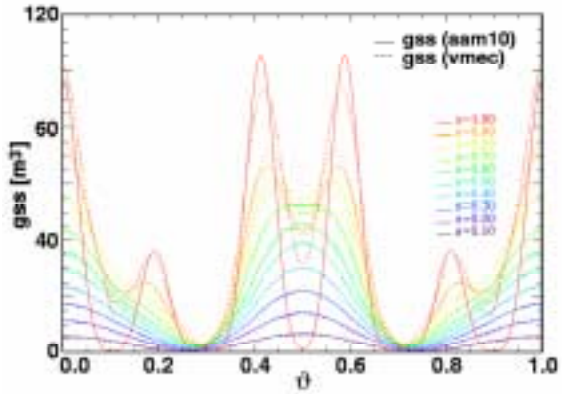

Figure 8: Comparison between the new algorithm and VMEC

To extend the transport models to ergodic configurations two different methods are used. The first model solves the transport equations with Monte-Carlo techniques making use of mappings. Special emphasis is put on the construction of local magnetic coordinates and their respective metric tensor. First applications of this technique to W7-X in a limiter-like configuration are shown in Fig. 9.
The reduction of the relative importance of parallel transport with respect to radial transport for electron heat, ion heat and particle transport results in less and less aligned profiles for the respective quantities in the islands.

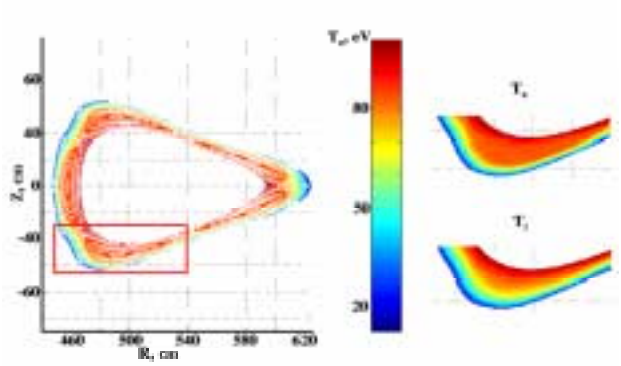

Figure 9: Temperature distribution in the W7-X edge

As an alternative ansatz a finite-difference discretization of the transport equations on a custom-tailored grid is used. This grid is generated by field-line tracing to guarantee an exact discretization of the dominant parallel transport (minimizing by this also the numerical diffusion problem). The perpendicular fluxes are then interpolated in a 2-D plane (using local magnetic coordinates), where the interpolation problem for a quasi-isotropic problem has to be solved by a constrained Delauney triangulation (keeping the structural information for magnetic surfaces if they exist) and discretization. All terms involving toroidal terms are discretized by finite differences. The first tests for W7-X were successfully performed.
In addition to the development of transport models for the plasma edge general problems of plasma-surface interactions are addressed. Modelling of ECR-heated methane plasmas is done to get a better understanding in the problem of carbon layer production and chemical sputtering in such plasmas, which serve as a model system of divertor plasmas being dominated by carbon sputtering, especially at detached conditions.

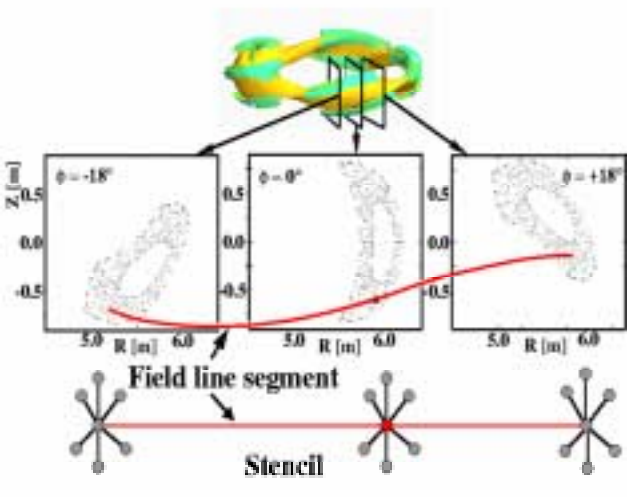

Figure 10: Discretization stencil for ergodic magnetic fields

A fully kinetic model (resolving also the sheath in front of the wall) including all relevant species and their reactions (neutrals, ions, electrons) was developped and applied /178/. The same model was used to study electron distribution functions for capacitive discharges, photon-created plasmas (which appear e.g. below the dome baffle of Asdex Upgrade) and plasma crystals.
In the area of plasma-surface interaction physics the new generalized version of the binary-collision codes TRIM and TRIDYN was completed and an extension to a 3D version was started. The problem of plasma-surface interaction processes for chemical sputtering is studied using molecular dynamics simulation of carbon microcrystallites. The resulting anisotropic diffusion coefficients and reaction rates are then used for a kinetic Monte-Carlo model accounting for real geometry effects like voids to calculate the chemical sputtering and hydrogen diffusion /757/.

6. Scientific Staff

X. Bonnin, M. Borchardt, M. Drevlak, R. Kleiber, A. Könies, V. Kornilov, K. Matyash, A. Mishchenko, N. McTaggart, P. Merkel, C. Nührenberg, J. Nührenberg, J. Riemann, A., Runov, R. Schneider, S. Sorge, M. Warrier. Guests: M. Behr[7], P. Beyer[8], B. Braams[9], R. Dewar[10], T. Fauster[11], A. Hatayama[12], M. Isaev[13], N. Jelic[14], S. Kasilov[15], E. Kaveeva[16], A. Kuyanov[13], V. Lutsenko[17], M. Mikhailov[13], I. Moeller[178], I. Morozov[16], V. Rozhansky[16], M. Samitov[13], I. Senichenkov[16], M. Shoucri[19], A. Subbotin[13], A. Tomasi[20], M. Umansky[21], S. Voskoboynikov[16], Y. Yakovenko[17], R. Zagorski[22].

[7]Rice University Houston, [8]Universität Marseille, [9]New York University, [10]Universität Canberra, [11]Universität Erlangen-Nürnberg, [12]Keio Universität Yokohama, [13]Kurchatov-Institute Moscow, [14]Universität Ljubljana, [15]National Science Center Kharkov, [16]State Technical University St. Petersburg, [17]Institute for Nuclear Research Kiev, [18]Ruhr-Universität Bochum, [19]Institut de recherche d´Hydro-Québec, [20]University of Sussex, [21]LLNL, [22]Institute of Plasma Physics and Laser Microfusion Warsaw.

IEA Implementing Agreement for Cooperation in Development of the Stellarator Concept

1 Objectives of the Agreement

The objective of the Implementing Agreement, first concluded in 1985, is to "improve the physics base of the Stellarator concept and to enhance the effectiveness and productivity of research and development efforts relating to the Stellarator concept by strengthening co-operation among Agency member countries". To achieve this, it was agreed to exchange information, conduct workshops, exchange scientists, do joint theoretical, design and system studies, coordinate experimental programmes in selected areas, exchange computer codes, and perform joint experiments. In 2000 the Agreement was extended until June 2005. The contracting parties are EURATOM, the U.S. DoE, Japan, and Australia. In September 1994, Russia became an Associate Contracting Party. In 2002, the Ukraine also joined the Implementing Agreement.

2 Status of the Agreement

In 2002, there have been two meetings of the Executive Committee. The 30th meeting was held on February 24 at Canberra, Australia. The 31st meeting took place on October 15 at Lyon, France, in conjunction with the IAEA Fusion Energy Conference. The next meeting is scheduled for 2003 at Greifswald.

3 Report on 2002 Activities

In 2002, 26 physicists participated in the exchange of scientists.

M. Osakabe from NIFS, Toki, held discussions on further collaboration with measurements on ion losses from January 27 to February 10. J. Howard from PPPL used a 4-day stay to work on the design of the MOSS spectrometer on WENDELSTEIN 7-AS in January. A. Kislyakov from Ioffe Institute, St. Petersburg, conducted neutral particle analyses for two months from February 6 to April 3. A second visit for two months started on June 1. Y. Kolesnychenko and V. Marchenko from NUCRESI, Kyiv, studied energetic ions in WENDELSTEIN 7-AS for 5 weeks from March 17 to April 21. During a short visit in April, D. Mikkelsen from PPPL discussed the collaboration on stellarator reactor studies. S. Murakami, K. Ida, S. Inagaki, M. Yoshinuma and H. Yamada, all from NIFS, Toki, participated in deuterium injection experiments in WENDELSTEIN 7-AS from April 18 to May 6. M. Zarnstoff and E. Fredrickson from PPPL worked on current-induced effects in high-beta discharges in WENDELSTEIN 7-ASfrom April 13 to 21. M. Zarnstoff continued the co-operation for a further 2.5 months, starting on May 25. V. Afanasiev and St. Koslovsky from Ioffe Institute, St. Petersburg, visited IPP to perform neutral particle analyses from April 1 to May 17. A short visit of A. Reimann and D. Monticello from PPPL at the end of June was devoted to studying high-beta equilibria with the PIES code. J. Lyon from Oak Ridge worked on pellet injection in WENDELSTEIN 7-AS from June 24 to 28. During a 2-week stay at Garching in June E. Suvorov from IAP, Nishny Novgorod, analysed the kinetic stability of distribution functions on W 7-AS. V. Timokine and V. Skokov from STU St. Petersburg worked on the impurity pellet injector and studied impurity pellets on WENDELSTEIN 7-AS for 2 months from June 12 to August 11. D. Mikkelsen from PPPL continued the collaboration on stellarator reactor studies from October 27 to November 8. A. Kislyakov from Ioffe Institute, St. Petersburg, participated in the studies on neutral particle analysis for 3 weeks from November 17 to December 8.

J. Knauer, H.-J. Hartfuss, F. Volpe and R. Konig attended the 14th Topical Conference on High Temperature Plasma Diagnostics at Madison, USA, from July 8 to 11. A. Weller participated in the NCSX Programme Advisory Committee Meeting at Princeton from December 7 to 13.

4 Conferences and Workshops

The 13th International Stellarator Workshop was held at Canberra, Australia, from February 25 to March 1, with 12 scientists from IPP participating.

Stellarator System Studies

Head: Dr. Horst Wobig (till 07/2002)
Provisional Head: Dr. Yuri Igitkhanov (since 08/2002)

1 Helias reactor

During this year, Helias reactors concepts (HSR) with 4 and 3 field periods were investigated. Changing of the number of field periods from 5 (as in W7-X) to 4 and 3, lowers the aspect ratio and reduces the size and cost of the reactor. Furthermore, a Helias ignition experiment, HSR4/18i, was considered with the basic aim the same as in ITER FDR - to demonstrate a burning plasma.

These concepts were presented at the 13th Stellarator Workshop in Canberra, the 9th EU-US Transport Task Force Workshop in Cordoba, the 22nd SOFT in Helsinki, the 19th IAEA Fusion Energy Conference in Lyon, and the International Conference in Alushta (September 16-21).

1.1 Coil system

The magnetic forces acting on the coils of the HSR configuration are balanced by an appropriate support system. The system consists of an intercoil structure and two toroidal support rings, connected to each other. To balance the torque the toroidal rings were designed as a framework. The coils were surrounded by stainless-steel housings. In regions of high coil curvature the coil housings were locally reinforced. Maximum values of the equivalent stress of about 670 MPa at maximum displacements of about 60 mm were found in the stainless-steel structure, see Fig.1

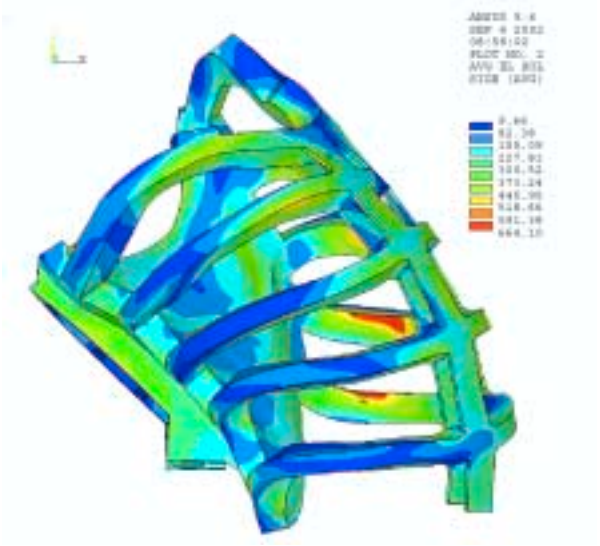

Figure 1: Half a field period of HSR4/18: equivalent stress distribution in the coil support structure.

Compression stress of the toroidal support rings mainly acts in the toroidal direction with a maximum value of about 400 MPa.

In summary, the large values of the magnetic forces call for strong support of the coil winding pack by a rigid coil housing and, in addition, a scheme of mutual support of the structure.

1.2 Reactor configuration with 3 field periods

To reduce the aspect ratio further, a configuration of the Helias type with 3 periods, HSR 3/15, was investigated. This device has a major radius of 15m, a minor radius of 2.5m, and an aspect ratio of 6. With 10 coils per period the total number of modular coils is 30. In Fig.2 the top view of the coils of one field period and in Fig.3 the magnetic surfaces of the vacuum field are shown. The main parameters of the configuration are listed in Table I.

Figure 2: View from top of one period of the coil set (winding packs) of HSR 3/15.

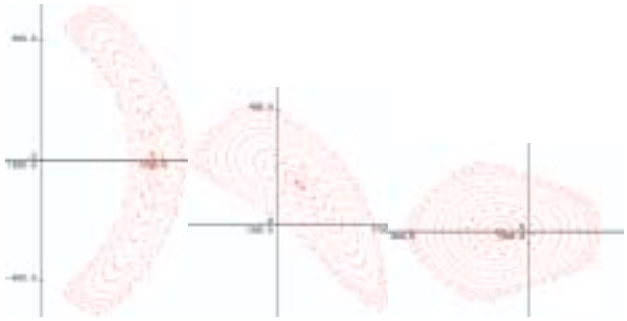

Figure 3: Poincaré plots of HSR 3/15 for planes $\varphi = 0, 30, 60^{o}$.

The stochastic region outside the last magnetic surface is impressed by the remnants of the 3/4 islands and the plasma flows along the certain channels towards the plates. Although iota per period is in the same range as in HSR 4/18 the total value is significantly by smaller and results in a higher ratio of the Pfirsch-Schluter currents to diamagnetic currents. The neoclassical transport

characterised by the effective ripple coefficient ε_{eff} is very small and amounts to about 0.65% at half-radius. The energy loss of fast α-particles is calculated to be about 6%. The main problem arises from the high value of the magnetic field at the coils. Further optimisation is required.

	HSR3/1	HSR4/18i	HSR 5/22
Major radius [m]	15	18	22
Av. minor radius [m]	2.5	2.1	1.8
Plasma volume [m^3]	1600	1560	1410
Av. field on axis [T]	4.4	4.4	4.75
Max. field on coils[T]	8.3	8.5	10
Number of coils	30	40	50
Magnetic energy [GJ]	72	76	100

Table 1: Main parameters of HSR3/15, HSR4/18, and HSR5/22 configurations.

1.3 Stellarator transport code

Development of the Stellarator transport code was established on the basis of international co-operation, aiming to provide an analytical and predictive tool. Neoclassical and anomalous transport models and also the equation for the radial electric field were incorporated into the code. The possible operational regimes for the Helias reactor were discussed by analysing the HDH and H* regimes in W7-AS.

2 Helias ignition experiment

Since a breeding blanket is not required in an ignition experiment, the distance between the plasma and coils can be made smaller than in a power reactor. For this reason the maximum field on the coils can be reduced to 8.5T, which allows one to utilise NbTi superconductors at a cooling temperature of 4K. Since self-sustained burn depends on the balance between alpha-particle heating and energy transport, current scaling laws of energy confinement were tested with respect to their compatibility with ignition conditions. Three of the empirical scaling laws (Lackner-Gottardi, W7 and NLHD2 scaling) predict confinement times which are larger than those required (2.5–3 sec). Self-sustained burn can be reached in the parameter regime: temperature T(0) = 11 keV, line-averaged density $2.1 \times 10^{20} m^{-3}$, averaged beta 3.6%, fusion power 1600 MW. The design point has rather high density and low temperature in comparison with a tokamak experiment. The choice of the high-density regime is justified by recent results in W7-AS, where line-averaged densities of up to $4 \times 10^{20} m^{-3}$ could be achieved. The Helias reactor is expected to operate at high density (central electron density of 3×10^{20} m^{-3}) and moderate temperature (T(0) less than 15keV). Under these conditions, neoclassical theory predicts that only the so-called 'ion-root' solution for the radial electric field exists, thus requiring strong optimisation of the magnetic field spectrum to minimise losses in the stellarator-specific 1/ν-regime. HSR4/18i is excellent in this regard, having an effective helical ripple considerably less than one per cent over the entire plasma cross-section. At this level, 1/ν-losses pose no threat to ignition. The divertor concept in the Helias reactor follows the same ideas applied for W7-AS and W7-X. However, the heat load on the target plates remains a critical issue: to keep the thermal load below the technical limits up to 90% of the alpha-particle power must be radiated. Since there is no need in stellarators to drive a toroidal current, neither transformer coils nor poloidal field coils are necessary. No provisions must be be made for controlling disruptions. The modular coils are based on conventional NbTi technology; its winding pack consists of 1040 tons of superconducting NbTi cable. The total weight of the coil system, including the support structure, is estimated to be about 9600 t, which is much less than the weight of the ITER FDR coil system.

3 WENDELSTEIN 7-X

The vacuum magnetic configurations of W7-X were calculated in detail and presented for nine operational cases. Documentation is available as an IPP report (IPP III/270) and also in electronic form under */afs/ipp/home/t/tya/w7x_vacuumconf*. The magnetic field at the conductor for the coils in the test arrangement of CEA-DAPNIA in Saclay was computed.

3.1 Neutron field in the W7-X hall

The (d,d)-reactions between the deuterons will produce neutrons with an average energy of 2.46 MeV, which are shielded by concrete wall 180 cm thick. Knowledge of the neutron field inside the hall is of special interest for the different diagnostic equipment including neutron diagnostics. Detailed analysis of the neutron field was carried out the MCNP, code together with the nuclear cross-section library, ENDF/B-VI. The divertor structure, graphite tiles, and openings for diagnostic and heating facilities are included in that cell model. A deuterium plasma with density $10^{14} cm^{-3}$ and temperature 4keV was assumed. The ring source for the neutrons is located at R = 550 cm, z = 0 and produces Q = 10^{16} neutrons/sec. Typically 20 to 60 energy groups are taken into account. The total neutron flux and the energy spectrum are computed at various radial and vertical positions by using a ring detector, a point detector, and control spheres (small radius 50 cm). There is only a weak dependence of the neutron flux on the radial position.

Scientific Staff

T. Andreeva, C.D. Beidler, E. Harmeyer, F. Herrnegger, Yu. Igitkhanov, J. Kisslinger, Yu. Turkin, H. Wobig

PLASMA-FACING MATERIALS AND COMPONENTS

Heads: Prof. Dr. Dr. Harald Bolt, Dr. Joachim Roth

During the operation of fusion devices the plasma-facing materials are subjected to particle fluxes from the plasma (ions, electrons, atoms) and to electromagnetic radiation. This results in a multitude of complex processes termed as "plasma wall interaction". The understanding of these processes helps to improve the materials used for applications on the first wall of fusion experiments. It also leads to optimised operation conditions and thus to performance improvement during the plasma discharge. New materials with improved properties in terms of e.g. erosion behaviour and heat flux capability are to be developed and characterised under plasma interactive conditions. The integration of new materials into plasma-facing components (PFC) also requires detailed work on interfacial engineering, since dissimilar materials with different functions have to be used. Within the project „Plasma-Facing Materials and Components" the areas of plasma wall interaction studies, material modification under plasma exposure, development of new plasma-facing materials and their characterisation have been merged to form a field of competence at IPP. The work supports the exploration and the further development of the fusion devices of IPP and also generates basic expertise with regard to the PFC related questions in ITER and fusion reactors. The tasks of the project are:

- Surface processes on plasma-exposed materials,
- Migration of materials in fusion devices,
- Tritium inventory – understanding and control,
- Materials – processing and characterisation,
- Component behaviour

1 Surface processes on plasma-exposed materials

1.1 Carbide formation on nickel and iron

The carbide formation on iron and nickel was measured using X-ray photoelectron spectroscopy (XPS). Carbide formation reactions are either exothermic (W, Ti, Si, Be) or endothermic (Fe, Ni). Thin carbon films on W, Ti, Si and Be were measured before, now carbidization on Ni and Fe was studied.

Thin carbon films (one to several monolayers) were repared at room temperature. The C 1s signal showed elementary (not reacted) carbon in an earlier described contribution. Despite the endothermic formation reactions, at the interface carbidic carbon could be observed in both cases.

During annealing experiments up to 970 K, carbon films on iron showed a decrease in carbidic contribution beginning at 470 K. At 670 K the fraction of carbidic carbon increased, accompanied by a decrease in elementary signal. Beginning at 770 K the C 1s signal intensity rapidly decreased due to carbon diffusion into the iron bulk. The remaining carbon detected at the surface is bound in carbide. Annealing of carbon films on nickel to higher temperatures, however, lead not to any loss of carbon into the bulk below 720 K. At 770 K the carbide formation set in. The carbon diffusion into nickel started at this temperature and lead to a decrease in the C 1s signal intensity. Up to 920 K both carbidic and elementary carbon are present in the XPS signal, in contrast to carbon films on iron.

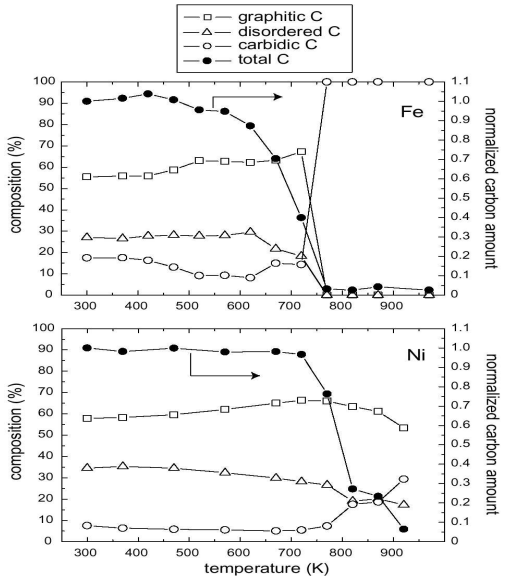

Figure 1: Carbide formation on iron and nickel (open symbols) and change of total carbon amount in the surface layer by diffusion (black symbols) during the annealing up to 920 K.

1.2 Mixed material erosion

1.2.1 Erosion of titanium/carbon mixtures

The interaction of deuterium ions with thin carbon layers on titanium was analysed using X-ray photoelectron spectroscopy (XPS). This technique allows identification of the chemical composition of the carbon surface layer. Comparison with bombardment by chemically inert noble gases verifies the chemical erosion mechanism of the carbon layer through deuterium at room temperature.

It was shown that erosion proceeds in two stages. Initially, an exponential decrease in the total carbon intensity, accompanied by a simultaneous increase in the carbidic carbon signal, are observed. Once only carbidic carbon remains, linear erosion is measured.

The initial exponential decrease of carbon results from a chemical erosion mechanism involving the whole carbon layer resembling ion-induced desorption of adsorbed

monolayers. This agrees with penetration depths of implanted ions exceeding the thickness of the carbon surface layer.
The cross-section for this erosion mechanism was determined as 4.7×10^{-17} cm^2. The linear erosion yield of carbidic carbon by deuterium ions was deduced from the measurements as 0.003, which compares reasonably well with the erosion yield calculated by a kinematic simulation.

1.2.2 Chemical erosion of atomically dispersed doped hydrocarbon layers by Deuterium

To study the influence of doping on the chemical erosion of carbon by hydrogen, atomically dispersed Ti-doped (~10 at.%) amorphous hydrocarbon layers were produced by magnetron sputtering and characterised (see Annual Report 2001).
The chemical erosion of these layers was investigated mass-spectroscopically in the temperature range of 300 K to 800 K for 30 eV deuterium impact with mass spectrometry. Compared to pyrolytic graphite, the methane production yield is strongly reduced at elevated temperatures. This reduction starts from temperatures just above room temperature and is even larger than for B-doped graphite, which has the highest reported reduction till now. The most likely explanation for the decreased hydrocarbon formation is a decreased activation energy for hydrogen release in the doped layer. The ratio of emitted CD_3 to CD_4 increases with temperature for pyrolytic graphite and even stronger for the doped layers.
The fluence dependence of the chemical erosion yield was also determined. The additionally observed reduction is explained by enrichment and the depth profile were measured with X-ray photoelectron spectroscopy.

1.2.3 Chemical erosion

A model of the chemical erosion of graphite during hydrogen ion bombardment has been implemented in the TRIDYN code. The model includes methane formation at the end of the ion track as well as kinetic emission of hydrocarbons from the near surface region. Model calculations were performed for hydrogen ion energies from 10 to 1000 eV, and at target temperatures ranging from 300 to 900 K. Good agreement between calculated and measured erosion yields is obtained.

1.3 New methods of surface analysis

In the ERDA-TOF apparatus put up at the tandem accelerator, time of flight and energy of the recoil particles have to be measured simultaneously. Flight times from 70 ns to 1.5 μs have to be detected with appropriate time resolution. The start and stop signals of the TOF measurement are given by secondary electrons released from a thin foil through which the particles pass. Time variances are minimised by deflecting the electrons to a micro channel plate (MCP) assembly in an isochronous electrostatic mirror. In order to reduce energy straggling within the foils, ultra thin diamond foils (0.6 μg/cm^2) developed at Kurchatov Institute Moscow with diameters up to 70 mm are employed to obtain acceptable solid angles. In co-operation with V. Liechtenstein from Kurchatov Institute different MCP assemblies and operating conditions were tested to optimise the time behaviour of the system. Investigations on different coatings of the foils were started to increase their secondary electron yield and to improve the detection efficiency especially for light ions

2 Migration of materials in fusion devices

2.1 ASDEX Upgrade

2.1.1 Carbon deposition in ASDEX Upgrade

The growth of carbon layers has been studied with long term samples below the divertor IIb and in a pump duct of ASDEX Upgrade from March to August 2001. The composition of re-deposited layers and their optical properties were analysed with ion beam techniques and ellipsometry. The deposition in the sub-divertor area showed a complicated deposition pattern with a maximum deposition of about 1.3 μm on the samples closest to the strike point. The thicknesses of deposited layers decreased strongly with increasing distance from the strike points. All deposits form soft hydrocarbon layers which consist mainly of deuterium and carbon with D/C from 0.7–1.4. Only a small deposition was observed in the pump duct, with a maximum of about 2.5×10^{15} D-atoms/cm^2 at the duct entrance. The observed deposition pattern in the duct was compared with simulation calculations assuming neutral hydrocarbon radicals as precursors for film deposition. The deposition pattern can be explained by 2 different radical species with surface loss probabilities $\beta < 10^{-3}$ and $0.1 \leq \beta \leq 0.9$. The most likely species are CD_3 and C_2D_x radicals.

2.1.2 Tungsten migration in ASDEX Upgrade

In ASDEX Upgrade, tungsten coated graphite tiles are employed as plasma-facing components in the main chamber and the divertor baffle region. In the 2002 campaign, sample tiles with an especially manufactured 350 nm thin W coating were exposed in the divertor excluding the strike point regions. Ion beam analysis before and after exposure of these tiles was performed to determine the erosion behaviour of tungsten in divertor IIb. The locations of these sample tiles were equivalent to those, where W is foreseen to be employed in ITER. On the outer baffle tiles strong sputtering of W occurred : After roughly 6000 s of total discharge time in the campaign, a peak erosion value of 100 nm was found. On all of the other sample tiles, erosion by sputtering was negligible. In these regions, however, a relatively strong erosion of the W coatings by arcing was found.
Re-deposition of eroded tungsten was investigated by quantitative PIXE analysis of deposited atoms on carbon tiles retrieved after the experimental campaign both from main chamber and divertor. Maximum deposition is found at divertor baffle tiles in contact with the far periphery of the plasma scrape-off layer. However, the total amount of re-deposited W accounts only for a small fraction of the total eroded W determined from spectroscopic detection of neutral tungsten emission lines. This is explained by the observation that tungsten is predominantly eroded during plasma ramp down phases where the plasma is not diverted and in direct contact with the central column surface.

DIVIMP transport simulations have shown that under these conditions most of the eroded tungsten is locally re-deposited close to its sputtering location.

2.2 TEXTOR

A new method for the determination of massive erosion and deposition on plasma-facing components was developed and tested successfully on a graphite tile of the ALT-II limiter of TEXTOR. The surface profile of the tile was measured before and after exposure to plasma discharges with an optical profiler, erosion or deposition is determined from the difference of the two profiles. The profiles were determined relative to specially machined holes, which provide stable reference points. An accuracy of about 1 µm can be achieved. After exposure for 7625 plasma seconds a maximum erosion of 28 µm carbon is observed in erosion dominated areas, while a maximum deposition of about 40µm is observed in net re-deposition areas. The composition and structure of the re-deposited layers were investigated with SIMS and scanning electron microscopy.

2.3 Wendelstein 7-X

For the upcoming stellarator experiment W7-X manipulator diagnostics are planned to allow exposure of material samples both in the plasma boundary region and in the divertor plasma for single discharges. Probe heads will be equipped with electrical connections to allow measurement of local plasma parameters and probe temperature. After identification of suitable vessel ports, design studies have been carried out in collaboration with the W7-X design team to detect possible collisions with other diagnostics. As a result of these studies, the probe manipulator for the plasma boundary region will be placed at the inboard side of the W7-X vessel while the manipulator for the divertor plasma will be placed at the outboard side.

3 Tritium inventory - understanding and control

3.1 Mechanisms of Tritium co-deposition

The surface loss probabilities of various hydrocarbon radicals have previously been determined in laboratory low-temperature plasma experiments using cavity probes. These data provide a basis to explain the formation of thick co-deposited layers in fusion devices. To determine sticking coefficients and other elementary surface reaction cross sections directly, a dedicated particle-beam experiment was commissioned. Using this set-up, the sticking coefficient of CH_3 radicals on a-C:H surfaces was measured to be around 10^{-4}. However, the combined interaction of atomic hydrogen and CH_3 radicals leads to a dramatic increase of the sticking coefficient to 10^{-2}.

Actual investigations aim at a microscopic understanding of plasma-surface-interaction processes such as chemical sputtering. Here it was found that the simultaneous interaction of low energy ions (10 to 1000 eV) and atomic hydrogen with a-C:H surfaces leads, in particular at low ion energies and low substrate temperatures, to a dramatic increase of the erosion rates compared with the interaction of the individual species alone.

3.2 Deuterium retention in tungsten

New measurements of ion-driven deuterium retention in polycrystalline W foil have been performed. Deuterium retention has been investigated as a function of ion fluence, implantation temperature, incident energy and surface conditions. Special attention has been given to the investigation of deuterium retention in thin films of W carbide and oxide which can be formed on W surfaces in a fusion device. Such kinds of films increase the deuterium retention in W. Several points are reviewed: (i) inventory in pure W, (ii) inventory in W pre-implanted by carbon ions and (iii) inventory in W oxide.

The main conclusions are: D retention increases approximately with the square root of the fluence, indicating diffusion limited trapping in intrinsic (E_t=0.85eV) and ion induced traps (E_t=1.45eV). D is retained far beyond the implantation range at room temperature in polycrystalline W. Pre-annealing at 1573K results in a decrease of the D retention in intrinsic traps. The retention decreases with increasing implantation temperature (Fig. 2).

Pre-implantation of 1 keV C^+ at room temperature and low fluence increases the D retention in intrinsic traps, but prevents the deuterium retention in radiation damage induced traps. D retention is strongly increased in WO_3/W compared to pure W.

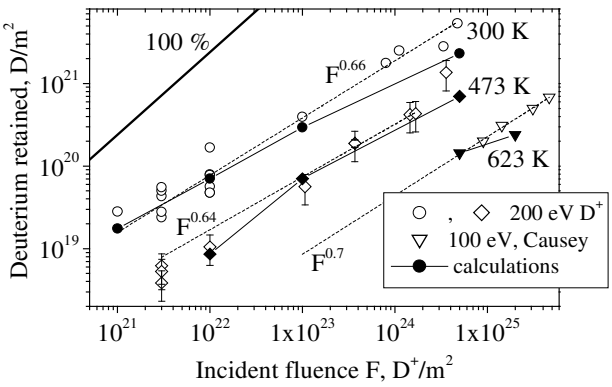

Figure 2: Fluence dependence of D retention in W for different temperatures

3.3 Hydrogen permeation measurements and diffusion barriers

The safe operation of a future fusion power plant will require a thorough control of the on-site inventory of radioactive tritium. Hydrogen isotopes in general diffuse into and through metals. Therefore the knowledge of the solubility and permeation of hydrogen isotopes in candidate materials as well as active measures to control this permeation are required. We perform direct measurements of the diffusion of hydrogen through thin samples and we also investigate the performance of ceramic coatings as diffusion barriers.

Deuterium permeation through a membrane made from the low activation steel EUROFER has been investigated at different driving pressures and both for the clean and oxidised state of the surface. For the clean surface state

when the permeation was very close to being diffusion limited, permeability values coincided well with literature data on the same material and on F82H (which is rather similar to EUROFER in composition) within all pressures and temperatures applied in the experiments. Surface oxidation lead to approximately one order of magnitude decrease in permeated flux.
Experiments on coating of EUROFER samples with Al_2O_3 thin films as diffusion barriers have been done and permeation measurements on barrier coated EUROFER are on the way.

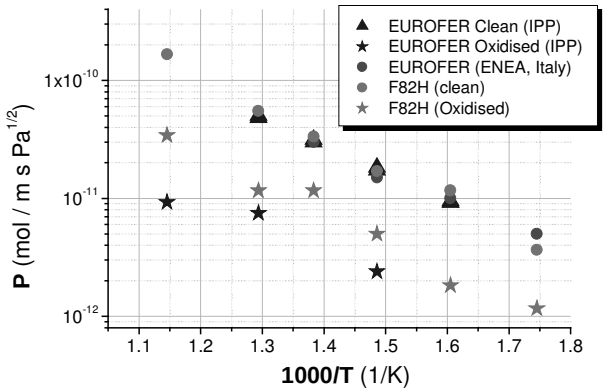

Figure 3: Arrhenius plots of D fluxes permeated through low-activation steels

4 Materials – processing and characterisation

4.1 Low-Z coatings for the first wall protection of Wendelstein 7-X

Vacuum plasma sprayed boron carbide (B_4C)-layers are considered as low-Z coatings for the first wall of W7-X. The development programme of low-Z coatings on water-cooled stainless steel panels was continued to examine the suitability of B_4C coatings. The B_4C coated wall panels will be used on the 70 m² outboard side, where the surface is not in direct plasma contact and receives a relatively low particle and power flux.
In order to investigate the probability of arcing on these nearly ceramic protection layers, B_4C coated samples were exposed at the vessel walls of the tokamak ASDEX Upgrade and the stellarator W7-AS. The position of the samples was similar to the expected plasma wall distance in W7-X. The total exposure time in ASDEX Upgrade was app. 2350 s (444 discharges) and 643 s in W7-AS (1445 discharges). The optical and electron microscopic analysis of the ASDEX Upgrade and W7-AS wall sample surfaces showed no visible arc traces, cracks or delaminations. This result is in contrast to the observation at TEXTOR, where B_4C layers were exposed on a highly loaded limiter and a large number of arc tracks was detected (see IPP Annual Report 2000).
The plasma-physical and thermo-mechanical evaluation of B_4C-coated water-cooled stainless steel panels is nearly finished. The selected VPS B_4C coating with 300 µm thickness and additional stainless steel interlayer fulfils all the requirements of the wall protection and can be manufactured industrially with an efficient plasma spray technique. In 2003 the final thermal cycling tests will be performed with a full scale mock-up.

Figure 4: Prototype of B_4C covered first wall panel (manufacturer: Plansee/Deggendorfer Werft)

4.2 Deuterium retention in carbide-doped graphites

Fine-grain graphites doped with different carbides (TiC, VC, WC, ZrC) were manufactured in the frame of a project dealing with the optimisation possibilities of doped fine-grain graphites with respect to high thermal conductivity, good mechanical properties, and reduced chemical erosion (see Annual Report 2001).
The retention of 1 keV deuterium implanted at room temperature in these doped graphites has been investigated up to a fluence of about 10^{24} D/m^2 by thermal desorption spectroscopy and ion beam analysis. The influences of the porosity, degree of graphitisation, and kind of dopant on the fluence dependence of the D retention were studied for graphites with different final heat treatment.
A strong decrease of the D retention for fluences higher than 10^{21} D/m^2 was observed for the undoped graphites graphitised at temperatures above 2000 K compared to material only calcined at 1270 K. Due to the identical manufacturing processes for the carbide-doped graphites used in this study, the structure is comparable for all of them. The choice of dopant as well as the ratio of open to closed porosity show no influence on the D retention. Therefore, these properties of the graphites can be neglected for hydrogen retention estimations.

4.3 Metal matrix composites

The development of new materials with high thermal conductivity and sufficient strength is decisive for the efficiency of future fusion reactors. In the case of the divertor, the copper alloys used allow for an operation temperature of 350°C under neutron irradiation. To increase efficiency it is necessary to develop materials for operation temperatures up to 550°C. Therefore, we investigate metal matrix composites with a copper matrix for thermal conductivity reinforced with silicon carbide long fibres for

strength. SiC fibres (SCS6, Textron) were electrolytically coated with a 100 µm thick copper layer. An additional heat treatment was performed to reduce the pores coming from chemical reactions between hydrogen and oxygen in the layer. The coated and degased fibres were hot isostatically pressed in a copper capsule. Hardness measurements and EDX analysis showed no diffusion of carbon from the fibre surface into the matrix. Push out tests were applied to investigate the bonding between the fibres and matrix (Figure 5). The calculated shear strength of this composite was about 8 MPa. One possibility to increase the shear strength is the deposition of an interface layer for reactive bonding between fibre and matrix.

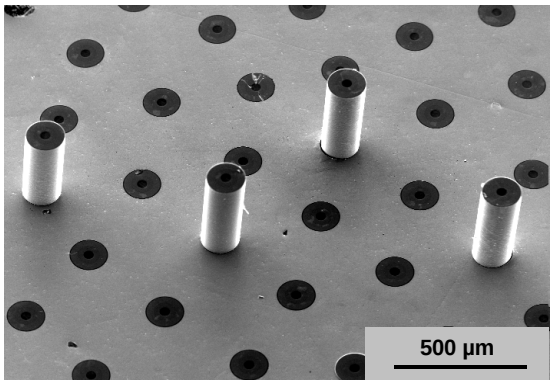

Figure 5: SiC fibres reinforced copper after push out test

5 Component behaviour

5.1 Micro- and macroscopic composite mechanics

In a fibrous metal matrix composite subjected to thermal loads, complex thermal stresses develop on micro-scale due to the thermal expansion misfit of the constituent materials. Dual scale stress analysis was performed for a copper alloy matrix/SiC long fibre composite system. Focus was placed on the non-linear deformation behaviour and local ductile damage evolution under thermal cycling. To this end, an incremental micro-mechanics technique combined with a finite element method was applied. Ten cycles of uniform temperature change between 150°C and 500°C were assumed as loading history. The residual stresses originating from the processing were also considered. A composite laminate structure consisting of laminae with 20% of fibre volume fraction was modelled. The effect of temperature-dependent matrix yield stress on the damage accumulation was quantitatively estimated.

Simulation results showed that soft copper would not be adequate as a matrix due to significant damage development whereas the use of a precipitation-hardened alloy led to an effective suppression of plastic strain accumulation despite of high hydrostatic stress states. In the latter case, the accumulated effective plastic strain in the matrix was less than 1 %. In the case of a laminate, the global total in-plane strain was about 0.2 %. The maximum compressive fibre stress is found at ambient temperature reaching about 3.6 GPa which is 95 % of the mean tensile fibre strength.

5.2 IPP high heat flux test facility

Plasma-facing components (PFC) for the divertors, limiters and first wall are the thermally highest loaded parts of a fusion experiment or a future fusion power plant.

The thermal stresses in highly loaded PFCs, generated from stationary heat loads up to 20 MW/m² and significantly higher transient heat loads, are the most important loading for such components. The development and the quality control of the manufacturing of actively cooled PFCs, especially for the next generation of long pulse fusion experiments, W7-X and ITER, requires thermal tests with heat loads similar to the operating conditions.

IPP plans to build a high heat flux (HHF) test facility on the basis of available ion sources and power supply of the closed W7-AS experiment. Start of construction will be in 2003. The increase of the pulse length of the ion sources up to 15-30 s and a maximal beam power of 1.1 MW allows an efficient testing of the divertor components for W7-X. It is planned to start the heat flux tests of W7-X divertor components in 2004. The modular concept of the water-cooled vacuum chamber ($\varnothing 1.5 \times 4.5$ m) enables easy future modifications of the facility. So, after the testing of the W7-X PFCs, it should be possible to offer an additional European HHF test facility for the tests of ITER divertor components.

6 Staff

M. Balden, M. Ben Hamdane, I. Bizyukov, A. Brendel, R. Brill, B. Böswirth, J. Dorner, W. Eckstein, K. Ertl, M. Fußeder, K. Gehringer, A. Golubeva, X. Gong, H. Greuner, T. Höschen, R. Hoffmann, W. Hohlenburger, A. Holzer, E. Huber, W. Jacob, E. de Juan Pardo, A. von Keudell, B.Y. Kim, J. Kißlinger, K. Klages, F. Koch, K. Krieger, R. Lang, S. Lessmann-Bassen, D. Levchuk, S. Levchuk, V. Liechtenstein, S. Lindig, Ch. Linsmeier, H. Maier, K. Marx, G. Matern, P. Matern, M. Mayer, J. Mazurelle, O. Ogorodnikova, E. Oyarzabal, B. Plöckl, C. Popescu, O. Poznansky, A. Röhreich, M. Roppelt, J. Roth, J. Schäftner, K. Schmid, R. Straßer, D. Valenza, A. Weghorn, A. Wiltner, M. Ye, J.-H. You

Contributors: W. Bohmeyer, A. Geier, M. Laux, R. Neu, H. Renner, V. Rohde, S. Schweizer

Tokamak Physics

Head of Project: Prof. Dr. S. Günter

The aims of the activities in the tokamak physics division are twofold: on the one hand to advance the theoretical basis of high temperature plasma physics with particular regard to tokamak physics, and on the other to give theoretical support to the tokamak program of IPP. The main topics of the theoretical activities are: modelling of the scrape-off layer and divertor plasmas, investigation of MHD stability, analysis of transport properties, propagation and absorption of waves in inhomogeneous plasmas, and the simulation of turbulent transport. The contributions described here are mostly concerned with model and code developments in the stage prior to specific applications or those aspects of theory where comparison with experiments is still in the qualitative rather than the quantitative phase. That part of the scientific work which has been carried out in close collaboration with experiments is reported in the respective sections on the projects: ASDEX Upgrade, JET and ITER.

1 Tokamak Edge Physics Group

D. Coster, K. Borrass, J. Kim, Y. Nishimura,V. Rozhansky*, S. O. Voskoboynikov*[1]

Development of the SOLPS code package. The edge physics group has, in collaboration with Prof. Rozhansky's group in St. Petersburg and Dr. Ralf Schneider's group in IPP Greifswald, continued the development of the SOLPS codes. In particular, a change in the implementation of the core heat boundary condition has enabled a significantly expanded domain of convergence for code runs with drift terms enabled. Support of the SOLPS package for groups around the world (including Japan, China, Russia, the USA) as well as within Europe has continued with increasing contributions to supporting the use of the code within the EFDA-JET workframe.

Since 2000, a version of the B2.5 code has been utilized to determine perpendicular transport from experimental profiles. Last year the possibility to use the determined profiles (or transport coefficients) in distinguishing between different physics models was suggested. The work is being extended to improve the profile determination in ASDEX Upgrade and to include other devices, which could give a size scaling.

Divertor and edge turbulence simulation by combined B2 and turbulence codes.[2] A new approach to edge plasma transport has been implemented, combining a 2D fluid turbulence simulation model (including dissipation and interchange-forcing) and a Braginskii type 2D transport code (B2), coupled through the perpendicular transport coefficients. The basic idea is to replace the fast time scale, repetitive turbulence vortex dynamics by a diffusion operator. To this end, parametrisation of transport coefficients "D and χ's" by turbulence runs is introduced. Selfconsistent turbulent transport coefficients and equilibrium plasma profiles are calculated in the ASDEX Upgrade divertor geometry. It has been shown that the transport is determined by the competition of the gradient drive and non-adiabatic electron response induced by collisionality.

On the other hand the B2 code incorporates the toroidicity induced drifts within a Braginskii type description and generates E_r shear in the presence of steep pressure gradients. This Braginskii type E_r-field can enter the turbulence model as a background $E \times B$ shear flow which suppresses the radial flux together with Reynolds stress induced electric fields. The transport coefficients now include the shear flow suppression effects (together with the drift wave dynamics described above) and – within the 2D turbulence model used – can lead to non-monotonic D and χ profiles which are the key component of the tokamak L-H transitions. As an example of the H-mode study, heat pulse induced L-H transitions (after sawtooth events, for example) are examined by controlling the influx at the core boundary (and thus to actively produce steepening of the edge gradients).

2 MHD Theory Group

S. Günter, V. Igochine, P. Lauber, P. Merkel, G. Pautasso, S. Pinches, S. Riondato, E. Strumberger, Q. Yu

The group deals with the theory of macroscopic instabilities in tokamak plasmas. There is a wide range of activities extending from first principle approaches (like the treatment of fast particle driven modes) to the interpretation of MHD instabilities observed in experiments

Fast particle driven instabilities. In a plasma with a significant population of suprathermal particles generated by external heating or fusion processes, kinetic effects can lead to additional destabilisation of MHD modes or even to additional (energetic particle) modes. To address this problem in a selfconsistent wary a gyrokinetic description (instead of the often used hybrid-MHD model) is required. Therefore a new linear gyrokinetic MHD code has been developed and is being tested. In the MHD limit known results on, e.g. internal kinks and TAE modes have been successfully reproduced. After completion, this code and the perturbative nonlinear code HAGIS will complement each other, with the new gyrokinetic model allowing to derive the linear stability properties (complex frequencies and eigenfunctions)

[1] * Visitors

[2] in collaboration with the TOK Turbulence Group

over a larger validity range, and HAGIS permitting to analyse the nonlinear consequences of these modes on the particular distribution in space and velocity.

Neoclassical tearing modes (NTMs). The previously existing code to describe the non-linear evolution of NTMs has been improved by refinement in the numerical techniques (implicite formulation and a novel, conservative treatment of parallel fluxes in the perturbed magnetic field) to enable it to deal with realistic ratios of parallel to perpendicular heat transport coefficients ($\chi_{\|}/\chi_{\perp} \sim 10^{10}$) and Lundquist numbers (up to $\sim 10^{9}$). This new code has been used to investigate the growth and saturation of NTMs. Future applications will be the study of heat transport in ergodised magnetic fields and the interaction of NTMs with external magnetic fields.

Resistive wall modes. The 2D linear stability code CASTOR has been extended by implementing a resistive wall (in the thin shell approximation) and finite viscosity. In cooperation with the stellarator theory group (C. Nührenberg) the 3D MHD stability code CAS3D has been generalized to study wall stabilization by arbitrarily shaped conducting structures including holes and poloidal and toroidal gaps. For the vacuum part of the code a parallelized version has been developed. The code has been applied to predict the influence of an ideal wall in realistic geometry on the MHD stability of ASDEX Upgrade type equilibria.

Equilibria for advanced tokamak scenarios. Usual tokamak equilibrium codes are not able to deal with strongly reversed magnetic shear and high-q core regions characteristic of some advanced tokamak scenarios. Therefore the 3D fixed/free boundary VMEC/NEMEC code (developed for stellarator equilibria) has been used for the study of tokamak equilibria with current holes, and – in a separate project – for the assessment of 3D effects. For general (not up-down symmetric) tokamak configurations new interfaces between this equilibrium code and the stability codes CASTOR and CAS3D have been developed.

Interpretation of complex MHD instabilities. The MHD interpretation code (MHD-IC) has been further developed to account for the toroidal coupling of modes with different poloidal mode numbers. The code has been successfully applied to identify and investigate MHD instabilities in advanced scenarios on ASDEX Upgrade.

Effect of plasma shaping on the ELM activity. On ASDEX Upgrade it has been found that plasma shaping is able to strongly influence the ELM size. Experimentally, closeness to double Null shape together with high plasma density have been found to lead to type II ELMs. In stability analyses the same conditions (plasma density entering through the collisionality dependence of bootstrap current) have been found to reduce the drive for low-mode number instabilities at the plasma edge. Furthermore the reduced bootstrap current (at high density) closes the access to the second stability regime allowing to limit the edge pressure gradient by $n \rightarrow \infty$ ballooning modes. These results are in agreement with the experimental observation of small energy losses per ELM as the unstable region becomes smaller with increasing mode number.

3 Transport Analysis Group

A. G. Peeters, C. Angioni, M. Apostoliceanu, G. Becker, A. Bergmann, O. Kardaun, G. Pereverzev, E. Poli, G. Tardini

The group studies neoclassical as well as anomalous transport. Work is done on global scaling laws, transport code development, heat and particle transport (theory and experiment), polarization current, physics of internal transport barriers (discussed under the ASDEX Upgrade section) and linear stability of micro instabilities. Below a few highlights are discussed in more detail.

*Extension of the transport code ASTRA.*The transport code Astra has been further developed. During the year 2002 the code was installed in 8 research Institutes and Universities worldwide in Europe, US and Japan. Presently a number of Laboratories where the code is installed approaches 40. New features were added to improve performance of the code. In addition to previously available transport models the multi-mode model (MMM 95) was added. Presently a user of the code has a choice of 5 theory-based transport models. Systematic studies show that ITG/TEM turbulent transport reasonably describes present tokamak experiments.

Theory based ITER predictions. A predictive transport modelling of ITER was performed. All theory-based models show that the ITG/TEM induced core transport allows ITER operation at $Q \geq 10$. Although an uncertainty in a minimum pedestal temperature required for such an operation remains. According to different models, the pedestal temperature required for achieving high performance in ITER varies between 3.5 and 5.5 keV. These values of T_{ped} overlap with the empirical scaling predictions for T_{ped} within the margins of uncertainty.

Modelling of density profile peaking. This year the study of anomalous tokamak transport has concentrated on the comparison of theory based transport models with the observed density profile behaviour. A new transport property of tokamak plasmas has been identified: the density peaking measured in H-mode plasmas of the ASDEX Upgrade tokamak is correlated with collisionality, and in particular decreases with increasing collision frequency as shown in Fig. 3.1. This experimental evidence can be explained with theoretical fluid transport models describing drift wave instabilities, ion temperature gradient and trapped electron modes, provided they include a valid description of the effects of collisions on these instabilities, like the GLF23 model. Collisionless models, like the Weiland model, are in disagreement with the experimental observations. The theoretically predicted anomalous particle pinch decreases with collisionality. The neoclassical Ware pinch plays an important role in plasmas at high collisionality, which is close to the density limit in present large tokamak experiments, while it is practically negligible at low collisionality. The present results reconciliate apparently contradictory observations on the existence of an anomalous particle pinch collected so far in tokamaks, and are of great relevance for the prediction of particle transport and density profiles in ITER burning plasmas.

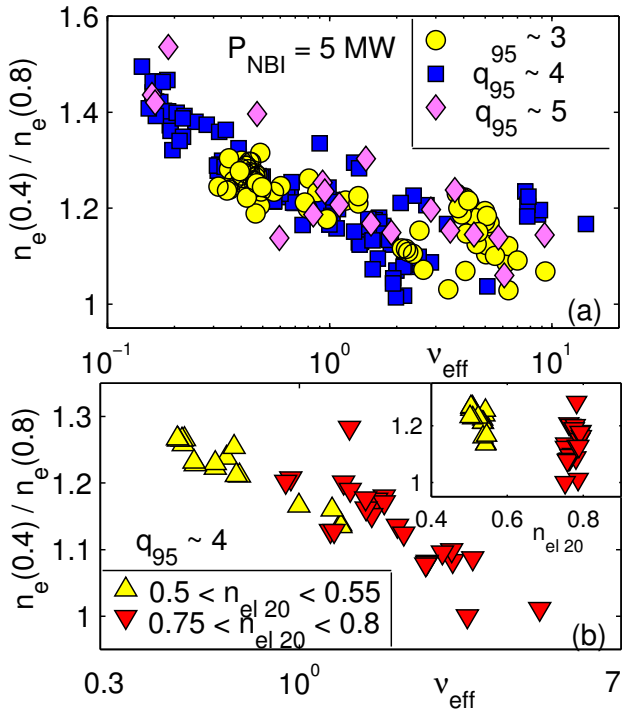

3.1 ASDEX Upgrade data clearly show the correlation between density peaking and normalized collisionality

Polarization current of rotating NTMs. The polarisation current due to the motion of a magnetic island with respect to the surrounding plasma has been studied by means of numerical simulations based on a Monte Carlo δf solution of the drift kinetic equation. This current is believed to play a role in determining the treshold for the onset of the neoclassical tearing mode (NTM) and its evolution before the saturation. At small island widths W (W comparable to the ion banana width w_b), the ion orbits overlapping the island are subject to a different electric potential inside and outside of it. This makes the local description of the standard analytic theory invalid. It has been found that this overlapping process leads to a drop of the polarisation current near the island (nearly proportional to W/w_b). The consequence is a reduction of the role of the polarisation-current term in the Rutherford equation for the NTM. The controversial problem of the transition from low to high collisionality regime (related to an increase of the polarisation current by a factor $\varepsilon^{-3/2}$, where ε is the inverse aspect ratio) has been investigated. It has been found that such a transition occurs for very high values of the collision frequency, quite far from the usual ASDEX Upgrade parameters.

4 Wave Physics Group

M. Brambilla, R. Bilato, D. Correa-Restrepo, K. Dimova, M. Götz, R. Meyer-Spasche, D. Pfirsch, G. Spies, H. Tasso, G. N. Throumoulopoulos

Modelling of heating and current drive with waves in the ICR frequency range. The efforts to improve numerical simulations of plasma heating and current drive in the Ion Cyclotron range of frequencies have been continued. The toroidal full-wave code TORIC has been modified to allow interfacing with MHD equilibrium codes. The range of applications for TORIC has been extended to higher frequencies by taking into account damping at higher ion cyclotron harmonics, and to lower frequencies by including ion Landau and Transit Time damping.

For the construction of the bounce-averaged quasilinear diffusion coefficient for the electrons using the wave fields evaluated by TORIC an algorithm has been developed, which ensures that power absorption profiles predicted by the solver of the Fokker-Planck kinetic equation and by TORIC will agree. This enables the evaluation of reliable profiles of the hf-driven current. Extensive explorations of Fast-Wave current drive scenarios for ASDEX Upgrade have been initiated.

Drift and gyrokinetic theories. Drift and gyrokinetic theories have been further investigated based on a previously derived Lagrangian for the system of Maxwell and kinetic equations, focusing in particular on the derivation of conservation laws. The method employed, contrary to other current approaches, enforces the exact gauge invariance in the definition of the approximate Lagrangian, thereby avoiding inconsistencies, in particular in the derivation of the energy-momentum tensor.

Analytic investigations of MHD equilibria and stability. Investigations of MHD equilibria with flows have been extended to take into account anisotropic resistivity, Hall term, and two-fluid theory. Many properties and exact solutions have been found, including ones with characteristics corresponding to Internal Transport Barrier plasmas.

Wall stabilization of MHD modes has been modelled by dissipative Mathieu-Hill equantions. "Negative energy" modes are found to be stabilized by the combined action of parametric excitation and damping coefficient. The region of stability is significantly increased for the "two-step" Hill's equation. This is a strong indication that the "resistive wall" mode could be stabilized by the joint action of a properly tailored time-dependent wall resistivity and sufficient viscous dissipation in the plasma.

Theoretical contributions to gyrotron optimization. Electron trajectories in a gyrotron were studied. Methods of optimum control were used to optimize the electron perpendicular efficiency in the so-called cold-cavity approximation of gyrotron theory.

Development of numerical methods. The nonlinear dynamical properties of Runge-Kutta difference schemes have been further investigated, in search for difference schemes allowing for large time-steps and improving the computing efficiency for the solution of evolution equations.

5 Turbulence Modelling Group

B. Scott, F. Jenko, A. Kendl, D. Strintzi, T. Schmidt-Dannert

Computational Studies of Turbulence in Magnetised Plasmas. Our studies of the low frequency fluidlike drift turbulence believed to underly anomalous transport in magnetically confined fusion experiments continue. We employ

fluid models extended to capture important kinetic effects (Landau damping, finite gyroradius), and kinetic models intended to treat all phenomena at the scales of interest (1mm to 10cm, 10 kHz to 1 MHz). The latter models are called gyrokinetic. Both fluid and gyrokinetic models are now reliable under generally electromagnetic conditions for phenomena from global scales down to the electron gyroradius, although it remains infeasible to cover such a wide range within the same computation.

Saturation of Self Generated Zonal Flows in the Edge. The fluid and gyrofluid codes DALF and GEM, respectively, have been used mainly to investigate edge turbulence. The main point of the studies is to determine the saturation mechanism not only of the turbulence but also to the zonal flow/sideband system to which it is nonlinearly coupled. The zonal flow results from the flux surface averaged electrostatic potential, and the sidebands are sinusoidal modes with up/down anti-symmetric structure. Both the geodesic acoustic oscillation and the global Alfvén oscillation whose end state is the Pfirsch-Schlüter current are involved. The energetic transfer mechanism have been identified by deriving the zonal and sideband energy theorem and measured in the computations. These have confirmed that the geodesic curvature mechanism limits the growth of self-generated zonal flows, to the point where this favoured mechanism for the L-to-H transition does not function.

Finite Beta and Finite Electron Mass Effects in Core Turbulence. The fluid codes have also been run for core turbulence cases, examining the effects of a finite plasma beta (i. e., electromagnetic induction) on the standard Cyclone Base Case for ion temperature gradient (ITG) turbulence. The studies find that the modifications are significant, including a substantial level of transport by parallel electron motion along disturbed magnetic field lines. This is consistent with the mode structure of the turbulence changing from ITG to kinetic ballooning (similar to MHD ballooning but limited to ITG scales by the kinetic dissipation mechanisms). These modifications are seen already at beta levels below normal for modern tokamaks, suggesting reduced relevance for established electrostatic results and an urgency for world wide development of electromagnetic core turbulence codes. An important companion result is a significant dependence of the mode structure and transport on the electron mass even at realistic values, suggesting that one should not use model ratios on the order of 100, as has been ongoing elsewhere.

Nonlinear Threshold for Kinetic Electron Temperature. The kinetic code GENE has been concentrating on electron temperature driven (ETG) turbulence, which is the corresponding case at the electron gyroradius scale to the ITG turbulence at the ion gyroradius scale. Of practical interest is the extent to which this model can account for experimentally observed stiffness in the electron temperature profiles. This situation is complicated by the presence in some regimes of a substantial trapped electron component to ITG turbulence, which would relax the stiffness. This is sometimes experimentally observed. The ETG computations cannot include this because it remains infeasible to carry both ion and electron gyroradius scales in the same computation with a realistic mass ratio. Nevertheless, it does emerge that the transport induced by ETG "streamer" turbulence as described in previous reports is large enough to establish a "floor value" for electron thermal transport which is consistent with the levels one finds in core transport barriers. A nonlinear analytic model has been derived using basic model assumptions, which captures both the linear threshold and the nonlinear "streamer" threshold as found by the computations.

Effects on Local Magnetic Shear Properties on Edge Turbulence. Reexamining the general damping effect of magnetic shear on edge turbulence we have found that much of the effect is due to a nonlinear change in the associated zonal flow layer structure, towards narrower vorticity layers for moderate to strong magnetic shear in general terms. In stellarator geometry, local shear generally plays the same role as global shear does, when the latter is absent; one should therefore expect low shear stellarators to exhibit a similar type of edge turbulence as existing configurations. Sharp local variations in the shear have a strong localised effect, mainly by changing the effective parallel wavelength.

6 Scientific Staff

Head: S. Günter, Deputy: M. Brambilla

C. Angioni, M. Apostoliceanu, G. Becker, A. Bergmann, R. Bilato, K. Borrass, D. Correa-Restrepo, D. Coster, K. Dimova, W. Feneberg, M. Götz, V. Igochine, F. Jenko, O. Kardaun, A. Kendl, J. Kim, R. Kochergov, P. Lauber, P. Martin, P. Merkel, R. Meyer-Spasche, Y. Nishimura, G. Pautasso, A. Peeters, G. Pereverzev, S. Pinches, E. Poli, S. Riondato, T. Schmidt-Dannert, W. Schneider, E. Schwarz, B. Scott, G. Spies, D. Strintzi, E. Strumberger, G. Tardini, H. Tasso, C. Tichmann, Q. Yu, H.-P. Zehrfeld

Guests: C.V. Atanasiu, Institute of Atomic Physics, Romania, A. H. Boozer, Columbia University, New York, USA, P. Lalousis, IESL.FORTH, Heraklion, Greece, P. McCarthy, University College, Cork, Ireland, G. J. Miron, Institute of Atomic Physics, Romania, E. Quigley, University College, Cork, Ireland, V. Rozhansky, State Technical University, St. Petersburg, Russia, Samuli Saarelma, Helsinki University of Technology, Finnland, J. Tataronis, University of Madison, USA, G. N. Throumoulopoulos, University of Ioannina, Greece, I. Veselova, State Technical University, St. Petersburg, Russia, S. Voskoboynikov, State Technical University, St. Petersburg, Russia, H. Weitzner, Courant Institute of Mathematical Sciences, New York, USA

CENTRE FOR INTERDISCIPLINARY PLASMA SCIENCE

(Prof. Dr. Dr. h.c. Volker Dose, IPP, Prof. Dr. Gregor Morfill, MPE)

1 PLASMA TECHNOLOGY

The Low-temperature Plasma Physics group (LTPP group) at IPP is concerned with the application of low-temperature plasmas for surface treatment, such as deposition of thin films, erosion, and surface modification. The main focus is on the investigation of plasma-surface interaction processes of hydrogen and hydrocarbon plasmas (e.g. CH_4) with hydrocarbon layers. These processes play an important role in the transport of carbon in the boundary layers of fusion experiments. The main activities in 2002 were to investigate deposition of amorphous, hydrogenated carbon films (a-C:H) from pulsed discharges and to study the synergistic interaction of ions and neutral radicals relevant to deposition and erosion of hydrogenated carbon films.

1.1 Synergistic Erosion of C:H Surfaces by Energetic Argon Ions and Thermal Hydrogen Atoms

Erosion of hard a-C:H films by simultaneous exposure to an Ar^+ ion beam and a beam of thermal, atomic hydrogen was investigated by in-situ real-time ellipsometry. Experiments were performed at room temperature, where erosion by atomic hydrogen is negligible. The energy of the Ar^+ ions was varied between 20 eV and 800 eV. Bombardment of the film with Ar^+ ions alone yields physical sputtering at energies higher than about 100 eV. Below that energy no physical sputtering is observed. This is in agreement with TRIM.SP computer simulations. However, if both beams are switched on, a strong increase of the erosion rate by a factor of more than 5 is observed at an ion energy of 800 eV, and even at 20 eV substantial erosion occurs which significantly exceeds that due to atomic hydrogen alone.

In the literature low-energy erosion of carbon at room temperature due to hydrogen ions is explained by so-called *kinetic hydrocarbon emission*: Chemical reaction of hydrogen leads to creation of weakly-bound hydrocarbon surface groups, which can then be sputtered at energies below the threshold for physical sputtering of the original material. To test the consistency of this explanation with our results, TRIM.SP calculations were performed for different surface binding energies of carbon. In order to simulate erosion yields of the order of those found experimentally, a surface binding energy of ≈0.1 eV has to be assumed (see blue line in Fig. 1), which is unreasonably low.

Alternatively, the following mechanism of *chemical sputtering* is proposed: Incident ions break C—C bonds within their penetration range. Atomic hydrogen, which is known to permeate a few nanometers into a-C:H, passivates the broken bonds. By repeated bond breaking and passivation by hydrogen, stable molecules are formed which thermally diffuse out of the film. The proposed mechanism is in agreement with various experimental observations reported in the literature.

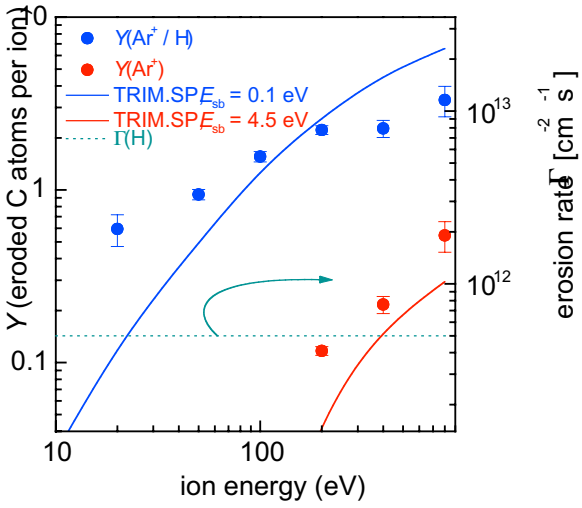

Figure 1: Erosion yield (eroded carbon atoms per incident Ar ion) as a function of Ar ion energy for the erosion of a-C:H layers due to bombardment of Ar ions alone (red circles) and Ar ions in the presence of a flux of atomic H (blue circles). The solid lines are TRIM.SP simulations. The dotted green line indicates the erosion rate (right-hand scale) due to atomic H alone.

1.2 Inductively-coupled Plasma Device for In-situ Studies

In a new plasma experiment set up in 2001, the plasma is produced by inductive coupling at a frequency of 13.56 MHz. Growth and erosion of layers are investigated by real-time, in-situ ellipsometry and in-situ infrared spectroscopy. In this device, the deposition of a-C:H layers from pulsed discharges was investigated. The total deposited film thickness d is divided by the number of pulses to obtain the film growth per cycle (δd/cycle). With a constant plasma on-time τ_{on} = 5 ms, the plasma off-time τ_{off} is varied. The resulting δd/cycle in a CH_4 and C_2H_6 plasma is plotted in Fig. 2. First the thickness gain per pulse increases steeply, reaches a maximum, and then decreases again. The rise time is of the order of 5 ms, whereas the decay time is of the order of 50 ms. This behaviour can be schematically understood as the incorporation of two different species: (i) high-reactive species (such as C_2H, CH) which chemisorb upon impact on the surface and (ii) low-reactive species (such as CH_3, C_2H_5) which chemisorb only if the surface is activated by plasma exposure during a plasma pulse.

The contribution of reactive species (i) to film growth increases with τ_{off} before it saturates, because the efficiency of dissociation depends on the pulse length and duty cycle. Optimal plasma operation with respect to growth rate is realised if two conditions are met: (a) The absorbed power needs to be tuned so that the minimum energy per molecule

is dissipated to cause film growth. This results for a given plasma power during the plasma on-phase and given residence time in a specific duty cycle; (b) the plasma off-time needs to be long enough so that all species are able to diffuse to the surfaces before a subsequent plasma pulse causes further dissociation reactions. These two conditions pose absolute boundary constraints for the duty cycle and the pulse length.

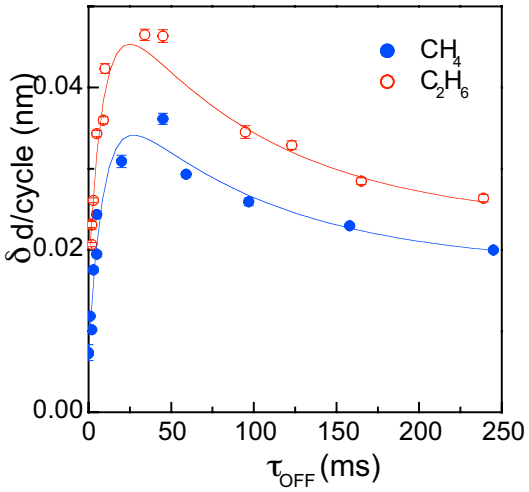

Figure 2: Thickness gain per pulse for a pulsed ICP discharge using methane (solid squares) and ethane (blank cycles) as working gas as a function of plasma off-time τ_{off}.

The contribution of low-reactive species (ii) increases at the beginning of the plasma off-phase because the recombination of radicals is no longer counter-balanced by electron-induced dissociation reactions. After this initial increase, the density again decreases on a time scale corresponding to the residence time of neutrals in the plasma reactor. The contribution of low-reactive species to film growth goes through a maximum with increasing τ_{off}. At the maximum the plasma off-phase is long enough to allow the density of low-reactive species to build up, but short enough for these species to be incorporated in the film in a subsequent plasma pulse before they are pumped away.
A simple rate equation model based on film growth by reactive and low-reactive species is able to reproduce the observed dependence of δd/cycle on τ_{off} as illustrated by the solid lines in Fig. 2.

1.3 Particle Growth Experiment

In a collaboration between the experimental groups 'Complex Plasmas' at MPE and 'Low-temperature Plasma Physics' at IPP, a new experiment for the growth of carbon microparticles in a hydrocarbon plasma was constructed and commissioned. Key points of the experiment are the possibility of controlling the electron energy distribution by a specific proprietary control to achieve diamond growth on diamond seed particles and levitation by thermophoresis.
First experiments showed the successful levitation of particles in a RF plasma and particle generation in methane plasmas. Particle clouds can be observed by a video system and first indications of crystallisation were found. For in-situ measurement of particle size distributions, Mie scattering ellipsometry was installed.

1.4 Quantitative Mass Spectrometry

In collaboration with the data analysis group, a novel method of decomposing mass spectra based on Bayesian probability theory was developed. The algorithm combines measured mass spectra of the gas mixture of unknown composition with calibration measurements of known gases and returns the relative concentrations and the associated margin of confidence for each component of the mixture. In addition to the concentrations, the procedure allows one to derive improved values of the cracking coefficients of all contributing species, even for those components for which no calibration measurements exist or cannot be performed. This latter feature also allows one to analyse mixtures which contain radicals in addition to stable molecules, a problem often encountered in the mass-spectrometric analysis of plasmas. The method was applied to the gas phase analysis of methane RF plasmas. Besides the stable hydrocarbon molecules containing one and 2 C atoms, the radical species H, CH_3, and C_2H_5 were identified.

2 PLASMA THEORY

2.1 Pinch Effect Studies

High-resolution gyrokinetic turbulence computations augmented by Braginskii fluid simulations were used to study particle transport in the tokamak core and edge plasma. Although the particle diffusivities are small compared to the heat diffusivities, they determine the final density profile, with obvious consequences for the energy confinement time. Especially important is the occurrence of inward particle transport (pinch) for realistic parameters, as it can lead to a profile instability incurring a steepening of the density, and result in a barrier for ITG turbulence.
Contrary to common wisdom, the residual particle transport in ITG and TEM turbulence is due not only to the trapped electron fraction. It is also controlled to a great extent by the passing electrons. In all ITG or TEM scenarios where a pinch effect has been found, the inward electron current is carried only by the circulating electrons, while the trapped electrons are advected outward. Analysis shows that the ITG/TEM pinch effect is caused by the non-adiabatic part of the collisionless parallel circulating electron response. The trapped electrons' response is mostly controlled by the local electric potential at the outboard midplane, which prevents parallel inhomogeneities.
Analogously for ETG turbulence, the residual particle transport is determined by the non-adiabatic part of the ion response at the electron gyroradius scale, and can also cause inward particle transport.

2.2 Edge Turbulence Simulations

For an L-mode reference discharge 3D edge turbulence simulations for comparison with the GPI images were carried out. The NLET turbulence code was expanded to include EFIT generated geometry data in the simulations. Open and closed field lines as well as the effect of limiter like boundary conditions were tested. The atomic emission efficiency curves for the D-alpha line were applied to the code results. Linear growth rates of the fluid code were found to agree with gyrokinetic results for the same plasma parameters in the relevant regime for the C-Mod L-Mode edge.

2.3 Low Collisionality Zonal Flows

A new interpretation of the computation of the effective inertia of collisionless zonal flows was studied. A very small fraction of the passing ions is found to nearly cancel the large inertia of the trapped ions. The effect of collisions on this small fraction of ions is currently being studied, since it might dramatically alter the effective mass density of the plasma with respect to the zonal flows.

2.4 Anisotropic Intermittency in Homogeneous Magnetohydrodynamic Turbulence

Homogeneous incompressible magnetohydrodynamic (MHD) turbulence was shown to be statistically anisotropic by considering higher-order two-point statistics of the turbulent fields parallel and perpendicular to the local magnetic field. The anisotropy is attributed to the influence of the magnetic field on the nonlinear energy cascade. An increasing mean magnetic-field damps the parallel-field dynamics, while in the perpendicular direction a gradual transition towards two-dimensional MHD turbulence is observed with perpendicular energy-spectra showing Iroshnikov-Kraichnan scaling. This is equivalent to higher parallel-field homogeneity of small-scale dissipative structures, i.e., current and vorticity microsheets, due to their stronger alignment along the mean field. A modified Log-Poisson model reproduces the corresponding anisotropic intermittency of energy dissipation by phenomenological tuning of the respective parallel and perpendicular energy-cascade rates.

2.5 Method of Characteristics for Ideal Magnetohydrodynamics

By applying the theory of characteristics to the hyperbolic set of partial differential equations governing deal magnetohydrodynamics (MHD), we were able to develop a three-dimensional Method-of-Characteristics algorithm (MoC). The Hartree-type scheme allows the maximum possible Courant-Friedrichs-Lewy time-step to be used by naturally respecting the physical domain of dependence of a fluid particle within the space-time of ideal MHD.The implementation allows the advance of shock fronts and other discontinuities arriving in ideal MHD as infinitely thin objects, obeying the MHD Rankine-Hugoniot relations. This renders the MoC approach superior to finite-difference methods when it comes to accuracy and physical consistency. The code is second-order accurate in space and time. In parallel, performance tests with state-of-the-art MHD Riemann solvers were carried out.

3 Data Analysis

The Data Analysis group at IPP is concerned with analysis of measured data to obtain most reliable results. Data sets may consist of measurements from different experiments (diagnostics). Measured data from one experiment may comprise various calibration measurements. The reliability of the results depends on the uncertainties of all measured data, the uncertainties of parameters entering the measurement descriptive model, and the quality of the physical model. A ubiquitous problem in data analysis is to identify and quantify sources of uncertainties of a measurement system and describe the data with a model including all uncertainties in order to obtain the most reliable result, including its credibility. This can only be achieved if all information relevant to the inference problem is combined in one concise formalism. Bayesian probability theory (BPT) provides a general and consistent frame for combining various kinds of information taking into account the degree of uncertainty of data and models.

3.1 Integrated Data Analysis

Integrated data analysis of fusion diagnostics is the combination of different, heterogeneous diagnostics in order to improve physics knowledge and reduce the uncertainties of results. One example is the validation of profiles of plasma quantities. Integration of different diagnostics requires systematic and formalised error analysis for all uncertainties involved. The BPT allows systematic combination of all information entering the measurement descriptive model that considers all uncertainties of the measured data, calibration measurements, physical model parameters, and measurement nuisance parameters.

Systematic error analysis was performed at the Nd:YAG and ruby Thomson scattering diagnostics (in collaboration with A. Dinklage, E. Pasch, J. Knauer, E3). A software package for n_e and T_e profile estimation for the Nd:YAG Thomson scattering system including a thorough error analysis was transfered to W7-AS. The analysis of the ECE diagnostic for T_e profile estimation is in progress.

The complete statistical model of the diagnostics allows the experimentalist to quantify the influence of different error sources on the reliability of the results, which has an impact on both diagnostic improvement and design. The reliability of the profiles can be studied by eliminating selected error sources or assuming exact calibration measurements. The error sources are of different importance for the various quantities of interest. Hence, the diagnostic improvement is strongly related to physics goals, i.e. one has to specify if n_e or T_e measurements are to be preferred in terms of accuracy. Diagnostics improvement can be achieved by reducing crucial uncertainties and by hardware upgrades, e.g. with additional spectral channels. The complete statistical description allows one to find the best operational settings for existing hardware and hardware upgrades. In addition, the Bayesian framework allows easy adaptation of the analysis to changes in the diagnostics due to new operational plasma regimes.

First steps towards an integrated data analysis were achieved by combining different heterogeneous data (see figure 3). The result of combining different diagnostics within the Bayesian framework affords a gain in information, since it contains all the correlations between different parameters. For example, the combination of a diagnostic allowing information only about T_e (soft X-ray) with a diagnostic containing information about T_e and n_e (Thomson scattering) yields more reliable results for n_e compared with the results from the second diagnostic only. The probabilistic description contains the full correlation structure of parameters.

3.2 Magnetic Island Dynamics of Tearing Modes in ASDEX Upgrade

Magnetic islands of neoclassical tearing modes have been found to limit the maximum achievable energy which can be stored in a fusion plasma and may therefore be a problem for a future reactor. Concepts of stabilising the plasma in order to handle these instabilities include electron cyclotron current drive, which can only be useful if it is

accurately adjusted to the quantity needed. A thorough understanding of the island is therefore necessary.
The time dependence of the magnetic island width is theoretically described by the generalised Rutherford equation. This first-order nonlinear differential equation with respect to time contains in our case three terms describing stabilising and destabilising effects in the plasma. Assigned to these terms are three free parameters which have to be determined from measured data since theoretical considerations can only provide estimates.
The square of the width of a magnetic island is proportional to the amplitude of the magnetic flux. The variation of the latter with time is contained in the signal of the Mirnov coils. However, this signal suffers from perturbing events such as ELMs (edge localised modes). In order to clear the signal one first has to look for the time incidents where the ELMs occur and then employ Fourier transformation together with integration over time to get the amplitude of the unhampered range in-between. Furthermore, that time interval has to be identified which is actually described by the Rutherford equation and not spoiled by fluctuations, which especially show up during the onset of the island, or additional modes. Since in the valid range of the Rutherford equation the signal is smoother and suffers less from noise, a typical Bayesian change point problem arises in identfying the time incident for which the behavior changes. But even more, with this numerical procedure it is now possible to separate sections of the signal with coupled modes from those of a single mode.

Finally, the pure signal in the valid time range was used to determine the three free parameters of the Rutherford equation employing BPT. Comparison of the result from theory obtained by inserting the calculated parameters with the signal from experiment gives very good agreement within the error margin. Moreover, it can be stated that one of the three terms, the so-called Glasser-Greene-Johnson term, may be neglected in the Rutherford equation because it does not lead to a better description of the data. The examinations will be continued with a more thorough consideration of the assumptions used for the Rutherford equation.

3.3 Resolution Enhancement

The growth process of tetrahedral amorphous carbon (ta-C) was studied with deconvolved ^{13}C depth profiles from elastic recoil detection measurements. The deconvolution was performed by the adaptive kernel method in the framework of BPT. The depth profiles were compared with TRIM and molecular dynamics calculations (in collaboration with P. Neumeier, G. Dollinger, TU Munchen).
The toroidal and poloidal distribution of tritium in the ASDEX Upgrade walls was measured by secondary ion mass spectroscopy. The total tritium content as well as the depth distribution were recovered by deconvolving the SIMS transfer matrix from the data. Specific toroidal and poloidal variations were found. The interpretation is still in progress (in collaboration with E. Nolte, TU Munchen).

3.4 Speckle Interferometry

Speckle interferometry is one of the best suited techniques for non-contact measurements of deformations of rough surfaces. Nevertheless, the evaluation of the obtained data suffers from a low signal-to-noise ratio of about 1. A novel approach based on combination of Bayesian hyperplane-priors and neural networks was developed and successfully applied.

3.5 Mass Spectroscopy with Incomplete Cracking Matrix

The analysis of samples by mass spectroscopy techniques is often hampered by limited knowledge of the cracking matrix. A fast technique based on the Generalized Maximum Entropy (GME) method for joint estimation of the concentrations and the cracking matrix was used to decompose multicomponent mass spectra of hydrocarbons containing radicals.

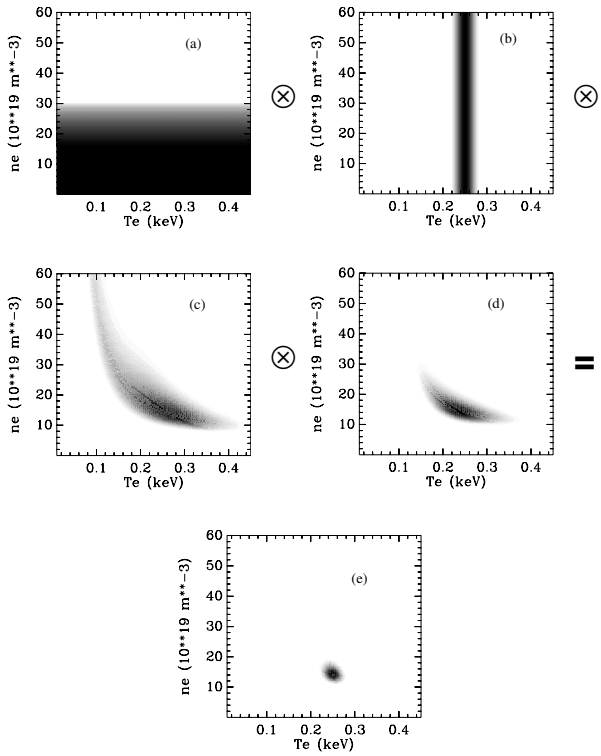

Figure 3: Posterior probability distributions for the electron temperature and electron density exploiting information from (a) the cut-off density from the operational regime of the μ-wave interferometer, (b) the soft X-ray diagnostic containing only information about T_e, (c) the Nd:YAG Thomson scattering diagnostic, (d) monotonicity constraints on neighbouring spatial channels of the Nd:YAG Thomson scattering diagnostic, (e) the result from the integrated information.

4.Scientific Staff

J.R. Abelson[1], M. Bąuer, A. Caticha[2], M. Daghofer[3], G. D'Agostini[4], Th. Durbeck, E. Edelmann[5], R. Fischer, S. Gori, F. Guglielmetti, K. Hallatschek, Ch. Hopf, W. Jacob, H. Kang, A. von Keudell, T. Loredo[6], M. Meier, W.-Ch. Muller, B. Plockl, K. Polozhiy[7], R. Preuss, E. Salonen[8], Th. Schwarz-Selinger, I. Sidorenko, U. von Toussaint, J.-S. Yoon.

[1]University of Illinois at Urbana Campaign, USA
[2]University at Albany-SUNY, USA
[3]Technical University Graz, Austria
[4]Universitá La Sapienza, Rome, Italy
[5]Department of Physical Sciences, Finland
[6]Cornell University, Ithaca NY, USA
[7]Kharkov State University, Ukraine
[8]Technical University Helsinki, Finland

Plasma Diagnostic

(Head of Division: Prof. Dr. G. Fussmann)

1 Introduction

The Plasma Diagnostics Division contributes to various WENDELSTEIN 7-X activities (conceptual studies and experimental testing of diagnostic components) and participates in the ASDEX Upgrade and WENDELSTEIN 7-AS fusion experiments at Garching. This work is reported under the sections dealing with the respective projects. Additional activities comprise experimental and theoretical investigations in Berlin. The areas covered are: PSI-2 plasma generator, UHV laboratory, electron beam ion trap (EBIT) experiment, and basic plasma physics studies using analytical and/or numerical methods.

2 PSI-2 Plasmagenerator

One major topic of investigation at PSI-2 was the hot-liner experiment. The experiment was designed to study the deposition/erosion behaviour of hydrocarbons under conditions such as those present in ITER and future fusion reactors (further information is given in the ITER part of this report).

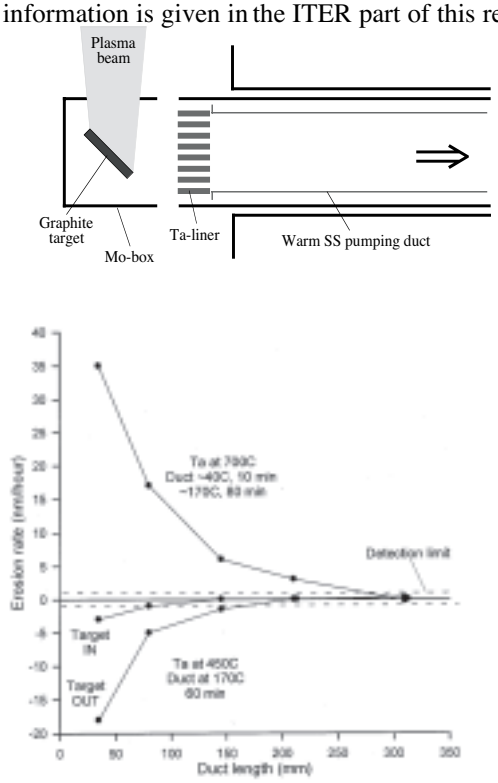

Figure 1: Schematic view of the hot-liner experiment (top). Growth rates of layers in the duct region for different experimental conditions (bottom).

To produce hydrocarbons in the PSI generator, chemical erosion of a graphite target was used. In a number of cases, the rate of hydrocarbon production was enhanced by injecting methane (CH_4) into the main chamber. Figure 1 illustrates the placement of the graphite target and the hot-liner with the attached liner tube (pump duct) relative to the plasma. As a general observation the growth process in the liner tube is found to be determined by the rates at which hydrocarbons are deposited, but also eroded by atomic hydrogen. This is of crucial importance for understanding the formation of hydrocarbon layers on surfaces. Furthermore, it was found that the temperature of the hot-liner has a large effect on the deposition/erosion behaviour. When this temperature was fixed at 450° C, for example, the process of erosion prevailed in the liner tube with the highest rate at the tube entrance (Fig. 1 bottom). Raising the liner temperature to 700° C resulted in net deposition, i.e., the formation of a-CH layers in the tube. An explanation of the qualitatively different results could be pyrolysis of the hydrocarbons at the hot surface producing fragments with a high sticking probability. Progress was also made concerning the data analysis for different methods of determining the electron temperature T_e in discharges with hydrogen. It was found that T_e can be correctly measured by Langmuir probes even if T_e is as low as 0.2 eV. The temperatures extracted from Boltzmann plots of the Balmer lines are systematically lower and it seems that this method is not reliably applicable for a wide temperature range.

Previous investigations on the heat flux in magnetized plasmas were continued by measuring the floating potential as well as the ion and electron fluxes to a probe. The PSI-2 device was furnished with a new rotatable target for simultaneous measurements of potential, energy flux and current; first experiments with this target are under way.

3 Electron beam ion trap (EBIT)

During 2002, the EBIT group has concentrated its work on a number of topics:

(i) Development of the beam line for guiding extracted ions from the trap to external analyses and experiment systems: With a reflectron time-of-flight (TOF) spectrometer the composition of the trap inventory can be analysed. In front of the TOF apparatus an atomic gas jet can intersect the ion beam to perform collision experiments.

(ii) Implementation of a normal-incidence spectrometer at the EBIT facility: The spectrometer is being employed to record fine structure transitions in the ground term of highly charged ions. Because the lifetimes of such magnetic dipole transitions (1-10 ms) are much larger than the ions' orbital periods (10^{-5}-10^{-2} ms), these lines can be used to monitor the extent of the ion cloud in a given experiment and to receive information on the ion temperature.

(iii) Extension of the database on the EUV spectra: Previous investigations of EUV spectra for tungsten were extended to

argon and xenon. Such experimental data are of great importance in plasma diagnostics, particularly for the diagnostics of fusion plasmas.

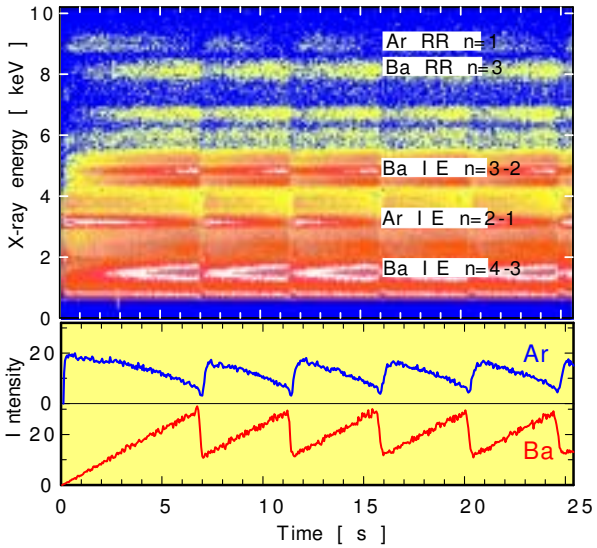

Figure 2: X-ray emission of highly charged Ar and Ba ions vs. time. Emission bands for Ar and Ba from different X-ray production mechanisms are marked. The lower plot is a projection of the Ar (n = 2-1) and Ba (n = 3-2) X-ray events onto the time axis. The feedback between the Ar and Ba ions is expressed by the mirrorlike behaviour of the X-ray intensities.

(iv) Investigation of the evolution of ions in EBIT: In the context of our EBIT physics studies, the dynamics of a two-component ion plasma was measured. An unexpected sawtooth behaviour in the X-ray emission was observed. To study the interaction between ions of a light and heavy element, time-resolved X-ray spectra were recorded for trapped ions whilst feeding the trap with a constant flux of Ar (Z=18) and Ba (Z=56) atoms. The data taken in such experiments are presented as a scatter plot in Fig. 2. A prominent feature is the time structure of the X-ray emission pointing to a periodic collapse in the ion population of the trap. The sawtooth effect is very sensitive to electron-beam current and axial trap depth, and there are thresholds for switching the activity on and off. Theoretical analysis of the sawtooth behaviour was made in terms of the feedback between low-Z and high-Z ions. Part of the experimental findings can be understood as arising from a bifurcation of temperature and density (Hopf bifurcation).

4 UHV laboratory

The application of plasma-sprayed B_4C layers is envisaged for use as plasma-facing material in the W7-X stellarator. B_4C layers combine excellent thermal properties, long erosion lifetime and high electrical resistivity. Modifications of B_4C layers were investigated after exposure of a suitable sample to the edge plasma of TEXTOR-94 tokamak discharges. The sample consisted of a Cu limiter coated with a 170 µm thick B_4C layer. The analysis methods revealed that interaction of the plasma with the surface has resulted in the formation of craters. The diameter of a single crater was found to vary from 25 to 100 µm; the crater edge is surrounded by re-solidified molten material. B and C material is deposited from the eroded B_4C layer in zones approximately 1 mm away from the craters. Further analyses were made to determine how crater formation has modified the electrical resistance of the B_4C layer (in co-operation with the Paul Drude Institut in Berlin). It was found that this quantity is about 200 times higher than that of massive B_4C from the literature. Additional variations in resistivity can be expected if the Cu substrate is involved in the deposition process. Placing a needle tip on different positions of a crater spot (controlled by a microscope) and measuring the resistivity to the underlying substrate, large reductions were found compared with regions of the surface where cratering was absent (40-160 kΩ). For example, in the crater hole 4Ω are measured, while at the rim of a crater and on its periphery, values of 0.2-1 kΩ and 2-6 kΩ, respectively, were found. Changes in resistivity due to arcing are a serious problem and may explain the re-ignition of arcs at the location of a crater. In the future, the possibility of reducing the arc-ignition probability of B_4C layers by adding impurities during the spraying process should be investigated.

5 Theory and Modelling

In the following, the main topics of the theory and plasma modelling group are listed:

(i) Bifurcation of temperature and anomalous transport in the edge region of W7-X: A 3-dimensional, time-dependent heat conduction equation was used to calculate the temperature in the edge region of W 7-X. By averaging over fluctuations and the geometry of closed field lines the equation was reduced to a 2-D problem. The effect of island structures on predicted temperature profiles was also studied within the framework of a cylindrical plasma model. For the plasma temperature, bifurcation phenomena are observed.

(ii) The particle-in-cellcode PLAS was used to investigate the behaviour of magnetized plasmas with respect to the following features: charge shielding, ion confinement, and electron transport across magnetic field lines. Starting with a thermal plasma (T_e=T_i=T) embedded in an external magnetic field B, the time evolution was calculated in 2-D geometry. In regions with an ion pressure gradient, an electric field occurs producing electron drift motion. Due to the Kelvin-Helmholtz instability this drift motion is instable. A large number of interacting vortices with different rotation directions then leads to electron transport across the magnetic field lines. It is important to note that this type of transport is proportional to the ratio of T/B, but independent of the plasma density.

(iii) Studies of material surfaces under high heat flux conditions: Investigation of the temperature evolution for targets exposed to intense laser pulses or plasma events like ELMs was continued. Modelling calculations were made for different heating scenarios and different target materials with non-isotropic heat conduction being taken into account.

6 Staff

F. Allen, I. Arkhipov[3], P. Bachmann, C. Biedermann, W. Bohmeyer, N. Ezumi[1], D. Hildebrandt, B. Juttner[2], H. Kastelewicz[2], B. Koch, P. Kornejew, M. Laux, A. Markin[3], D. Naujoks, R. Radtke, H.-D. Reiner, A. Stareprawo, D. Sunder, U. Wenzel.

1 Guest, Nagano College of Technology, Japan
2 Humboldt University, Berlin
3 Guest, Ac. Sci. Inst. of Chemistry, Moscow, Russia

Energy and System Studies

Thomas Hamacher

1 Objectives

The energy and system studies group evaluates possible future developments of the energy system. Special emphasis is put on the possible role of fusion in the very long-term. Therefor the studies need to consider a time horizon far beyond the next fifty years.

The group is involved in two European projectes, the SERF and the VLEEM studies. At the university of Augsburg the group is involved in stetting up the Wissenschaftszentrum Umwelt. As part of this work a co-operation with the adminstration and city government of Augsburg and local utility (Stadtwerke Augsburg) is formed.

2 Very Long Energy and Environmental Model (VLEEM)

The VLEEM project came to a first end in 2002 by issuing the final report to the European Commission. The report can be found under www.vleem.org. A second phase of the project was launched in autumn 2002. Objective of the study is develop a new energy model being well suited to talk about the very long term. The model should be used by the European Commission to shape the energy R&D portfolio. The model applies a so called back-casting methodology. The IPP was involved in setting up the overall framework of the methodology and to co-ordinate the activities to describe the supply side technologies.
The IPP developed a simulation tool called TASES, which is well able to simulate energy systems on various levels of spatial and temporal detail.

The final goal is to develop pictures of a sustainable energy future being either based on fossil, nuclear or renewable primary energy carriers and to describe the path that could lead into these futures.

3 Socio-Economic Research on Fusion (SERF)

Four different major tasks were attacked in 2002 within the SERF framework. The ongoing studies on External Costs very finalised. IPPs main contribution was a critical review of the ExternE methodology itself. The main criticism can be summarised as follows: it is rather doubtful that all values, including human life, can be monetised and second that ethical judgements can not be replaced by an automatically algorithm. An alternative way to judge environmental damages was proposed, which is mainly based on concepts of A. Sen.

The fruitful co-operation with the Indian Institute of Management in Ahmedabad was continued. More and refined scenarios of the development of the Indian energy system were developed.

A new co-operation with the institute Elektrische Energietechnik at the university of Rostock was formed. Objective of the co-operation are detailed studies about the development of the future electricity grid and the role fusion could play with in this grid. In a first step it was assumed that the number of intermittent electricity sources, mainly wind and solar PV increased considerable. Two sound conclusions could be drawn already from the first part of the study: the electricity network needs to be strengthen considerable and large amount of back-up capacity to guarantee the tertiary control of the network need to be installed. It is also obvious that the introduction of off-shore wind power will influence not only the German network but the UCTE net as a whole.

A third co-operation was launched with the IER at the university of Stuttgart. Goal of the co-operation was to develop a global energy model based on TIMES. TIMES is a software tool that was created within the ETSAP group, which is a special IEA agreement. The task of the IER was to design the topology of the model. TIMES was successfully implemented at the IPP.

4 URBS

The energy and system studies groups is actively involved in setting up the Wissenschaftszentrum Umwelt (WZU) at the university of Augsburg. Task of the WZU is to co-ordinate all kinds of environmental studies at the university. More information on the WZU and the annual report can be found under www.wzu.uni-augsburg.de. The IPP is affiliated to the WZU via the EPP institute at the university of Augsburg which is lead in personal union by one of the IPP directors. The main contribution of the IPP is the development of the URBS methodology. URBS should become a tool to analyse and optimise urban energy systems. The development of URBS have lead to a close co-operation with the local utility (Stadtwerke Ausburg) and to the city government and administration. Numerous scenarios for the future development in Augsburg are prepared. Special emphasis is put on the potentials of combined heat and power and the use of renewables.

5 Staff

Markus Biberacher, Tahir Farid, Thomas Hamacher, Jochen Oelke and Stephan Richter.

WEGA

Head: Dr. Johann Lingertat

1 Introduction

WEGA (Wendelstein Experiment in Greifswald fur Ausbildung) is a classical stellarator and was established as a EURATOM collaboration between Max-Planck-Institut fur Plasmaphysik/Garching, the C.E.N. Institute/Grenoble, and the Institute ERM Institute/Bruxelles. The machine was originally built in the ´70s in Grenoble/France as a tokamak with 40 field coils. Later it was converted to a stellarator by changing the torus (now R = 0.72 m and a = 0.19 m) and adding 4 helical coil packets forming a l=2, m=5 configuration.

After successful operation in Grenoble the WEGA was transferred via Institut fur Plasmaforschung, Stuttgart, to Max-Planck-Institut fur Plasmaphysik, TI Greifswald in 2000 and rebuilt in a modernised version. The machine is used mainly for educational training, testing of new diagnostic equipment, and basic research in plasma physics and for test and continuous operation of the new technical infrastructure of the institute. In July 2001 the first stellarator discharge was carried out in the new WEGA device.

2 Device and diagnostics

The plasma is ignited and heated from the low-field side by ECRH at 2.45 GHz (O-mode). The maximum power available is 6 kW. Typically, the resonant field of B_o = 87.5 mT (first harmonic) or of $B_0/2$ (second harmonic) is located in the centre of the vacuum vessel. ι_0 is varied between 0.2 and 0.5. The standard length of a discharge is a few minutes. As wall cleaning procedures either glow discharges in nitrogen, argon, and helium or stellarator discharges are used. The routinely achieved base pressure is in the 10^{-8} mbar range. Working gases are H_2, He and Ar.

The established operational limits for the magnetic fields in steady-state operation are $I_{tor} \leq 2.6$ kA ($B_{tor} \leq 0.37$ T) and $I_{hel} \leq 3.5$ kA ($\iota_0 \leq 0.18$ at $I_{tor} = 2.6$ kA).

The following diagnostics are operational: residual gas analyser, Langmuir probe with slow manipulator, H_α - detector, single-channel interferometer, and optical overview spectrometer. A bolometer and a fast manipulator for a second Langmuir probe are commissioned.

3 Experimental results

3.1 Flux surface measurements

One of the first tasks performed on the WEGA device was to evaluate the magnetic field structure. For experimental mapping of the magnetic flux surfaces the well-established fluorescent method was chosen.

The experiments were carried out to scan a wide range of ι_0 ($0.1 \leq \iota_0 \leq 1$) by changing the current in the helical field coils at a constant toroidal field B_o = 87.5 mT. For some configurations up to 40 single striking points, each representing one toroidal turn of the electron beam, could be distinguished experimentally. The experiments show good agreement with the calculations on the existence of closed nested magnetic field surfaces as well as the position of the magnetic axis. As can be seen from Figs. 1 and 2 (left side), the magnetic surfaces at ι = 1/7 and ι = 1/3 are disturbed by non-natural islands caused by error fields. In fact, all islands for ι = (n =1) / m with m = 3...7 were distinguished experimentally.

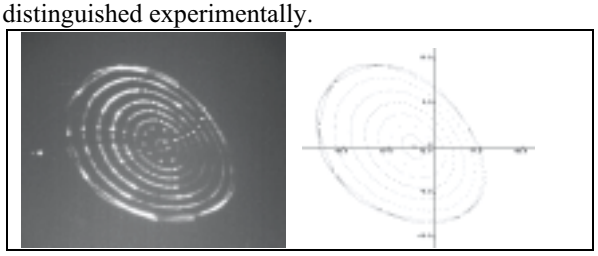

Figure 1: Measured and computed magnetic surfaces for ι = 1/7 at φ = 72°

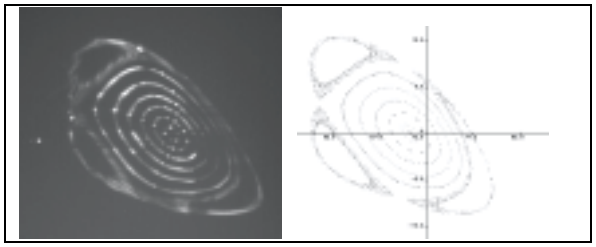

Figure 2: Measured and computed magnetic surfaces for ι = 1/3 at φ = 72°

In Figs. 1 and 2 the results of calculations using the *Gourdon* code are shown on the right side. In order to obtain a similar shape and position of the experimentally observed islands a horizontal shift of approximately 3 mm between the axis of the toroidal and helical field coils was assumed.

To compensate the error fields an additional coil was recently installed. As calculations show, this coil will suppress formation of non-natural islands and, moreover, will allow islands to be moved poloidally. The related experiments will start in the near future.

3.2 Characterisation of the plasma

One of the basic diagnostics implemented at WEGA is a Langmuir probe. Given the low power density of the WEGA plasma, the probe can be used throughout the whole cross-section to measure the electron density, electron temperature, and plasma potential as function of the radius. Different probe geometries, materials, and arrangements were used to study specific features of probe characteristics and develop procedures for data evaluating the characteristics.

One common feature of all characteristics is the absence of ion current saturation even at relatively high probe voltages

of –150V. A model capable of fitting the measured characteristics relies on the assumption of a two-temperature Maxwellian distribution of electron energies where only a small number of electrons belong to the high-temperature component. This assumption is consistent with the heating method used. Typical values obtained after fitting the probe characteristics with a two-temperature model are: $T_{e,low} \leq 15$ eV, $T_{e,high} \leq 700$ eV, $n_{e,\ low} \leq 5\times10^{17}$ m^{-3}, $n_{e,high}/n_{e,low} \leq 0.05$.

The measured profiles of the electron temperature and density for discharges heated by the first-harmonic are hollow with maxima located outside the separatrix. Here the maximum density is always above the cut-off density for O-mode ($n_{cut\text{-}off} = 7.5\times10^{16}$ m^{-3}). The electron density obtained by fitting the Langmuir characteristics was regularly cross-checked with interferometer measurements.

The hollowness of profiles may be explained by assuming that the O-mode wave is reflected at the cut-off layer outside the separatrix and thereby partially converted into X-mode. The X-mode fraction is effectively absorbed at the upper-hybrid layer, which is located between the cut-off and the outer wall. The remaining O-mode part is converted through multiple reflections into a X-mode wave which is finally absorbed at the upper-hybrid resonance. Additionally, wave conversion into Bernstein modes may contribute to absorption.

Attempts to avoid build-up of the cut-off layer outside the separatrix by reducing the density (lower gas flow) were not successful. The plasma extinguishes before the cut-off layer moves into the separatrix.

By using second-harmonic ECRH at half the standard magnetic field value the situation improves. As shown in Fig. 3, the density profile becomes peaked. However, the electron temperature profile stays hollow, although the temperature maximum moves with increasing heating power inside the separatrix. Probably, the efficiency of mode conversion into Bernstein waves is increased at second-harmonic ECRH. These waves may easily propagate towards the plasma centre and be absorbed there.

Experiments with changed geometry of the microwave injection port are under preparation. The aim is to increase the mode conversion efficiency by more tangential injection.

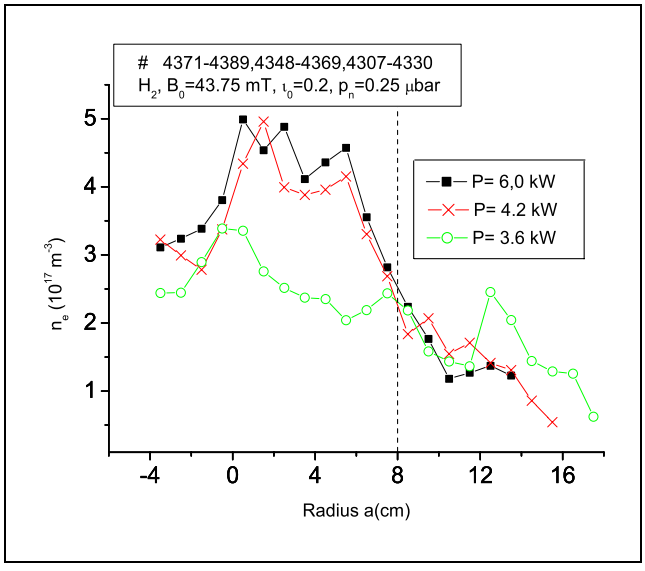

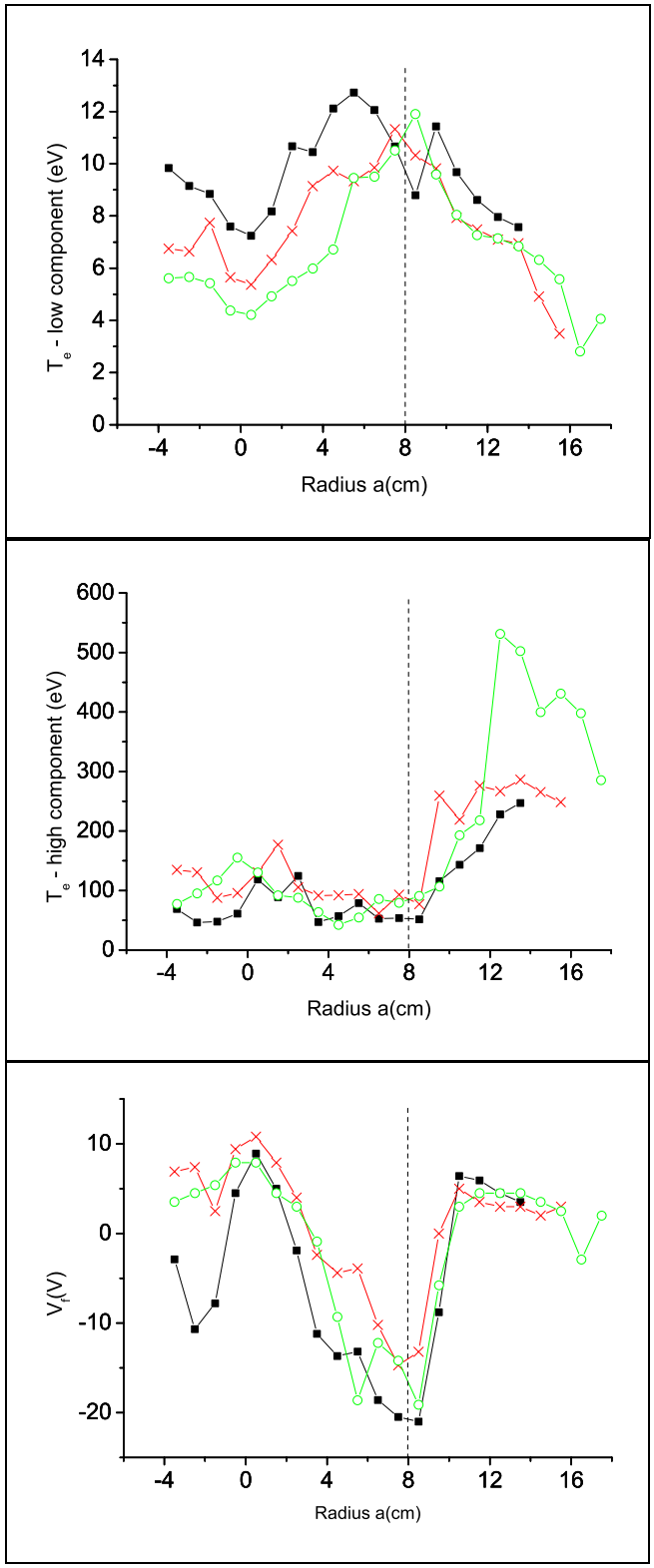

Figure 3: Measured profiles for 2nd – harmonic ECRH (separatrix at a=8cm)

4 Scientific Staff

K. Horvath*, J. Lingertat, M. Otte
* International Max Planck Research School

VINETA

Head: Prof. Dr. Thomas Klinger

1 Introduction

The linearly magnetized helicon plasma device, VINETA, went into full operation at IPP Greifswald branch in spring 2001. It is designed for conducting basic research in general plasma dynamics and is accordingly equipped with specialized diagnostics. The current scientific programme is also the subject of project A15 in the special collaborative research centre (SFB 198) "kinetics of partially ionized plasmas" of DFG (German Science Fund), established at Greifswald University. The project is focused on electromagnetic plasma waves and instabilities in bounded, inhomogeneous geometries, e.g., whistler waves, Alfven waves, and drift waves.

2 Device Design and Diagnostics

The VINETA device is designed for versatile operation and maximum flexibility. It consists of four identical cylindrical modules; each of them is immersed in a set of 8-9 water-cooled magnetic field coils that can be freely adjusted along the axis. The assembled device has a homogeneous magnetic field of maximum B = 0.1 T. If required, axial gradients in the magnetic field can be tailored to create magnetic bottle, mirror or separatrix configurations. The total length of the VINETA device is 5 m. Figure 1 shows a photo of the experiment. VINETA can be run either in steady-state or pulsed operation. A long, large-volume (V = 40 l) magnetized plasma column (argon, helium, xenon) is created with electron densities 10^{16} - 10^{19} m^{-3}. The electron temperature is in the range of 2-5 eV.

3 Experimental Programme

3.1 Discharge Physics

Main tool for plasma production is the RF source, installed in form of a glass tube at the one end of the VINETA device. The RF power is coupled into the plasma by a Nagoya type III double-half-turn right-helical antenna. Such an antenna geometry drives on m=1 helicon mode. Figure 2 shows density profiles in the poloidal plane of the plasma column. The three discharge modes – capacitive, inductive, helicon – are established if the RF input power is increased from zero to a few kW. In the capacitive mode, a hollow profile forms since plasma production takes place in the antenna sheaths only. Above a certain power threshold ~1 kW, in a sudden jump the helicon-wave-sustained discharge mode is established. The helicon discharge mode is characterized by high plasma densities (up to 10^{19} m^{-3}) and a peaked density profile. By lowering

Figure1: Full view of the VINETA device. The magnetic field coils (red) can be adjusted along the axis. The helicon plasma source is installed on the right-hand side.

the RF power below a different power threshold, the discharge jumps from the helicon mode into the inductive mode with a flat-top density profile (plasma density in the centre is 10^{17} - 10^{18} m^{-3}).

In all three cases, the electron temperature remains in the range 2-5 eV. Higher electron temperatures could be achieved specifically by electron cyclotron resonance heating (ECR) of the helicon target plasma. As an alternative plasma source, a quiescent DC hot-cathode discharge is currently under construction.

3.2 Whistler Waves in Bounded Plasmas

Whistler waves are right-hand polarized electromagnetic waves with frequencies in the range of $\omega_{LH} << \omega << \omega_{ce}$. They are of fundamental importance in ionospheric plasma physics and radio sciences. Whistler waves have regained attention in the context of helicon discharges, where the long-wavelength whistler waves are used to heat the plasma non-resonantly. The primary goal of the project is systematic investigation of the transition from unbounded-plasma whistler waves to bounded-plasma helicon modes with special attention to the wave dynamics. This is understood only if the problem of a plasma-filled

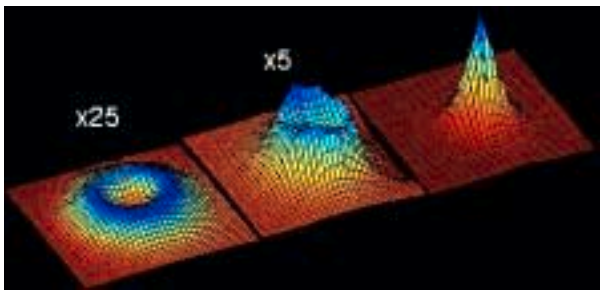

Figure. 2: Poloidal plasma density profiles for capacitive, inductive, and helicon discharge mode (left to right).

waveguide is considered, i. e. the complete plasma-edge-boundary system must be taken into account. The numerical solution of the resulting equations gives a reasonable answer to questions arising from experimental observation. In the long wave-length regime (~10 MHz ~ ω_{LH}), relevant to helicon wave physics, measurements of the amplitude and phase of the RF-driven wave magnetic field were done in a plane section parallel to the magnetic field. Figure 3 shows the result.

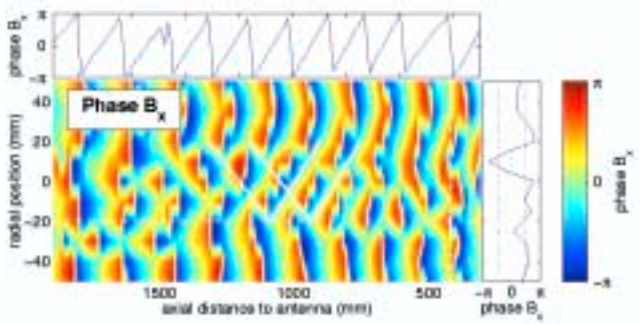

Figure 3: The B_x-component of the magnetic field fluctuations measured in a plane parallel to B_0 .Top diagram (a): amplitude. Bottom diagram (b): phase. The dashed lines indicate the 1d sections.

The phase fronts (bottom diagram) show a surprisingly complicated pattern. The coarse structure indicates a more or less constant phase in the radial direction, but the fine structure with curved and broken fronts is only to be understood if obliquely propagating waves are taken into account that are totally reflected at the plasma (cut-off) boundary layer. This reflection process is well consistent with the dispersion properties of whistler waves and supports the analogue to electromagnetic waves propagating in an optical fibre.

3.3 Drift and drift-Alfven waves

The high density achieved in the helicon discharge mode allows one to approach the $\beta >> m_e/m_i$ regime of drift waves. This project aims to make systematic investigation of electrostatic drift waves observed in the density gradient regions of the VINETA device. Basically one expects to enter the electromagnetic drift (Alfven) wave regime if $\beta \geq m_e/m_{i\ and}$ $\beta' = \beta(L_\parallel/2\pi L_\perp)^2 \sim 1$, where $L_\perp$ is the profile length scale perpendicular to B_0 and $L_\parallel$ is the parallel magnetic con-nection length. However, since the collisionality at T_e = 2-5 eV is comparetively high, the electron response parallel to B_0 is strongly damped and the drift waves keep electrostatic. Shown in Fig. 5 is an m = 2 electrostatic drift wave mode (β = 160 m_e/m_i and ν_{ei}= 50 MHz) as recorded with the probe array.

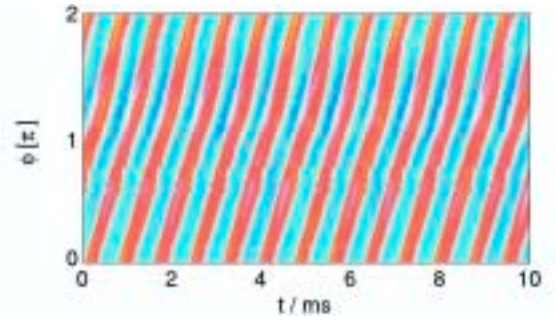

Figure 4: Space-time diagram of density fluctuations caused by an m = 2 electrostatic drift mode.

Work in progress is a comparison between linear eigenmode calculations (in cooperation with Risø National Laboratory), fully taking into account the radial collision profile, and measured frequencies and mode numbers/structures. As a next step, by ECR heating the electron temperature is increased above $T_e \geq 10$eV. This reduces the collisionality and opens the parameter space for electromagnetic drift wave studies. An appropriate ECR heating system is under construction.

3.4 Alfvén waves

For high-density helicon plasmas, the Alfvén wavelength $\lambda_A = v_A/f_{ci}$ is much less than the axial plasma column length. It is thus feasible to study torsional Alfvén waves under steady-state laboratory conditions. Alfven waves are launched by small exciter electrodes or current loops. The measurement of propagating wave fields is currently being done by relatively large magnetic probes, in future with miniaturized Hall probes and optical (LIF) techniques. Of particular interest are kinetic Alfvén waves, where $v_A \sim v_{e,th}$. Kinetic Alfvén waves play an important role in ionospheric plasma physics but also in electromagnetic drift wave dynamics. Figure 6 shows the wave dispersion measured in a helium plasma. Also shown is the theoretically expected dispersion curve of a torsional Alfvén wave. The agreement is quite reasonable. Note the long wavelengths at low frequencies.

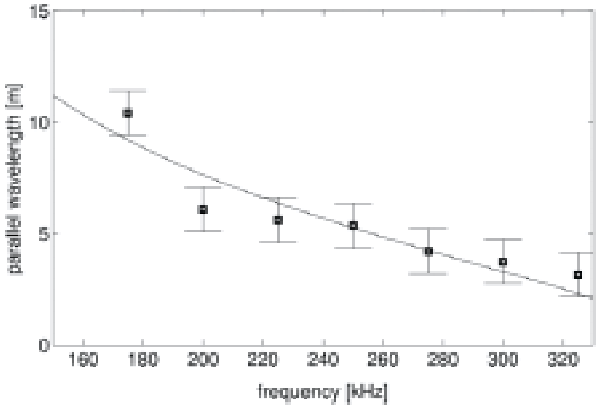

Figure 5: Dispersion measurements of a kinetic torsional Alfvén wave. The theoretically Expected dispersion behaviour is also included (solid line).

4 Scientific Staff*

T. Klinger, C.M. Franck, O. Grulke, C. Schröder, A. Stark, J. Zalach

Guests: G. Bonhomme[1], V. Naulin[2]

*

1 L.P.M.I., Université Henri Poincaré, Nancy (France)

2 FZ Risø (Denmark)

Electron Spectroscopy Group

Head: Uwe Hergenhahn

1 Introduction

The electron spectroscopy group uses synchrotron radiation in fundamental investigations of the detection of charged particles, which are important for the characterization of species in the cold region of fusion plasmas.

2 Results

Important results have been achieved in 2002 mainly in two areas, namely electron spectroscopy of free clusters and in coincident detection of electron pairs. For the latter project, a new apparatus, in which a number of electron time-of-flight analysers are coupled with a hemispherical electron spectrometer, has been completed.

2.1 Autoionization of clusters

Photoelectron spectroscopy of free van-der-Waals clusters can reveal important information on the electronic structure of these weakly bound systems and substantially benefits from the use of synchrotron radiation.

A new process, which has recently been investigated theoretically, is the autoionization of singly ionized van-der-Waals clusters. Here, as compared to the monomer, the number of dicationic states is greatly increased since the two positive charges can be distributed among two different sites in the cluster. Calculations of the energies of these states, e.g. for $(Ne_N)^{2+}$ clusters, have shown that these 'two-site' states have a significantly smaller binding energy than atomic Ne^{2+} states. By that, autoionization of inner-valence vacancy states, like $(Ne_N)^+ 2s^{-1}$, is energetically possible, whereas this state would decay by fluorescence in the atom.

Other than conventional Auger decay, this process is only possible in the presence of the environment surrounding the vacancy, and therefore has been termed Interatomic Coulombic Decay (ICD).

The detection of ICD would be of great interdisciplinary interest, since the same decay mechanism is expected to be present in other weakly bonded systems, like aggregates bound by hydrogen bridges.

To collect evidence for the ICD hypothesis, electron spectra of Ne clusters at photon energies below and above the 2*s* ionization threshold were collected. The cluster bulk and surface components of the 2*s* line and the monomer component due to uncondensed atoms in the beam can be distinguished (Fig. 1). Apart from that a peak-like feature with kinetic energies between 1.2 and 2 eV appears, when the photon energy is tuned above the 2*s* ionization threshold. In Ar clusters, where ICD of the 3*s* levels is not allowed, a corresponding feature is absent. We interpret this as the first experimental proof for the existence of ICD.

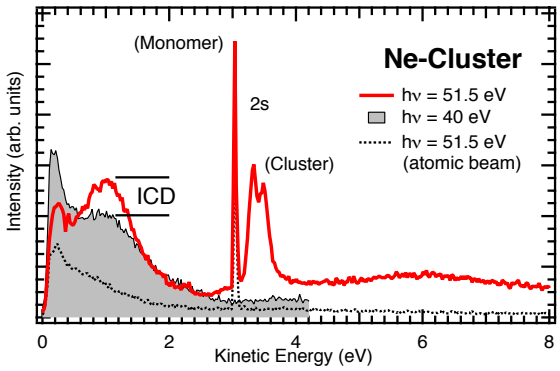

Figure 1: Electron spectrum of free Ne clusters showing strong evidence for electrons resulting from ICD with kinetic energies around 1.6 eV.

2.2 Photoelectron – Auger electron coincidence measurements

Molecular Auger spectra are complex due to the large number of doubly charged final states that can be populated. Moreover, in conventional Auger electron spectroscopy contributions of all intermediate states are present in the final spectrum. By that, in molecules, where core holes can be created at several chemically inequivalent atoms with the same nuclear charge, contributions of these atoms will overlap. A simple example of the latter case is the nitrogen K-shell photoionization of dinitrogenoxide, N_2O.

N_2O, or $N_T{=}N_C{=}O$, is a linear molecule, where N_T and N_C are called the terminal and the central nitrogen atom. Their N 1*s* photoionization thresholds are 408.5 and 412.5 eV, resp. In this project, we have used a new apparatus to separately record the K-VV Auger spectra of the two chemically shifted nitrogen core hole species. To this end, the Auger electrons were detected in coincidence with the pertaining photoelectrons. Significant differences between the two Auger spectra were found, which are in rough agreement with theoretical predictions.

For the last experiment carried out in 2002, our high-resolution electron spectrometer was combined with a projective ion spectrometer constructed in the group of Prof. U. Becker, FHI Berlin. This allowed to carry out high resolution detection of photoelectrons from axis selected molecules.

3 Scientific Staff

S. Marburger, O. Kugeler, U. Hergenhahn

Scientific Computing, Data Management and Data Acquisition

Head: Stefan Heinzel

1 Introduction

Rechenzentrum Garching (RZG) traditionally provides supercomputing power and archival services for IPP and other Max Planck Institutes throughout Germany. Besides operation of the systems, application support is given to Max Planck Institutes with high-end computing needs in fusion research, materials science, astrophysics, and other fields. Large amounts of experimental data from the fusion devices of IPP (ASDEX Upgrade, WENDELSTEIN 7-AS, and, later, WENDELSTEIN 7-X), satellite data of MPI of Extraterrestrial Physics (MPE) at the Garching site, and data from supercomputer simulations are administered and stored with high lifetimes. In addition, RZG provides network and standard services for IPP and part of the other MPIs at the Garching site. The experimental data acquisition software development group for the new WENDELSTEIN 7-X fusion experiment and the current ASDEX Upgrade fusion experiment operates as part of RZG.

2 Major Hardware Changes

The massively parallel Cray T3E system (with 816 processors, 102 GB main memory, and a peak performance of 0.49 TeraFlop/s) has been replaced by a new IBM supercomputer. In the first half of 2002 a one TeraFlop/s system with 208 Power 4 processors was available. Upgrade to a 3.8 TeraFlop/s system with 704 Power 4 compute processors and 1.8 TeraBytes of main memory occurred in summer. In the Nov 2002 list of the top 500 supercomputers worldwide the system was ranked no 1 in Germany, no 5 in Europe and no 21 world-wide. The performance of the new system exceeds that of the Cray T3E system by one order of magnitude. For non-parallel vectorizing codes, a NEC SX-5 vector system with high single processor performance with 3 processors and 12 GB of main memory is available. As general purpose machine, the 20 processor IBM SP2 system has been replaced by an 8 processor IBM power 4 system. The following dedicated compute servers for different institutes have been installed or upgraded and are being operated by RZG: Linux cluster with 64 Pentium 4 processors for Fritz-Haber-Institute; SGI Origin 3400 system (12 processors, 24 GB main memory) for IPP; SUNFIRE 3800 system (8 processors US III, 32 GB main memory) for MPI of Developmental Biology; SUNFIRE V880 system (4 processors, 8 GB of main memory) for MPI of Extraterrestrial Physics.

3 Data Management

3.1 Multiple-resident AFS and OpenAFS

RZG developed the OpenAFS client for IBM AIX 5.1, which is used on the new Regatta systems. The major advantage over the IBM supplied AFS client are large file support and the MR-AFS extensions to allow for data-migration commands. The OpenAFS client for AIX 5.1 works, however, presently only in the 32-bit-kernel. Further development is needed to support the 64-bit-kernel as well.
On the server side RAID systems, which use inexpensive IDE disks, but appear to the host as SCSI disks are going to replace more and more the traditional SSA disks. The new RAID systems show better performance at much higher capacities and lower price. They can be used not only with Linux PCs, but with any hard- and software supporting SCSI or fibre channel.

Especially for the Regatta systems a high performance AFS solution based on GPFS data transfer protocol is being developed.

3.2 Archival and Backup System

Concerning mass storage of data, a basic distinction is made between experiment-type data sets with requirements for long-time conservation and short-lifetime data of the backup type, which are replaced by new versions at short intervals. Meanwhile, besides MR-AFS, TSM (Tivoli Storage Manager from IBM) is routinely in use. The tape drive capacity of the TSM server (an IBM H80 machine) has been extended by additional tape drives to a total of fourteen (four STK 9940 and ten STK 9840 drives) served by the Grau/ADIC and STK robot systems and tape silos. The “Arc” service stayed in operation only for the high-performance systems Cray T3E and NEC SX-5, for which no TSM clients are available. For TSM archival data the second tape copy is being routinely generated at Leibniz Rechenzentrum Munchen (LRZ) in downtown Munich.

4 Developments for High End Computing

High-performance computing is a key technology for IPP and other Max Planck Institutes. Application development and support for high-end parallel computing is of great importance for disciplines especially in the fields of plasma physics, materials science, and astrophysics. Projects to support new developments in close collaboration with the respective scientists are described in detail.

4.1 Fusion Research

4.1.1 MHDT Code

The general turbulence code MHDT (magneto-hydro-dynamic turbulence) with Cray-specific communication routines was ported to the new IBM system. Usage of the Cray shmem compatibility library was helpful. Fast Fourier Transformation library routines had also to be converted from the Cray to the IBM system. In the first approach IBM specific routines from the pESSL library were tested. Due to scalability problems alternatively better scaling routines from the FFT package FFTW from MIT were implemented.

4.1.2 SDTrimSP Code

The functionality of the SDTrimSP (static/dynamic Trim sputtering) code of the generalized TRIDYN code package was further extended in co-operation with R. Schneider. Target compositions can now be taken from an input file so that previous runs may serve as starting points for new simulations. Further on the option for the variation of isotopes was implemented. A single code version is maintained for all potential computer systems (Linux cluster, IBM regatta systems, Cray T3E) depending on compute and main memory requirements.

4.1.3 TORB Code

The TORB code was extended by an important functionality. Support was given for the implementation of "Zonal Flows" as an extension of the physical model and the adaptation of the diagnostic possibilities. For graphical display of the results the corresponding analysis program was extended. The parallelization of the code was adapted to the hybride architecture of the IBM "Regatta" systems by cloning/farming.

4.1.4 EUTERPE Code

Support was given for porting the code to the IBM regatta system and to integrate the essential diagnostics of the TORB code.

4.2 Materials Sciences

4.2.1 WIEN2K Package

The new WIEN2K version of the LAPW programme package with important new functionalities replaces the previous WIEN97 code. WIEN2K was now adapted to the new Power4-based IBM system. Initial test runs with large data sets showed that the achievable scaling behaviour stayed behind the expectations. Because of the complex structure of the code several reasons can be considered. The parallel solver for the Eigenvalue problem is an essential component which is a set of ScaLAPACK library routines in WIEN2K. In a first approach it was investigated whether analogous routines from the IBM optimized pESSL library scale better. Furtheron the existence of alternative suitable parallel solver algorithms was evaluated. So far better alternatives could not be found. Usage of pESSL routines showed now improvement over the public domain ScaLAPACK routines. A potential for improvement, however, lies in the usage of an improved MPI communication library with shorter latencies. There are two other larger program parts besides the Eigenvalue solver, which deal with the set up of the matrix. Detailed timings showed a need for improvements. Work is in progress, in close co-operation with the authors at TU Vienna.

4.2.2 FHImd97 Code

The ab-initio molecular dynamics code FHImd97 with T3E specific optimizations and Cray proprietary communication and numeric routines was ported to the new IBM system. Significant code revisions were necessary especially for the specific implementation of the Fast Fourier transformations. By further optimizing the ported code, a tenfold acceleration of the code could be achieved on 32 IBM processors compared to 32 Cray T3E processors.

4.2.3 CHARMm

The molecular dynamics programme CHARMm was implemented on the new IBM system. Especially the introduction of the 64-bit version, which was not yet supported for IBM systems, caused problems. The new code is now used for production runs by MPI for Biophysics, Dep. Prof. Michel.

4.2.4 STRIP code

For the STRIP simulation code of MPI for Metal Research support was given to significantly enhance the performance on the IBM system.

4.3 Astrophysics

4.3.1 Adaptive Mesh Refinement

Installation work has been carried out for the CHOMBO and CHOMBO-Vis package, which provides a general adaptive mesh refinement procedure with integrated visualization. Interoperability with additionally necessary software packages like Python, HDF and VTK turned out to be very complicated.

4.3.2 Rady/2D

The performance of the supernova simulation code Rady/2D (radiation hydro code) could be considerably improved on the new IBM Power 4 system. Especially correct usage of highly optimized IBM specific library routines (from ESSL and MASS libraries) together with an additional particular compiler option increased the performance of the 2D version over 1 Gflop/s and the 1D version over 1.4 Gflop/s.

4.3.3 AMRA/Genesis

For the parallel usage of the integrated AMRA/Genesis code performance bottlenecks were analyzed and solved together with the author. Removal of Divide Exceptions led to a significant performance enhancement.

4.4 Earth Sciences / Climate Research

4.4.1 ECHAM

After the parallelization of the advection procedures in ECHAM model version 5 had been finished and delivered to MPI for Meteorology for inclusion into the ECHAM5-standard version, the need for parallelization of extension

functions, especially the so-called nudging arose. An additional term creates a necessary guidance along a given (measured) trajectory. This additional term and the filtering for normal mode initialisation was now also parallelized.

4.4.2 C-HOPE

The sequential C-HOPE code for ocean modelling was parallelized using the OpenMP model for shared memory systems on IBM machines at RZG and the transferred to the large NEC SX-6 system at DKRZ. The code can now be used with a performance of 13 to 15 Gflop/s on a SX-6 node at DKRZ.

5 Vector Computing

Support was given to implement a molecular dynamics code of the CIPS group on the NEC SX-5 system. The performance analysis showed, however, that a scalar cache-based system is more suitable for this code. As an alternative to parallelization of this code there was a screening for suitable, already existing parallel molecular dynamics codes. The LAMMPS package from Sandia Labs appeared to be principally suitable and was ordered by the author.

6 Multimedia

6.1 Video Conferencing

The RZG video group, established in 2002, gives central support to guarantee effective use of the increasing number of systems in- and outside IPP. 188 video conferences with about 60 minutes per session have been run between the lecture halls at Garching and Greifswald. Only two meetings had to be cancelled due to GWiN failures, minor problems were: 8 presentations had to be shown by video and 11 technical bugs deteriorated sound or video quality.
The AUG seminar room was equipped with hard- and software comparable to the lecture hall in D2. The IPP VC now consists of 3 high-end systems Tandberg 6000, 6 settop systems - 1 Tandberg 880, 5 Tandberg 500 –20 desktop systems Polycom ViaVideo, and 2 PictureTel ISDN systems. Software clients like Sun Forum, NetMeeting and GnoMeMeeting are tested at AUG. Most systems are operated over the GWiN, alternatively over up to 6 S0 ISDN lines. Multipoint conferences are run on in-built MCUs or the VC service of the DFN-Verein (still in pilot phase, steadily improved and used for 3 conferences per week). The firewall and safety problem has been solved by testing, improving and installing a software gatekeeper / proxy on a dedicated Linux PC (to be moved to RZG DMZ). All VC systems inside IPP are registered on that gatekeeper, which restricts in and out going VC traffic to those machines only. The global dialling system (GDS) of the Internet2 is used, allowing standardized world-wide connections. To schedule and administrate the IPP systems, the VSA software of MVC-AG has been installed.

The requirements for an EFDA teleconferencing infrastructure have been summarized in an ad hoc report to the EFDA leader: The unstable inter-operating of the ITU standards H.320 and H.323 at IPP and the free software VRVS should be further tested, the situation will be evaluated again in 2003. Where high quality video and audio is needed, H.323 hardware is recommended. The Generalverwaltung of the MPG has been supported in installing 5 high end desktop system for the president, the general secretary and the three vice presidents, together with one videoconferencing room. Another 15 systems are currently installed in MPIs of the biological medical section of MPG. The DFN VC service is used.

7 Developments in Networking

New network infrastructure was implemented at IPP. The goal was to use a cabling structure that can easily be adapted to future technologies. The data network realized was therefore based on the concept of a “collapsed backbone“, consisting of switches at a few central locations which directly connect to all endpoints via links based on copper or fibre. This structure drastically enhances overall network performance, for all connections between centralized switches are now at a speed of 1 Gigabit/s (Gigabit Ethernet technology) with the option of implementing even more powerful trunks. Due to the availability of both multi-mode and mono-mode fibre optic cables between the premises it is also possible to adopt upcoming new network technologies such as 10 or 40-Gigabit Ethernet. With this structure we also improved the security and integrity of data because eavesdropping is almost impossible.

For logical security based on the functionality of the internet protocol suite TCP/IP a packet filter firewall at the access point to the internet was implemented, where all the incoming/outgoing packets are checked against a set of blocking or granting rules. Additionally all incoming electronic mail is scanned for viruses and only clean and unobjectionable data (based on known problems) will be passed to the internal network. Spam mail filtering has also been installed. Users can now individually define and set filter threshold values.

8 Data Acquisition and Data Bases for Plasma Fusion Experiments

The XDV group supports the experiments at IPP in data acquisition, archiving and processing. The complete design concept for the data acquisition system of WENDELSTEIN 7-X was reviewed. All known requirements concerning real time control, data visualization in near real time, data archiving, data analysis and configuration were incorporated in the design. The primary goal in the design process was to achieve a state in the software development, ready to support the first data acquisition stations in measuring and archiving data. Those stations, needed for lab testing of heating subsystems and for the first tests on diagnostic construction, are expected to operate by the middle of 2003.

Another test for the design principles is the implementation of a diagnostic system for ASDEX-Upgrade (the shot based tokamak at the IPP) that will operate with the newly developed software. The first stage of this MSX diagnostic is nearly finished and will start operation at the beginning

of 2003. More work has to be done on real time processing of incoming data.

The interface to the object-oriented Objectivity database was further developed. The database is used for archiving of all measured data streams and to log the used parameters and configurations. The database also contains all information that an analysis task needs for processing. The setup parameters and the start configuration are stored in a second federation. A GUI-based object editor, which is needed for generating and editing parameter and configuration objects, was tested and adapted to the urgent needs of the XDV users. This tool is still under development.

Together with the control group of WENDELSTEIN 7-X we started the process of designing GUI-based editors for the discharge programs of the WENDELSTEIN 7-X stellarator. A discharge program is a planned sequence of segments. Each segment describes the state of the machine for a planned duration of time. During the run of a program there is always one and only one segment active. The control system is responsible for changing of segments. These editors are necessary, to give the users of the experiment access to the overwhelming amount of free parameters of the subsystems. The tools are crucial to the experimental program and must be thoroughly designed to be accepted by the users. There is still work to be done in the design process as well as in the implementation.

The time-measuring system of WENDELSTEIN 7-X consists of a central clock and a time-generating device that connects via a star-like fiber optic network to numerous slave time-capturing devices (TDC's and TTE's). The development of the slave devices as well as a simple central timer is finished. All interfaces are implemented as PCI cards. The TDC ("time to digital converter") was tested and reviewed. Drivers for VxWorks, Solaris, Windows NT and Linux have been developed. The TTE ("Trigger Time Event") is also finished, but the drivers for Windows NT and Linux have still to be developed. Together with the simple central timer, a star-like networks was implemented and connects now the prototype DAQ ("data acquisition") stations. The accurate comparison in time of measured data between different stations is now possible.

The duration of a discharge of WENDELSTEIN 7-X is planned to be up to 30 minutes. This means, that most of the important state parameters have to be monitored and supervised during the discharge. This is also true for the diagnostic subsystems during the data acquisition phase. This monitoring system for the DAQ stations is a two step process. The collected data is reduced on the DAQ stations and sent by IP multicast protocol to one or more monitor servers. The servers analyze the data and publish evaluated and physically meaningful data back to the net. This data is then visualized by monitor clients on the physicist's workstation. Again the IP multicast protocol is used to reduce the amount of network traffic. The tasks of the monitor server have to be investigated in close co-operation with the physicists and have still to be defined. Several prototype clients with different visualizing methods have been implemented.

Data communication and event transmission with the control system will be done via the "real time network". An implementation of an ethernet real time protocol, proposed by the control group of WENDELSTEIN 7-X, was accomplished for Windows NT and Linux. The functionality and the performance of this system is still under test and has to be further improved.

9 Staff

I. Ahlert, A. Altbauer, G. Bacmeister, K. Desinger, R. Dohmen, S. Gross, A. Hackl, R. Hatzky, S. Heinzel, C. Hennig, A. Jacob, K. Lehnberger, H. Lederer, R. Muhlberger, K. Näckel*, W. Nagel, M. Panea-Doblado, P. Pfluger, F. Pirker, A. Porter-Sborowski, H. Reuter, S. Sagawe*, H.-G. Schätzko, R. Schmid, J. Schmidt, A. Schott, H. Schurmann*, T. Soddemann**, H. Soenke, U. Schwenn, K. Stockigt**, R. Tisma, S. Valet*, Th. V. Weber*, I. Weidl

Data Acquisition Group:
P. Heimann, J. Maier, J. Reetz, M. Zilker
* IPP Greifswald ** since Aug 2002

Lehrstuhl für Experimentelle Plasmaphysik

Prof. Dr. Kurt Behringer

In collaboration with the "Experimental Plasma Physics Division E4" the research of the department is focused on diagnostics of low temperature plasmas including fusion edge plasmas. Main emphasis is given on the development and application of diagnostic methods, in particular on molecular diagnostics. The investigations are basically carried out at several laboratory experiments (ECR, MW and RF plasmas), however, some methods are applied also to the divertor plasma of ASDEX Upgrade.

1 Molecular Hydrogen

Radiation of molecular hydrogen is a diagnostic tool to determine molecular densities in laboratory plasmas and molecular fluxes in the edge plasma of fusion experiments. Interpretation of the radiation is based on a collisional radiative model which has to be verified by experimental results. Furthermore, the vibrational population in the ground state is deduced from the measured vibrational population in the excited state. Since the vibrational population in the ground state plays a key role in a manifold of processes, the interaction of hydrogen plasmas with surfaces is also a point of interest.

1.1 Collisional Radiative Model

The collisional radiative model for molecular hydrogen was further improved. A comparison of measured with calculated population densities in an electronically excited state of the triplet system ($d\ ^3\Pi_u$) showed the relevance of quenching processes (Q), charge exchange (CX) and dissociative attachment (DA) of electronically excited states. This is illustrated by Fig. 1, which shows calculated photon efficiencies (destruction events, such as ionisation S and dissociation D, per emitted Fulcher photon XB). The (S+D)/XB ratio increases systematically with each further process. The enhancement is up to an order of magnitude for $n_e > 10^{18}$ m^{-3}. These additional processes are clearly verified by the experimental data point which is obtained from gas puff experiments with calibrated valves in the outer divertor of ASDEX Upgrade. T_e and n_e were taken from Langmuir probe measurements.

In order to resolve underlying rate coefficients for electronic impact excitation into the vibrational states, Franck-Condon factors and transition probabilities are needed. These data were calculated on the basis of potential curves and electronic transition dipole moments with a previously developed computer code TraDiMo. Calculations of corresponding cross sections are currently started. The knowledge of transition probabilities for the isotopes allow predictions for the wavelength range of intense vibrational transitions. This is now available for selected transitions in H_2, HD, D_2, DT and T_2.

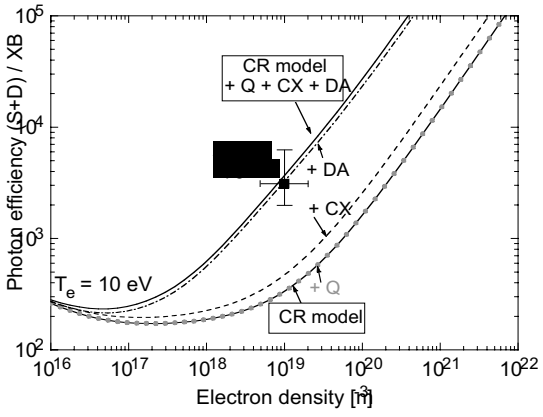

Figure 1: Extensions of the collisional radiative model verified by an experimental data point (ASDEX Upgrade).

1.2 Interaction with Surfaces

The vibrational population of the first five vibrational quantum numbers in the ground state of molecular hydrogen can be characterised by a vibrational temperature $T_{vib}(X)$. This quantity is accessible by emission spectroscopy. Modifications of $T_{vib}(X)$ were observed in hydrogen plasmas being in contact with several surfaces (plasma treated) as shown in Fig. 2. Tungsten and graphite lead to an enhancement of $T_{vib}(X)$ in comparison to steel, Cu and Al. Gas blow experiments of methane above steel result in the highest value. This might be due to dissociation of hydrocarbons into already vibrationally excited hydrogen molecules. First investigations show a dependence of $T_{vib}(X)$ on the substrate temperature, i.e. a decrease from

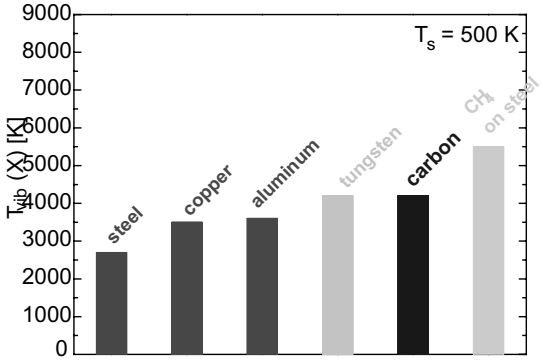

Figure 2: Influence of surfaces on the vibrational population of hydrogen in a hydrogen plasma.

T_s= 500 K to T_s= 300 K enhances $T_{vib}(X)$ from 4200 K to 5400 K above tungsten.

2 Hydrocarbons

Hydrocarbons are formed by chemical erosion of carbon in hydrogen plasmas. Measurements of erosion yields require knowledge of the incoming hydrogen flux and the released carbon flux. Both quantities can be determined by spectroscopic techniques using the Balmer line radiation and radiation of hydrocarbon radicals, e.g. CH. A similar technique (density instead of flux measurements) is applied to laboratory plasmas with the advantages of having well defined plasma and surface parameters. Furthermore, weight loss measurements are applicable. The combination of these methods is used to quantify the formation of higher hydrocarbons.

2.1 Erosion yields

The composition of ions in a H_2/He plasma was measured in an ICP discharge by using mass spectrometry. It is typical for these low pressure plasmas that H_3^+ is the most dominant ion. Ratios of ion to atomic fluxes are shown in Fig. 3 (left). Due to the simultaneous bombardment of atoms and ions, the chemical enhanced erosion of graphite is observed in these plasmas. The additional existence of low energy rare gas ions leads to the chemical sputtering (ion-neutral synergism) as shown in Fig. 3 (right). A dependence on the rare gas ion species is observed.

2.2 Higher Hydrocarbons and Photon Efficiencies

The method to determine the methane particle flux from the photon flux of CH is well established. Detailed investigations of hydrocarbon plasmas in ICP and ECR discharges have shown that the radiation of the C_2 molecule (Swan band, around 516 nm) is correlated with the C_2 density and, due to a dominant formation mechanism, to the C_2H_x densities. Therefore, it is suggested to use the C_2 emission as diagnostics for the formation of higher hydrocarbons (C_2H_x) released from a carbon surface.

The quantity, which gives the correlation between a measured photon flux and the carbon flux, is the so-called photon efficiency D/XB. Due to complex reaction channels of hydrocarbons, calculated D/XB ratios (dissociation models) have to be checked by experimental results. This was done for CH_4 particles and CH radiation in a special campaign (gas puff experiments) at ASDEX Upgrade in a limited parameter range of T_e and n_e. The radiation of C_2 was simultaneously observed by the transportable spectroscopic system which is maintained from Augsburg. A comparison of CH radiation originating from CH_4 puffs with CH radiation from C_2H_6 puffs gives almost equal photon efficiencies. As a consequence CH radiation can refer to both, CH_4 and C_2H_6 formation and the contribution of higher hydrocarbons to CH radiation has to be considered in spectroscopic measurements of erosion yields. For C_2 radiation the situation is more clear: the contribution of CH_4 particles is almost negligible. The photon efficiency for C_2 from C_2H_6 is comparable with the photon efficiency of CH from CH_4, both being in the range of 55 – 60. On this basis, spectroscopically determined carbon fluxes can be corrected now by the contribution of the C_2H_6 formation. Work is ongoing for other hydrocarbons such as C_2H_2, C_2H_4 and C_3H_8.

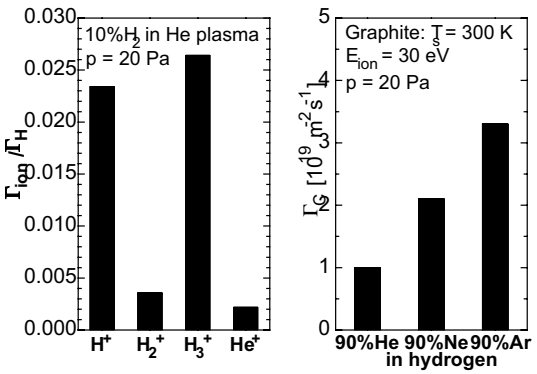

Figure 3: Left: measured ion to atomic flux ratio in a H_2/He plasma. Right: carbon fluxes released from graphite using He, Ne or Ar as background gas.

3 Publications and Lectures

U. Fantz: *Emission Spectroscopy of Hydrogen Molecules in Technical and Divertor Plasmas*, Contrib. Plasma Phys. **42** (2002) 6-7, 675-684

U. Fantz and P.T. Greenland: *Discussion on Data Needs for Molecular Hydrogen Modelling*, Contrib. Plasma Phys. **42** (2002) 6-7, 694-696

U. Fantz: *Atomic and Molecular Emission Spectroscopy in Low Temperature Plasmas Containing Hydrogen and Deuterium*, IPP Report, **IPP 10/21**, March 2002

U. Fantz: *Diagnostikmethoden zur Bestimmung der Elektronenenergieverteilungsfunktion in Niederdruckplasmen*, Seminar, Technische Physik, AG Dünnschichttechnologie, Universität Essen, Januar 2002

U. Fantz: *Optische Erscheinungen in der Atmosphäre*, Institut für Plasmaforschung, Universität Stuttgart, Mai 2002

U. Fantz: *Spectroscopic Characterisation of a Negative Ion Source*, 3th Workshop on Inductively Coupled Plasma Sources (WICP), Bochum, June 2002

U. Fantz: *Spectroscopic Characterisation of a Negative Ion Source*, Max-Planck-Institut für Plasmaphysik, Garching, Seminar der Abteilung Neutralteilcheninjektion, July 2002

U. Fantz: *Molecular Emission Spectroscopy of Low Temperature Plasmas in Hydrogen*, New Trends in Plasma Physics II, Max-Planck-Institut für Plasmaphysik, Garching, July 2002

U. Fantz: *Molecular Diagnostics of Cold Edge Plasmas*, IAEA Technical Meeting on "Atomic and Molecular and Plasma Material Interaction Data for Fusion", Jülich, October 2002

U. Fantz: *Optische Erscheinungen in der Atmosphäre*, Max-Planck-Institut für Plasmaphysik, IPP Instituts-kolloquium, Garching, Dezember 2002

4 Scientific Staff

K. Behringer, U. Fantz, B. Heger, S. Meir, P. Starke, D. Wünderlich, M. Berger, J. Günther, A. Zymara, S. Riegg, M. Regler

Lehrstuhl für Experimentalphysik III der Universität Bayreuth

Head: Prof. Dr. Jürgen Küppers

1. Elementary reactions of hydrogen atoms with adsorbates and solid surfaces

Cooperation between IPP and the University of Bayreuth is concentrated on investigating fusion-relevant plasma-wall interaction processes. Accordingly, the hydrogen atom surface chemistry on possible reactor wall materials is the primary research topic.

A considerable fraction of the species impinging on the first wall of a fusion experimental vessel are neutrals and ions in the energy range below a kinetic energy of about 10 eV. These particles are not capable of causing physical sputtering, but can induce several processes, such as chemical erosion, abstraction etc, which contaminate the plasma. It is therefore desirable to understand the elemental processes and mechanisms of these processes. Recent work of the IPP/UBT collaboration was concentrated on investigating these issues. Since low-energy ions are neutralised in the immediate vicinity of a substrate by resonance neutralisation, it is sufficient to study the low-energy atom-surface interaction. For experimental reasons, the present work utilised only thermal atoms with energies in the range of a few tenth of an eV.

Despite the fact that impinging ions from the boundary plasma transform a considerable fraction of the surfaces of carbon tiled walls into hydrogenated a-C:H, it is of interest to know whether H atoms exhibit strong interaction with graphite surfaces.

Graphite is available in various forms: quasi-crystalline C flakes with mm sized surface areas of C(0001) orientation, HOPG (highly oriented pyrolytic graphite) samples of different qualities with µm-sized surface patches of (0001) orientation, oriented pyrolytic graphite with (0001) layers oriented normally or almost normally to the surface, and pyrolytic graphite with random orientation of the (0001) planes in sub-µm-sized crystallites.

Prior to 2002 there was no experimental evidence that H adsorbs on the C(0001) surface and this surface was considered as essentially “inert”, even with respect to adsorption of atoms. This was plausible taking the sp^2-hybridization of C in the C(0001) plane and the strong in-plane C-C interaction into account. However, in 1999 and in 2001 two theoretical papers were published (Sidis et al., Jackson et al.) in which strong chemisorption of H on the C(0001) plane was suggested by allowing the C atom to which the H was bonded to relax outward from the C(0001) plane by a few tenth of an Å.

Our experimental studies on the H/graphite interaction confirmed these theoretical predictions and provided the first experimental evidence for H adsorption on the C(0001) plane, with a binding energy of about 1 eV, and parallel and normal vibrational frequencies very close to theoretical values.

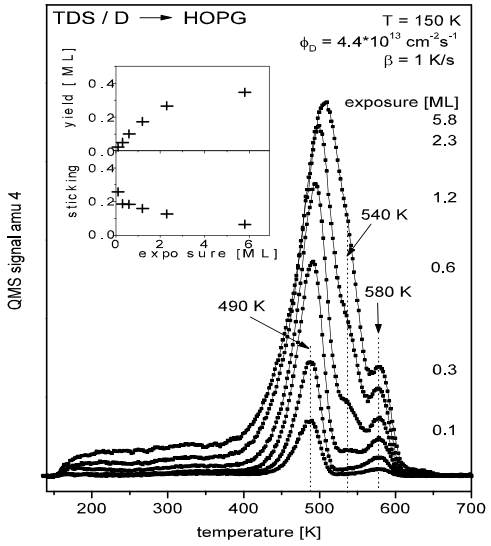

Figure 1: Thermal desorption spectra of D on HOPG surfaces.

Fig.1 shows thermal desorption spectra of D exposed HOPG surfaces. The main peak around 500 K stems from D adsorbed on (0001) terraces, the minor peak at 580 K is probably due to defect sites. The saturation coverage was obtained as close to 0.5, i.e. H atoms adsorb on every other C atom.

Concerning abstraction of D on C(0001) by gaseous H theoretical calculations predicted surprisingly large cross sections, up to 12 Å^2 at low D coverages. These cross sections illustrate that D by H abstraction on graphite is governed by the D-H interaction and that the H-substrate interaction plays a minor role in the abstraction process. As a consequence, the abstraction kinetics is of the Eley-Rideal type, i.e. the HD rate as a function of the H fluence (= time at constant H flux) exhibits a purely exponential decay, as apparent in fig.2.

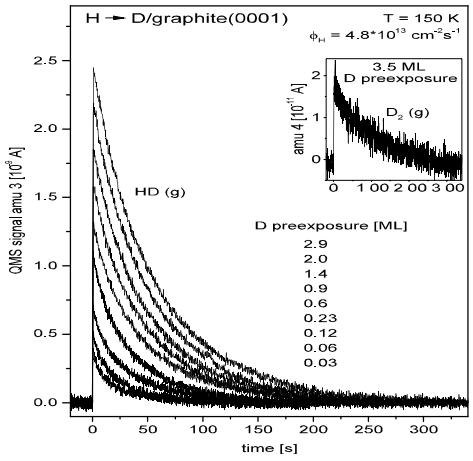

Figure 2: HD kinetics measured during abstraction of D on C(0001) with gaseous H atoms at various D precoverages. The inset illustrates the background D_2 rate.

2. Publications

C. Lutterloh, M. Wicklein, A. Dinger, J. Biener, and J. Küppers
Thermal stability and hydrogen induced abstraction of silyl groups on Si(100) surfaces.
Surf. Sci. 498 (2002) 123

T. Zecho, B. Brandner, J. Biener, and J. Küppers
Hydrogen induced chemical erosion of amorphous hydrogenated carbon thin films: structure and reactivity.
J. Phys. Chem. B 106 (2002) 610

J. Biener, E. Lang, C. Lutterloh, and J. Küppers
Reactions of gas-phase H atoms with atomically and molecularly adsorbed oxygen on Pt(111) surfaces.
J. Chem. Phys. 116 (2002) 3063

A. Güttler, D. Kolovos-Vellianitis, T. Zecho, and J. Küppers
Abstraction of sulfur from Pt(111) surfaces with thermal H atoms toward adsorbed and gaseous H_2S.
Surf. Sci. 516 (2002) 219

T. Zecho, A. Güttler, X. Sha, B. Jackson, and J. Küppers
Adsorption of hydrogen and deuterium atoms on the (0001) graphite surface.
J. Chem. Phys. 117 (2002) 8486

T. Zecho, A. Güttler, X. Sha, D. Lemoine, B. Jackson, and J. Küppers
Abstraction of D chemisorbed on graphite (0001) with gaseous H atoms.
Chem. Phys. Lett.366 (2002) 188

D. Kolovos-Vellianitis and J. Küppers
Kinetics of abstraction of D and O on Cu(110) surfaces by gaseous H atoms.
J. Phys. Chem. B in press

S. Wehner, F. Baumann, and J. Küppers
Kinetic hysteresis in the CO oxidation reaction on Ir(111) surfaces.
Chem. Phys. Lett. in press

T. Zecho, A. Güttler, and J. Küppers
Suppression of D adsorption and D by H abstraction on graphite (0001) surfaces by adsorbed water.
Chem. Phys. Lett. in press

J. Biener, C. Lutterloh, M. Wicklein, A. Dinger, and J. Küppers
Thermal stability and hydrogen atom induced etching of nm-thick a-Si:H films grown by ion-beam deposition on Si(100) surfaces.
J. Vac. Sci. Technol. A submitted

S. Wehner, F. Baumann, M. Ruckdeschel, and J. Küppers
Kinetic phase transitions in the reaction CO + O → CO_2 on Ir(111) surfaces.
J. Chem. Phys. submitted

3. Conference contributions

D. Kolovos-Vellianitis and J. Küppers
The kinetics of abstraction of adsorbed D on Ag(100) surfaces with gaseous H atoms.
ECOSS 21, Malmö, 6/2002

T. Zecho
Reactions of H(D) atoms on the graphite (0001) surface.
Dept. of Chemistry, Univ. Massachusetts, Amherst, 11/2002

T. Zecho, A. Güttler, C. Drummer, X. Sha, B. Jackson, and J. Küppers
Adsorption and abstraction of H atoms on the graphite (0001) surface.
49th AVS Symposium, Denver, 11/2002

4. Doctoral thesis

B. Brandner: Thermische Eigenschaften und Wasserstoff-induzierte Erosion von a-Si:H Filmen. Dissertation Universität Bayreuth 2002

5. Diploma thesis

A. Güttler: Wechselwirkung thermischer Wasserstoffatome mit auf Platin (111) adsorbiertem Schwefel. Diplomarbeit Universität Bayreuth 2002

6. Scientific staff

F. Baumann, J. Biener, B. Brandner, A. Dinger, C. Lutterloh, A. Güttler, D. Kolovos-Vellianitis, T. Zecho

Lehrstuhl für Experimentelle Plasmaphysik der Christian-Albrechts-Universität zu Kiel

Head: Prof. Dr. Ulrich Stroth

1 The Torsatron TJ-K

The objective of this project is the experimental and numerical investigation of plasma turbulence. The experiments are carried out on the torsatron TJ-K. The device magnetically confines a low-temperature plasma at typical electron temperatures of 10 eV and densities of up to 6×10^{18} m^{-3}. Hydrogen, Helium and Argon plasmas are heated with helicon waves and with ECRH. The magnetic field is up to B = 0.3 T. The moderate parameters allow for Langmuir probe access. Therefore probe arrays can be used to measure a full set of turbulence data in the entire plasma cross-section. The results are closely compared with simulations of drift-wave turbulence using the DALF3 code. Furthermore, the physics of helicon-wave heating and ECRH In toroidal low-temperature plasmas is studied.

2 Turbulence simulations

Turbulence simulations are carried out with the drift-Alfvén turbulence code DALF3, which was written for fusion plasmas. The dimensionless parameters which govern the equations solved are such that they are relevant both for the edge of a fusion and the core of the TJ-K plasma. Systematic numerical studies have shown that poloidal wave-number spectra of density and transport fluctuations can serve to reveal the relevant turbulence driving mechanism. Drift-wave transport spectra have a maximum in the range where the density spectrum already decays exponentially. The density-potential cross-phase is in the vicinity of zero. Curvature driven instabilities create a spectrum which is peaked at long wavelengths with cross-phases of about $\pi/2$. For the whole range of TJ-K parameters, the drift-wave mechanism is predicted to clearly dominate the interchange mechanism.

The simulated data were also applied to assess advanced analyses tools which are usually applied to experimental data. In particular, bi-spectral analysis has been proposed as a diagnostic for Reynolds stress as a driving mechanism of zonal flows. The analysis of the simulated data showed that the geodesic acoustic mode dominates the poloidal flow spectrum and that it reduces radial transport in the same way as does a low frequency zonal flow. Using the total cross-bicoherence a correlation between Reynolds stress and large scale poloidal flows could be detected. The experimentally more accessible auto-bicoherences did not proof to be a useful quantity to study this interaction. However, Reynold's stress was not observed as a precursor of the flow, it rather appears simultaneously in the region of radial flow shear.

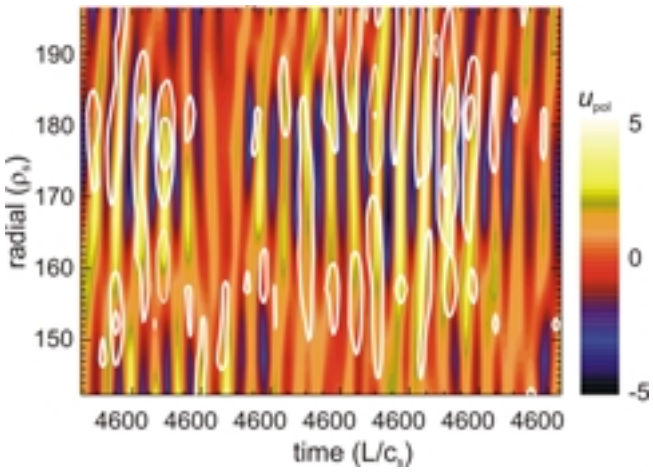

Figure 1: Radial poloidal flow profile as function of time. Overlayed in white are regions of high values of the total integrated bicoherence between the fluctuations in poloidal and radial flow and the low frequency poloidal flow.

3 Turbulence measurements

Systematic turbulence measurements were carried out in the entire parameter range accessible in TJ-K. The characteristics of the detected fluctuations are similar to those reported from fusion experiments. Turbulent power spectra are found decaying over more than 2 decades in frequency space. The density fluctuation amplitude increases when the plasma density decreases. The probability density functions of density and potential fluctuations have a Gaussian shape. Transport fluctuations, on the other hand, are intermittent. In order to investigate intermittency more in detail, wavelet tools were applied to achieve scale separation. A typical result is depicted in Fig. 3. The upper part of the figure compares power spectra calculated from Fourier and wavelet transforms. The agreement is rather satisfactory. The wavelet transforms, however, yield time traces which represent a characteristic frequency of the fluctuations. Hence it can be used to calculate the PDFs as function of the characteristic frequency. The Kurtosis of these PDFs is shown in the lower part of the figure. An increase of the Kurtosis with frequency is found. This is a clear signature of intermittency.

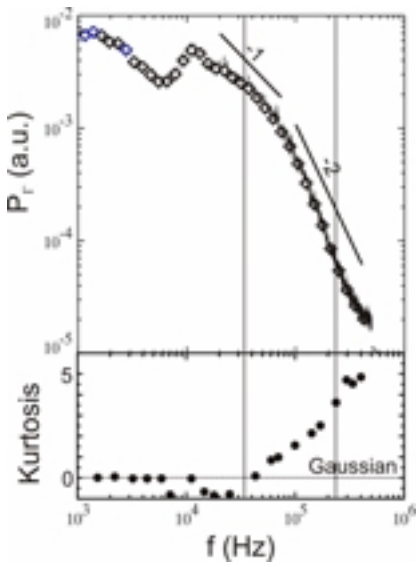

Figure 2: Power spectra from turbulent transport data using Fourier (line) and wavelet (diamonds) methods. The Kurtosis of the wavelet are shown in the lower part.

4 Plasma Heating

Helicon-wave heating at 27.12 MHz and a power of 2 kW is successfully applied at neutral pressures from 10^{-4} to 5×10^{-3} mbar.

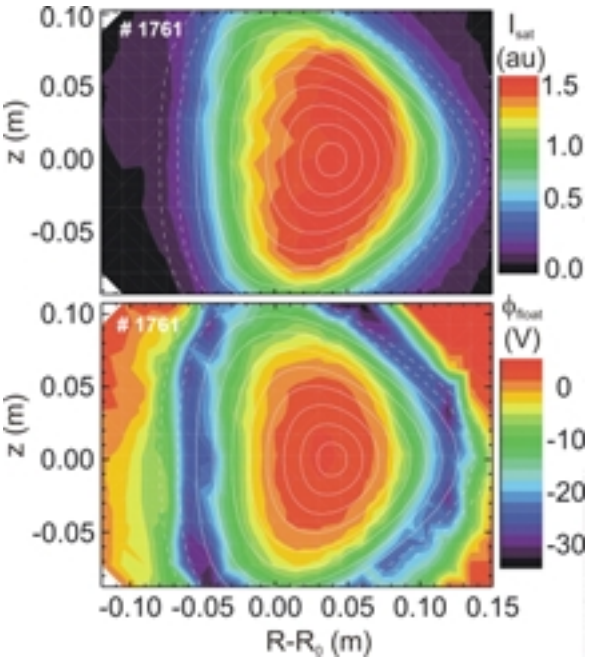

Figure 3: 2D profiles of the ion-saturation current and the floating potential in an ECRH Helium discahrge. Flux surfaces are overlaid.

The heating mechanism depends on plasma species and magnetic field strength. In Argon, the line averaged density rises with B up to 6×10^{18} m^{-3}. Discontinuities in the density increase are consistent with the assumption of wavelength changes of a toroidally closed wave. Peaked density profiles indicate that heating is due to the helicon wave, which has largest amplitudes in the plasma centre. Hydrogen discharges have an inductive character. The profiles are hollow and the density is independent of B. In Helium a transition from helicon to inductive heating occurs at $B \approx 0.17$ T.

Recently an ECRH system at 2.45 GHz and 6 kW power went into operation. The wave is coupled in O-mode from a bottom flansch to the plasma. In Hydrogen, Helium and Argon at a neutral pressure of 5×10^{-5} mbar, over-dense plasma up to 6×10^{18} m^{-3} were achieved, pointing to an O-X-B mode-conversion process. The density profiles are centrally peaked. Fig. 3 depicts a 2D profile of the ion-saturation current and the floating potential measured in a poloidal plasma cross-section. Both nicely follow the calculated flux surfaces. In potential profile has a shear layer at the separatrix.

5 Publications

N. Krause, C. Lechte, U. Stroth, E. Ascasibar, S. Niedner, J. Stöber, R. Westphal, *The Torsatron TJ-K, a toroidal experiment for low-temperature plasma physics research*, Sub. Rev. Sci. Instruments, 73(10),3474 (2002).

S. Niedner, B. D. Scott, U. Stroth, *Statistical Properties of Drift Wave Turbulence in Low Temperature Plasmas*, Plasma Phys. Contr. Fusions, **44**,397(2002).

S. Lechte, J. Stöber, U. Stroth, *Parameter Limits of Magnetically Confined Low-Temperature Plasmas from a combined Particle and Power Balance*, Phys. Plasmas, **9**(6)2839(2002).

U. Stroth, K. Itoh, S.-I. Itoh, *Bifurcations in toroidal plasmas*, Part IV. Ed. S.-I. Itoh and Y. Kawai, Fukuoka, Japan, 2002;

C. Lechte, S. Niedner, U. Stroth, *Comparison of Turbulence Measurements and Simulations of the Low-Temperature Plasma in the Torsatron TJ-K*, New J. of Phys. **4**,34 (2002)

M. Ramisch, U. Stroth, S. Niedner, B. Scott, *On the Detection of Reynolds Stress as Driving and Damping Mechanism of Zonal Flows*, New J. of Phys., **5**,12(2003)

E. Ascasíbar, T. Estrada, F. Castejón, A. López-Fraguas, I. Pastor, U. Stroth, J. Qin, *Rotational Transform Dependence of the Energy Confinement Time for ECR Heated TJ-II Plasmas*, Nucl. Fusion., submitted

U. Stroth, E. Ascasíbar, N. Krause, C. Lechte, S. Niedner, *Comparison of Measured and Simulated Turbulence in the Torsatron TJ-K*, Proc. of the 13th Int. Stellarator Workshop, Canberra, 2002

E. Ascasíbar, U. Stroth, A. López-Fraguas, T. Estrada, F. Castejón et.\ al., *Parametric Scaling Studies of the Energy Confinement Time for ECR Heated TJ-II Plasmas*, Proc. of the 13th Int. Stellarator Workshop, Canberra, 2002

6 Scientific Staff

F.Greiner N. Krause, C. Lechte, N. Mahdi-Zadeh, , M. Michel, M. Ramisch, K.Rahbarnia, V. Senger, H. Stenzel, U. Stroth

Lehrstuhl für Messsystem- und Sensortechnik

Prof. Dr.-Ing. Alexander W. Koch

1 Introduction

The cooperation of the IPP and the Technische Universität München is concentrated on the development of speckle measurement techniques for the detection arc traces, surface deformation, surface erosion, surface roughness, surface structure and surface contours in the divertor region of experimental fusion devices.

2 Correlation of Speckle Images

The appearance of speckle photographs is mainly determined by the microstructure of the irradiated surface, and is therefore very sensitive to any changes thereof, caused e.g. by surface erosion. The determination of the similarity of sequentially recorded speckle images can assist in detecting of changes of the surface microstructure using the so called *pearson's coefficient* $C_{I1,I2}$ according to eq. (1), where $I_{1,n,m}$ denotes the intensity I of a pixel at the position of the coordinates n, m of the first image.

$$C_{I1,I2} = \frac{\sum_{n=1}^{N}\sum_{m=1}^{M}\left(I_{1,n,m} - \overline{I_1}\right)\left(I_{2,n,m} - \overline{I_2}\right)}{\sqrt{\sum_{n=1}^{N}\sum_{m=1}^{M}\left(I_{1,n,m} - \overline{I_1}\right)^2 \cdot \sum_{n=1}^{N}\sum_{m=1}^{M}\left(I_{2,n,m} - \overline{I_2}\right)^2}} \qquad (1)$$

It can be shown [1)] that the value $C_{I1,I2}$ corresponds to the variance of surface height changes $\sigma_{\Delta h}$ according to eq. (2), where λ denotes the irradiation wavelength and θ the angle between the observation direction and the surface normal.

$$C_{I1,I2} = \exp\left\{-k^2 \cdot (1+\cos\Theta)^2 \cdot \sigma_{\Delta h}^2\right\}; \quad k = \frac{2\pi}{\lambda}; \qquad (2)$$

Using a wavelength λ of 496,5 nm (Ar-Ion-Laser) at an angle of $\theta \approx 0°$ (long-range measurement) as an example, it can be seen that already a very small variance of surface height changes of $\sigma_{\Delta h}$ = 20 nm leads to a value of $C_{I1,I2} \approx 0.77$ und thus becomes easily detectable. In order to monitor a continuous erosion process, several images with small steps of $\sigma_{\Delta h}$ have to be recorded and each corresponding surface state has to be correlated with each proceeding one. In Fig. 1, an erosion of an aluminium plate, induced by pulses of a Nd:YAG-Laser (energy ≈ 200 mJ/pulse) is imaged using this method. By applying the same procedure to small sub-sections of the images, this method permits to obtain spatial information of the erosion process, too.

This technique was implemented in the interferometric set-up introduced already in former annual reports.

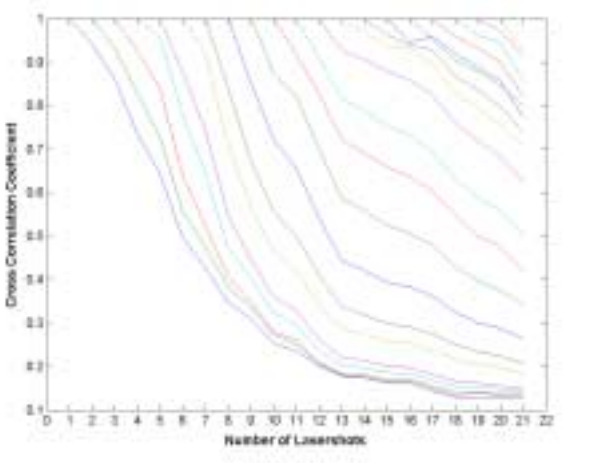

Figure 1: Decreasing correllation coefficient caused by laser induced erosion of an aluminium plate

3 Interferometry at Moving Objects

A research set-up of a two wavelength speckle-interferometer was developed and already presented in former reports. By synchronizing a two-camera system the set-up is capable of recording two interferograms of different wavelengths simultaneously and thus to perform surface contouring even if movements of the measurement object with respect to the interferometer should occur. At a laser power of 300 mW and an exposure time of 250 µs of the CCD-camera, recent tests demonstrate that a surface contour can still be measured when the object is shifted at a velocity of 12 mm/s during observation.

4 Scientific Staff

Andreas Meixner
Andreas Purde
Markus Riemenschneider
Thomas Zeh

---

1) Hinsch, K.D., Fricke-Begemann, T., Gülker, G., Wolff, K.; Speckle correlation for the analysis of random processes at rough surfaces; Optics and Lasers in Engineering 2000, Vol. 33, p. 87 - 105

Institut für Plasmaforschung (IPF) der Universität Stuttgart

Head: Prof. Dr. Uwe Schumacher

The Max-Planck-Institut für Plasmaphysik (IPP) at Garching and Institut für Plasmaforschung (IPF) at University of Stuttgart are collaborating closely for more than three decades on technological developments, measurements, and interpretations of heating and diagnostic systems. The main topics of the co-operation are applications of millimetre waves for heating, current drive, plasma stabilization and diagnostics - mainly for W7-X, ASDEX Upgrade and W7-AS – and contributions to emission, absorption and LIF spectroscopy for bulk and divertor plasma diagnostics.

1 Plasma Heating and Diagnostics

The investigations of the application of millimetre waves to fusion plasmas for electron cyclotron resonance heating (ECRH), current drive, and neoclassical tearing mode stabilization were continued. On the technical side, work on the ECRH system of W7-X formed the major part. Nevertheless, technical support, research and development for W7-AS, ASDEX Upgrade and ITER was continued. Studies of the MHD stability of high-β discharges in ASDEX Upgrade and the use of ECRH / ECCD to control instabilities continued to be a major issue. Moreover, general developments in the field of millimetre wave technology as well as the study of microwaves as a plasma diagnostic tool are reported here.

1.1 Electron cyclotron resonance heating (ECRH)

1.1.1 ECRH on W7-AS

Technical support of the ECRH system on W7-AS was continued. The generator as well as the transmission system could be maintained at a high level of reliability, although two gyrotrons became defect. Until the shut-down of W7-AS in August 2002, plasma experiments with ECRH were performed with two gyrotrons at 140 GHz and one gyrotron at 70 GHz, each of them delivering 0.5 MW. Details can be found in the IPP part of this report.

1.1.2 ECRH system on ASDEX Upgrade

The present ECRH system at ASDEX Upgrade (140 GHz, 4 x 0.5 MW, pulse length 2 s, steerable launchers in poloidal and toroidal direction) is running routinely. To analyse the experimental data of the power absorption in the plasma the shape of the RF beam should be well known. Therefore, the launching structure of ASDEX Upgrade has been rebuilt and low power measurements have been performed to determine the beam profile in the plasma. The results (FWHM ≈ 15 mm) are in good agreement with calculations of the beam propagation.

A new ECRH system with 4 gyrotrons, 1 MW each, has been planned and is currently under construction. These gyrotrons will allow operation at frequencies between 104 GHz and 140 GHz, where the first tube emits only at these two frequencies, the others shall be step-tuneable. The transmission system is a combination of a quasi-optical mirror line (matching of gyrotron output beam, polarisation adjustment) and a HE_{11} corrugated waveguide (I.D. 87 mm, for the transmission from gyrotron hall to the plasma), both operating at atmospheric pressure. The beam parameters have been defined, and the construction of the support structure for the mirrors is finished. The performance of the system with respect to broadband transmission has been improved. Various surface profiles of the corrugated polarizers have been manufactured and tested; significant increase of the bandwidth compared to sinusoidal polarizers was found.

1.1.3 MHD stability studies on ASDEX Upgrade

The occurrence of neoclassical tearing modes (NTM), driven by the gradients of the toroidal current density and the plasma pressure limit the energy content in a Tokamak plasma. To maximise the fusion power of a future machine the operation at high plasma pressure is foreseen – a regime where the occurrence of these modes is highly probable. Therefore possibilities are explored to control or prevent such instabilities. The NTM's are associated with the development of magnetic islands with an initially relatively small width. Electron cyclotron current drive (ECCD) and electron cyclotron resonance heating (ECRH) which have a well localised power deposition to modify the current distribution within the islands are excellent candidates to stabilise the NTM's. On the tokamak ASDEX Upgrade both, ECCD and ECRH, are used to study the MHD stability of fusion plasmas.

1.1.3.1 Active control of neoclassical tearing modes using ECRH / ECCD on ASDEX Upgrade

Experiments have been conducted to investigate the possibilities of stabilising the m = 3, n = 2 mode at high β_N. Fig. 1 illustrates a typical discharge where the 3/2 NTM is completely stabilised. In this discharge B_t is changed during the shot, thus ensuring that the ECCD deposition coincides with the resonant q-surface and consequently keeps the discharge free from the 3/2 NTM in a steady state for about 300 ms at $\beta_N \approx 2.6$. This situation is constant until the NBI power is increased from 12.5 to 15 MW at t = 3.25 s. In that

case β_N increases temporarily up to 3.0 and the 3/2 NTM is triggered again at the end of the B_t scan. At t = 2.8 s the NBI power is increased up to 12.5 MW and β_N increases also up to 2.7 until the NTM is triggered again at t ≈ 3.1 s and grows to its saturated width. Since this happens in the presence of ECCD injection it is assumed that the positions of deposition and island do not coincide any more. This assumption is supported by the analysis of the ECE signals which show a radial shift of the island by about 5 cm.

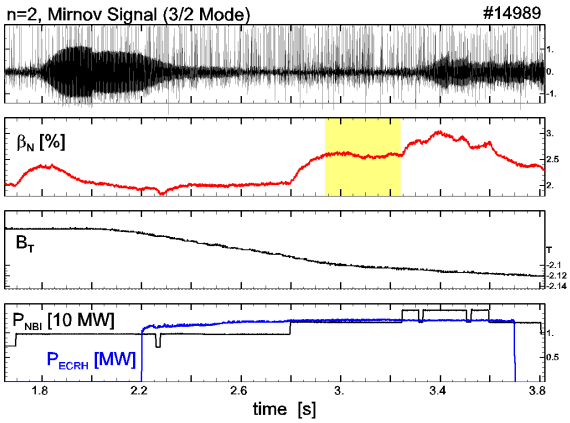

Figure 1: Stabilisation of 3/2 mode with a quasi stationary region (2.9 ≤ t ≤ 3.2 s).

Many discharges at ASDEX Upgrade are limited by the 2/1 mode situated at the q=2 surface which is closer to the wall. In some cases these modes can lead to a slowing-down of plasma rotation and to a dramatic loss of confinement. A special discharge scenario has been developed to allow reproducible experiments on 2/1 mode stabilisation at ASDEX Upgrade. A first result of such an experiment is

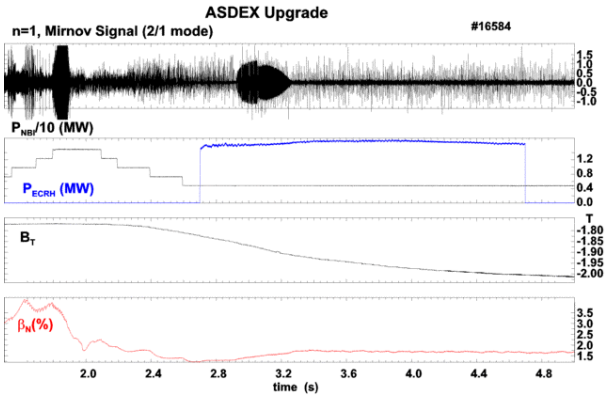

Figure 2: First results of stabilization of 2/1 mode.

given in Figure 2. This example shows that ECRH releases a locked 2/1 mode and finally suppresses the instability.

1.1.4 ECRH system for W7-X

Work on the 140 GHz, 10 MW-CW ECRH system for the stellarator W7-X continued. IPF has taken responsibility for the quasi-optical transmission lines as well as for the development of the acceleration voltage modulator, the thyratron crowbars and cathode heater supplies for the depressed collector gyrotrons which are under development at FZK Karlsruhe.

1.1.4.1 Multi-beam transmission system

The prototype transmission line at IPF Stuttgart was completed by water-cooled components as foreseen for the ECRH system in Greifswald. Measurements on the prototype line which at present consists of 17 mirrors confirm the expected power transmission efficiency of ≈ 90 %. The mode analysis of the beams at the exit of the multi-beam section yields a TEM_{00}-mode purity of ≥ 98 %. Further tests, where the heat load of the reflectors due to microwaves was simulated by infrared radiators and heating of the cooling water, show negligible reduction of the quality of the lines. In Table 1, a summary of results from the various channels of the prototype line is presented.

Channel of MBWG	A	B	BN	C	D	E	F
transm. efficiency (%)	89.5	86.8	89.8	89.1	90.7	90.0	90.5
purity of TEM_{00} (%)	98.8	99.1	99.2	98.9	99.0	97.3	99.2

Table 1: Transmission data for the prototype beam conditioning systems and multi-beam waveguide (17 reflectors)

The mirrors, which are installed in the gyrotron test bed at Forschungszentrum Karlsruhe did not show any fatigue for the present power levels of 890 kW for 3 min or 520 kW for 17 min. After integration of polarizers into the test chamber, arcing in the dummy load could be completely avoided owing to the use of a circularly polarized beam. Also, no arcing was detected on the corrugated surfaces of the polarizers, provided that they were clean.

At present, most of the transmission system for Greifswald has been designed. All mirrors for the transmission up to the torus hall are being manufactured or have been delivered already. Prototypes of a calorimeter and mirrors with directional couplers have been fabricated. The cooling system for the mirrors was installed. At present, data acquisition and mirror control are in preparation.

Work now concentrates on detailed design of beam diagnostics as well as on absorbers for stray radiation. A prototype of the last mirror in front of the torus window was designed, machined and equipped with a diagnostic hologram to measure the quality of alignment of the lines. First tests confirm the principle and show the potential for an automatic alignment system. Furthermore, the drafting of the launchers has been started.

1.1.4.2 High-voltage system for gyrotron power control and tube protection

The high-voltage system as shown in Fig. 3 for each of the 1 MW, 140 GHz gyrotrons consists of a high-power supply (65 kV, 50 A) for the electron beam current and a low-power, high-voltage source for the beam acceleration. The gyrotron output power is controlled by fast control of this low-power high-voltage source. The high-power source is realised by THALES in PSM (pulse-step modulator) technology, which consists of individual 1 kV DC sources connected in series via semiconductor switches. The output voltage is determined by the number of connected sources. The sequence of connected sources is changed at a repetition rate of 100 kHz. A low pass output filter reduces the voltage ripple.

First tests of the PSM module showed poor transient behaviour during voltage steps and a high voltage ripple in the frequency spectrum of the switching sequence. For the analysis of these phenomena the whole 65 kV module consisting of 84 stages was modelled by PSpice. The inclusion of the stray capacitances from stage to stage and stage to ground via the isolation transformers and the design of the low-pass filter were recognized as key issues for the explanation of the high ripple. By detailed numerical circuit simulation a new low-pass filter was designed. After a change of the components, new tests showed a remarkable improvement of the output voltage behaviour, which is close to the specified data for gyrotron application. Simulations show that the design of the low-pass filter has to be matched to the load in operation.

In addition to the redesign of the PSM low-pass filter the function of the crowbar circuit for gyrotron protection was simulated to limit the released energy into an arc in the tube to the specified maximum value.

As a fast low-power HV source for beam acceleration and gyrotron output-power control, a high voltage servo-amplifier is used which suppresses the influence of the residual ripple from the PSM supply on the acceleration voltage. The required high slew-rate of the amplifier output voltage of 600 V/µs could be attained by separate feed-back loops for the regulation of value and slew-rate of the output voltage sketched in Fig.3. The frequency behaviour of ripple suppression is shown in Fig. 4. The ripple with a frequency of up to 1 kHz is suppressed by 60 dB, and the 100 kHz ripple from the PSM switching is reduced by 18 dB, leaving a gyrotron output power ripple of only 0.2 % .

The prototype of such a servo amplifier is in construction. After completion and test this device will be the basis for 10 units needed for the ECRH system on W7-X.

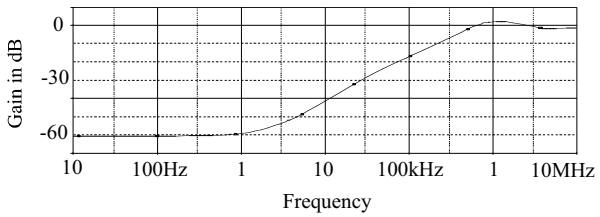

Figure 4: Servo amplifier. Suppression of voltage noise from main supply.

1.1.5 ITER contributions

In 2002, the investigations of the ITER-relevant concept of remotely steerable antennas based on the imaging properties of a four-wall corrugated square waveguide were continued. The work concentrated on detailed measurements of the loss, which is introduced by the integration of mitre bends into the antenna (e.g. for neutron screening). Compared to a straight antenna, and in spite of an optimum position of these "dog-legs", the measurements yield an increase of the transmission loss for polarization parallel to the scanning plane (see Fig. 5). The reason is an abrupt change of the boundary conditions in the side walls of the mitre bends, which cannot be avoided in standard bends. At present, work is going on to optimize the mitre bend design, and first improvements are obtained.

For characterisation and quality control of square waveguides, a method based on resonator techniques to measure the complex propagation constants of HE_{1n} modes is under development. First investigations yield promising results, and further work is planned.

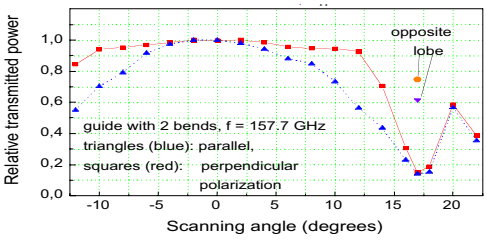

Figure 5: Power transmission of a remote steering antenna with two mitre bends as function of the steering angle

2.1 General developments in millimetre wave technology

1.2.1 Investigations of materials for in-vessel components and absorbers

For the characterization of the in-vessel reflections as well as for development of absorbers and loads, investigations of absorbing plates made from vacuum plasma-sprayed B_4C and atmospheric plasma sprayed mixtures of Al_2O_3 and TiO_2 on metallic substrates (Cu, Mo and Al) or alloy TZM (Ti-Zr-Mo) were carried out. To determine the dielectric constants ε_1 and ε_2 of the coating, the reflection coefficient

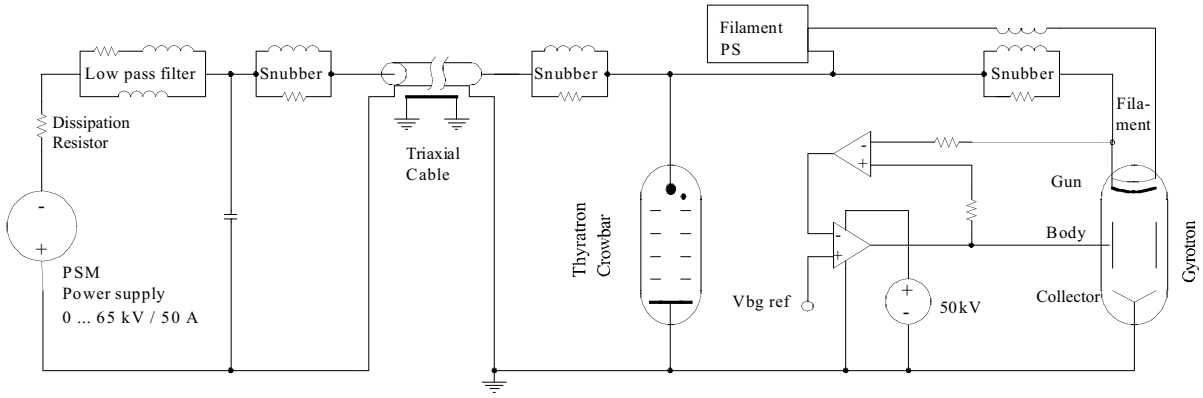

Figure 3: HV-supply for the 1 MW cw, 140 GHz gyrotron.

R_p (i) as a function of incidence angle at a fixed frequency and (ii) as a function of frequency f at a fixed incidence angle of 20° was measured with polarization parallel to the plane of incidence. From a fit of both data sets to theory, ε_1 and ε_2 as well as the dielectric parameters n and k can be determined unambiguously. Results for various coatings are summarized in Table 2.

Coating	Sub-strate	d (mm)	R(α=0) (db)	n	k
B_4C	Cu	0.15	-4.96	2.7	1.1
	Mo	0.3	-3.26	3.9	2.1
	TZM	0.1	-2.7	3.8	2.7
	TZM	0.19	-1.95	4.8	0.8
0.25 TiO_2 0.75 Al_2O_3	Al	0.21	-2.36	5.2	2.9
		0.56	-3.06	4.9	2.1
		0.85	-3.0	5.0	2.2
0.5 TiO_2 0.5 Al_2O_3	Al	0.3	-1.57	8.2	5.0
		0.4	-1.74	6.8	4.6
		0.6	-1.85	7.8	4.1

Table 2: Dielectric parameters n and k: var. samples at 140 GHz

As a main result, the analysis of the tables shows a strong dependence of the data on the production process. For mixtures of materials, a non-linear variation of the constants as function of the mixing ratio due to formation of semiconductors is found.

1.2.2 Design of components for oversized waveguide systems

The existing computer codes for numerical optimisation and design of overmoded waveguide systems (based on scattering matrix method, coupled wave equations and simulated annealing) were further improved. The development focuses on calculations of far-field patterns radiated from waveguide antennas based on the mode mixtures generated in the corrugated or smooth waveguide structures. The programs use analytic formulas and are suitable for both cylindrical and rectangular waveguides. In addition, the implementation of optimisation algorithms for waveguide structures with varying diameter (tapers, mode converters, horn antennas) is in progress.

1.2.3 Frequency diplexers for oversized waveguides

A program was developed to design and optimize frequency diplexers based on the *spatial* Talbot effect in rectangular waveguides. Such diplexers can be used, if microwaves with two different frequencies must be transmitted in one waveguide (e.g. reflectometers). The diplexer consists of a combining section with two input waveguides (TE_{10}-mode) at one side and the output waveguide at the other side (see Fig. 6). A fourth waveguide (top right in Fig. 6, not shown) with an integrated absorber prevents reflections of spurious field components. By optimizing the dimensions of the diplexer, one can find solutions, where the power losses of the TE_{10}-mode are below 3 % for both frequencies. A scaled diplexer is currently under construction and will be tested soon. Further developments will include an investigation of a different design, which is based on the *angular* Talbot-effect, as well as the possibility to build other components (triplexers, band filters).

1.2.4 Microwave beam propagation and diagnostics

The available computer code for the analysis of microwave beam profiles was developed further. It now makes possible to find the position and the direction of the beam's axis as well as the position of the beam waist, and it delivers the contents of all Hermite-Gaussian modes up to TEM_{55}. This code was applied to analyse the measured profiles of the test beam used in evaluating the prototype multi-beam waveguide for ECRH on W7-X and of the resulting beams at various positions along the waveguide. Improved beam propagation calculations were done for the design of the new microwave lines on ASDEX-Upgrade.

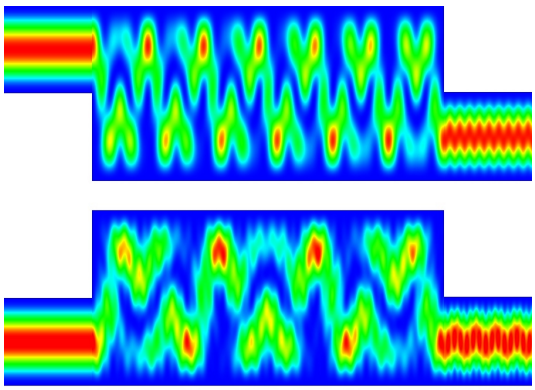

Figure 6: Field distribution in a diplexer for 45 GHz (top) and 70 GHz (bottom).

1.2.5 Wood's anomaly in the design of corrugated mirrors

For broadband polarizers, where the groove period p is in the region $\lambda/2 < p < \lambda$, *Wood's anomaly* can occur, which leads to the almost total extinction of the 0^{th} order reflected power in a narrow frequency band. The lost power is converted into heat or radiated away as a leaky wave which can lead to serious problems at the MW levels considered.
In experiments, the occurrence of Wood's anomaly was found to be a function of frequency, the geometry (depth, period length) and shape (rectangular, rounded) of the polarizing grating as well as the angle of incidence. Modelling was performed with the FDTD (Finite Difference Time Domain) method, and very good agreement with the measurements is found. The results are used for the final optimization of broadband polarizers for the multi-frequency ECRH system on ASDEX upgrade.

1.2.6 Corrugated mode converters with varying wall impedance

Efficient transmission of high power microwaves and their launching can be achieved in corrugated waveguides by special mixtures of hybrid modes. For this purpose, mode converters based on varying wall impedance without inner diameter change were studied.

In Fig.7, mode coupling between HE_{11} and other HE_{1n} or EH_{1n} modes as function of corrugation depth is shown for constant width w and period p of the corrugations. The mode conversion of the input HE_{11} mode and the HE_{12} can be optimized by different periods of the perturbation, the number of beat-wavelengths and the corrugation depth. As plotted in Fig. 7, significant coupling occurs only at corrugation depths between 0.1·_/4 and 0.6·_/4. For a variation of the corrugation depth given by

d (z) = d_0 – d_1 sin [(2π/ $\__w$)z + $\__0$], the wanted mode mixture of 85% HE_{11} and 15% HE_{12} was achieved after 4 beat-wavelengths, each $\__w$ = 0.12 m, with d_0 = 0.77 mm and d_1 = 0.3mm, and a phase shift of $\__0$ = 1.57. At z = 480 mm, the maximum spurious mode was 1.7% in the EH_{12} mode.

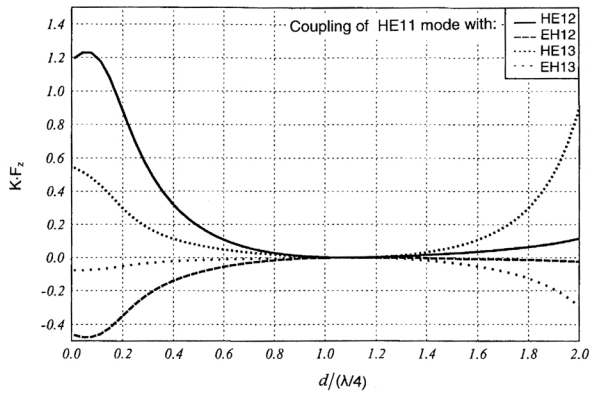

Figure 7. Coupling coefficients due to varying wall impedance as function of the normalized corrugation depth (f= 70 GHz, a = 13.9 mm).

1.3 Millimetre wave diagnostics

1.3.1 Doppler reflectometer for density fluctuation and plasma rotation studies

Doppler reflectometry is a new diagnostic method for the investigation of propagating density perturbations. Whereas in a standard reflectometer transmitter and receiver antennas are oriented perpendicularly to the plasma surface the Doppler reflectometer probes the plasma by a microwave signal with a line of sight which is non-perpendicular with respect to the reflecting layer. The diagnostic selects density perturbations with finite wave number $k_\perp$ in the reflecting layer defined by the tilt angle. For a given propagation velocity of these fluctuations this leads to a *Doppler shift* of the returning microwave. The accuracy in the measurement of both reflected power and its frequency shift is determined by the integration time and the statistical properties of the signals.

Numerical simulations were carried out to optimise the antenna spot size with respect to plasma curvature effects in order to obtain maximum k-resolution. From the Doppler shift of the returning microwave the propagation velocity of the selected density perturbations $v_\perp$ can then be directly obtained.

In the experiments W7-AS and ASDEX-Upgrade Doppler reflectometry is used to measure the frequency spectrum which contains information on propagation velocity, wavenumber and power of the plasma turbulence.

It was found that a useful interpretation of the measurements in general is only possible if the design of the reflectometer (antenna geometry, receiver) and relevant plasma discharge parameters (density profile, magnetic field configuration) are taken in consideration. Especially developed computer programs (FDTD-code, equivalent network code) allow to calculate the propagation of the microwave in the inhomogenous plasma. These computations yield the *instrument function* of the reflectometer, which depends on the input plasma parameters. The solutions of both numerical codes were benchmarked against analytical solution. These investigations are carried out in collaboration with other groups at IST (Portugal) and CEA (Marseille, Nancy) .

Numerically calculated turbulence (e.g. B. Scott, IPP) has been implemented into the *numerical reflectometer*. This allows to find out if and to what degree characteristic parameters of the turbulence can be observed by the *instrument function* of the Doppler reflectometer.

The comparison of numerically generated time-series of the *numerical reflectometer* with receiver signals in actual plasma experiments with corresponding discharge parameters also allows conclusions about the relevance of numerical turbulence codes. Such a comparison has been carried out for an L-mode discharge on ASDEX –Upgrade and corresponding numerical turbulence (B. Scott, IPP).

The 2000-2002 experimental campaign of W7-AS comprises the first island-divertor operation as well as externally triggered radial electric fields. For this campaign fast changes in the radial profile of turbulence level and propagation velocity were diagnosed. A total of seven homodyne reflectometers spanning the range 70 GHz to 110 GHz were installed.

For an antenna with a fixed tilt angle of +14 deg with respect to the normal onto the reflecting layer values of up to 10 MHz were observed for the Doppler frequency shift which correspond to a poloidal velocity of up to 70 km/s. A second symmetric antenna with -14 deg allows differential measurements if the orientation of the cut-off layer changes with the magnetic configuration. A fast spectrum analyzer has been built in Stuttgart from which frequency shift and intensity of the Doppler-shifted spectral component were determined with a temporal resolution of less than 10 microseconds. The main results are:

- Temporal and radial dependence of the signal power in discharges with different confinement properties.
- Dependence of poloidal propagation velocity of the turbulence in the gradient region and energy confinement. In cases where a comparison of the poloidal propagation velocity of the turbulence with the results from radial electric field measurements (CRX spectroscopy) were available agreement was found within the error bars of the diagnostics.
- *Time-of–flight*-measurements with 2 poloidally separated antennas as second independent diagnostic for the measurement of the propagation velocity of the turbulence. The results agree with those of the Doppler reflectometer.

Near the end of the experimental campaign a conventional reflectometer with perpendicular incidence was installed to

look specifically for long-wavelength components of the turbulence. The main results are:

- Radial movement of the steep density profile in the H*-mode and the HDH-mode.
- In search for long-wavelength quasi-coherent fluctuations as a possible concomitant for the HDH-mode, no sign of such a dependence could be found.

1.3.2 Microwave reflectometry on ASDEX Upgrade

The optimised O- and X-mode antennas together with the improved receiver module of the Doppler reflectometer now allow measurements of rotation velocities $v_\perp$ perpendicular to the magnetic field, even for the low level of the density fluctuations in the H-mode barrier.
The *k*-selectivity of the antenna system with respect to fluctuations was calculated by numerical modelling of the Doppler reflectometer experiment. It could be shown that in principle the comparison of this *k*-selectivity with the measured *k*-spectrum yields the *k*-spectrum of density fluctuations. A numerical simulation of the reflectometer was found to be required to interpret the measurements. The main results are:

- Determination of the radial extent of the layer with suppressed turbulence in the H-mode barrier.
- Measurement of the ExB-rotation of the plasma and its radial shear with high temporal and radial resolution. This high resolution was exploited during the investigation of the L-H-transition. As can be seen in Fig. 8, a spin-up occurs before the transition in the region of the later H-mode barrier.
- The comparison with spectroscopy allows to estimate the contribution of the intrinsic propagation velocity of the turbulence in different discharge regimes.
- Analysis of the changes in turbulence during the L-H transition with high temporal resolution.

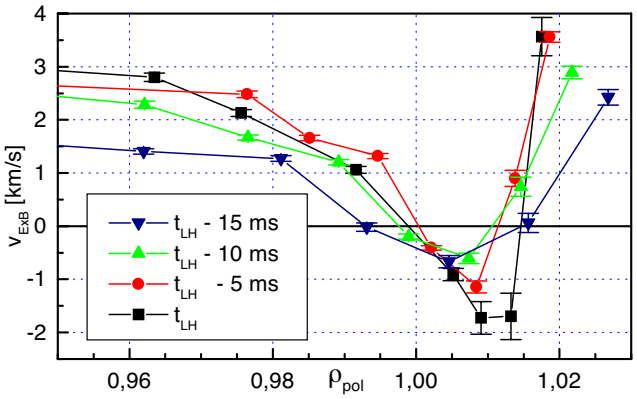

Figure 8: Rotation velocity profiles before the L-H-transition at the plasma edge (shot No. 14516). Note that there is a radial offset of $\rho \approx 0.02$ due to uncertainties in the profiles of magnetic field and density.

1.3.3 Microwave components for multiplex reflectometry

A multiplex reflectometer performs simultaneous measurements at different frequencies through a single antenna. This requires frequency multiplexers with a minimum of power loss. Using the Talbot principle (c.f. 1.2.3), multiplexers can be realised in oversized geometries. Therefore, the properties of multiplexers (losses, cross-talk, mechanical dimensions) in the frequency range relevant for reflectometry will be further investigated.

1.4 WEGA

With respect to the measurements of magnetic flux surfaces in WEGA some useful adjustments were applied to the Gourdon code, accompanying calculations were done and hints for measurement and evaluation were given.

1.5 Staff

(W. Kasparek, P. Brand, H. Braune[1], G. Gantenbein, M. Grünert[2], H. Hailer, E. Holzhauer, S. Klenge[3], H. Kumric, G. A. Müller, R. Munk, B. Plaum, J. Shi[4], K. Schwörer, R. Wacker), in collaboration with IPP Garching, FZK Karlsruhe, and IAP Nizhny Novgorod.

2 PLASMA EDGE DIAGNOSTICS

2.1 Spectroscopic measurements of plasma parameters in the divertor of ASDEX Upgrade

Laser induced fluorescence (LIF) via fiber is a new diagnostic for the investigation of space resolved temperature and density profiles of hydrogen isotopes, wall materials and impurities.
LIF is an established method in plasma physics to determine spatially and spectrally resolved measurements of atomic and molecular species, with the opportunity to measure the velocity distribution of the species.
Furthermore, preparation of the laser system was done to qualify the laser system, frequency conversion and wavelength tuning as well as the detection system. In a first test in the laboratory the applicability of LIF via fibre was analysed.

---

[1] on leave from IPP since Sept. 15, 2002
[2] from November 1, 2002
[3] until March 31, 2002
[4] from August 1, 2002

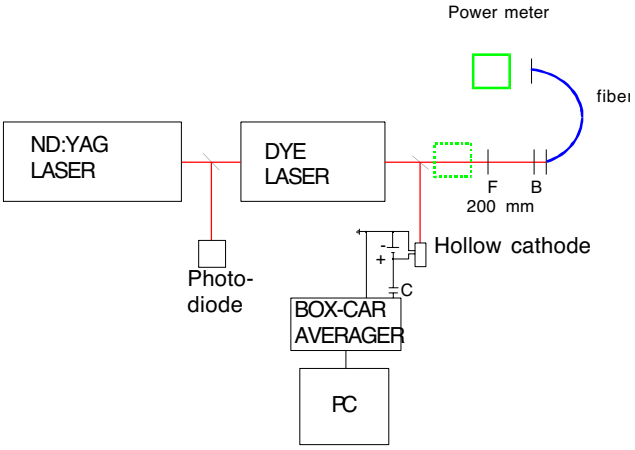

Figure 2.1: Experimental set-up for measurements of the fiber peak power threshold level.

Figure 2.1 shows the experimental set up of the laboratory LIF-system. The frequency doubled Nd:YAG-Laser (l=532 nm, t_{pulse}=7ns) is used as a pump laser for the dye laser. The spectral ranges of the system depend on the applied dye. The first measurement was done with the DCM dye with a specified spectral range between 600-660 nm. A new dye laser is used with a spectral resolution of
which will allow to determine the velocity distribution of the detected species.
The opto-galvanic effect on a neon filled hollow cathode lamp is used to calibrate the dye laser wavelength by tuning with the grating.
One of the critical points of this new diagnostic development is the power that can be transmitted via fibers into the divertor of ASDEX Upgrade. There are two goals in this point:
The first one is to estimate the detection limit of the diagnostic system. The threshold peak power level of the fiber is 1 GW /cm_. This threshold was measured with the experimental set-up which is shown in Figure 2.1. The measurement is shown in Figure 2.2 where the upper line illustrates the peak power threshold level of the fiber referring to the diameter of the fiber and the lower line shows the calculated detection limit of the LIF diagnostic. This result illustrates that the detection limit is more than one order of magnitudes lower than the threshold power level of the fiber.
The second one is to demonstrate that the laser light system does not heat the coupling of the fiber to the vacuum vessel of ASDEX Upgrade. For this experiment the laser was coupled in to the fiber with a power near to the damage threshold, and a fiber coupler was used to connect the two fibers. The temperature was measured with a thermocouple. The measurement shows a 10 % loss of power in the coupler but not a measurable increase of the temperature of the fiber coupling.

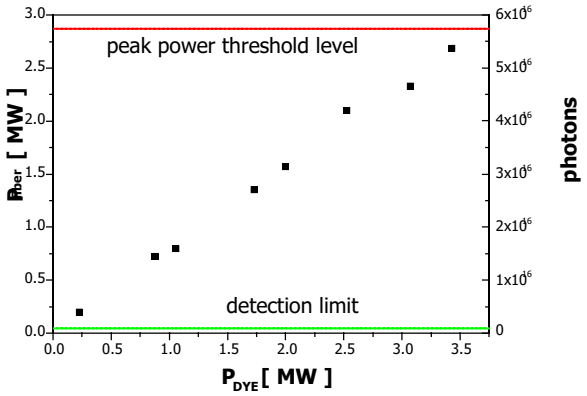

Figure 2.2: Power transmission measurements via fiber: The upper line illustrates the peak power threshold level, and the lower line gives the detection limit of the LIF diagnostic system. The detection limit of the LIF diagnostic could be improved after a redesign of the optical path of the laser beam in the ASDEX Upgrade Divertor by a factor of 5. The line of sight was adjusted during the last shut down phase further more: fibers were installed from ASDEX Upgrade to the laser room.

The schematic experimental set-up of the laser and detection system on ASDEX Upgrade is shown in Figure 2.3.

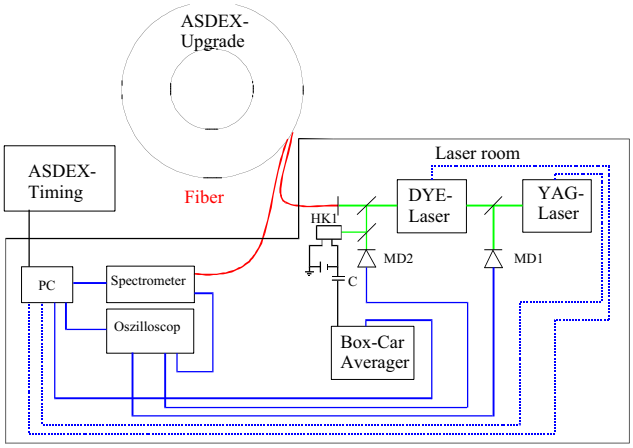

Figure 2.3: Scheme of the experimental set-up of the LIF diagnostic system on ASDEX-Upgrade

Further investigation will be performed to change the wavelength calibration to the hollow cathode with a Hydrogen/Deuterium gas filling. The automation of the laser and detection system has to be completed and further LIF test measurements on Neon, Helium and Hydrogen will be performed on a laboratory ECR-Plasma. The LIF diagnostic will be transferred to ASDEX Upgrade in the second quarter of 2003.

2.2 Erosion studies from emission and absorption spectroscopy

The determination of erosion mechanisms and erosion rates as a function of the plasma parameters and surface temperature is of major importance not only for tests of thermal protection materials for reusable space transportation systems but also for plasma facing components in thermonuclear fusion devices. Plasma jets interacting with targets of the material in question are

applied for these measurements and material tests. One of the methods is to study the erosion of a C/C-SiC target in such a plasma jet by high-resolution emission and absorption spectroscopy of Si I resonance spectra of the multiplet lines at 251 nm and the singlet lines at 263 nm, 288 nm or 390nm, respectively. The silicon is eroded by the plasma jet and forms a disc like radiating cloud in front of the target.

Further improvement of the experimental set up was done to measure the silicon density as a function of time and surface temperature. Figure 2.4 shows an Arrhenius plot of the measured silicon neutral density as a function of inverse surface temperature. The measurement was done with an uncoated C/C-SiC sample and coated with TiO_2. The sample with TiO_2 coating shows an increase of the effective surface binding energy of a factor of 3. Furthermore the plot shows the low and high temperature transition from active to passive oxidation.

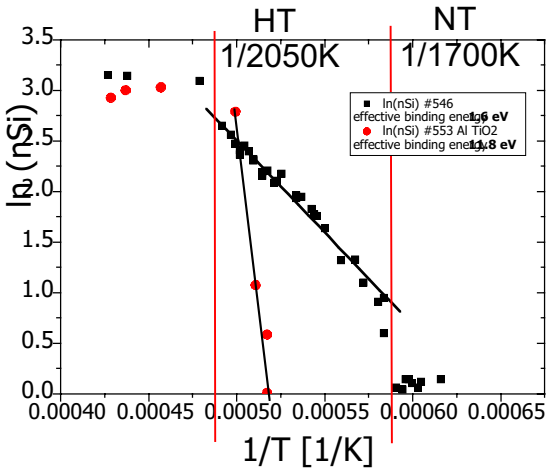

FIGURE 2.4: Measurements of silicon neutral density as a function of surface temperature

The change in the surface composition as a result of coating and plasma wall interaction makes it necessary to determine in situ the emissivity of the sample. In addition, an increasing emissivity allows an increasing thermal load to be tolerable. The ex-situ measurement of emissivity as a function of temperature and different coatings is shown in Figure 2.5. This graph illustrates that the emissivity increases up to a value of 0.9 at 1900 K for the TiO_2 protection layer.This demonstrates the necessity of the in-situ determination of the emissivity.

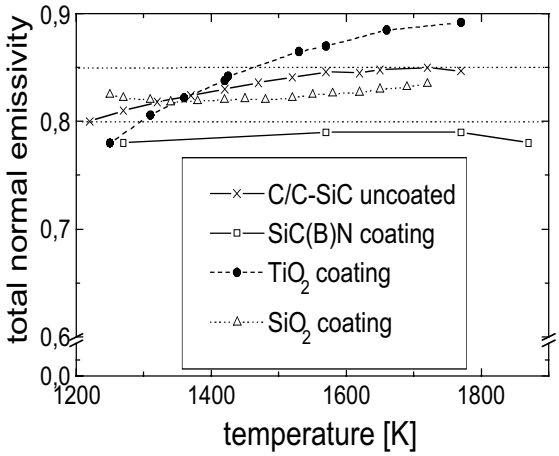

FIGURE 2.5: Total normal emissivity as a function of the surface temperature for uncoated C/C-SiC and as well as for different coatings

2.3 Staff

(U. S c h u m a c h e r, K. Burm[5], G. Dodel, P. Hießl, K. Hirsch, P. Lindner, B. Roth, R. Stirn)

3 Publications, Conference Reports, Patents, Doctoral Theses, Diploma Theses, Reports, And Seminar Talks

3.1 Publications

Dammertz, G., S. Alberti, A. Arnold, E. Borie, V. Erckmann, G. Gantenbein, E. Giguet, R. Heidinger, J.P. Hogge, S. Illy, W. Kasparek, K. Koppenburg, M. Kuntze, H.P. Laqua, G. LeCloarec,, Y. LeGoff, W. Leonhardt, C. Lievin, R. Magne, G. Michel, G.A. Müller, G. Neffe, B. Piosczyk, M. Schmid, K. Schwörer, M. Thumm, and M.Q. Tran: Development of a 140-GHz 1-MW continuous wave gyrotron for the W7-X Stellarator. IEEE Trans. Plasma Science, **PS-30** (2002) 808-818.

Jaenicke, R., S. Bäumel, J. Baldzuhn, R. Brakel, R. Burhenn, H. Ehmler, M. Endler, V. Erckmann, Y. Feng, F. Gadelmeier, J. Geiger, L. Giannone, P. Grigull, H. J. Hartfuß, D. Hartmann, D. Hildebrandt, M. Hirsch, E. Holzhauer, M. Kick, J. Kisslinger, T. Klinger, S. Klose, J. Knauer, R. König, G. Kühner, H. Laqua, H. Maaßberg, K. McCormick, R. Narayanan, H. Niedermeyer, E. Pasch, N. Ruhs, N. Rust, J. Saffert, F. Sardei, F. Schneider, M. Schubert, E. Speth, F. Wagner, A. Weller, U. Wenzel, A. Werner, and E. Würsching: A new quasi-stationary, very high density plasma regime on the W7-AS stellarator, Plasma Phys. Controlled Fusion **44** (2002) 193 - 205.

M. Thumm and W. Kasparek: Passive high-power microwave wave components. IEEE Trans. Plasma Science, PS-30 (2002) 755-786.

5 from October 1, 2002

3.2 Conference Reports

29th EPS Conference on Controlled Fusion and Plasma Physics, Montreux, Switzerland, June 17-21, 2002

G. Gantenbein, A. Keller, F. Leuterer, M. Maraschek, W. Suttrop, H. Zohm, ASDEX Upgrade Team: On the Stabilisation of Neoclassical Tearung Modes at high b_N in ASDEX Upgrade.
Jaenicke, R., S. Bäumel, J. Baldzuhn, R. Brakel, R. Burhenn, H. Ehmler, M. Endler, V. Erckmann, Y. Feng, F. Gadelmeier, J. Geiger, L. Giannone, P. Grigull, H. J. Hartfuß, D. Hartmann, D. Hildebrandt, M. Hirsch, E. Holzhauer, M. Kick, J. Kisslinger, T. Klinger, S. Klose, J. Knauer, R. König, G. Kühner, H. Laqua, H. Maaßberg, K. McCormick, R. Narayanan, H. Niedermeyer, E. Pasch, N. Ruhs, N. Rust, J. Saffert, F. Sardei, F. Schneider, M. Schubert, E. Speth, F. Wagner, A. Weller, U. Wenzel, A. Werner, and E. Würsching: A new quasi-stationary, very high density plasma regime on the W7-AS stellarator, Plasma Phys. Controlled Fusion 44 (2002) B193B205.
P.Lindner, M.Brix Ph.Mertens, A.Pospieszczyk, U.Samm, B.Schweer, B.Unterberg : Spectroscopic Studies Of The Velocity Distribution Of Helium And Neon Atoms Released From Carbon And Tungsten Limiters In TEXTOR-94. P-2.059

12th Joint Workshop on ECE and ECRH, EC-12, Aix-en Provence (France), May 13-16, 2002

Idei, H., T. Notake, M. Shapiro, W. Kasparek, T. Shimozuma, S. Kubo,
S. Ito, M. Sato, R. J. Temkin and K. Ohkubo, Development of Quasi-Optical Components for Electron Cyclotron Heating based on Phase Measurements. Conference Proceedings 060.

Laqua, H.P., V. Erckmann, F. Volpe, W7-AS team, ECRH-group IPF Stuttgart, Electron Bernstein wave heating and current drive in overdense plasmas at the Wendelstein7-AS stellarator. Conference proceedings 088.

W. Kasparek, G. Gantenbein, B. Plaum, R. Wacker, E. Filipovic, A.V. Chirkov, G.G. Denisov, S.V. Kuzikov, K. Ohkubo, F. Hollmann, D. Wagner: Performance of a Remote Steering Antenna for ECRH/ECCD Applications using 4-Wall Corrugated Square Waveguide. Conference Proceedings 033.

F. Leuterer, R. Dux, G. Gantenbein, T. Goodman, J. Hobirk, F. Imbeaux, K. Kirov, P. Mantica, M. Maraschek, A. Mück, R. Neu, A.G. Peeters, G. Pereverzev, F. Ryter, J. Stober, G. Tardini, E. Westerhof, H. Zohm, AUG Team: Recent ECRH Results in ASDEX Upgrade. Conference Proceedings 087.

G. Michel, P. Brand, G. Dammertz, V. Erckmann, G. Gantenbein, F. Hollmann, L. Jonitz, W. Kasparek, H.P. Laqua, W. Leonhardt, G. Müller, F. Purps, M. Schnid, T. Schulz, M. Thumm, Karlsruhe and Stuttgart ECRH Teams: Progress of the 10 MW ECRH System for W7-X Conference proceedings 044.

19th IAEA Fusion Energy Conference, Lyon, France, 14 - 19 October 2002

S. Günter, G. Gantenbein, A. Gude, V. Igoshine, M. Maraschek, O. Sauter, A.C.C. Sips, H. Zohm and the ASDEX Upgrade Team: Neoclassical Tearing Modes an the ASDEX Upgrade: Improved Scaling Laws, High Confinement at high b_N and New Stabilization Experiments.

F. Wagner, R. Burhenn, F. Gadelmeier, J. Geiger, M. Hirsch, H. P. Laqua, A. Weller, A. Werner, S. Bäumel, J. Baldzuhn, R. Brakel, A. Dinklage, P. Grigull, M. Endler, V. Erckmann, H. Ehmler, Y. Feng, R. Fischer, F. Gadelmeier, L. Giannone, H.-J. Hartfuss, D. Hildebrandt, E. Holzhauer, Y. Igitkhanov, R. Jänicke, M. Kick, A. Kislyakov, A. Kreter, J. Kisslinger, T. Klinger, S. Klose, J. P. Knauer, R. König, G. Kühner, H. Maassberg, K. McCormick, D. Naujoks, H. Niedermeyer, C. Nührenberg, E. Pasch, N. Ramasubramanian, N. Rust, E. Sallander, F. Sardei, U. Wenzel, H. Wobig, E. Würsching, M. Zarnstorff, S. Zoletnik, and the W7-AS Team: Major Results from Wendelstein 7-AS Stellarator, Proc IAEA-CN-94, 2002

25th Symposium on Fusion Technology, Helsinki, Finnland, September 2002

H. Hailer, G. Dammertz, V. Erckmann, G. Gantenbein, F. Hollmann, W. Kasparek, W. Leonhardt, M. Schmid, P.G. Schüller, M. Thumm, M. Weissgerber: Mirror Development for the 140 GHz ECRH system of the stellarator W7-X. Conference proceedings to be published in Fusion Eng. Design.

Brand, P. and G. Müller: Circuit Design and Simulation of a HV-Supply Controlling the Power of 140 GHz 1MW Gyrotrons for ECRH on W7-X. Conference proceedings to be published in Fusion Eng. Design.

Förster, W., P. Brand, G. Müller: A novel Approach of High Voltage Filter Design for Smoothing the Output Voltage of High Voltage High Power Pulse Step Modulators. Conference proceedings to be published in Fusion Eng. Design.

15th International Conference on Plasma-Surface Interactions in Controlled Fusion Devices (Gifu, Japan, May 2002)

K. McCormick, P. Grigull, R. Burhenn, R. Brakel, H. Ehmler, Y. Feng, R. Fischer, F. Gadelmeier, L. Giannone, D. Hildebrandt, M. Hirsch, E. Holzhauer, R. Jaenicke, J. Kisslinger, T. Klinger, S. Klose, J-P. Knauer, R. König, G. Kühner, H.P. Laqua, D. Naujoks, H. Niedermeyer, E. Pasch, N. Ramasubramanian, N. Rust, F. Sardei, F. Wagner, A. Weller, U. Wenzel and A. Werner: Island Divertor Experiments on the Wendelstein 7-AS Stellarator. Conference Proceedings, to be published in J. Nucl. Mater.

14th Joint Russian German Meeting on ECRH and Gyrotrons, Nizhny Novgorod and Moscow (Russia), June 25-July 2, 2002

M. Thumm, A. Arnold, G. Dammertz, R. Heidinger, S. Illy, K. Koppenburg, M. Kuntze, W. Leonhardt, G. Neffe, B. Piosczyk, M. Schmid, X. Yang, M.Q. Tran, G. Müller, E. Giguet, G. LeCloarec, F. Legrand, C. Lievin: Experimental results of the 140 GHz, 1 MW long-pulse gyrotron for W7-X

W. Kasparek, G. Gantenbein, H. Hailer, P.G. Schüller, K. Schwörer, R. Wacker), F. Hollmann, M. Weissgerber, V. Erckmann: Status of the transmission system for ECRH on W7-X .

K. Schwörer, G. Gantenbein, H. Hailer, W. Kasparek, R. Wacker (IPF), H. Hollmann (IPP): Performance tests of the multi-beam transmission lines for ECRH on W7-X

W. Kasparek, G. Gantenbein, H. Idei, S. Kubo, T. Notake: Simulation and experiments on various methods for in- situ alignment of beam waveguides

F. Leuterer, K. Kirov, F. Monaco, M. Münich, H. Schütz, F. Ryter, D. Wagner, R. Wilhelm, H. Zohm, T. Franke, K. Voigt, M. Thumm, R. Heidinger, G. Dammertz, K. Koppenburg, W. Kasparek, G. Gantenbein, H. Hailer, G.A. Müller, A. Bogdashov, G. Denisov, V. Kurbatov, A. Kuftin, A. Litvak, S. Malygin, E. Tai, V. Zapevalov: Plans for the new ECRH system of ASDEX Upgrade

F. Leuterer, R. Dux, J. Hobirk, K. Kirov, M. Maraschek, A. Mück, R. Neu, A.G. Peeters, F. Ryter, J. Stober, W. Suttrop, G. Tardini, H. Zohm, AUG Team, G. Gantenbein: ECRH results from ASDEX Upgrade

27th International Conference on Infrared and Millimeter Waves, San Diego, USA, September 22-26, 2002.

Dammertz, G., S. Alberti, E. Borie, V. Erckmann, G. Gantenbein, E. Giguet, R. Heidinger, J.P. Hogge, S. Illy, W. Kasparek, K. Koppenburg, M. Kuntze, H.P. Laqua, G. LeCloarec,, F. Legrand, W. Leonhardt, C. Lievin, R. Magne, G. Michel, G. Müller, G. Neffe, B. Piosczyk, M. Schmid, M. Thumm, and M.Q. Tran: Progress of the 1 MW, 140 GHz CW gyrotron for W7-X. Conference Digest.

E. Holzhauer, G. Gantenbein, W. Kasparek: Wood´s anomaly in the design of corrugated mirrors for high-power millimeter waves. Conference Digest.

Kasparek, W., H. Kumric, G.A. Müller, B. Plaum, A. Girard, D. Hitz, G. Melin: Development of transmission lines at frequencies of 28 – 37 GHz for application with ECR ion sources. Conference Digest.

Kumric, H. and H. Hasch: Corrugated mode converters with varying wall impedance. Conference Digest.

Wacker, R., F. Leuterer, D. Wagner, H. Hailer, W. Kasparek: Characterization of absorber materials for high-power millimetre waves. Conference Digest.

5th International Workshop „Strong Microwaves in Plasmas“, Nizhny Novgorod, Russland, August 1-8, 2002.

Erckmann, V., G. Gantenbein, W. Kasparek, H.P. Laqua, H. Maaßberg, G. Michel, G.A. Müller, N. Marushchenko, W7-AS Team: 20 Years of ECRH at W7-A and W7-AS

Kasparek, W., G. Dammertz, V. Erckmann, G. Gantenbein, H. Hailer, F. Hollmann, L. Jonitz, H.P. Laqua, W. Leonhardt, G. Michel, M. Schmid*, P.G. Schüller, K. Schwörer, R. Wacker, M. Weissgerber: The transmission system for ECRH on the stellarator W7-X: design issues and tests of prototype components

Ohkubo, K., S. Kubo, T. Shimozuma, H. Idei, H. Yoshimura, T. Notake and W. Kasparek: Theoretical Analysis of Remote Steering Antenna Comparing with Experiments

H. Zohm, G. Gantenbein, A. Keller, F. Leuterer, M Maraschek, A. Mück, R. Neu, F. Ryter, J. Stober, W. Suttrop and the ASDEX Upgrade Team: Confinement and Stability Studies with ECRH in ASDEX Upgrade

5th International Workshop on Transmission lines, San Diego, USA, September 18-20, 2002.

G. Gantenbein, F. Hollmann, W. Kasparek, B. Plaum, E. Filipovic, D. Wagner, A.V. Chirkov, G.G. Denisov, S.V. Kuzikov: Performance of a Remote Steering Antenna for ECRH/ECCD Applications using 4-wall Corrugated Square Waveguide

W. Kasparek, G. Dammertz, V. Erckmann, G. Gantenbein, H. Hailer, F. Hollmann, L. Jonitz, H.P. Laqua, W. Leonhardt, G. Michel, M. Schmid, P.G. Schüller, K. Schwörer, R. Wacker, M. Weissgerber: The transmission system for ECRH on the stellarator W7-X: design and tests of prototype components

16th ECTP2002: European Conference on Thermophysical Properties, 1-4.09.2002, Imperial College, London (National Physical Laboratory)

K.Hirsch, I.Altmann, G. Bauer, R.Brandt, P.Lindner, G.Neuer, B.Roth, J.Schneider, R.Stirn und U.Schumacher: In Situ Determination of the Emissivity and of the Erosion Rate of Heat Shield Materials in Re-entry Simulation Experiments

German-Polish Euro-Conference on Plasma Diagnostics for Fusion and Applications,
4.-6.9.2002, IPP Greifswald

J.Krüger, T.Kubach, P.Lindner, U. Schumacher:
Comparisen of probe and spectroscopic Diagnostics in Microwave Generated Plasmas for Technical Applications

R.Stirn, P.Hießel, K. Hirsch, P.Lindner, B.Roth, U.Schumacher:
Spectroscopic Diagnostics and Investigations of Plasma Target Interaction

3.3 Diploma Thesis

Stirn, R.: Untersuchung der Erosion beschichteter und unbeschichteter Hitzeschutzmaterialien durch einen Plasmastrahl, Universität Stuttgart

3.4 Seminar Talks

U. Schumacher: Strahlenphysik in der Plasmaforschung, Kolloquium, Institut für Strahlenphysik, Universität Stuttgart, 16.05.2002

U. Schumacher: Plasma - Extrem heiße Materie im Universum und im Labor, Arbeitskreis Astronomie, Universität Stuttgart, 03.07.2002

U.Schumacher: Photonenspektroskopie: Lichtblicke der Plasma- analyse, Kolloquium Humboldt-Universität Berlin, 12.07.2002

U.Schumacher: Development of microwave and plasma technology at Stuttgart Institute of Plasma Research, 2nd Intern. Workshop on Far-Infrared Technologies, Fukui University, Fukui, Japan, 13.10.2002

Department of Electrical and Electronic Engineering at Rostock University

Prof. H. Weber, Dipl.-Ing. T. Haase, Dipl.-Ing. A. Holst

1 Future electricity networks

Especially the introduction of intermittent electricity sources and the diffusion of distributed generation will make it necessary to improve the electricity network capacities and control mechanisms and will make the introduction of completely new dispatching philosophies necessary. The dispatching philosophy has to be changed from a demand driven to a supply driven philosophy, which distinguishes between renewable primary supplies and back-up secondary supplies. Basis for the following analysis is the software tool DIgSILENT PowerFactory.

The picture shows the additional power flow in the European UCTE net due to the installation of off-shore wind turbines

Within this tool the UCTE grid is modelled using 1488 nodes, 2401 transmission lines, 533 power plants, 92 transformers and 948 consumer loads. Information on the production and consumption in the UCTE states, distribution of produced power on the individual power plants and plant types, load-curves for high and low demand cases and the dynamic of power plants are available. In a first step the static electricity transport capacities in the German grid was analysed. Basis for the analysis are the existing capacities of the high-voltage transmission system. In a second step the planned development of the offshore wind energy was examined into the year 2030. In the picture the change of the load flow is presented with a feed of seven Gigawatt from offshore wind parks in the north and Baltic Sea opposite a basic scenario. The extension of the high-voltage transmission system in Northern Germany should take place in the same speed, as the establishment of the offshore wind parks. Otherwise it is not possible to transfer power from several Gigawatts. Further the supply of control power will be a large problem for the utilities. It depends not only on the load prognosis, but also on the wind prognosis. However in principle it is possible to feed twenty Gigawatt from offshore wind power into the German grid, if the high-voltage transmission system is accordingly developed and enough control power is available.

2 Influence of WENDELSTEIN 7-X on the electricity grid

The heating power of the experiment WENDELSTEIN 7-X is taken from the 110-kV-distribution network of the e.dis Energie Nord AG. These heavy pulsating load causes network reaction effects for consumers close to the IPP e.g. the city of Greifswald. In cooperation with IPP Institute of Greifswald and the utility e.dis the University of Rostock analyses the effects to the supplying high-voltage-network and the distribution subsystems. The aim of the study is the evaluation of the network reaction effects and to find possibilities to influence or to reduce the effects.

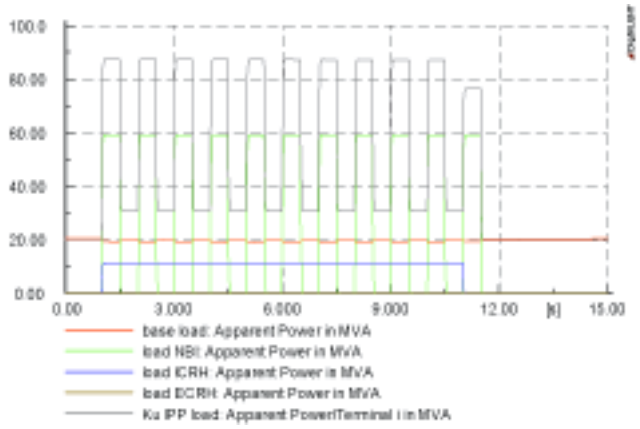

A detailed network model is used for the investigations. All parts of the local network levels are included inside of the model. The heating scenarios are simulated and the network reaction effects are detected. Some various load- and network conditions, different heating scenarios and future network constellations are considered within the simulation. The results show that the sudden load rises are problematically. There are some possibilities to improve the situation, which are studied more exactly at present.

Publications

1. *Allfrey*, S.J., R. Hatzky, A. Bottino* and L. Villard*:* Global Gyrokinetic Simulations of Nonlinear Interaction of Zonal Flows with ITG Modes. In: Proceedings of the 29th EPS Conference on Plasma Physics and Controlled Fusion, Montreux 2002, (Eds.) R.Behn, C.Varandas. ECA 26B, European Physical Society, Geneva 2002, P-4.059.

2. *Allfrey*, S.J., R. Hatzky, A. Bottino* and L. Villard*:* Role of Self-Generated and Externally Applied Radial Electric Fields in the Development of ITG Driven Modes. In: Proceedings of the Joint Varenna-Lausanne International Workshop on Theory of Fusion Plasmas, Varenna 2002. (Eds.) J.W.Connor, O. Sauter, E. Sindoni. Editrice Compositori, Bologna 2002, 171-182.

3. *Arnold*, A., G. Dammertz*, D. Wagner and M. Thumm*:* Measurements on a Mode Generator for Cold Tests of Step-Tunable Gyrotrons. In: Proceedings of the 27th International Conference on Infrared and Millimeter Waves, San Diego,CA 2002, (Ed.) R.J.Temkin. IEEE Press, New York,NY 2002, 289-290.

4. *Bachmann, P.:* Chaos in 1D Radiative Edge Plasmas. Contributions to Plasma Physics **42**, 425-430 (2002).

5. *Bachmann, P., J. Kisslinger, D. Sünder and H. Wobig:* Bifurcation of Temperature and Anomalous Transport in the Boundary Region of Wendelstein 7-X. Plasma Physics and Controlled Fusion **44**, 83-102 (2002).

6. *Bachmann, P., J. Kisslinger, D. Sünder and H. Wobig:* Bifurcation of Temperature and Anomalous Transport in the Edge Region of W-7X. In: Proceedings of the 29th EPS Conference on Plasma Physics and Controlled Fusion, Montreux 2002, (Eds.) R.Behn, C.Varandas. ECA 26B. European Physical Society, Geneva 2002, P-1.113.

7. *Baldzuhn, J., A. Werner and H. Wobig:* Radial Electric Field Modification by Perpendicular Neutral Beam Injection in the Stellarator W7-AS. In: Proceedings of the 13th International Stellarator Workshop, Canberra 2002, PPPL, Princeton,NJ 2002, PIIA.10.

8. *Basse*, N.P., P.K. Michaelsen*, S. Zoletnik*, M. Saffman*, M. Endler and M. Hirsch:* Spatial Distribution of Turbulence in the Wendelstein 7-AS Stellarator. Plasma Sources Science and Technology **11,** A138-A142 (2002).

9. *Basse*, N., S. Zoletnik*, M. Saffman*, J. Baldzuhn, M. Endler, M. Hirsch, J.-P. Knauer, G. Kühner, K. McCormick, A. Werner and W7-AS Team:* Low- and High-Mode Separation of Short Wavelength Turbulence in Dithering W7-AS Plasmas. Physics of Plasmas **9**, 3035-3049 (2002).

10. *Becker, G.:* Elongation and Current Scalings of Local and Global Energy Transport. Nuclear Fusion **42**, L8-L9 (2002).

11. *Becoulet*, M., V. Parail*, G. Huysmans*, S. Sharapov*, P.J. Lomas*, G. Saibene*, R. Sartori*, A. Loarte*, G.F. Matthews*, W. Suttrop, J. Stober, A. Kallenbach, E. Joffrin*, Y. Sarazin*, X. Litaudon*, A. Becoulet*, Ph. Ghendrih* and Contributors to the EFDA-JET Work Programme:* ELMs Behaviour and Edge Plasma Stability in JET. Plasma Physics and Controlled Fusion **44**, A103-A112 (2002).

12. *Behrisch, R.:* Contribution of Different Erosion Processes to Material Release from the Vessel Walls of Fusion Devices during Plasma Operation. Contributions to Plasma Physics **42**, 431-444 (2002).

13. *Beidler, C.D., S.V. Kasilov*, W. Kernbichler*, H. Maaßberg, D.R. Mikkelsen*, S. Murakami*, V.V. Nemov*, M. Schmidt, V. Tribaldos*, A. Wakasa* and R. White*:* Initial Results from the International Collaboration on Neoclassical Transport in Stellarators. In: Proceedings of the 13th International Stellarator Workshop, Canberra 2002, PPPL, Princeton,NJ 2002, OI.10.

14. *Beikler, R. and E. Taglauer:* Quantitative Layer Analysis of Single Crystal Surfaces by LEIS. Nuclear Instruments and Methods in Physics Research B **193**, 455-459 (2002).

15. *Bergmann, A.:* Transport of Edge-Localized Mode Energy in a Scrape-off Layer in the Presence of Collisionless Fast Electrons. Nuclear Fusion **42**, 1162-1167 (2002).

16. *Bergmann, A.:* Two-Dimensional Particle Simulation of the Current Flow to a Flush-Mounted Langmuir Probe in a Strong Oblique Magnetic Field. Physics of Plasmas **9**, 3413-3420 (2002).

17. *Biedermann, C., R. Radtke and K.B. Fournier*:* Spectroscopy of Heliumlike Argon Resonance and Satellite Lines for Plasma Temperature Diagnostics. Physical Review E **66**, 066404 (2002).

18. *Biel*, B., G. Bertschinger*, R. Burhenn and R. König:* Design of VUV/XUV Spectrometers for Impurity Studies on W7-X. In: Proceedings of the 29th EPS Conference on Plasma Physics and Controlled Fusion, Montreux 2002, (Eds.) R.Behn, C.Varandas. ECA 26B, European Physical Society, Geneva 2002, P-5.098.

19. *Bilato, R., M. Brambilla, I. Pavlenko* and F. Meo:* Simulation of Fast Wave Current Drive in Tokamaks in the Ion Cyclotron Frequency Range. Nuclear Fusion **42**, 1085-1093 (2002).

20. *Bindemann, T., J.C. Fuchs, H.-J. Hartfuß and M. Hirsch:* Robust Line Density Measurements at W7-AS Using a Cotton-Mouton Polarimeter. In: Advanced Diagnostics for Magnetic and Inertial Fusion, (Eds.) P.E.Stott, A.Wooton. Kluwer, New York,NY 2002, 323-326.

21. *Bleuel*, J., M. Endler, H. Niedermeyer, M. Schubert, H. Thomsen and W7-AS Team:* The Spatial Structure of Edge Fuctuations in the Wendelstein 7-AS Stellarator. New Journal of Physics **4**, 38.1-38.38 (2002).

22. *Bogusch*, E., H. Bolt, A. Chevalier*, C. Forty*, F. Gnesotto*, R. Heller*, A. Laurenti*, G. Link*, J. Lister*, R. Munther*, G. Reyk*, B. Schedler*, M. Thumm*, A. Vallée* and N. Waterman*:* Benefits to European Industry from Involvement in Fusion. Fusion Engineering and Design **63-64**, 679-687 (2002).

23. *Bolt, H., V. Barabash*, G. Federici*, J. Linke*, A. Loarte*, J. Roth and K. Sato*:* Plasma Facing and Heat Flux Materials-Needs for ITER and Beyond. Journal of Nuclear Materials **307-311**, 43-52 (2002).

24. *Bolzonella*, T., E. Martines*, M. Maraschek, H. Zohm, S. Günter, S. Saarelma* and ASDEX Upgrade Team:* ELM-Related High Frequency MHD Activity in ASDEX Upgrade. In: Proceedings of the 29th EPS Conference on Plasma Physics and Controlled Fusion, Montreux 2002, (Eds.) R.Behn, C.Varandas. ECA 26B. European Physical Society, Geneva 2002, P-1.038.

25. *Bonnin, X., H. Bürbaumer*, R. Schneider, D.P. Coster, F. Aumayr* and H.P. Winter*:* The Two-Mesh Grid Refinement Method for the B2 Code. Contributions to Plasma Physics **42**, 175-180 (2002).

26. *Borba*, D., H.L. Berk*, B.N. Breizman*, A. Fasoli*, F. Nabais*, S.D. Pinches, S. Sharapov*, D. Testa* and Contributors to the EFDA-JET Work Programme:* Modelling of Alfvén Waves in JET Plasmas with the CASTOR-K Code. Nuclear Fusion **42**, 1029-1038(2002).

27. *Borowski*, S., S. Thiel*, T. Kluner*, H.-J. Freund*, R. Tisma and H. Lederer:* High Dimensional Quantum Dynamics of Molecules on Surfaces: a Massively Parallel Implementation. Computer Physics Communications **143**, 162-173 (2002).

28. *Borrass, K., ASDEX Upgrade Team and EFDA-JET Work Programme Collaborators:* Natural Density Formation as an H-Mode Operational Limit. Nuclear Fusion **42**, 1251-1256 (2002).

29. *Borrass, K., EFDA-JET Work Programme Collaborators and ASDEX Upgrade Team:* Study of the Natural Density Formation in JET and ASDEX Upgrade. In: Proceedings of the 29th EPS Conference on Plasma Physics and Controlled Fusion, Montreux 2002, (Eds.) R.Behn, C.Varandas. ECA 26B. European Physical Society, Geneva 2002, P-1.028.

30. *Bosch, H.-S.:* Alles Blasen, oder was? Physik Journal **1** (5), 21-22 (2002).

31. *Bosch, H.-S.:* Erste Erfolge bei "sphärischen Tokamaks". Physik Journal **1** (4), 19-20 (2002).

32. *Bottino*, A., S.J. Allfrey*, A.G. Peeters, O. Sauter*, L. Villard* and ASDEX Upgrade Team: E x B* Flow Effects on ITG Modes in Reverse Shear ASDEX Upgrade Discharge. In: Proceedings of the 29th EPS Conference on Plasma Physics and Controlled Fusion, Montreux 2002, (Eds.) R.Behn, C.Varandas. ECA 26B. European Physical Society, Geneva 2002, P-1.040.

33. *Bottino*, A., R. Hatzky, S.J. Allfrey*, O. Sauter* and L. Villard*:* Global Nonlinear Gyrokinetic Simulations of ITG Modes Using Particles in Tokamak Geometry. In: Proceedings of the Joint Varenna-Lausanne International Workshop on Theory of Fusion Plasmas, Varenna 2002. (Eds.) J.W.Connor, O.Sauter, E.Sindoni. Editrice Compositori, Bologna 2002, 351-356

34. *Bradshaw, A.M. and T. Hamacher:* Our Energy Future. Physicalia Magazine **24**, 127-137 (2002).

35. *Bradshaw, A.M. and I. Milch:* Fusionsforschung im Max-Planck-Institut für Plasmaphysik. Atw - Internationale Zeitschrift für Kern-energie **47,** 37-42 (2002).

36. *Brakel, R. and W7-AS Team:* Electron Energy Transport in the Presence of Rational Surfaces in the Wendelstein 7-AS Stellarator. Nuclear Fusion **42**, 903-912 (2002).

37. *Brambilla, M.:* "Quasi-Local" Wave Equations in Toroidal Geometry, with Applications to Fast Wave Propagation and Adsorption at High Harmonics of the Ion Cyclotron Frequency. Plasma Physics and Controlled Nuclear Fusion **44**, 2423-2443 (2002).

38. *Bruchhausen*, M., R. Burhenn, A. Pospieszczyk*, S. Zoletnik* and W7-AS Team:* Measurements of Electron Density Fluctuations in the Scrape-off Layer (SOL) and Edge Plasma of the Stellarator Wendelstein 7-AS by Means of Lithium Laser Blow-off. In: Proceedings of the 29th EPS Conference on Plasma Physics and Controlled Fusion, Montreux 2002, (Eds) R.Behn, C.Varandas. ECA 26B, European Physical Society, Geneva 2002, P-3.214.

39. *Bubert*, H., X. Ai*, S. Haiber*, M. Heintze*, V. Brüser*, E. Pasch, W. Brandl* and G. Marginean*:* Basic Analytical Investigation of Plasma-Chemically Modified Carbon Fibers. Spectrochimica Acta B **57**, 1601-1610 (2002).

40. *Budny*, R.V., R. Andre*, A. Becoulet*, C.D. Challis*, G.D. Conway, W. Dorland*, D.R. Ernst*, T. Hahm*, T.C. Hender*, D. McCune*, G. Rewoldt* and Contributors to the EFDA-JET Work Programme:* Microturbulence and Flow Shear in High-Performance JET ITB Plasma. Plasma Physics and Controlled Fusion **44**, 1215-1228 (2002).

41. *Burhenn, R., K. Ida*, R. Brakel, L. Giannone, P. Grigull, J.-P. Knauer, F. Kunkel, H. Maaßberg, K. McCormick, E. Pasch, A. Weller, W7-AS Team, ECRH Group and NI Group:* Characterization of Impurity Transport in the W7-AS Stellarator during the Transition to the Improved Confinement Regime. In: Proceedings of the 29th EPS Conference on Plasma Physics and Controlled Fusion, Montreux 2002, (Eds) R.Behn, C.Varandas. ECA 26B, European Physical Society, Geneva 2002, P-4.043.

42. *Cattanei, G. and W7-AS Team:* Resonant Faraday Shield ICRH Antenna. Nuclear Fusion **42**, 541-546 (2002).

43. *Cecconello*, M., J.A. Malmberg*, E. Sallander and J.R. Drake*:* Self-Organisation and Intermittent Coherent Oscillations in the EXTRAP-T2 Reversed Field Pinch. Physica Scripta **65**, 69-75 (2002).

44. *Cho*, B., T. Schwarz-Selinger, K. Ohmori*, D.G. Cahill* and J.E. Greene*:* Effect of Growth Rate on the Spatial Distributions of Dome-Shaped Ge Islands on Si(001). Physical Review B **66**, 195407 (2002).

45. *Conway, G.D., G.M.D. Hogeweij*, M. De Baar*, Yu. Baranov*, R. Barnsley*, N.C. Hawkes*, X. Litaudon*, J. Mailloux*, E. Righi*, F.G. Rimini*, K.-D. Zastrow* and Contributors to the EFDA-JET Work Programme:* Turbulence Behaviour during Electron Heated Reversed Shear Discharges in JET. Plasma Physics and Controlled Fusion **44**, 1167-1180 (2002).

46. *Conway, G.D., B. Kurzan, B.D. Scott, E. Holzhauer and M. Kaufmann:* Coupling of Turbulence and Reflectometer Simulation Codes and Comparison with Experiment. Plasma Physics and Controlled Fusion **44**, 451-463 (2002).

47. *Conway, G.D., P.J. McCarthy, I. Nunes*, A.C.C. Sips, F. Serra*, S. Sesnic*, M. Maraschek, A. Mück, W. Suttrop, M. Manso*, ASDEX Upgrade Team and CFN Teams:* Locating Rational Surfaces from Reflectometer Fluctuations. In: Proceedings of the 29th EPS Conference on Plasma Physics and Controlled Fusion, Montreux 2002, (Eds.) R.Behn, C.Varandas. ECA 26B. European Physical Society, Geneva 2002, P-4.075.

48. *Cooper*, W.A., S. Ferrando i Margalet*, S.J. Allfrey*, M.Yu. Isaev*, M.I. Mikhailov*, V.D. Shafranov*, A.A. Subbotin*, Y. Narushima*, S. Okamura*, C. Suzuki*, K. Yamazaki*, J. Nührenberg and T.N. Todd*:* Bootstrap Current Destabilization of Ideal MHD Modes in 3D Reactor Configurations. Plasma Physics and Controlled Fusion **44**, 357-373 (2002).

49. *Cooper*, W.A., J. Nührenberg, V. Drozdov*, A.A. Ivanov*, A.A. Martynov*, S.Yu. Medvedev*, Yu.Yu. Poshekhonov*, M.Yu. Isaev* and M.I. Mikhailov*:* 3D Equilibrium Averaged Description and Consistency Check. In: Proceedings of the 29th EPS Conference on Plasma Physics and Controlled Fusion, Montreux 2002, (Eds.) R.Behn, C.Varandas. ECA 26B, European Physical Society, Geneva 2002, P-2.113.

50. *Cordey*, J.G., D.C. McDonald*, K. Borrass, M. Charlet*, I. Coffey*, A. Kallenbach, K. Lawson*, P.J. Lomas*, J. Ongena*, J. Rapp*, F. Ryter, G. Saibene*, R. Sartori*, M. Stamp*, J. Strachan*, W. Suttrop, M. Valovic* and Contributors to the EFDA-JET Work Programme:* Energy Confinement in Steady-State ELMy H-Modes in JET. Plasma Physics and Controlled Fusion **44**, 1929-1935 (2002).

51. *Coster, D.P., J.-W. Kim, Y. Nishimura, R. Schneider, X. Bonnin, V. Rozhansky* and S. Voskoboynikov*:* Tokamak Edge Model Validation and Improvement. Plasma Physics and Controlled Fusion **44**, 979-984 (2002).

52. *Crisanti*, F., X. Litaudon*, J. Mailloux*, D. Mazon*, E. Barbato*, Yu. Baranov*, A. Becoulet*, M. Becoulet*, C.D. Challis*, G.D. Conway, R. Dux, L.G. Eriksson*, B. Esposito*, D. Frigione*, P. Hennequin*, C. Giroud*, N.C. Hawkes*, G. Huysmans*, F. Imbeaux*, E. Joffrin*, P.J. Lomas*, P. Lotte*,

P. Maget, M. Mantsinen*, D. Moreau*, F.G. Rimini*, M. Riva*, Y. Sarazin*, G. Tresset*, A.A. Tuccillo* and K.-D. Zastrow*:* JET Quasistationary Internal-Transport-Barrier Operation with Active Control of the Pressure Profile. Physical Review Letters **88**, 145004 (2002).

53. *Dammertz*, G., S. Alberti*, A. Arnold*, E. Borie*, V. Erckmann, G. Gantenbein*, E. Giguet*, R. Heidinger*, J.P. Hogge*, S. Illy*, W. Kasparek*, K. Koppenburg*, M. Kuntze*, H.P. Laqua, G. LeCloarec*, F. Legrand*, Y. Legoff*, W. Leonhardt*, C. Lievin*, R. Magne*, G. Michel, G. Müller*, G. Neffe*, B. Piosczyk*, M. Schmid*, K. Schwörer*, M. Thumm* and M.Q. Tran*:* Progress of the 1 MW, 140 GHz. CW Gyrotron for W7-X. In: Proceedings of the 27th International Conference on Infrared and Millimeter Waves, San Diego,CA 2002, (Ed.) R.J.Temkin. IEEE Press, New York,NY 2002, 3-4.

54. *Dammertz*, G., S. Alberti*, A. Arnold*, E. Borie*, V. Erckmann, G. Gantenbein*, E. Giguet*, R. Heidinger*, J.P. Hogge*, S. Illy*, W. Kasparek*, K. Koppenburg*, M. Kuntze*, H.P. Laqua, G. LeCloarec*, F. Legrand*, Y. Legoff*, W. Leonhardt*, C. Lievin*, R. Magne*, G. Michel, G. Müller*, G. Neffe*, B. Piosczyk*, M. Schmid*, M. Thumm* and M.Q. Tran*:* 140 GHz, 1 MW. CW Gyrotron for Fusion Plasma Heating. In: Proceedings of the 3rd IEEE International Vacuum Electronics Conference, Monterey,CA 2002. IEEE Operations Center, Piscataway,NJ 2002, 330-331.

55. *Dinklage, A.:* Laser Absorption Spectroscopy with a Blue Diode Laser in an Aluminium Hollow Cathode Discharge. Review of Scientific Instruments **73**, 378-382 (2002).

56. *Dinklage, A., R. Fischer, G. Kühner, H. Maaßberg, E. Pasch and J. Svensson:* Steps towards an Integrated Data Analysis: Basic Concepts and Bayesian Analysis of Thomson Scattering Data. In: Proceedings of the 29th EPS Conference on Plasma Physics and Controlled Fusion, Montreux 2002, (Eds.) R.Behn, C.Varandas. ECA 26B, European Physical Society, Geneva 2002, P-5.103.

57. *D'Ippolito*, D.A., J.R. Myra*, P.M. Ryan*, E. Righi*, J.A. Heikkinen*, P. Lamalle*, J.-M. Noterdaeme and Contributors to the EFDA-JET Work Programme:* Modeling of Mixed-Phasing Antenna-Plasma Interactions on JET A2 Antennas. Nuclear Fusion **42,** 1356-1364 (2002).

58. *Düchs, D. and J.A. Heikkinen* (Eds.):* Proceedings of the 8th International Workshop on Plasma Edge Theory in Fusion Devices, Espoo 2001. Contributions to Plasma Physics **42** (2002), 136-463.

59. *Dumortier*, P., P. Andrew*, G. Bonheure*, R.V. Budny*, R.J. Buttery*, M. Charlet*, I. Coffey*, M. De Baar*, P. de Vries*, T. Eich, D. Hillis*, L.C. Ingesson*, S. Jachmich*, G. Jackson*, A. Kallenbach, H.R. Koslowski*, K. Lawson*, C. Liu*, G. Maddison*, A. Messiaen*, P. Monier-Garbet*, M. Murakami*, M.F.F. Nave*, J. Ongena*, V. Parail*, M.E. Puiatti*, J. Rapp*, R.Sartori*, M. Stamp*, J. Strachan*, W. Suttrop, G. Telesca*, M. Tokar*, B. Unterberg*, M. Valisa*, M. von Hellermann*, B. Weyssow* and Contributors to the EFDA-JET Work Programme:* Confinement Properties of High Density Impurity Seeded ELMy H-Mode Discharges at Low and High Triangularity on JET. Plasma Physics and Controlled Fusion **44**, 1845-1862 (2002).

60. *Ehmler, H., R. Burhenn, J. Baldzuhn, A. Dinklage, L. Giannone, D. Hartmann, M. Kick, J.-P. Knauer, A. Kreter, K. McCormick, E. Pasch, T. Klinger, A. Weller and W7-AS Team:* Comparative Study of Intrinsic Edge Impurities in the W7-AS Stellarator during High Confinement Discharges In: Proceedings of the 29th EPS Conference on Plasma Physics and Controlled Fusion, Montreux 2002, (Eds.) R.Behn, C.Varandas. ECA 26B, European Physical Society, Geneva 2002, P-4.044.

61. *Ehmler, H., K. McCormick, E. Wolfrum, R. Burhenn, P. Grigull, T. Klinger and W7-AS Team:* Carbon Concentration in the Wendelstein 7-AS Stellarator Measured with the High-Energy Li Beam. Plasma Physics and Controlled Fusion **44,** 1411-1422 (2002).

62. *Ehmler, H., A. Rehmet*, K. Rätzke* and F. Faupel*:* Limits of Ion-Beam Depth-Profiling as Used in Diffusion Studies on Oxidation-Sensitive Materials. Defect Diffusion Forum **203** (2), 147-152 (2002).

63. *Endler, M., M. Bruchhausen*, J. Bleuel*, M. Schubert and W7-AS Team:* The Impact of Magnetic Shear on the Spatial Structure of Edge Fluctuations in Wendelstein 7-AS. Stellarator News **83**, 1-4 (2002).

64. *Endler, M., S. Davies*, I. García-Cortés*, G.F. Matthews*, ASDEX Upgrade Team and JET Team:* The Fine Structure of ELMs. In: Proceedings of the 29th EPS Conference on Plasma Physics and Controlled Fusion, Montreux 2002, (Eds.) R.Behn, C.Varandas. ECA 26B, European Physical Society, Geneva 2002, O-3.24.

65. *Fantz, U., S. Meir and M. Berger*:* Optical Diagnostics of Molecular Carbon Densities in Methane Plasmas and their Correlation with Higher Hydrocarbons. In: Proceedings of the 16th ESCAMPIG and 5th ICRP Joint Conference, Grenoble 2002, (Eds.) N.Sadeghi, H.Sugai. European Physical Society, Geneva 2002, 123-127.

66. *Feist, J.-H. and W7-X Construction Team:* Status of Wendelstein 7-X Construction. In: Proceedings of the 19th IEEE/ NPSS Symposium on Fusion Engineering, Atlantic City,NJ 2002, (Ed.) IEEE, Piscataway,NJ 2002, 264-267.

67. *Feneberg, W. and H. Weitzner*:* Electrostatic Potential and Plasma Flow near the Edge of a Divertor Tokamak. Physics of Plasmas **9**, 1036-1038 (2002).

68. *Feng, Y., F. Sardei, P. Grigull, K. McCormick, J. Kisslinger, L. Giannone, D. Reiter* and Y. Igitkhanov:* Transport Study on the W7-AS Island Divertor. Physics, Modelling and Comparison to Experiment. In: Proceedings of the 29th EPS Conference on Plasma Physics and Controlled Fusion, Montreux 2002, (Eds.) R.Behn, C.Varandas. ECA 26B, European Physical Society, Geneva 2002, O-1.06.

69. *Feng, Y., F. Sardei, P. Grigull, K. McCormick, J. Kisslinger, D. Reiter* and Y. Igitkhanov:* Transport in Island Divertors: Physics, 3D Modelling and Comparison to First Experiments on W7-AS. Plasma Physics and Controlled Fusion **44**, 611-625 (2002).

70. *Feng, Y., F. Sardei, J. Kisslinger, D. Reiter* and Y. Igitkhanov:* Island Divertor Transport Modelling and Comparison with Experiment. Contributions to Plasma Physics **42**, 187-192 (2002).

71. *Fischer, R.:* Depth Profiles and Resolution Limits in Accelerator-Based Solid State Analysis. Analytical and Bioanalytical Chemistry **374**, 619-625 (2002).

72. *Fischer, R. and V. Dose:* Physical Mixture Modeling with Unknown Number of Components. In: Proceedings of the 21st International Workshop on Bayesian Inference and Maximum Entropy Methods in Science and Engineering, Baltimore,MD 2001, (Ed.) R.L.Fry. AIP Conference Proceedings 617, AIP Press, Melville,NY 2002, 143-154.

73. *Fischer, R., C. Wendland, A. Dinklage, S. Gori, V. Dose and W7-AS Team:* Thomson Scattering Analysis with the Bayesian Probability Theory. Plasma Physics and Controlled Fusion **44**, 1501-1519 (2002).

74. *Franck, C.M., O. Grulke and T. Klinger:* Magnetic Fluctuation Probe Design and Capacitive Pickup Rejection. Review of Scientific Instruments **73**, 3768-3771 (2002).

75. *Franck, C.M., O. Grulke and T. Klinger:* Transition from Unbounded to Bounded Plasma Whistler Wave Dispersion. Physics of Plasmas **9**, 3254-3258 (2002).

76. *Fuchs, J.C., J. Gafert, A. Herrmann, F. Mast and ASDEX Upgrade Team:* Detailed Investigation of the Divertor Radiation in ASDEX Upgrade. In: Proceedings of the 29th EPS Conference on Plasma Physics and Controlled Fusion, Montreux 2002, (Eds.) R.Behn, C.Varandas. ECA 26B. European Physical Society, Geneva 2002, P-1.047.

77. *Fundamenski*, W., S. Sipilä*, G.F. Matthews*, V. Riccardo*, P. Andrew*, T. Eich, L.C. Ingesson*, T.P. Kiviniemi*, T. Kurki-Suonio*, V. Philipps* and Contributors to the EFDA-JET Work Programme:* Interpretation of Recent Power Width Measurements in JET MkIIGB ELMy H-Modes. Plasma Physics and Controlled Fusion **44**, 761-794 (2002).

78. *Gadelmeier, F., P. Grigull, K. McCormick, R. Brakel, R. Burhenn, H. Ehmler, Y. Feng, L. Giannone, D. Hartmann, D. Hildebrandt, R. Jaenicke, J. Kisslinger, T. Klinger, J.-P. Knauer, R. König, D. Naujoks, E. Pasch, F. Sardei, F. Wagner, U. Wenzel, A. Werner and W7-AS Team:* Island Divertor Experiments on the W7-AS Stellarator. In: Proceedings of the 29th EPS Conference on Plasma Physics and Controlled Fusion, Montreux 2002, (Eds.) R.Behn, C.Varandas. ECA 26B, European Physical Society, Geneva 2002, P-3.212.

79. *Gafert, J., J.C. Fuchs and ASDEX Upgrade Team:* Determination of 2D-Emissivity-Distributions from a Digital 12-Bit-CCD-System Viewing the Divertor of ASDEX Upgrade Tangentially and Poloidally. In: Proceedings of the 29th EPS Conference on Plasma Physics and Controlled Fusion, Montreux 2002, (Eds.) R.Behn, C.Varandas. ECA 26B. European Physical Society, Geneva 2002, P-1.123.

80. *Gantenbein*, G., F. Hollmann*, W. Kasparek*, B. Plaum*, E. Filipovic*, D. Wagner, A.V. Chirkov*, G.G. Denisov* and S.V. Kuzikov*:* Performance of a Remote Steering Antenna for ECRH/ECCD Applications Using 4-Wall Corrugated Sqare Wave-guide. In: Proceedings of the 12th Joint Workshop on Electron Cyclotron Emission and Electron Cyclotron Heating, Aix-en-Provence 2002, 481-487.

81. *Gantenbein*, G., A. Keller, F. Leuterer, M. Maraschek, W. Suttrop, H. Zohm and ASDEX Upgrade Team:* On the Stabilisation of Neoclassical Tearing Modes with ECRH at High β_N ASDEX Upgrade. In: Proceedings of the 29th EPS Conference on Plasma Physics and Controlled Fusion, Montreux 2002, (Eds.) R.Behn, C.Varandas. ECA 26B. European Physical Society, Geneva 2002, P-1.036.

82. *García-Rosales*, C., N. Ordás*, E. Oyarzabal, J. Echeberria*, M. Balden, S. Lindig and R. Behrisch:* Improvement of the Thermo-Mechanical Properties of Fine Grain Graphite by Doping with Different Carbides. Journal of Nuclear Materials **307-311**, 1282-1288 (2002).

83. *Gavrilin*, A.V., J.R. Miller*, F. Schauer and S.W. Van Sciver*:* Comparative Analysis of Design Options for Current Leads for Wendelstein 7-X Magnet System. IEEE Transactions on Applied Superconductivity **12**, 1301-1304 (2002).

84. *Geier A., H. Maier, R. Neu, K. Krieger and ASDEX Upgrade Team:* Determination of the Tungsten Divertor Retention at ASDEX Upgrade Using a Sublimation Probe. Plasma Physics and Controlled Fusion **44**, 2091-2100 (2002).

85. *Geier, A., R. Neu, R. Dux, V. Rohde, R. Pugno, K. Krieger, H. Maier and ASDEX Upgrade Team:* Operation of ASDEX Upgrade with a Fully Tungsten Coated Central Column - Results from Experiments and Modeling. In: Proceedings of the 29th EPS Conference on Plasma Physics and Controlled Fusion, Montreux 2002, (Eds.) R.Behn, C.Varandas. ECA 26B, European Physical Society, Geneva 2002, P-2.048.

86. *Geiger, J.:* HINT Equilibrium Calculations for W7-AS. In: Proceedings of the 29th EPS Conference on Plasma Physics and Controlled Fusion, Montreux 2002, (Eds.) R.Behn, C.Varandas. ECA 26B, European Physical Society, Geneva 2002, P-5.035.

87. *Giannone, L., R. Burhenn, P. Grigull, K. McCormick and W7-AS Team:* Density Limit Studies with a Divertor in the W7-AS Stellarator. In: Proceedings of the 13th International Stellarator Workshop, Canberra 2002, PPPL, Princeton,NJ 2002, PIIA2.

88. *Giannone, L., R. Burhenn, K. McCormick, R. Brakel, Y. Feng, P. Grigull, Y. Igitkhanov, NBI Team, ECRH Team and W7-AS Team:* Radiation Power Profiles and Density Limit with a Divertor in the W7-AS Stellarator. Plasma Physics and Controlled Fusion **44**, 2149-2165 (2002).

89. *Giannone, L., K. McCormick, J. Baldzuhn, R. Brakel, R. Burhenn, H. Ehmler, Y. Feng, P. Grigull, J. Knauer, E. Pasch, R. Narayanan, N. Rust and W7-AS Team:* Bolometer Tomography and Density Limit of the High Density H-Mode in the W7-AS Stellarator. In: Proceedings of the 29th EPS Conference on Plasma Physics and Controlled Fusion, Montreux 2002, (Eds.) R.Behn, C.Varandas. ECA 26B, European Physical Society, Geneva 2002, D-5.002.

90. *Golan*, A. and V. Dose:* Tomographic Reconstruction from Noisy Data. In: Proceedings of the 21st International Workshop on Bayesian Inference and Maximum Entropy Methods in Science and Engineering, Baltimore,MD 2001, (Ed.) R.L.Fry. AIP Conference Proceedings 617, AIP Press, Melville,NY 2002, 248-258.

91. *Gong, X., K. Krieger, J. Roth, H. Maier, R. Neu, V. Rohde and ASDEX Upgrade Team:* Erosion and Deposition of Tungsten as Plasma Facing Material at the Central Column Heat Shield of ASDEX Upgrade. In: Proceedings of the 29th EPS Conference on Plasma Physics and Controlled Fusion, Montreux 2002, (Eds.) R.Behn, C.Varandas. ECA 26B, European Physical Society, Geneva 2002, P-2.052.

92. *Grulke, O. and T. Klinger:* Large-Scale Fluctuation Structures in Plasma Turbulence. New Journal of Physics **4**, 67.1-67.23 (2002).

93. *Gude, A., S. Günter, P. Merkel, E. Schwarz, C. Tichmann and H.-P. Zehrfeld:* Temporal Evolution of Neoclassical Tearing Modes and its Effect on Confinement Reduction in ASDEX Upgrade. Nuclear Fusion **42**, 833-840 (2002).

94. *Hamacher, T.:* Nuclear Fusion: A Possible Vision of the Future. In: Proceedings of the Power-Gen Europe, Milano 2002, Pennwell Corp., London 2002, 19 pp.

95. *Harmeyer, E., J. Kisslinger, A. Wieczorek* and H. Wobig:* Superconducting Coil System for a Stellarator Fusion Reactor. IEEE Transactions on Applied Superconductivity **12**, 558-561 (2002).

96. *Harmeyer, E. and A. Wieczorek*:* Computer Simulations of the Protection System for the Stellarator Fusion Reactor Superconducting Coils. In: Proceedings of the ANSOFT Workshop, Chemnitz 2002, Ed. ANSOFT GmbH, Chemnitz 2002, 27-38.

97. *Hartfuß, H.-J. and W7-X Diagnostics Team:* Diagnostics for the W7-X Stellarator. In: Advanced Diagnostics for Magnetic and Inertial Fusion, (Eds.) P.E.Stott, A.Wooton. Kluwer, New York,NY 2002, 371-374.

98. *Hatzky, R., T.M. Tran*, A. Könies, R. Kleiber and S.J. Allfrey*:* Energy Conservation in a Nonlinear Gyrokinetic Particle-in-Cell Code for Ion-Temperature-Gradient-Driven (ITG) Modes in θ-Pinch Geometry. Physics of Plasmas **9**, 898-912 (2002).

99. *Hawkes*, N.C., Y. Andrew*, C.D. Challis*, R. DeAngelis*, V. Drozdov*, J. Hobirk, E. Joffrin*, P. Lotte*, D. Mazon*, E. Rachlew*, S. Reyes-Cortes*, F. Sattin*, E. Solano*, B.C. Stratton*, T. Tala*, M. Valisa* and Contributors to the EFDA-JET Work Programme:* The Formation and Evolution of Extreme Shear Reversal in JET and its Influence on Local Thermal Transport. Plasma Physics and Controlled Fusion **44**, 1105-1125 (2002).

100. *Hergenhahn, U., A. Kolmakov*, M. Riedler*, A.R.B. de Castro*, O. Löfken* and T. Möller*:* Observation of Excitonic Satellites in the Photoelectron Spectra of Ne and Ar Clusters. Chemical Physics Letters **351**, 235-241 (2002).

101. *Hergenhahn, U., O. Kugeler, E.E. Rennie, A. Rüdel* and S. Marburger*:* Vibrational Excitation in the C 1s-Ionized Ethane. Surface Reviews and Letters **9**, 13-19 (2002).

102. *Herrmann, A.:* Overview on Stationary and Transient Divertor Heat Loads. Plasma Physics and Controlled Fusion **44**, 883-903 (2002).

103. *Hildebrandt, D., M. Laux, J. Sachtleben, J. Boscary, H. Grote, H.-D. Reiner and Divertor Team of W7-X:* Design and Operational Diagnostics of the W7-X Divertor. In: Proceedings of the 13th International Stellarator Workshop, Canberra 2002, PPPL, Princeton,NJ 2002, PII B.10.

104. *Hobirk, J., N.C. Hawkes*, P.J. McCarthy, D. Merkl, R. Wolf, ASDEX Upgrade Team and Contributors to the EFDA-JET Workprogramme:* Measurements of the Poloidal Magnetic and Radial Electric Field Profiles in ASDEX Upgrade and JET. In: Advanced Diagnostics for Magnetic and Inertial Fusion, (Eds.) P.E.Stott, A.Wooton. Kluwer, New York,NY 2002, 197-204.

105. *Hogeweij*, G.M.D., Yu. Baranov*, G.D. Conway, S.R. Cortes*, M. De Baar*, N.C. Hawkes*, F. Imbeaux*, X. Litaudon*, J. Mailloux*, F.G. Rimini*, S. Sharapov*, B.C. Stratton*, K.-D. Zastrow* and Contributors to the EFDA-JET Work Programme:* Electron Heated Internal Transport Barriers in JET. Plasma Physics and Controlled Fusion **44**, 1155-1165 (2002).

106. *Hopf, C., A. von Keudell and W. Jacob:* Chemical Sputtering of Hydrocarbon Films by Low-Energy Ar^+ Ion and H Atom Impact. Nuclear Fusion **42**, L27-L30 (2002).

107. *Horton, L.D., J.C. Fuchs, S. Günter, M. Jakobi, B. Kurzan, P.J. McCarthy, H. Murmann, J. Neuhauser, S.D. Pinches, S. Saarelma*, J. Stober, W. Suttrop and ASDEX Upgrade Team:* Pedestal Physics at ASDEX Upgrade. In: Proceedings of the 29th EPS Conference on Plasma Physics and Controlled Fusion, Montreux 2002, (Eds.) R.Behn, C.Varandas. ECA 26B. European Physical Society, Geneva 2002, P-2.047.

108. *Horton, L.D., T. Hatae*, A. Hubbard*, G. Janeschitz*, Y. Kamada*, B. Kurzan, L. Lao*, P.J. McCarthy, D. Mossessian*, T.H. Osborne*, S.D. Pinches, S. Saarelma*, M. Sugihara*, W. Suttrop, K. Thomsen* and H. Urano*:* Dependence of H-Mode Pedestal Parameters on Plasma Magnetic Geometry. Plasma Physics and Controlled Fusion **44**, A273-A278 (2002).

109. *Idehara*, T., I. Ogawa*, S. Maeda*, R. Pavlichenko*, S. Mitsudo*, D. Wagner and M. Thumm*:* Observation of Mode Patterns for High Purity Mode Operation in the Submillimeter Wave Gyrotron. International Journal of Infrared and Millimeter Waves **23**, 973-980 (2002).

110. *Igitkhanov, Y., O.P. Pogutse*, H.R. Wilson*, J.W. Connor*, H. Wobig, P.Grigull, M. Hirsch, G. Janeschitz*, M. Sugihara*, A. Loarte*, G. Saibene*, R. Sartori*, G. Pacher* and H.D. Pacher*:* A Physics Picture of Type I ELMs. Contributions to Plasma Physics. **42**, 272-276 (2002).

111. *Igitkhanov, Y., Y. Turkin, H. Wobig, T. Andreeva, C.D. Beidler, F. Castejon*, J. Geiger, J. Kisslinger, H. Maaßberg, D.R. Mikkelsen* and K. Yamazaki*:* 1-D Predictive and Analysis Transport Model for Particle and Energy Transport in Stellarators. In: Proceedings of the 13th International Stellarator Workshop, Canberra 2002, PPPL, Princeton,NJ 2002, OIV.3.

112. *Igitkhanov, Y., H. Wobig, L. Giannone, K. McCormick, D. Morozov*, J. Herrera*, A. Loarte* and O. Shishkin*:* Impurity Shielding Effect in an H-Mode Rotating Plasma. In: Proceedings of the 29th EPS Conference on Plasma Physics and Controlled Fusion, Montreux 2002, (Eds.) R.Behn, C.Varandas. ECA 26B, European Physical Society, Geneva 2002, P-1.106.

113. *Jachmich*, S., G. Maddison*, M. Beurskens*, P. Dumortier*, T. Eich, A. Messiaen*, M.F.F. Nave*, J. Ongena*, J. Rapp*, J. Strachan*, M. Stamp*, G. Telesca*, B. Unterberg* and Contributors to the EFDA-JET Work Programme:* Seeding of Impurities in JET H-Mode Discharges to Mitigate the Impact of ELMs. Plasma Physics and Controlled Fusion **44**, 1879-1891 (2002).

114. *Jaenicke, R., S. Bäumel, J. Baldzuhn, R. Brakel, R. Burhenn, H. Ehmler, M. Endler, V. Erckmann, Y. Feng, F. Gadelmeier, J. Geiger, L. Giannone, P. Grigull, H.-J. Hartfuß, D. Hartmann, D. Hildebrandt, M. Hirsch, E. Holzhauer, M. Kick, J. Kisslinger, T. Klinger, S. Klose, J. Knauer, R. König, G. Kühner, H. Laqua, H. Maaßberg, K. McCormick, R. Narayanan, H. Niedermeyer, W. Ott, E. Pasch, N. Ruhs, N. Rust, J. Saffert, F. Sardei, F. Schneider, M. Schubert, E. Speth, F. Volpe*, F. Wagner, A. Weller,U. Wenzel, A. Werner, E. Würsching:* Overview on Recent W7-AS Results. In: Proceedings of the 13th International Stellarator Workshop, Canberra 2002, PPPL, Princeton,NJ 2002, OI.6

115. *Jaenicke, R., S. Bäumel, J. Baldzuhn, R. Brakel, R. Burhenn, H. Ehmler, M. Endler, V. Erckmann, Y. Feng, F. Gadelmeier, J. Geiger, L. Giannone, P. Grigull, H.-J. Hartfuß, D. Hartmann, D. Hildebrandt, M. Hirsch, E. Holzhauer, M. Kick, J. Kisslinger, T. Klinger, S. Klose, J. Knauer, R. König, G. Kühner, H. Laqua, H. Maaßberg, K. McCormick, R. Narayanan, H. Niedermeyer, E. Pasch, N. Ruhs, N. Rust, J. Saffert, F. Sardei, F. Schneider, M. Schubert, E. Speth, F. Wagner, A. Weller, U. Wenzel, A. Werner and E. Würsching:* A New Quasi-Stationary, Very High Density Plasma Regime on the W7-AS Stellarator. Plasma Physics and Controlled Fusion **44**, B193-B205 (2002).

116. *Jakobi, M., B. Kurzan, H. Murmann, J. Neuhauser and ASDEX Upgrade Team:* Measurement of Electron Temperature and Density of Intermittent Plasma Objects by Thomson Scattering in ASDEX Upgrade. In: Proceedings of the 29th EPS Conference on Plasma Physics and Controlled Fusion, Montreux 2002, (Eds.) R.Behn, C.Varandas. ECA 26B. European Physical Society, Geneva 2002, P-1.122.

117. *Jenko, F. and W. Dorland*:* Prediction of Significant Tokamak Turbulence at Electron Cyroradius Scales. Physical Review Letters **89**, 225001 (2002).

118. *Jenko, F. and A. Kendl:* Radial and Zonal Modes in Hyperfine-Scale Stellarator Turbulence. Physics of Plasmas **9**, 4103-4106 (2002).

119. *Jenko, F. and A. Kendl:* Stellarator Turbulence at Electron Gyroradius Scales. New Journal of Physics **4**, 35.1-35.12 (2002).

120. *Joffrin*, E., R. Wolf, B. Alper*, Yu. Baranov*, C.D. Challis*, M. De Baar*, C. Giroud*, C. Gowers*, N.C. Hawkes*, T.C. Hender*, M. Maraschek, D. Mazon*, V. Parail*, A.G. Peeters, K.-D. Zastrow* and Contributors to the EFDA-JET Work Programme:* q = 1 Advanced Tokamak Experiments in JET and Comparison with ASDEX Upgrade. Plasma Physics and Controlled Fusion **44**, 1203-1214 (2002).

121. *Kallenbach, A., Y. Andrew*, M. Beurskens*, G. Corrigan*, T. Eich, K. Erents*, W. Fundamenski*, J. Gafert, A. Korotkov*, G.F. Matthews*, T. Pütterich*, M. Stamp* and Contributors to the EFDA-JET Work Programme:* Edge Transport Analysis of JET H-Mode Discharges and the Possible Influence of Radial Drift Velocities. In: Proceedings of the 29th EPS Conference on Plasma Physics and Controlled Fusion, Montreux 2002, (Eds.) R.Behn, C.Varandas. ECA 26B. European Physical Society, Geneva 2002, O-3.22.

122. *Kallenbach, A., M. Beurskens*, A. Korotkov*, P.J. Lomas*, W. Suttrop, M. Charlet*, D.C. McDonald*, F. Milani*, J. Rapp*, M. Stamp*, Contributors to the EFDA-JET Work Programme and ASDEX Upgrade Team:* Scaling of the Pedestal Density in Type-I ELMy H-Mode Discharges and the Impact of Upper and Lower Triangularity in JET and ASDEX Upgrade. Nuclear Fusion **42**, 1184-1192 (2002).

123. *Kang, H.D., R. Preuss, T. Schwarz-Selinger and V. Dose:* Decomposition of Multicomponent Mass Spectra Using Bayesian Probability Theory. Journal of Mass Spectrometry **37**, 748-754 (2002).

124. *Kardaun, O.:* On Estimating the Epistemic Probability of Realizing $Q = P_{fus}/P_{aux}$ Larger than a Specified Lower Bound in ITER. Nuclear Fusion **42**, 841-852 (2002).

125. *Kasilov*, S.V., D. Reiter*, A.M. Runov, W. Kernbichler* and M.F. Heyn*:* On the 'Magnetic' Nature of Electron Transport Barriers in Tokamaks. Plasma Physics and Controlled Fusion, **44**, 985-1004 (2002).

126. *Kausch*, C., B. Sandow*, M. Bessenrodt-Weberpals and S. Bargstädt-Franke*:* The Status of Women in Physics in Germany. In: Proceedings of the IUPAP International Coference on Women in Physics, Paris 2002, (Eds.) B.K. Hartline, D.Li. AIP Conference Proceedings 628, AIP Press, Melville,NY 2002, 163-164.

127. *Kendl, A.:* Turbulent Times in Fusion Research. Science's Next Wave: Careers in Energy Science. 2002. http://nextwave.sciencemag.org/cgi/content/full/2002/01/02/3.

128. *Keudell, A. von:* Formation of Polymer-Like Hydrocarbon Films from Radical Beams of Methyl and Atomic Hydrogen. Invited Review. Thin Solid Films **402**, 1-37 (2002).

129. *Keudell, A. von and J.R. Abelson*:* Advantages of the "Optical Cavity Substrate" for Real Time Infrared Spectroscopy of Plasma-Surface Interactions. Journal of Applied Physics **91**, 4840-4845 (2002).

130. *Keudell, A. von, M. Meier and C. Hopf:* Growth Mechanism of Amorphous Hydrogenated Carbon. Diamond and Related Materials **11**, 969-975 (2002).

131. *Kirov, K., F. Leuterer, G. Pereverzev, F. Ryter, W. Suttrop and ASDEX Upgrade Team:* ECRH Power Deposition Studies in ASDEX Upgrade. Plasma Physics and Controlled Fusion **44**, 2583-2602 (2002).

132. *Kirov, K., F. Leuterer, G. Pereverzev, F. Ryter, W. Suttrop and ASDEX Upgrade Team:* ECRH Power Deposition Studies in ASDEX Upgrade. In: Proceedings of the 29th EPS Conference on Plasma Physics and Controlled Fusion, Montreux 2002, (Eds.) R.Behn, C.Varandas. ECA 26B, European Physical Society, Geneva 2002, P-2.046.

133. *Kiviniemi*, T.P., J.A. Heikkinen* and A.G. Peeters:* Neoclassical Radial Electric Field and Ion Heat Flux in the Presence of the Transport Barrier. Contributions to Plasma Physics **42**, 236-240 (2002).

134. *Klinger, T., F. Greiner and A. Piel:* Bifurcations in Simple Plasma Diodes. In: Bifurcation Phenomena in Plasmas, (Eds.) S.-I.Itoh, Y.Kawai. Hyushu University Press, Hyushu 2002, 57-77.

135. *Klose, S., A. Weller, J. Geiger, A. Werner and W7-AS Team:* Asymmetries of Impurity Radiation in the W7-AS Observed with Soft-X-Ray Tomography. In: Proceedings of the 29th EPS Conference on Plasma Physics and Controlled Fusion, Montreux 2002, (Eds.) R.Behn, C.Varandas. ECA 26B, European Physical Society, Geneva 2002, P-5.032.

136. *Klose, S., A. Weller, P. Schötz*, A. Werner and H. Greve:* X-Ray Multi Camera Tomography System of Wendelstein 7-X. In: Advanced Diagnostics for Magnetic and Inertial Fusion, (Eds.) P.E.Stott, A.Wooton. Kluwer, New York,NY 2002, 229-232.

137. *Kolesnichenko, Ya.I., V.V. Lutsenko*, H. Wobig and Yu.V. Yakovenko*:* Alfvén Eigenmodes and their Stabilization by Energetic Circulating Ions in the Wendelstein-Line Stellarators. Nuclear Fusion **42**, 949-958 (2002).

138. *Kolesnichenko, Ya.I., V.V. Lutsenko*, H. Wobig and Yu.V. Yakovenko*:* Alfvén Instabilities Driven by Circulating Ions in Optimized Stellarators and their Possible Consequences in a Helias Reactor. Physics of Plasmas **9**, 517-528 (2002).

139. *König, R., P. Grigull, K. McCormick, N. Ohyabu*, T. Obiki*, A. Komori*, K. Matsuoka*, S. Masuzaki*, H. Renner, F. Wagner, Y. Feng, F. Sardei, J. Kisslinger and A. Werner:* The Divertor Program in Stellarators. Plasma Physics and Controlled Fusion **44**, 2365-2422 (2002).

140. *Korotkov*, A., K. McCormick, P.D. Morgan*, J. Schweinzer, J. Vince* and Contributors to the EFDA-JET Workprogramme:* Line Ratio Method for Poloidal Magnetic Field Measurement Using Li-Multiplet (2^2S-2^2P) Emission. In: Advanced Diagnostics for Magnetic and Inertial Fusion, (Eds.) P.E.Stott, A.Wooton. Kluwer, New York,NY 2002, 209-212.

141. *Kraus, W., P. McNeely, E. Speth, B. Heinemann, O. Vollmer and R. Wilhelm:* Development of Large Radio Frequency Negative-Ion Sources for Nuclear Fusion. Review of Scientific Instruments **73**, 1096-1098 (2002).

142. *Kreter, A., J. Baldzuhn, H. Ehmler, M. Hirsch, M. Kick, A. Kislyakov*, H. Maaßberg and W7-AS Team:* Optimised Confinement Discharges with High Ion Temperatures after Installation of the Island Divertor in W7-AS. In: Proceedings of the 29th EPS Conference on Plasma Physics and Controlled Fusion, Montreux 2002, (Eds.) R.Behn, C.Varandas. ECA 26B, European Physical Society, Geneva 2002, P-5.033.

143. *Krieger, K., X. Gong, M. Balden, D. Hildebrandt, H. Maier, V. Rohde, J. Roth, W. Schneider and ASDEX Upgrade Team:* Erosion and Migration of Tungsten Employed at the Central Column Heat Shield of ASDEX Upgrade. Journal of Nuclear Materials **307-311**, 139-143 (2002).

144. *Kröger*, J., S. Lehwald*, M. Balden and H. Ibach*:* Anomalous Dispersion of Adsorbate Phonons of Mo(110)-H. Physical Review B **66**, 073414 (2002).

145. *Kukushkin*, A.S., H.D. Pacher*, G. Janeschitz*, A. Loarte*, D.P. Coster, G.F. Matthews*, D. Reiter*, R. Schneider and V. Zhogolev*:* Basic Divertor Operation in ITER-FEAT. Nuclear Fusion **42**, 187-191 (2002).

146. *Kuntze*, M., G. Dammertz*, S. Illy*, W. Leonhardt*, B. Piosczyk*, M. Schmid*, S. Alberti*, M.Q. Tran*, M. Thumm*, E. Giguet*, Y. Legoff*, V. Erckmann, G. Michel, W. Kasparek* and G. Moller*:* Advanced High Power Gyrotrons. In: Proceedings of the 28th International Conference on Plasma Science and the 13th International Pulsed Power Conference, Las Vegas,NV 2001, (Ed.) R. Reinovsky. IEEE, Piscataway,NJ 2002, 508-511.

147. *Kurki-Suonio*, T., J.A. Heikkinen*, T.P. Kiviniemi* and J. Stober:* Monte Carlo Simulations of Edge Ion Temperature Profile in ASDEX Upgrade. Contributions to Plasma Physics **42**, 224-229 (2002).

148. *Kurki-Suonio*, T., J.A. Heikkinen*, S. Sipilä*, H.-U. Fahrbach, J. Neuhauser, J. Stober and ASDEX Upgrade Team:* Monte Carlo Simulations of Edge Ion Distribution and NPA Fluxes in ASDEX Upgrade. In: Proceedings of the 29th EPS Conference on Plasma Physics and Controlled Fusion, Montreux 2002, (Eds.) R.Behn, C.Varandas. ECA 26B. European Physical Society, Geneva 2002, P-2.049.

149. *Kurki-Suonio*, T., S. Sipilä*, J.A. Heikkinen*, H.-U. Fahrbach, A. Khudoleev and ASDEX Upgrade Team:* Monte Carlo Simulations of Central Ion Temperature Measurements Using Neutral Particle Analysers. Plasma Physics and Controlled Fusion **44**, 475-491 (2002).

150. *Kurzan, B., H. Murmann, D. Bolshukhin, M. Jakobi and ASDEX Upgrade Team:* Determination of the Electron Density and Mean Energy for Anisotropic Velocity Distributions by Thomson Scattering. In: Advanced Diagnostics for Magnetic and Inertial Fusion, (Eds.) P.E.Stott, A.Wooton. Kluwer, New York,NY 2002, 327-330.

151. *La Haye*, R.J., S. Günter, D.A. Humphreys*, J. Lohr*, T.C. Luce*, M. Maraschek, C.C. Petty*, R. Prater*, J.T. Scovilli* and E.J. Strait*:* Control of Neoclassical Tearing Modes in DIII-D. Physics of Plasmas **9**, 2051-2260 (2002).

152. *Lang, P.T., B. Alper*, L.R. Baylor*, M. Beurskens*, J.G. Cordey*, R. Dux, R. Felton*, L. Garzotti*, G. Haas, L.D. Horton, S. Jachmich*, T.T.C. Jones*, P.J. Lomas*, A. Lorenz, M. Maraschek, H.W. Müller, J. Ongena*, J. Rapp*, M. Reich, K.F. Renk*, R. Sartori*, G. Schmidt*, M. Stamp*, W. Suttrop, E. Villedieu* and EFDA-JET Work Programme Collaborators:* Optimization of Pellet Scenarios for Long Pulse Fuelling to High Densities at JET. Nuclear Fusion **42**, 388-402 (2002).

153. *Lang, P.T., B. Alper*, L.R. Baylor*, M. Beurskens*, J.G. Cordey*, R. Dux, R. Felton*, L. Garzotti*, G. Haas, L.D. Horton, S. Jachmich*, T.T.C. Jones*, A. Lorenz, P.J. Lomas*, M. Maraschek, H.W. Müller, J. Ongena*, J. Rapp*, K.F. Renk*, M. Reich, R. Sartori*, G. Schmidt*, M. Stamp*, W. Suttrop, E. Villedieu*, D. Wilson* and Contributors to the EFDA-JET Work Programme:* High Density Operation at JET by Pellet Refuelling. Plasma Physics and Controlled Fusion **44**, 1919-1928 (2002).

154. *Lang, P.T., M. Reich, R. Dux, T. Eich, L. Fattorini*, J.C. Fuchs, O. Gehre, J. Gafert, A. Herrmann, M. Jakobi, M. Kaufmann, S. Kalvin*, G. Kocsis*, B. Kurzan, M. Manso*, V. Mertens, H.W. Müller, H. Murmann, J. Neuhauser, I. Nunes*, D. Reich*, K.F. Renk*, W. Sandmann, J. Stober, U. Vogl and ASDEX Upgrade Team:* Advanced High Field Side Pellet Refuelling and Mitigation of ELM Effects in ASDEX Upgrade. In: Proceedings of the 29th EPS Conference on Plasma Physics and Controlled Fusion, Montreux 2002, (Eds.) R.Behn, C.Varandas. ECA 26B. European Physical Society, Geneva 2002, P-1.044.

155. *Laqua, H., H. Niedermeyer and I. Willmann*:* Ethernet-Based Real-Time Control Data Bus. IEEE Transactions on Nuclear Science **49**, 478-482 (2002).

156. *Laqua, H.P., V. Erckmann, F. Volpe*, H. Maaßberg, W7-AS Team and ECRH Group:* Electron Bernstein Wave Heating and Current Drive in Overdense Plasmas at the Wendelstein 7-AS Stellarator. In: Proceedings of the 29th EPS Conference on Plasma Physics and Controlled Fusion, Montreux 2002, (Eds.) R.Behn, C.Varandas. ECA 26B, European Physical Society, Geneva 2002, D-5.010.

157. *Laqua, H.P., V. Erckmann, F. Volpe*, H. Maaßberg, W7-AS Team and ECRH-Group:* Electron Bernstein Wave Heating and Current Drive in Overdense Plasmas at the Wendelstein 7-AS Stellarator. In: Proceedings of the 12th Joint Workshop on Electron Cyclotron Emission and Electron Cyclotron Resonance Heating, Aix-en-Provence 2002, 403-407.

158. *Laqua, H.P., V. Erckmann, F. Volpe*, W7-AS Team and ECRH Group:* Electron Bernstein Wave Heating and Current Drive in Over-dense Plasmas at the Wendelstein 7-AS Stellarator. In: Proceedings of the 13th International Stellarator Workshop, Canberra 2002, PPPL, Princeton,NJ 2002, OIV.3.

159. *Laux, M., W. Schneider, E. Hantzsche*, B. Jüttner*, H. Kostial* and P. Wienhold*:* Arcing through a Thick B_4C Layer. In: Proceedings of the 20th International Symposium on Discharges and Electrical Insulation in Vacuum, Tours 2002, Ed. Societé Française du Vide, Paris 2002, 630-633.

160. *Lederer, H.:* Der neue IBM-Hochleistungsrechner der MPG. In: 17. und 18. DV-Treffen der Max-Planck-Institute, (Eds.) H.Hayd, R.Kleinrensing, GWDG-Bericht 57, Gesellschaft für wissenschaftl. Datenverarbeitung mbH, Göttingen 2002, 31-40.

161. *Lederer, H.:* Wie die Flops laufen lernten. Max Planck Forschung **1**, 50-51 (2002).

162. *Letsch*, A., H. Zohm, F. Ryter, W. Suttrop, A. Gude, F. Porcelli*, C. Angioni* and I. Furno*:* Incomplete Reconnection in Sawtooth Crashes in ASDEX Upgrade. Nuclear Fusion **42**, 1055-1059 (2002).

163. *Leuterer, F., R. Dux, G. Gantenbein*, T.P. Goodman*, J. Hobirk, K. Kirov, H.R. Koslowski*, M. Maraschek, A. Mück, R. Neu, A.G. Peeters, F. Ryter, J. Stober, W. Suttrop, E. Westerhof*, H. Zohm, ECRH Team and ASDEX Upgrade Team:* Recent ECRH Results in ASDEX Upgrade. In: Proceedings of the 12th Joint Workshop on Electron Cyclotron Emission and Electron Cyclotron Heating, Aix-en-Provence 2002, 267-276.

164. *Litaudon*, X., F. Crisanti*, B. Alper*, J.F. Artaud*, Yu. Baranov*, E. Barbato*, V. Basiuk*, A. Becoulet*, M. Becoulet*, C. Castaldo*, C.D. Challis*, G.D. Conway, R. Dux, L.G. Eriksson*, B. Esposito*, C. Fourment*, D. Frigione*, X. Garbet*, C. Giroud*, N.C. Hawkes*, P. Hennequin*, G. Huysmans*, F. Imbeaux*, E. Joffrin*, P.J. Lomas*, P. Lotte*, P. Maget*, M. Mantsinen*, J. Mailloux*, D. Mazon*, F. Milani*, D. Moreau*, V. Parail*, E. Pohn*, F.G. Rimini*, Y. Sarazin*, G. Tresset*, K.-D. Zastrow*, M. Zerbini* and Contributors to the EFDA-JET Work Programme:* Towards Fully Non-Inductive Current Drive Operation in JET. Plasma Physics and Controlled Fusion **44**, 1057-1086 (2002).

165. *Loarte*, A., M. Becoulet*, G. Saibene*, R. Sartori*, D.J. Campbell*, T. Eich, A. Herrmann, M. Laux, W. Suttrop, B. Alper*, P.J. Lomas*, G.F. Matthews*, S. Jachmich*, J. Ongena*, P. Innocente* and EFDA-JET Work Programme Collaborators:* Characteristics and Scaling of Energy and Particle Losses during Type I ELMs in JET H-Modes. Plasma Physics and Controlled Fusion **44**, 1815-1844 (2002).

166. *Lorenzini*, R., P.T. Lang, G. Pereverzev, J. Stober and ASDEX Upgrade Team:* Particle Transport in ASDEX Upgrade Discharges Undergoing Strong Density Peaking. In: Proceedings of the 29th EPS Conference on Plasma Physics and Controlled Fusion, Montreux 2002, (Eds.) R.Behn, C.Varandas. ECA 26B. European Physical Society, Geneva 2002, P-1.041.

167. *Maddison*, G., J.A. Snipes*, J.M. Chareau*, G.D. Conway, I.H. Hutchinson*, L.C. Ingesson*, H.R. Koslowski*, A. Loarte*, P.J. Lomas*, M. Mantsinen*, G.F. Matthews*, L. Meneses*, M.F.F. Nave*, E. Righi*, G. Saibene*, R. Sartori*, O. Sauter*, K.-D. Zastrow* and Contributors to the EFDA-JET Work Programme:* ELM Moderation with ICRH Heating on JET. Plasma Physics and Controlled Fusion **44**, 1937-1952 (2002).

168. *Maggi, C., K. Borrass, J.C. Fuchs, L.D. Horton, V. Mertens and ASDEX Upgrade Team:* Isotope Effect on the L-Mode Density Limit in ASDEX Upgrade. In: Proceedings of the 29th EPS Conference on Plasma Physics and Controlled Fusion, Montreux 2002, (Eds.) R.Behn, C.Varandas. ECA 26B. European Physical Society, Geneva 2002, P-1.046.

169. *Maier, H., J. Luthin, M. Balden, S. Lindig, J. Linke*, V. Rohde, H. Bolt and ASDEX Upgrade Team:* Development of Tungsten Coated First Wall and High Heat Flux Components for Application in ASDEX Upgrade. Journal of Nuclear Materials **307-311**, 116-120 (2002).

170. *Mailloux*, J., B. Alper*, Yu. Baranov*, A. Becoulet*, A. Cardinali*, C. Castaldo*, R. Cesario*, G.D. Conway, C.D. Challis*, F. Crisanti*, M. De Baar*, P. de Vries*, A. Ekedahl*, K. Erents*, C. Gowers*, N.C. Hawkes*, G.M.D. Hogeweij*, F. Imbeaux*, E. Joffrin*, X. Litaudon*, P.J. Lomas*, G.F. Matthews*, D. Mazon*, V. Pericoli*, R. Prentice*, F.G. Rimini*, Y. Sarazin*, B.C. Stratton*, A.A. Tuccillo*, T. Tala*, K.-D. Zastrow* and Contributors to the EFDA-JET Work Programme:* Progress in Internal Transport Barrier Plasma with Lower Hybrid Current Drive and Heating in JET (Joint European Torus). Physics of Plasmas **9**, 2156-2164 (2002).

171. *Manini*, A., J.-M. Moret*, F. Ryter, A. Sushkov* and ASDEX Upgrade Team:* Interpretation of Plasma Dynamic Response to Additional Heating Power. In: Proceedings of the 29th EPS Conference on Plasma Physics and Controlled Fusion, Montreux 2002, (Eds.) R.Behn, C.Varandas. ECA 26B, European Physical Society, Geneva 2002, P-2.050.

172. *Mantica*, P., G. Gorini*, F. Imbeaux*, J. Kinsey*, Y. Sarazin*, R.V. Budny*, I. Coffey*, R. Dux, X. Garbet*, L. Garzotti*, L.C. Ingesson*, M. Kissick*, V. Parail*, C. Sozzi*, A. Walden* and Contributors to the EFDA-JET Work Programme:* Perturbative Transport Experiments in JET Low or Reverse Magnetic Shear Plasmas. Plasma Physics and Controlled Fusion **44**, 2185-2216 (2002).

173. *Mantsinen*, M., L.C. Ingesson*, T. Johnson*, V. Kiptily*, M.L. Mayoral*, S. Sharapov*, B. Alper*, L. Bertalot*, S. Conroy*, L.G. Eriksson*, T. Hellsten*, J.-M. Noterdaeme, S. Popovichev*, E. Righi* and A.A. Tuccillo*:* Controlling the Profile of Ion-Cyclotron-Resonant Ions in JET with the Wave-Induced Pinch Effect. Physical Review Letters **89**, 115004 (2002).

174. *Mantsinen*, M., M.L. Mayoral*, V. Kiptily*, S. Sharapov*, B. Alper*, A. Bickley*, M. De Baar*, L.G. Eriksson*, A. Gondhalekar*, T. Hellsten*, K. Lawson*, F. Nguyen*, J.-M. Noterdaeme, E. Righi*, A.A. Tuccillo* and M. Zerbini*:* Alpha Tail Production with Ion Cyclotron Resonance Heating of ^{4}He-Beam Ions in JET Plasmas. Physical Review Letters **88**, 105002 (2002).

175. Maras*chenko*, V.S., S. Günter and Ya.I. Kolesnichenko:* Nonideal Fishbone Instability. Physics of Plasmas **9**, 1065-1068 (2002).

176. *Marushchenko, N.B., H. Maaßberg, A. Dinklage, N. Rust and W7-AS Team:* High Power NBCD Analysis at W7-AS. In: Proceedings of the 29th EPS Conference on Plasma Physics and Controlled Fusion, Montreux 2002, (Eds.) R.Behn, C.Varandas. ECA 26B, European Physical Society, Geneva 2002, D-5.003.

177. *Mattioli*, M., M.E. Puiatti*, M. Valisa*, I. Coffey*, R. Dux, P. Monier-Garbet*, M.F.F. Nave*, J. Ongena*, M. Stamp*, J. Strachan*, M. von Hellermann* and Contributors to the EFDA-JET Work Programme:* Simulation of the Time Behaviour of Impurities in JET Ar-Seeded Discharges and its Relation with Sawteething. In: Proceedings of the 29th EPS Conference on Plasma Physics and Controlled Fusion, Montreux 2002, (Eds.) R.Behn, C.Varandas. ECA 26B. European Physical Society, Geneva 2002, P-2.042.

178. *Matyash, K., R. Schneider, A. Bergmann, W. Jacob, U. Fantz and P. Pecher*:* Modeling of ECR Methane Plasmas. Czechoslovak Journal of Physics **52**, Suppl. D, 515-521 (2002).

179. *Mayer, M.:* Ion Beam Analysis of Rough Thin Films. Nuclear Instruments and Methods in Physics Research B **194**, 177-186 (2002).

180. *Mayer, M.:* SIMNRA 5.0, Computerprogramm, als Shareware. IPP Garching 2002, http://www.ipp.mpg.de/~mam/.

181. *Mayer, M., J. Roth and K. Ertl:* Rutherford Backscattering Spectroscopy and Elastic Recoil Detection Analysis with Lithium Ions - The Better Alternative to Helium? Nuclear Instruments and Methods in Physics Research B **190**, 405-409, (2002).

182. *Mayoral*, M.L., E. Westerhof*, O. Sauter*, B. Alper*, R.J. Buttery*, M. De Baar*, T.C. Hender*, D.F. Howell*, M. Mantsinen*, A. Mück, M.F.F. Nave* and Contributors to the EFDA-JET Work Programme:* Neo-Classical Tearing Mode Control through Sawtooth Destabilisation in JET. In: Proceedings of the 29th EPS Conference on Plasma Physics and Controlled Fusion, Montreux 2002, (Eds.) R.Behn, C.Varandas. ECA 26B. European Physical Society, Geneva 2002, P-1.026.

183. *Mazon*, D., X. Litaudon*, D. Moreau*, M. Riva*, G. Tresset*, Yu. Baranov*, A. Becoulet*, J.M. Chareau*, F. Crisanti*, R. Dux, R. Felton*, E. Joffrin* and Contributors to the EFDA-JET Work Programme:* Real-Time Control of Internal Transport Barriers in JET. Plasma Physics and Controlled Fusion **44**, 1087-1104 (2002).

184. *McCarthy, P.J., M. Foley*, J. Hobirk, O. Kardaun and ASDEX Upgrade Team:* Fast Recovery of the q Profile on ASDEX Upgrade Using a Nonlinearly Optimized Function Parameterization Model. In: Proceedings of the 29th EPS Conference on Plasma Physics and Controlled Fusion, Montreux 2002, (Eds.) R.Behn, C.Varandas. ECA 26B. European Physical Society, Geneva 2002, P-1.125.

185. *McCormick, K., P. Grigull, R. Burhenn, R. Brakel, H. Ehmler, Y. Feng, F. Gadelmeier, L. Giannone, D. Hildebrandt, M. Hirsch, R. Jaenicke, J. Kisslinger, T. Klinger, S. Klose, J.-P. Knauer, R. König, G. Kühner, H.P. Laqua, R. Narayanan, D. Naujoks, H. Niedermeyer, E. Pasch, N. Rust, F. Sardei, F. Wagner, A. Weller, U. Wenzel and A. Werner:* New Advanced Operational Regime on the W7-AS Stellarator. Physical Review Letters **89**, 015001 (2002).

186. *McCormick, K., P. Grigull, R. Burhenn, R. Brakel, H. Ehmler, Y. Feng, F. Gadelmeier, L. Giannone, D. Hildebrandt, M. Hirsch, R. Jaenicke, J. Kisslinger, T. Klinger, S. Klose, J.-P. Knauer, R. König, G. Kühner, H.P. Laqua, R. Narayanan, D. Naujoks, H. Niedermeyer, E. Pasch, N. Rust, F. Sardei, F. Wagner, A. Weller, U. Wenzel and A. Werner:* Plasma Performance of Wendelstein 7-AS with the New Boundary-Island Divertor Modules. In: Proceedings of the 13th International

Stellarator Workshop, Canberra 2002, PPPL, Princeton,NJ 2002, OIV.4.

187. *McNeely, P., M. Bandyopadhyay, P. Franzen, B. Heinemann, C. Hu, W. Kraus, R. Riedl, E. Speth and R. Wilhelm:* Studies on the Extraction Region of the Type VI RF Driven H^- Ion Source. In: Proceedings of the 9th International Symposium on the Production and Neutralization of Negative Ions and Beams, Gif-sur-Yvette 2002, (Ed.) M.P.Stockli. AIP Conference Proceedings 639, AIP Press, Melville,NY 2002, 90-111.

188. *Meier, M. and A. von Keudell:* Temperature Dependence of the Sticking Coefficient of Methyl Radicals at Hydrocarbon Film Surfaces. Journal of Chemical Physics **116**, 5125-5136 (2002).

189. *Michel, G., V. Erckmann, F. Hollmann*, L. Jonitz, H.P. Laqua*, F. Purps, T. Schulz and ECRH Teams* at FZK and IPF:* Progress of the 10 MW ECRH System for W7-X. In: Proceedings of the 12th Joint Workshop on Electron Cyclotron Emission and Electron Cyclotron Resonance Heating, Aix-en-Provence 2002, 493-497.

190. *Mikhailov*, M.I., V.D. Shafranov*, A.A. Subbotin*, M.Yu. Isaev*, J. Nührenberg, R. Zille and W.A. Cooper*:* Improved Alpha-Particle Confinement in Stellarators with Poloidally Closed Contours of the Magnetic Field Strength. Nuclear Fusion **42**, L23-L26 (2002).

191. *Milch, I.:* Plasma mit Dreiecksquerschnitt. Auf Zukunftskurs: 10 Jahre Fusionsforschung mit ASDEX Upgrade. HGF Jahresheft 2002, 32-33 (2002).

192. *Mück, A., T.P. Goodman*, H.R. Koslowski*, F. Ryter, E. Westerhof*, H. Zohm and ASDEX Upgrade Team:* Sawtooth Tailoring Experiments with ECRH in ASDEX Upgrade. In: Proceedings of the 29th EPS Conference on Plasma Physics and Controlled Fusion, Montreux 2002, (Eds.) R.Behn, C.Varandas. ECA 26B. European Physical Society, Geneva 2002, P-1.037.

193. *Müller, H.W., V. Bobkov*, G. Haas, M. Jakobi, M. Laux, M. Maraschek, J. Neuhauser, M. Reich, V. Rohde, J. Schweinzer, E. Wolfrum and ASDEX Upgrade Team:* Profile and Transport Studies in the outer Scrape off Layer at ASDEX Upgrade. In: Proceedings of the 29th EPS Conference on Plasma Physics and Controlled Fusion, Montreux 2002, (Eds.) R.Behn, C.Varandas. ECA 26B. European Physical Society, Geneva 2002, O-2.06.

194. *Müller, H.W., R. Dux, M. Kaufmann, P.T. Lang, A. Lorenz, M. Maraschek, V. Mertens, J. Neuhauser and ASDEX Upgrade Team:* High β Plasmoid Formation, Drift and Striations during Pellet Ablation in ASDEX Upgrade. Nuclear Fusion **42**, 301-309 (2002).

195. *Müller, W.-C. and D. Carati*:* Dynamic Gradient-Diffusion Subgrid Models for Incompressible Magnetohydrodynamic Turbulence. Physics of Plasmas **9**, 824-834 (2002).

196. *Müller, W.-C. and D. Carati*:* Large-Eddy Simulation of Mag-netohydrodynamic Turbulence. Computer Physics Communications **147**, 544-547 (2002).

197. *Müller, W.-C., A. Zeiler and G.E. Morfill:* Direct Numerical Simulation of Yukawa Systems by Particle-in-Cell Methods. In: Dusty Plasmas in the New Millenium, (Eds.) R.Bharuthram, M.A.Hellberg, P.K.Shukla. AIP Conference Proceedings 649, AIP, Melville,NY 2002, 365-368.

198. *Murakami*, S., A. Wakasa*, H. Maaßberg, C.D. Beidler, H. Yamada*, K.Y. Watanabe* and LHD Experimental Group:* Neoclassical Transport Optimization of LHD. Nuclear Fusion **42**, L19-L22 (2002).

199. *Na, Y.-S., A.C.C. Sips, O. Gruber, J. Hobirk, G. Pereverzev and ASDEX Upgrade Team:* Transport in High Normalized Beta Discharges on ASDEX Upgrade. Plasma Physics and Controlled Fusion **44**, 1285-1297 (2002).

200. *Nagel, M. and F. Schauer:* Thermohydraulic Behavior of the Wendelstein 7-X Magnet System. IEEE Transactions on Applied Superconductivity **12**, 1537-1540 (2002).

201. *Nakamura, Y., G. Pautasso, O. Gruber and S.C. Jardin*:* Axisymmetric Disruption Dynamics Including Current Profile Changes in the ASDEX Upgrade Tokamak. Plasma Physics and Controlled Fusion **44**, 1471-1481 (2002).

202. *Narayanan, N., R. König, P. Grigull, K. McCormick, L. Giannone, Y. Feng, A. John, B. Schweer, M. Brix* and W7-AS Team:* Spectroscopic Characterization of W7-AS Island Divertor Plasmas. In: Proceedings of the 29th EPS Conference on Plasma Physics and Controlled Fusion, Montreux 2002, (Eds.) R.Behn, C.Varandas. ECA 26B, European Physical Society, Geneva 2002, P-5.034.

203. *Naujoks, D.:* Ion Confinement in a Linear Plasma Column. Contributions to Plasma Physics **42**, 356-361 (2002).

204. *Neu, R., R. Dux, A. Geier, A. Kallenbach, R. Pugno, V. Rohde, D. Bolshukhin, J.C. Fuchs, O. Gehre, O. Gruber, J. Hobirk, M. Kaufmann, K. Krieger, M. Laux, C. Maggi, H. Murmann, J. Neuhauser, F. Ryter, A.C.C. Sips, A. Stäbler, J. Stober, W. Suttrop, H. Zohm and ASDEX Upgrade Team:* Impurity Behaviour in the ASDEX Upgrade Divertor Tokamak with Large Area Tungsten Walls. Plasma Physics and Controlled Fusion **44**, 811-826 (2002).

205. *Neu, R., J.C. Fuchs, G. Haas, A. Herrmann, A. Kallenbach, M. Laux, J. Neuhauser, F. Ryter, J. Gafert, O. Gruber, M. Kaufmann, B. Kurzan, V. Mertens, H.W. Müller, V. Rohde, A.C.C. Sips, J. Stober, B. Streibl, W. Treutterer and ASDEX Upgrade Team:* Properties of the New Divertor IIb in ASDEX Upgrade. Plasma Physics and Controlled Fusion **44**, 1021-11029 (2002).

206. *Neuhauser, J., D.P. Coster, H.-U. Fahrbach, J.C. Fuchs, G. Haas, A. Herrmann, L.D. Horton, M. Jakobi, A. Kallenbach, M. Laux, J.-W. Kim, B. Kurzan, H.W. Müller, H. Murmann, R. Neu, V. Rohde, W. Sandmann, W. Suttrop, E. Wolfrum and ASDEX Upgrade Team:* Transport into and across the Scrape-off Layer in the ASDEX Upgrade Divertor Tokamak. Plasma Physics and Controlled Fusion **44**, 855-869 (2002).

207. *Nguyen*, F., J.-M. Noterdaeme, I. Monakhov*, F. Meo, H.-U. Fahrbach, C. Maggi, R. Neu, W. Suttrop, M. Brambilla, D. Hartmann, F. Wesner and ASDEX Upgrade Team:* ICRF Ion Heating with Mode Conversion on the Tokamak ASDEX Upgrade. In: Proceedings of the 29th EPS Conference on Plasma Physics and Controlled Fusion, Montreux 2002, (Eds.) R.Behn, C.Varandas. ECA 26B. European Physical Society, Geneva 2002, P-1.045.

208. *Niedner, S., B.D. Scott and U. Stroth:* Statistical Properties of Drift Wave Turbulence in Low-Temperature Plasmas. Plasma Physics and Controlled Fusion **44**, 397-408 (2002).

209. *Nishijima*, D., U. Wenzel, K. Ohsumi*, N. Ohno*, Y. Uesugi* and S. Takamura*:* Characteristics of Detached Plasmas Associated with Electron-Ion and Molecular Assisted Recombinations in NAGDIS-II. Plasma Physics and Controlled Fusion **44**, 597-610 (2002).

210. *Nishimura, Y., D.P. Coster, J.-W. Kim and B.D. Scott:* Coupling of Perpendicular Transport in Turbulence and Divertor Codes. Contributions to Plasma Physics **42**, 379-383 (2002).

211. *Nishimura, Y., D.P. Coster and B.D. Scott:* Tokamak Edge E_r and Transport Studies by Turbulence and Divertor Codes. In: Proceedings of the 29th EPS Conference on Plasma Physics and Controlled Fusion, Montreux 2002, (Eds.) R.Behn, C.Varandas. ECA 26B. European Physical Society, Geneva 2002, P-1.110.

212. *Nunes*, I., G.D. Conway, M. Manso*, M. Maraschek, F. Serra*, W. Suttrop, CFN Team and ASDEX Upgrade Team:* Study of ELMs on ASDEX Upgrade Using Reflectometry Measurements with High Temporal and Spatial Resolution. In: Proceedings of the 29th EPS Conference on Plasma Physics and Controlled Fusion, Montreux 2002, (Eds.) R.Behn, C.Varandas. ECA 26B. European Physical Society, Geneva 2002, O-5.06.

213. *Ogawa*, I., T. Idehara*, R. Pavlichenko*, S. Mitsudo*, D. Wagner and M. Thumm*:* High Quality Operation of High Frequency Gyrotron. In: Proceedings of the 27th International Conference on Infrared and Millimeter Waves, San Diego,CA 2002, (Ed.) R.J.Temkin. IEEE Press, New York,NY 2002, 293-294.

214. *Ott, W., E. Speth and W7-AS Team:* Plasma Build-up in Stellarators by Neutral Beams Alone. Nuclear Fusion **42**, 796-804 (2002).

215. *Otte, M. and J. Lingertat:* Initial Results of Magnetic Surface Mapping in the WEGA Stellarator. In: Proceedings of the 29th EPS Conference on Plasma Physics and Controlled Fusion, Montreux 2002, (Eds.) R.Behn, C.Varandas. ECA 26B, European Physical Society, Geneva 2002, P-5.036.

216. *Pamela*, J., D. Stork*, E. Solano*, Yu. Baranov*, D. Borba*, C.D. Challis*, H.P.L. de Esch*, R.D. Gill*, A. Gondhalekar*, V. Kiptily*, T. Johnson*, M. Mantsinen*, K.G. McClements*, M.F.F. Nave*, S.D. Pinches, O. Sauter*, S. Sharapov*, D. Testa* and Contributors to the EFDA-JET Work Programme:* Overview of Results and Possibilities for Fast Particle Research on JET. Nuclear Fusion **42**, 1014-1028 (2002).

217. *Pautasso, G., A. Savtchkov*, S. Egorov, R. Dux, K.-H. Finken*, O. Gruber, G. Haas, G. Mank*, M. Maraschek, V. Rohde, U. Seidel and ASDEX Upgrade Team:* Mitigation of Disruptions with Fast Impurity Puff on ASDEX Upgrade. In: Proceedings of the 29th EPS Conference on Plasma Physics and Controlled Fusion, Montreux 2002, (Eds.) R.Behn, C.Varandas. ECA 26B. European Physical Society, Geneva 2002, P-2.051.

218. *Pautasso, G., C. Tichmann, S. Egorov, T. Zehetbauer, O. Gruber, M. Maraschek, K.-F. Mast, V. Mertens, I, Perchermeier, G. Raupp, W. Treutterer, C.G. Windsor* and ASDEX Upgrade Team:* On-Line Prediction and Mitigation of Disruptions in ASDEX Upgrade. Nuclear Fusion **42**, 100-108 (2002).

219. *Pedemonte*, L., G. Bracco*, R. Tatarek*, R. Beikler, E. Taglauer, K. Brüning* and W. Heiland*:* The Surface Structure and Thermal Vibrations of Ag(110) Studied by Low Energy Ion Scattering. Nuclear Instruments and Methods in Physics Research B **193**, 557-562 (2002).

220. *Peeters, A.G., O. Gruber, S. Günter, M. Kaufmann, H. Meister, G. Pereverzev, F. Ryter, A.C.C. Sips, J. Stober, W. Suttrop, G. Tardini, R. Wolf, H. Zohm and ASDEX Upgrade Team:* Confinement Physics of the Advanced Scenario with ELMy H-Mode Edge in ASDEX Upgrade. Nuclear Fusion **42**, 1376-1382 (2002).

221. *Pereverzev, G., G. Janeschitz*, A.S. Kukushkin*, V.S. Mukhovatov*, G. Pacher*, H.D. Pacher*, A.R. Polevoi* and O.V. Zolotukhin*:* Simulation of Core Transport in ITER Plasmas with First-Principle-Based Transport Models. In: Proceedings of the 29th EPS Conference on Plasma Physics and Controlled Fusion, Montreux 2002, (Eds.) R.Behn, C.Varandas. ECA 26B. European Physical Society, Geneva 2002, P-1.072.

222. *Perry*, A., G.D. Conway, R. Boswell* and H. Persing*:* Modulated Plasma Potentials and Cross Field Diffusion in a Helicon Plasma. Physics of Plasmas **9**, 3171-3177 (2002).

223. *Poli, E., A.G. Peeters, A. Bergmann, S. Günter and S.D. Pinches:* Drift Kinetic Simulations of the Current Driving the Neoclassical Tearing Mode. In: Proceedings of the 29th EPS Conference on Plasma Physics and Controlled Fusion, Montreux 2002, (Eds.) R.Behn, C.Varandas. ECA 26B. European Physical Society, Geneva 2002, O-4.01.

224. *Poli, E., A.G. Peeters, A. Bergmann, S. Günter and S.D. Pinches:* Reduction of the Ion Drive ρ^*_θ Scaling of the Neoclassical Tearing Mode. Physical Review Letters **88**, 075001 (2002).

225. *Poulipoulis*, G., G.N. Throumoulopoulos* and H. Tasso:* Tokamak Equilibria with Reversed Magnetic Shear and Sheared Flows. In: Proceedings of the 29th EPS Conference on Plasma Physics and Controlled Fusion, Montreux 2002, (Eds.) R.Behn, C.Varandas. ECA 26B. European Physical Society, Geneva 2002, P-4.076.

226. *Preuss, R., H.D. Kang, T. Schwarz-Selinger and V. Dose:* Quantitative Analysis of Multicomponent Mass Spectra. In: Proceedings of the 21st International Workshop on Bayesian Inference and Maximum Entropy Methods in Science and Engineering, Baltimore,MD 2001, (Ed.) R.L.Fry. AIP Conference Proceedings 617, AIP Press, Melville,NY 2002, 155-162.

227. *Preuss, R., M. Maraschek, H. Zohm and V. Dose:* Bayesian Analysis of Magnetic Island Dynamics of Tearing Modes in ASDEX Upgrade. In: Proceedings of the 29th EPS Conference on Plasma Physics and Controlled Fusion, Montreux 2002, (Eds.) R.Behn, C.Varandas. ECA 26B, European Physical Society, Geneva 2002, P-1.042.

228. *Quigley, E., P.J. McCarthy, A.G. Peeters, J. Hobirk and ASDEX Upgrade Team:* Formation Criterion and Position of Internal Transport Barriers in ASDEX Upgrade. In: Proceedings of the 29th EPS Conference on Plasma Physics and Controlled Fusion, Montreux 2002, (Eds.) R.Behn, C.Varandas. ECA 26B. European Physical Society, Geneva 2002, P-3.206.

229. *Rafiq*, T., R. Kleiber, M. Nadeem* and M. Persson*:* Unstable Ion-Temperature-Gradient Modes in the Wendelstein 7-X Stellarator Configuration. Physics of Plasmas **9**, 4929-4938 (2002).

230. *Rapp*, J., T. Eich, M. von Hellermann*, A. Herrmann, L.C. Ingesson*, S. Jachmich*, G.F. Matthews*, V. Philipps*, G. Saibene* and Contributors to the EFDA-JET Work Programme:* ELM Mitigation by Nitrogen Seeding in the JET Gas Box Divertor. Plasma Physics and Controlled Fusion **44**, 639-652 (2002).

231. *Raupp, G., K. Behler, G. Neu, R. Merkel, W. Treutterer, D. Zasche, T. Zehetbauer and ASDEX Upgrade Team:* Integrating Discharge Control and Data Acquisition at ASDEX Upgrade. Fusion Engineering and Design **60**, 353-359 (2002).

232. *Reinecke, N., S. Reiter, S. Vetter and E. Taglauer:* Steps, Facets and Nanostructures: Investigation of Cu(11*n*) Surfaces. Applied Physics A **75**, 1-10 (2002).

233. *Renner, H., J. Boscary, H. Greuner, H. Grote, F.W. Hoffmann, J. Kisslinger, E. Strumberger and B. Mendelevitch:* Divertor Concept for the W7-X Stellarator and Mode of Operation. Plasma Physics and Controlled Fusion **44**, 1005-1019 (2002).

234. *Rennie, E.E., I. Powis*, U. Hergenhahn, O. Kugeler, G. Garcia*, T. Lischke* and S. Marburger*:* Valence and C 1s Core Level Photo-electron Spectra of Camphor. Journal of Electron Spectroscopy and Related Phenomena **125**, 197-203 (2002).

235. *Rennie, E.E., I. Powis*, U. Hergenhahn, O. Kugeler, S. Marburger* and T.M. Watson*:* Valence and C 1s Core Level Photoelectron Spectra of Butan-2-ol. Journal of Physical Chemistry A **106**, 12221-12228 (2002).

236. *Rennie, E.E., U. Hergenhahn, O. Kugeler, A. Rüdel*, S. Marburger* and A.M. Bradshaw:* A Core Level Photoionisation Study of Furan. Journal of Chemical Physics **117**, 6524-6532 (2002).

237. *Robin*, A., W. Heiland*, R. Beikler, E. Taglauer, L. Pedemonte* and G. Bracco*:* Surface Structure and Dynamics of the Ag(110) Surface Studied by Low Energy Ion Scattering. Reports of the Academy of Science (Moscow), Physical Series **66**, 492-494 (2002).

238. *Robin*, D.M., U. von Toussaint and P.C. Cheeseman*:* High Resolution Surface Geometry and Albedo by Combining Laser Altimetry and Visible Images. International Archives of Photogrammetry and Remote Sensing **34** (3), 105-111 (2002).

239. *Rohde*, D., P. Pecher*, H. Kersten*, W. Jacob and R. Hippler*:* The Energy Influx during Plasma Deposition of Amorphous Hydrogenated Carbon Films. Surface and Coatings Technology **149**, 206-216 (2002).

240. *Rossignol*, J., B. Jüttner* and C.H. Wu:* Glow-to-Arc Transition at the Left Branch of the Paschen-Curve. In: Proceedings of the 20th International Symposium on Discharges and Electrical Insulation in Vacuum, Tours 2002, Ed. Societé Française du Vide, Paris 2002, 243-246.

241. *Rozhansky*, V., E. Kaveeva*, S. Voskoboynikov*, D.P. Coster, X. Bonnin and R. Schneider:* Modelling of Electric Fields in Tokamak Edge Plasma and L-H Transition. Nuclear Fusion **42**, 1110-1115 (2002).

242. *Rozhansky*, V., E. Kaveeva*, S. Voskoboynikov*, D.P. Coster, X. Bonnin and R. Schneider:* Radial Electric Field in the Biasing Experiments and Effective Conductivity in a Tokamak. Physics of Plasmas **9**, 3385-3394 (2002).

243. *Rozhansky*, V., E. Kaveeva*, S. Voskoboynikov*, D.P. Coster, X. Bonnin and R. Schneider:* The Structure of the Radial Electric Field in the Vicinity of the Separatrix and the L-H Transition. Contributions to Plasma Physics **42**, 230-235 (2002).

244. *Rubel*, M., V. Philipps*, A. Pospieszczyk*, T. Tanabe* and S. Kötterl:* Overview of Fuel Retention in Composite and Tungsten Limiters. Journal of Nuclear Materials **307-311**, 111-115 (2002).

245. *Rummel, T., O. Gaupp*, G. Lochner* and J. Sapper:* Quench Protection for the Superconducting Magnet System of Wendelstein 7-X. IEEE Transactions on Applied Superconductivity **12**, 1382-1385 (2002).

246. *Runov, A.M., S.V. Kasilov*, J. Riemann, M. Borchardt, D. Reiter* and R. Schneider:* Benchmark of the 3-Dimensional Plasma Transport Codes E3D and BoRiS. Contributions to Plasma Physics **42**, 169-174 (2002).

247. *Rust, N., J. Baldzuhn, M. Kick, A. Werner and E. Speth:* Recent Results from W7-AS with the New Radial NBI Injector. In: Proceedings of the 29th EPS Conference on Plasma Physics and Controlled Fusion, Montreux 2002, (Eds.) R.Behn, C.Varandas. ECA 26B, European Physical Society, Geneva 2002, P-4.045.

248. *Ryter, F., H.-U. Fahrbach, A. Gude, R. Neu, V. Rohde, J. Stober and ASDEX Upgrade Team:* Survey of H-Mode Transition and Confinement from ASDEX Upgrade 'H-Mode Standard Shot'. Plasma Physics and Controlled Fusion **44**, A407-A413 (2002).

249. *Ryter, F. and H-Mode Threshold Database Group*:* Progress of the International H-Mode Power Threshold Database Activity. Plasma Physics and Controlled Fusion **44**, A415-A421 (2002).

250. *Ryter, F., G. Tardini, H.-U. Fahrbach, K. Kirov, F. Leuterer, A.G. Peeters, G. Pereverzev, W. Suttrop and ASDEX Upgrade Team:* Electron Heat Transport in ASDEX Upgrade: Experiment and Modelling. In: Proceedings of the 29th EPS Conference on Plasma Physics and Controlled Fusion, Montreux 2002, (Eds.) R.Behn, C.Varandas. ECA 26B, European Physical Society, Geneva 2002, P-1.048.

251. *Saarelma*, S., S. Günter, T.P. Kiviniemi*, T. Kurki-Suonio* and ASDEX Upgrade Team:* MHD Stability Analysis of Type II ELMs in ASDEX Upgrade. Contributions to Plasma Physics **42**, 277-282 (2002).

252. *Saibene*, G., R. Sartori*, A. Loarte*, D.J. Campbell*, P.J. Lomas*, V. Parail*, K.-D. Zastrow*, Y. Andrew*, S. Sharapov*, A. Korotkov*, M. Becoulet*, G. Huysmans*, H.R. Koslowski*, R.V. Budny*, G.D. Conway, J. Stober, W. Suttrop, A. Kallenbach, M. von Hellermann* and M. Beurskens*:* Improved Performance of ELMy H-Modes at High Density by Plasma Shaping in JET. Plasma Physics and Controlled Fusion **44**, 1769-1800 (2002).

253. *Salzedas*, F., G. Pautasso, I. Nunes*, W. Suttrop, M. Maraschek, M. Manso* and ASDEX Upgrade Team:* Observations of the Onset of the Energy Quench in ASDEX Upgrade Density Limit Disruptions. In: Proceedings of the 29th EPS Conference on Plasma Physics and Controlled Fusion, Montreux 2002, (Eds.) R.Behn, C.Varandas. ECA 26B. European Physical Society, Geneva 2002, P-1.039.

254. *Sandow*, B., M. Bessenrodt-Weberpals, C. Kausch* and J. McKenna*:* Balancing Family and Career. In: Proceedings of the IUPAP International Coference on Women in Physics, Paris 2002, (Eds.) B.K.Hartline, D.Li. AIP Conference Proceedings 628, AIP Press, Melville,NY 2002, 29-31.

255. *Sartori*, R., G. Saibene*, M. Becoulet*, P.J. Lomas*, A. Loarte*, D.J. Campbell*, Y. Andrew*, R.V. Budny*, M. Beurskens*, A. Kallenbach, V. Parail*, W. Suttrop, J. Stober, K.-D. Zastrow*, M. Zerbini*, R.D. Monk and Contributors to the EFDA-JET Work Programme:* Edge Operational Space for High Density/High Confinement ELMY H-Modes in JET. Plasma Physics and Controlled Fusion **44**, 1801-1814 (2002).

256. *Schacht, J., H. Niedermeyer, C. Wiencke*, J. Hildebrandt* and A. Wassatsch*:* A Trigger-Time-Event System for the W7-X Experiment. Fusion Engineering and Design **60**, 373-379 (2002).

257. *Scheibner*, H., S. Franke*, S. Solyman*, J.F. Behnke*, C. Wilke and A. Dinklage:* Laser Absorption Spectroscopy with a Blue Diode Laser in an Aluminum Hollow Cathode Discharge. Review of Scientific Instruments **73**, 378-382 (2002).

258. *Schild*, T., D. Bouziat*, P. Bredy*, G. Dispau*, A. Donati*, P. Fazilleau*, L. Genini*, M. Jacquemet*, B. Levesy*, F. Molinié*, J. Sapper, C. Walter*, M. Wanner and L. Wegener:* Overview of a New Test Facility for the W7-X Coils Acceptance Tests. IEEE Transactions on Applied Superconductivity **12**, 639-643 (2002).

259. *Schmidt, M.:* δf Monte Carlo Simulations for Stellarators. In: Proceedings of the 29th EPS Conference on Plasma Physics and Controlled Fusion, Montreux 2002, (Eds.) R.Behn, C.Varandas. ECA 26B, European Physical Society, Geneva 2002, P-4.112.

260. *Schneider, R., H. Renner, X. Bonnin, D.P. Coster and J. Neuhauser:* Divertor for W7-X: II. Comparison of Island and Axisymmetric Divertor. Plasma Physics and Controlled Fusion **44**, 665-672 (2002).

261. *Schubert, M., M. Hron*, M. Endler and W7-AS Team:* Spatially Resolved Fast Swept Langmuir Probe Measurements at the Wendelstein 7-AS Stellarator. In: Proceedings of the 29th EPS Conference on Plasma Physics and Controlled Fusion, Montreux 2002, (Eds.) R.Behn, C.Varandas. ECA 26B, European Physical Society, Geneva 2002, P-3.218.

262. *Schwarz-Selinger, T., Y.L. Foo*, D.G. Cahill* and J.E. Greene*:* Surface Mass Transport and Island Nucleation during Growth of Ge on Laser Textured Si(001). Physical Review B **65**, 125317 (2002).

263. *Sharapov*, S., B. Alper*, H.L. Berk*, D. Borba*, B.N. Breizman*, C.D. Challis*, A. Fasoli*, N.C. Hawkes*, T.C. Hender*, J. Mailloux*, S.D. Pinches, D. Testa* and Contributors to the EFDA-JET Work Programme:* Alfvén Wave Cascades in a Tokamak. Physics of Plasmas **9**, 2057-2036 (2002).

264. *Sips, A.C.C., R. Arslanbekov*, C. Atanasiu*, W. Becker, G. Becker, K. Behler, K. Behringer, A. Bergmann, R. Bilato, D. Bolshukhin, K. Borrass, B. Braams*, M. Brambilla, F. Braun, A. Buhler, G.D. Conway, D.P. Coster, R. Drube, R. Dux, S. Egorov, T. Eich, K. Engelhardt, H.-U. Fahrbach, U. Fantz, H. Faugel, M. Foley*, K.B. Fournier*, P. Franzen, J.C. Fuchs, J. Gafert, G. Gantenbein*, O. Gehre, A. Geier, J. Gernhardt, O. Gruber, A.Gude, S. Günter, G. Haas, D. Hartmann, B. Heger, B. Heinemann, A. Herrmann, J. Hobirk, F. Hofmeister, H. Hohenöcker, L.D. Horton, V. Igochine, D. Jacobi, M. Jakobi, F. Jenko, A. Kallenbach, O. Kardaun, M. Kaufmann, A. Keller, A. Kendl, J.-W. Kim, K. Kirov, R. Kochergov, H. Kollotzek, W. Kraus, K. Krieger, B. Kurzan, P.T. Lang, P. Lauber, M. Laux, F. Leuterer, A. Lohs, A. Lorenz, C. Maggi, H. Maier, K. Mank, M. Manso*, M. Maraschek, K.-F. Mast, P.J. McCarthy, D. Meisel, H. Meister, F. Meo, R. Merkel, D. Merkl, V. Mertens, F. Monaco, A. Mück, H.W. Müller, M. Münich, H. Murmann, Y.-S. Na, G. Neu, R. Neu, J. Neuhauser, J.-M. Noterdaeme, I. Nunes*, G. Pautasso, A.G. Peeters, G. Pereverzev, S.D. Pinches, E. Poli, M. Proschek*, R. Pugno, E. Quigley, G. Raupp, T. Ribeiro*, R. Riedl, S. Riondato, V. Rohde, J. Roth, F. Ryter, S. Saarelma*, W. Sandmann, S. Schade, H.-B. Schilling, W. Schneider, G. Schramm, S. Schweizer, B.D. Scott, U. Seidel, F. Serra*, S. Sesnic*, C. Sihler, A. Silva*, E. Speth, A. Stäbler, K.-H. Steuer, J. Stober, B. Streibl, E. Strumberger, W. Suttrop, A. Tabasso, A. Tanga, G. Tardini, C. Tichmann, W. Treutterer, M. Troppmann, P. Varela*, O. Vollmer, D. Wagner, U. Wenzel, F. Wesner, R. Wolf, E. Wolfrum, E. Würsching, Q. Yu, D. Zasche, T. Zehetbauer, H.-P. Zehrfeld and H. Zohm:* Steady State Advanced Scenarios at ASDEX Upgrade. Plasma Physics and Controlled Fusion **44**, B69-B83 (2002).

265. *Sips, A.C.C., G.D. Conway, R. Dux, A. Herrmann, J. Hobirk, O. Gruber, S. Günter, C. Maggi, M. Manso*, M. Maraschek, F. Leuterer, Y.-S. Na, A.G. Peeters, J. Stober and R. Wolf:* Progress towards Steady-State Advanced Scenarios in ASDEX Upgrade. Plasma Physics and Controlled Fusion **44**, A151-A157 (2002).

266. *Sips, A.C.C., A.G. Peeters, F. Ryter, R. Wolf, M. Greenwald*, P. Gohil*, C. Greenfield*, J. Kinsey*, E. Barbato*, G. Bracco*, P. Buratti*, B. Esposito*, Yu. Baranov*, T. Hellsten*, T. Aniel*, A. Becoulet*, L.G. Eriksson*, X. Garbet*, T. Hoang*, F. Imbeaux*, X. Litaudon*, P. Maget*, T. Fukuda*, T. Fujita*, S. Ide*, Y. Kamada*, Y. Sakamoto*, H. Shirai*, T. Suzuki*, T. Takizuka*, G.M.D. Hogeweij*, Yu. Esipchuk*, N. Ivanov*, N. Kirneva*, K. Razumova*, T. Hahm*, E. Synakowski* and E. Doyle*:* An International Database for the Study of the Formation of ITBs in Tokamaks. Plasma Physics and Controlled Fusion **44**, A391-A398 (2002).

267. *Smelyanskiy*, V.N., U. von Toussaint and D.A. Timucin*:* Dynamics of Quantum Adiabatic Evolution Algorithm for Number Partitioning. Los Alamos Preprint Server, http://arxiv.org/abs/quant-ph/0202155 (2002).

268. *Snead*, L.L., M. Balden, R.A. Causey* and H. Atsumi*:* High Thermal Conductivity of Graphite Fiber Silicon Carbide Composites for Fusion Reactor Application. Journal of Nuclear Materials **307-311**, 1200-1204 (2002).

269. *Sorge, S. and R. Hatzky:* Ion-Temperature-Gradient Driven Modes in Pinch Configurations within a Linear Gyrokinetic Particle-in-Cell Simulation of Ions and Electrons. Plasma Physics and Controlled Fusion **44**, 2471-2481 (2002).

270. *Spong*, D.A., R. Sanchez*, A. Weller and S.P. Hirshman*:* Shear Alfvén Eigenmodes in Compact Stellarators. In: Proceedings of the 13th International Stellarator Workshop, Canberra 2002, PPPL, Princeton,NJ 2002, PI-25.

271. *Stäbler, A., P. Franzen, J. Hobirk, A.G. Peeters, A.C.C. Sips and ASDEX Upgrade Team:* The Role of Neutral Beam Injection Geometry in Advanced Discharge Scenarios on ASDEX Upgrade. In: Proceedings of the 29th EPS Conference on Plasma Physics and Controlled Fusion, Montreux 2002, (Eds.) R.Behn, C.Varandas. ECA 26B, European Physical Society, Geneva 2002, O-5.03.

272. *Stan-Sion*, C., L. Rohrer*, F. Kubo*, V. Lazarev*, P. Hartung*, E. Nolte*, R. Behrisch and J. Roth:* Upgrading of the Ultra-Clean Injector for Depth Profiling at the Munich AMS Facility. Nuclear Instruments and Methods in Physics Research B **192,** 331-338 (2002).

273. *Stober, J., O. Gruber, M. Kaufmann, R. Neu, F. Ryter, W. Sandmann, H. Zohm and ASDEX Upgrade Team:* Behaviour of Density Profiles of H-Mode Discharges in ASDEX Upgrade. Plasma Physics and Controlled Fusion **44**, A159-A164 (2002).

274. *Strumberger, E., S. Günter, P. Merkel, E. Schwarz, C. Tichmann, H.-P. Zehrfeld and ASDEX Upgrade Team:* Application of Three-Dimensional Codes to Tokamaks. In: Proceedings of the 29th EPS Conference on Plasma Physics and Controlled Fusion, Montreux 2002, (Eds.) R.Behn, C.Varandas. ECA 26B. European Physical Society, Geneva 2002, P-2.090.

275. *Strumberger, E., S. Günter, P. Merkel, E. Schwarz, C. Tichmann and H.-P. Zehrfeld:* Numerical Computation of Magnetic Fields of Two- and Three-Dimensional Equilibria with Net Toroidal Current. Nuclear Fusion **42**, 827-832 (2002).

276. *Subba*, F., X. Bonnin, R. Schneider and S. Kuhn*:* Computational Modeling of Purely Neo-Classical Scrape-off Layer. Contributions to Plasma Physics **42**, 350-355 (2002).

277. *Subba*, F., D. Tskhakaya*, R. Schneider and S. Kuhn*:* Kinetic and Fluid Study of Classical Transport Phenomena in Scrape-off Layer Plasmas. Contributions to Plasma Physics **42**, 372-378 (2002).

278. *Subbotin*, A.A., W.A. Cooper*, M.Yu. Isaev*, M.I. Mikhailov*, J. Nührenberg, M.F. Heyn*, V.N. Kalyuzhnyi*, S.V. Kasilov*, W. Kernbichler*, V.V. Nemov*, M.A. Samitov*, V.D. Shafranov* and R. Zille:* Quasi-Isodynamical Configurations without Transitional Particle Orbits. In: Proceedings of the 29th EPS Conference on Plasma Physics and Controlled Fusion, Montreux 2002, (Eds.) R.Behn, C.Varandas. ECA 26B, European Physical Society, Geneva 2002, P-5.086.

279. *Sudo*, S., H.-J. Hartfuß, T. Mizuuchi*, T. Ozaki*, Y. Nagayama*, T. Akiyama*, A. Fujisawa*, Y. Hamada*, K. Ida*, T. Ido*, H. Iguchi*, S. Kado*, K. Kawahata*, K. Kondo*, K. Narihara*, A. Nishizawa*, H. Okada*, B.J. Peterson*, F. Sano*, M. Sasao*, K. Sato*, M. Shoji*, K. Tanaka*, S. Tsuji-Iio*, K.Y. Watanabe*, A. Weller and I. Yamada*:* Diagnostics for Helical Systems. In: Advanced Diagnostics for Magnetic and Inertial Fusion, (Eds.) P.E.Stott, A.Wooton. Kluwer, New York,NY 2002, 363-370.

280. *Summers*, H.P., N.R. Badnell*, M.G. O'Mullane*, A.D. Whiteford*, R. Bingham*, B.J. Kellet*, J. Lang*, K. Behringer, U. Fantz, K.-D. Zastrow*, S.D. Loch*, M.S. Pindzola*, D.C. Griffin* and C.P. Ballance*:* Atomic Data for Modelling Fusion and Astrophysical Plasmas. Plasma Physics and Controlled Fusion **44,** B323-B338 (2002).

281. *Suttrop, W., K. Behler, H.C. van der Bij* and S. Klenge*:* Fast Economical Data Acquisition Systems Based on the CERN S-LINK Interface Standard. Fusion Engineering and Design **60**, 297-304 (2002).

282. *Suttrop, W., D. Kinna*, J. Farthing*, O. Hemming*, J. How*, V. Schmidt, EFDA-JET Remote Participation Users Group and Contributors to the EFDA-JET Work Programme:* Remote Participation at JET Task Force Work: Users' Experience. Fusion Engineering and Design **60**, 459-465 (2002).

283. *Suttrop, W., J. Ongena*, M. Becoulet*, J.G. Cordey*, P. Dumortier*, G. Huysmans*, P.T. Lang, A. Loarte*, P.J. Lomas*, G. Saibene*, R. Sartori*, V. Parail*, M. Valovic*, P. Andrew*, Y. Andrew*, M. Beurskens*, R.V. Budny*, M. Charlet*, I. Coffey*, T. Eich, L.C. Ingesson, S. Jachmich*, A. Kallenbach, H.R. Koslowski*, K. Lawson*, G. Maddison*, M. Maraschek, D.C. McDonald*, A. Messiaen*, F. Milani*, P. Monier-Garbet*, M.F.F. Nave*, M.E. Puiatti*, J. Rapp*, E. Righi*, O. Sauter*, F. Sartori*, J. Schweinzer, M. Stamp*, J. Strachan*, J. Stober, G. Telesca*, B. Unterberg*, M. Valisa*, P. de Vries*, B. Weyssow* and K.-D. Zastrow*:* High Density High Performance High-Confinement-Mode Plasmas in the Joint European Torus (JET). Physics of Plasmas **9**, 2103-2112 (2002).

284. *Suttrop, W., F. Ryter, J.G. Cordey*, R. Barnsley*, M. Beurskens*, J.M. Chareau*, M. Jakobi, C. Maggi, D.C. McDonald*, P.J. Lomas*, G. Maddison*, A. Meigs*, R. Neu, J. Schweinzer, M. Stamp*, J. Stober, J. Strachan*, V. Parail*, ASDEX Upgrade Team and Contributors to the EFDA-JET Work Programme:* Testing H-Mode Parameter Similarity in JET and ASDEX Upgrade. In: Proceedings of the 29th EPS Conference on Plasma Physics and Controlled Fusion, Montreux 2002, (Eds.) R.Behn, C.Varandas. ECA 26B. European Physical Society, Geneva 2002, P-1.030.

285. *Svensson, J.:* An MLP Training Algorithm Taking into Account Known Errors on Inputs and Outputs. International Journal of Neural Systems **12**, 369-379 (2002).

286. *Svensson, J., M. von Hellermann* and R. König:* High Precision Measurement of Fuel Density Profiles in Nuclear Fusion Plasmas. In: Proceedings of the International Conference on Artificial Neural Networks, Madrid 2002, (Ed.) J.R.Dorronsoro. Lecture Notes in Computer Science 2415, Springer Verlag, Berlin 2002, 498-503.

287. *Swiech*, W., T. Schwarz-Selinger and D.G. Cahill*:* Phase Coexistence and Morphology at the Si(110) Surface Phase Transition. Surface Science **519**, L599-L603 (2002).

288. *Tardini, G., A.G. Peeters, G. Pereverzev, F. Ryter and ASDEX Upgrade Team:* Theory-Based Modelling of ASDEX Upgrade Discharges with ECH Modulation. Nuclear Fusion **42**, L11-L14 (2002).

289. *Tardini, G., A.G. Peeters, G. Pereverzev, F. Ryter, J. Stober and ASDEX Upgrade Team:* Comparison of Theory Based Transport Models with ASDEX Upgrade Data. Nuclear Fusion **42**, 258-264 (2002).

290. *Tasso, H. and G.N. Throumoulopoulos*:* Wall Stabilization and the Mathieu-Hill Equations. Physics of Plasmas **9**, 2662-2666 (2002).

291. *Thomsen, H., M. Endler, J. Bleuel*, A.V. Chankin, K. Erents*, G.F. Matthews* and Contributors to the EFDA-JET Work Programme:* Parallel Correlation Measurements in the Scrape-off Layer of the Joint European Torus (JET). Physics of Plasmas **9**, 1233-1240 (2002).

292. *Thomsen, H., R. König, M. Endler, T. Klinger and W7-AS Team:* Characterization of ELM Phenomena by Means of Visible Imaging in the Wendelstein 7-AS Stellarator. In: Proceedings of the 29th EPS Conference on Plasma Physics and Controlled Fusion, Montreux 2002, (Eds.) R.Behn, C.Varandas. ECA 26B. European Physical Society, Geneva 2002, P-4.079.

293. *Thumm*, M., A. Arnold*, G. Dammertz*, R. Heidinger*, S. Illy*, K. Koppenburg*, M. Kuntze*, W. Leonhardt*, G. Neffe*, B. Piosczyk*, M. Schmidt, X. Yang*, M.Q. Tran*, G. Müller*, E. Giguet*, G. LeCloarec*, F. Legrand* and C. Lievin*:* Experimental Results of the 140 GHz, 1 MW Longpurse Gyrotron for W7-X. In: Proceedings of the 14th Joint Russian-German Workshop on ECRH and Gyrotrons, Nizhny Novgorod 2002, (Ed.) Russian Academy of Science. Viewgraphs Collection 1, Moskva 2002, 104-123.

294. Ti*mokhin*, V.M., B.V. Kuteev*, V.Yu. Sergeev*, V.A. Belopolsky*, O.A. Bakhareva*, R.Burhenn and W7-AS Team:* Studies of Three Dimensional Cloud Structure of Carbon Pellets Ablated in the W7-AS Plasma. In: Proceedings of the 29th EPS Conference on Plasma Physics and Controlled Fusion, Montreux 2002, (Eds.) R.Behn, C.Varandas. ECA 26B, European Physical Society, Geneva 2002, P-4.047.

295. *Timokhin*, V.M., B.V. Kuteev*, V.Yu. Sergeev, V.G. Skokov*, R. Burhenn and W7-AS Team:* Studies of Suprathermal Electrons in the W7-AS by Means of Pellet Injection. In: Proceedings of the 29th EPS Conference on Plasma Physics and Controlled Fusion, Montreux 2002, (Eds.) R.Behn, C.Varandas. ECA 26B, European Physical Society, Geneva 2002, P-5.031.

296. *Tsitrone*, E., J. Bucalossi*, T. Loarer*, Ph. Ghendrih*, A. Loarte*, P. Andrew*, J.P. Coad*, W. Fundamenski*, M. Stamp*, D.P. Coster and Contributors to the EFDA-JET Work Programme:* Particle Recirculation Studies in JET. Plasma Physics and Controlled Fusion **44**, 701-716 (2002).

297. *Valenza, D., M. Balden, H. Bolt, H. Greuner, S. Kötterl, M. Mayer, A. Pospieszczyk* and G. Sergienko*:* Development and Characterisation of B_4C Coatings for Plasma Facing Applications of the Wendelstein 7-X Fusion Experimental Device. In: Proceedings of Materials Week, München 2001, (Ed.) Werkstoff-Informationsges., Frankfurt a.M. 2002, CD-ROM.

298. V*alenza, D., H. Greuner, G. Hofmann, S. Kötterl, J. Roth and H. Bolt:* Characterisation and Thermal Loading of Low-Z Coatings for the First Wall of W7-X. Journal of Nuclear Materials **307-311**, 89-94 (2002).

299. *Valovic*, M., J. Rapp*, J.G. Cordey*, R.V. Budny*, D.C. McDonald*, L. Garzotti*, A. Kallenbach, M.A. Mahdavi*, J. Ongena*, V. Parail*, G. Saibene*, R. Sartori*, M. Stamp*, O. Sauter*, J. Strachan*, W. Suttrop and Contributors to the EFDA-JET Work Programme:* Long Timescale Density Peaking in JET. Plasma Physics and Controlled Fusion **44**, 1911-1918 (2002).

300. *Volpe*, F., H.P. Laqua and W7-AS Team:* Electron Bernstein Emission Diagnostic of Electron Temperature Profiles at W7-AS Stellarator. In: Advanced Diagnostics for Magnetic and Inertial Fusion, (Eds.) P.E.Stott, A.Wooton. Kluwer, New York,NY 2002, 347-354.

301. *Volpe*, F., H.P. Laqua and W7-AS Team:* Electron Bernstein Emission Diagnostic of Electron Temperature Profiles at W7-AS Stellarator. In: Proceedings of the 12th Joint Workshop on Electron Cyclotron Emission and Electron Cyclotron Resonance Heating, Aix-en-Provence 2002, 221-224.

302. *Wacker*, R., F. Leuterer, D. Wagner, H. Hailer* and W. Kasparek*:* Characterization of Absorber Materials for High-Power Millimeter Waves. In: Proceedings of the 27th International Conference on Infrared and Millimeter Waves, San Diego,CA 2002, (Ed.) R.J.Temkin. IEEE Operations Center, Piscataway,NJ 2002, 159-160.

303. *Wagner, D., M. Thumm* and A. Arnold*:* Mode Generator for the Cold Test of Step-Tunable Gyrotrons. In: Proceedings of the 27th International Conference on Infrared and Millimeter Waves, San Diego,CA 2002, (Ed.) R.J.Temkin. IEEE Press, New York,NY 2002, 303-304.

304. *Wanner, M. and W7-X Team:* Technical Status of Wendelstein 7-X. In: Proceedings of the 13th International Stellarator Workshop, Canberra 2002, PPPL, Princeton,NJ 2002, OV11.

305. *Wegener, L., W. Gardebrecht, R. Holzthüm, N. Jaksic, F. Kerl, J. Sapper and M. Wanner:* Status of the Construction of the W7-X Magnet System. IEEE Transactions on Applied Superconductivity **12**, 653-658 (2002).

306. *Weller A., J. Geiger, A. Werner, S. Klose, J. Baldzuhn, R. Brakel, H. Ehmler, G. Fu*, F. Gadelmeier, L. Giannone, J.-P. Knauer, G. Kühner, C. Nührenberg, E. Pasch, N. Rust, R. Sanchez*, E. Speth, D.A. Spong*, U. Wenzel, W7-AS Team and NBI Group:* Performance and Stability of High-β Discharges in W7-AS. In: Proceedings of the 13th International Stellarator Workshop, Canberra 2002, PPPL, Princeton,NJ 2002, OIV2.

307. *Wenzel, U., K. McCormick, D. Hildebrandt, S. Klose, D. Naujoks and H. Thomsen:* Experimental Observation of Marfes in the W7-AS Stellarator. Plasma Physics and Controlled. Fusion **44**, L57-L62 (2002).

308. *Werner, A., D.S. Darrow*, R. Kuduk* and A. Weller:* Fast Ion Loss Diagnostic for the Wendelstein 7-X Stellarator. In: Advanced Diagnostics for Magnetic and Inertial Fusion, (Eds.) P.E.Stott, A.Wooton. Kluwer, New York,NY 2002, 137-140.

309. *Westerhof*, E., O. Sauter*, M.L. Mayoral*, D.F. Howell*, M. Mantsinen*, M.F.F. Nave*, B. Alper*, C. Angioni*, P. Belo*, R.J. Buttery*, A. Gondhalekar*, T. Hellsten*, T.C. Hender*, T. Johnson*, P. Lamalle*, M. Maraschek, K.G. McClements*, F. Nguyen*, A.L. Pécquet*, S. Podda*, J. Rapp*, S. Sharapov*, M. Zabiego* and Contributors to the EFDA-JET Work Programme:* Control of Sawteeth and Triggering of NTMs with Ion Cyclotron Resonance Frequency Waves in JET. Nuclear Fusion **42**, 1324-1334 (2002).

310. *Wolf, R., Yu. Baranov*, M. De Baar*, C.D. Challis*, W. Dorland*, X. Garbet*, C. Giroud*, N.C. Hawkes*, E. Joffrin*, D. Mazon*, A.G. Peeters, K.-D. Zastrow* and Contributors to the EFDA-JET Work Programme:* Ion Heat Transport in JET and ASDEX Upgrade Tokamak Plasmas. In: Proceedings of the 29th EPS Conference on Plasma Physics and Controlled Fusion, Montreux 2002, (Eds.) R.Behn, C.Varandas. ECA 26B. European Physical Society, Geneva 2002, P-2.043.

311. *Yamada-Takamura*, Y., F. Koch, H. Maier and H. Bolt:* Hydrogen Permeation Barrier Performance Characterization of Vapor Deposited Amorphous Aluminium Oxide Films Using Coloration of Tungsten Oxide. Surface and Coatings Technology **153**, 114-118 (2002).

312. *Yang*, X., B. Piosczyk*, D. Wagner, E. Borie*, R. Heidinger*, G. Dammertz* and M. Thumm*:* Analysis of Transmission Characteristics for Single and Double Disk Windows. In: Proceedings of the 27th International Conference on Infrared and Millimeter Waves, San Diego,CA 2002, (Ed.) R.J.Temkin. IEEE Press, New York,NY 2002, 157-158.

313. *You, J.-H. and H. Bolt:* Overall Mechanical Properties of Fiber Reinforced Metal Matrix Composites for Fusion Applications. Journal of Nuclear Materials **305**, 14-20 (2002).

314. *You, J.-H. and H. Bolt:* Prediction of Plastic Deformation of Fiber-Reinforced Copper Matrix Composites. Journal of Nuclear Materials **307-311**, 74-78 (2002).

315. *Zastrow*, K.-D., M. Brix*, R. Dux, K.-H. Finken*, C. Giroud*, M. von Hellermann*, D. Hillis*, P.D. Morgan*, M.G. O'Mullane*, A.D. Whiteford* and Contributors to the EFDA-JET Work Programme:* Helium Ash Simulation Studies with Divertor Helium Pumping in JET Internal Transport Barrier Discharges. In: Proceedings of the 29th EPS Conference on Plasma Physics and Controlled Fusion, Montreux 2002, (Eds.) R.Behn, C.Varandas. ECA 26B. European Physical Society, Geneva 2002, O-5.02.

316. *Zehrfeld, H.-P. and E. Strumberger:* Computational Models of Toroidal Steady-State Plasmas for the Purpose of Stability Investigations. In: Proceedings of the 29th EPS Conference on Plasma Physics and Controlled Fusion, Montreux 2002, (Eds.) R.Behn, C.Varandas. ECA 26B. European Physical Society, Geneva 2002, P-5.048.

317. *Zohm, H., H.-S. Bosch, O. Gruber, R. Neu, H.-P. Schweiss, A. Stäbler, J. Stober and ASDEX Upgrade Team:* Neutron Production in High Performance Scenarios in ASDEX Upgrade. In: Proceedings of the 29th EPS Conference on Plasma Physics and Controlled Fusion, Montreux 2002, (Eds.) R.Behn, C.Varandas. ECA 26B. European Physical Society, Geneva 2002, P-1.043.

318. *Zoletnik*, S., N.P. Basse*, M. Saffman*, W. Svendsen*, M. Endler, M. Hirsch, A. Werner, J.C. Fuchs and W7-AS Team:* Changes in Density Fluctuations Associated with Confinement Transitions Close to a Rational Edge Rotational Transform in the W7-AS Stellarator. Plasma Physics and Controlled Fusion **44**, 1581-1607 (2002).

319. *Zurro*, B., M.A. Ochando*, P.J. McCarthy, F. Medina*, A. Baciero*, R. Dux, E. Ascasibar*, A. López-Fraguas*, A. López-Sánchez*, T. Estrada*, E. de la Luna*, J. Vega* and TJ-II Team:* Study of Impurity Transport Injected by Laser Ablation in the TJ-II. In: Proceedings of the 29th EPS Conference on Plasma Physics and Controlled Fusion, Montreux 2002, (Eds.) R.Behn, C.Varandas. ECA 26B. European Physical Society, Geneva 2002, P-5.025.

320. *Zvonkov*, A.V., A.Yu. Kuyanov*, J. Nührenberg, A.A. Skovoroda* and R. Zille:* Toroidal Mirror System. Plasma Physics Reports **28**, 756-764 (2002).

321. *Zweben*, S.J., D.P. Stotler*, J.L. Terry*, B. LaBombard*, M. Greenwald*, M. Muterspaugh*, C.S. Pitcher*, K. Hallatschek, R.J. Maqueda*, B. Rogers*, J.L. Lowrance*, V.J. Mastrocola* and G.F. Renda*:* Edge Turbulence Imaging in the Alcator C-Mod Tokamak. Physics of Plasmas **9**, 1981-1989 (2002).

Diploma Theses

322. *Lorenz, K.:* Untersuchungen an einer Hohlkathodenentladung zur Erzeugung negativer Wasserstoffionen. TU München 2002.

323. *Mazurelle, J.:* Plasma Deposition and Characterization of Al_2O_3 Coating. Ecole Nationale Supérieure de Chimie, Paris 2002.

324. *Oyarzabal, E.:* Influence of Small Carbide Additions on the Deuterium Retention of Isotropic Graphite Manufactured from Microspheres of Carbonaceous Mesophase. Universidad de Navarra, San Sebastián 2002.

325. *Pütterich, T.:* Messungen des Verunreinigungsflusses auf den Schutzlimitern in ASDEX Upgrade. Universität Augsburg 2002.

326. *Reusch, R.:* Bestimmung von Besetzungsdichten des He-Atoms in einer Plasmaentladung mit Hilfe laserinduzierter Fluoreszenz. Humboldt-Universität Berlin 2002.

327. *Schröder, D.:* Messung der Elektronentemperatur in rekombinierenden Plasmen. Humboldt-Universität Berlin 2002.

Doctoral Theses

328. *Bäumel, S.:* Zweidimensionale Charakterisierung von Elektronen-Temperaturfluktationen an W7-AS. Universität Greifswald 2002.

329. *Heger, B.:* Untersuchung und Interpretation der Molekülstrahlung von Wasserstoff und Deuterium in Niederdruckplasmen. Universität Augsburg 2002.

330. *Igochine, V.:* Investigation of MHD Instabilities in Conventional and Advanced Tokamak Scenarios on ASDEX Upgrade. TU München 2002.

331. *Kim, J.-W.:* An Analysis of the Anomalous Transport of the Plasma Edge in ASDEX Upgrade. TU München 2002.

332. *Meier, M.:* Elementare Mechanismen bei der Wechselwirkung von Methylradikalen und Wasserstoffatomen mit der Oberfläche amorpher Kohlenwasserstoff-Filme. Universität Bayreuth 2002.

333. *Niedner, S.:* Numerical Studies of Plasma Turbulence. Universität Kiel 2002.

334. *Pasternak, A.:* Experimentelle Plasmaphysik. Universität Greifswald 2002.

335. *Thomsen, H.:* A Dynamics Investigation into Edge Plasma Turbulence. Universität Greifswald 2002.

Habilitation

336. *Fantz, U.:* Atomic Molecular Emission Spectroscopy in Low Temperature Plasmas Containing Hydrogen and Deuterium. Universität Augsburg 2002.

Patents

337. *Biedermann, C., R. Radtke and S. Deuchler:* Bestrahlungseinrichtung mit einem hochflexiblen Membranbalg. Erteilung des deutschen Patents wird rechtskräftig: 3.4.2002. Einleitung der nationalen Phase der PCT-Anmeldung: 24.4.2002. Veröffentlichung der PCT-Anmeldung Nr. 1240 505: 18.9.2002.

338. *Bohmeyer, W.:* Optische Sonde mit räumlicher Auflösung. Erfindermeldung: 25.4.2002. Freigabe der Erfindermeldung: 2.8.2002.

339. *Mast, K.-F., G. Schramm and M. Münich:* Folienmanometer. Einleitung der nationalen Phasen der PCT-Anmeldung Nr. EP0968407 B1: 15.2.2002. Erteilung des US-Patents Nr. 6,383,031: 7.5.2002. Korrektur der US-Patentschrift: 15.9.2002.

340. *Schacht, J. and H. Niedermeyer:* Verfahren und Vorrichtung zum Synchronisieren und Steuern von technischen Systemen. Keine Auslandsanmeldungen: 6.6.2002.

341. *Schauer, F.:* Gasdurchlässige Hochspannungsisolation. Freigabe des deutschen Patents Nr. 19504857.1 und des europäischen Patents Nr. 0809852: 15.1.2002.

342. *Steinberger, J.:* Vakuumdurchführung für Ultrahochvakuumanlagen. Europäische Patentanmeldung Nr. 02006087.7: 18.3.2002. Veröffentlichung der europäischen Patentanmeldung: 25.09.2002. Offenlegung der deutschen Patentanmeldung DE 10114336 A1: 10.10.2002. Benennung der europäischen Länder: 28.11.2002.
1. Prüfbescheid der deutschen Patentanmeldung: 18.12.2002.

Lectures

343. *Andreeva, T.:* Characteristics of Main Configurations of Wendelstein 7-X. International Conference and School of Plasma Physics and Controlled Fusion, Alushta (Crimea) 2002.

344. *Andrew*, P., J.P. Coad*, T. Eich, E. Gauthier*, A. Herrmann, G.F. Matthews*, V. Riccardo*, M. Stamp* and Contributors to the EFDA-JET Work Programme:* Thermal Effects of Surface Layers on Divertor Target Plates. 15th International Conference on Plasma Surface Interactions in Controlled Fusion Devices, Gifu 2002.

345. *Balden, M.:* Chemical Erosion Processes of Carbon Materials under Hydrogen Bombardment and their Mitigation by Doping. Seminar, Universität Greifswald 2002.

346. *Balden, M.:* Chemical Erosion Processes of Carbon Materials under Reactive Plasma Contact and their Mitigation. European Materials Research Society Spring Meeting, Strasbourg 2002.

347. *Balden, M., E. Oyarzabal, E. de Juan Pardo, K. Durocher*, J. Roth and C. García-Rosales*:* Deuterium Retention by Implantation in Carbide-Doped Graphites. International Workshop on Hydrogen Isotopes in Fusion Reactor Materials, Tokyo 2002.

348. *Balden, M., J. Roth, E. de Juan Pardo and A. Wiltner:* Chemical Erosion by Deuterium of Atomically Dispersed Doped Hydro-Carbon Layers. 15th International Conference on Plasma Surface Interactions in Controlled Fusion Devices, Gifu 2002.

349. *Bandyopadhyay, M.:* Surface-Assisted Volume Production. Coordinating Committee on Neutral Beams, Schloss Ringberg 2002.

350. *Bauer, M.:* Schichtwachstum in gepulsten Plasmen: In-situ Diagnostik - Pulsaufgelöst? 9. Erfahrungsaustausch "Oberflächentechnologie mit Plasmaprozessen", Mühlleithen 2002.

351. *Bauer, M. and A. von Keudell:* Bedeutung von Wachstumssynergismen für die Schichtbildung in gepulsten Plasmen. Treffen des BMBF-Forscherverbundes, "Analyse und Modellierung der Einwirkung gepulster Plasmen auf Oberflächen", Bochum 2002.

352. *Bäumel, S.:* 2-d ECE Correlation Measurements at W7-AS. German-Polish Conference on Plasma Diagnostics for Fusion and Applications, Greifswald 2002.

353. *Bäumel, S.:* JET Lost Alpha Particle Diagnostic - Status Report on Design and Definition Phase of the Scintillator Probe. General Review Meeting, JET, Abingdon 2002.

354. *Bäumel, S.:* Radial-Poloidal Correlation of Electron Temperature Fluctuations at W7-AS. Workshop on Turbulence and Anomalous Transport in Plasmas and Fluids, Roskilde 2002.

355. *Bäumel, S.:* Two-Dimensional Correlation Measurement of Electron Cyclotron Emission Fluctuations on the Stellarator W7-AS. 14th Topical Conference on High Temperature Plasma Diagnostics, Madison,WI 2002.

356. *Bäumel, S.:* Two Dimensional Electron Cyclotron Emission Measurements. 9th EU-US Transport Task Force Meeting, Cordoba 2002.

357. *Behringer, K.:* Einführung in die Plasmaspektroskopie. Vorlesung, Universität Augsburg, WS 2002/2003.

358. *Behringer, K.:* Interpretation von Linienstrahlung von Wasserstoff und Helium in Labor- und Divertorplasmen. Plasma-Kolloquium, Institut für Plasmaforschung, Universität Stuttgart 2002.

359. *Behringer, K.:* Seminar über aktuelle Fragen der Plasmaphysik. Seminar, Universität Augsburg, SS 2002.

360. *Behringer, K.:* Spektroskopie von Nichtgleichgewichtsplasmen. Vorlesung, Universität Augsburg, SS 2002.

361. *Behringer, K. and U. Fantz:* Physikalisches Praktikum für Fortgeschrittene, Teil B. Seminar, Universität Augsburg, SS 2002.

362. *Behringer, K., U. Fantz and T. Hamacher:* Physikalische Grundlagen der Energiewandlung und Verteilung. Seminar, Universität Augsburg, WS 2002/2003.

363. *Behringer, K., U. Fantz and T. Hamacher:* Probleme der zukünftigen Energieversorgung. Seminar, Universität Augsburg, SS 2002.

364. *Behringer, K., U. Fantz and M. Schreck*:* Anwendungen und Diagnostik von Niederdruckplasmen. Seminar, Universität Augsburg, SS 2002.

365. *Behringer, K., M. Stritzker*, U. Fantz and H. Schreck*:* Diagnostik von Niederdrucktemperaturplasmen als industrielle Schlüsseltechnologie. Seminar, Universität Augsburg, WS 2002/2003.

366. *Behrisch, R.:* Tritium in the Vessel Walls for High Plasma Performance D/D Discharges. University of Nagoya 2002.

367. *Behrisch, R., G. Federici*, A.S. Kukushkin* and D. Reiter*:* Material Erosion at the Vessel Walls of Fusion Devices. 15th International Conference on Plasma Surface Interactions in Controlled Fusion Devices, Gifu 2002.

368. *Beidler, C.D., E. Harmeyer, F. Herrnegger, Y. Igitkhanov, J. Kisslinger, Ya.I. Kolesnichenko, V.V. Lutsenko*, V.S. Marchenko*, C. Nührenberg, I.N. Sidorenko, Y. Turkin, A. Wieczorek*, H. Wobig and Yu.V. Yakovenko*:* Recent Developments in Helias Reactor Studies. 13th International Stellarator Workshop, Canberra 2002.

369. *Berger*, M., U. Fantz and K. Behringer:* Besetzungsdichten von Edelgasen in ECR-Plasmen mit Molekülanteil. Verhandl. DPG (VI) **37**, 23, P7.2 (2002).

370. *Bergmann, A., E. Poli and A.G. Peeters:* Monte Carlo δf Simulations of Neoclassical Phenomena in Tokamak Plasmas. 19th IAEA Fusion Energy Conference, Lyon 2002.

371. *Bessenrodt-Weberpals, M.:* Chancen und Risiken für Physikerinnen in Dual Career Couples. Verhandl. DPG (VI) **37**, 152, AKC 1.2 (2002).

372. *Bessenrodt-Weberpals, M.:* Plasma-Material-Bearbeitung (Plasma-Aided Manufacturing). Vorlesung, Universität Düsseldorf 2002.

373. *Bessenrodt-Weberpals, M.:* Plasmaphysik in technischen Anwendungen. Vorlesung, Universität Düsseldorf 2002.

374. *Bessenrodt-Weberpals, M.:* Ziel "Diversity" - Neue Zielgruppen für Hochschulen und Unternehmen. Zukunftschancen durch eine neue Vielfalt in Studium und Lehre. Gender Mainstreaming als Impuls und Motor für die Studienreform in Informatik, Ingenieur- und Naturwissenschaften, München 2002.

375. *Biedermann, C.:* Übungen zu "Struktur der Materie (a): Atom- und Molekülphysik". Humboldt-Universität Berlin, SS 2002.

376. *Biedermann, C., R. Radtke and K.B. Fournier*:* Line Ratios and Wavelengths of Helium-Like Argon n=2 Satellite Transitions and Resonance Lines. 11th International Conference on the Physics of Highly Charged Ions, Caen 2002.

377. *Bindemann, T., H.-J. Hartfuß and M. Hirsch:* Robust Line Density Measurements at W7-AS Using the Cotton-Mouton Effect. German-Polish Conference on Plasma Diagnostics for Fusion and Applications, Greifswald 2002.

378. *Bobkov, Vl.V., S.S. Alimov*, Yu.V. Slyusarenko* and R.I. Starovoitov*:* Growth of Metal Newborn Formations on Cathode Surface under Influence of Plasma Flow. 8th International Conference on Plasma Surface Engineering, Garmisch-Partenkirchen 2002.

379. *Bobkov, Vl.V., M. Azarenkov*, V. Bobkov*, O. Bizyukov*, J.-M. Noterdaeme and R. Wilhelm:* Development of Coatings to Improve RF Voltage Stand-off: 8th International Conference on Plasma Surface Engineering, Garmisch-Partenkirchen 2002.

380. *Bobkov, Vl.V., J.-M. Noterdaeme, F. Wesner, R. Wilhelm and ASDEX Upgrade Team:* Influence of the Plasma on ICRF Antenna Voltage Limits. 15th International Conference on Plasma Surface Interactions in Controlled Fusion Devices, Gifu 2002.

381. *Bobkov, Vl.V., J.-M. Noterdaeme, F. Wesner, R. Wilhelm and ASDEX Upgrade Team:* Studies of ICRF Antenna Voltage Stand-off. Verhandl. DPG (VI) **37**, 42, P23.23 (2002).

382. *Bolt, H.:* Dünne Schichten. Vorlesung, Technische Universität München, SS 2002.

383. *Bolt, H.:* Fast Track Concept in the European Fusion Programme. International Symposium for ITER, Tokyo 2002.

384. *Bolt, H.:* Materials for the Plasma-Interactive Components of Fusion Devices. European Materials Research Society Spring Meeting, Strasbourg 2002.

385. *Bolt, H.:* Plasma-Facing and High Heat Flux Materials for Reactors beyond ITER. 3rd IAEA Technical Committee Meeting on Steady-State Operation of Magnetic Fusion Devices, Greifswald and Arles 2002.

386. *Bonnin, X., D.P. Coster, C.S. Pitcher*, R. Schneider, D. Reiter*, V. Rozhansky*, S. Voskoboynikov* and H. Bürbaumer*:* Improved Modelling of Detachment and Neutral-Dominated Regimes Using the B2.5-Solps Code. 15th International Conference on Plasma Surface Interactions in Controlled Fusion Devices, Gifu 2002.

387. *Bonoli*, P., E. D'Azevedo* and M. Brambilla:* Fully Converged Solutions of Ion Bernstein Wave Mode Conversion in Toroidal Geometry. International Sherwood Fusion Theory Conference, Rochester,NY 2002.

388. *Bonoli*, P., J.C. Wright*, Y. Lin*, M. Porkolab*, S. Wukitch*, E. D'Azevedo* and M. Brambilla:* Mode Conversion Current Drive Calculations Using a Spectral ICRF Field Solver. 44th Annual Meeting of the Division of Plasma Physics, Orlando,FL 2002. Bulletin of the American Physical Society **47** (9), 140 (2002).

389. *Borchardt, M., J. Riemann and R. Schneider:* Numerics in BoRiS. Parallel CFD 2002, Nara 2002.

390. *Borie*, E., K. Koppenburg*, G. Dammertz*, A. Arnold*, S. Illy*, W. Leonhardt*, G. Neffe*, M. Schmid*, B. Piosczyk*, M. Thumm*, E. Giguet*, G. LeCloarec*, Y. Legoff*, V. Erckmann, G. Michel, S. Alberti* and M.Q. Tran*:* Development of a High-Power, CW Gyrotron for the W7-X Stellarator. A Multifrequency Step-Tunable Gyrotron at FZK. Workshop on Far Infrared Technology, Fukui 2002.

391. *Boscary, J., H. Greuner, M. Czerwinski, B. Mendelevitch, K. Pfefferle and H. Renner:* Water-Cooled Target Modules for Steady-State Operation of the W7-X Divertor. 3rd IAEA Technical Committee Meeting on Steady-State Operation of Magnetic Fusion Devices, Greifswald and Arles 2002.

392. *Bosch, H.-S.:* Basic Nuclear Fusion. IPP Summer University on Plasma Physics, Greifswald 2002.

393. *Bosch, H.-S.:* Einführung in die Plasmaphysik I. Vorlesung, Universität Ulm, WS 2001/02.

394. *Bosch, H.-S.:* Einführung in die Plasmaphysik II. Vorlesung, Universität Ulm, SS 2002.

395. *Bosch, H.-S.:* Die Energie der Sterne – auch auf der Erde nutzbar? Vortrag "Physik Modern 2002", Universität München 2002.

396. *Bosch, H.-S.:* Fusionsenergie für das 21. Jahrhundert. Vortrag "Münchner Wissenschaftssommer", Technische Universität München 2002.

397. *Bosch, H.-S.:* Kernfusion - können wir das Sonnenfeuer auf die Erde holen? Vortrag "Energie: Physik - Chemie - Technik am Samstagvormittag", Universität Bayreuth 2002.

398. *Bosch, H.-S.:* Kernfusion: Tokamaks, Stellaratoren, ITER. Vortrag "Kernenergie, Nichtverbreitung und Exportkontrolle", Auswärtiges Amt, Berlin 2002.

399. *Bosch, H.-S.:* Physics of Nuclear Fusion. "Energy for Europe": European Summer University in Physics, Strasbourg 2002.

400. *Bosch, H.-S.:* Praktikum zur Plasmaphysik. Universität Ulm, WS 2001/02.

401. *Bozhko, Y. and F. Schauer:* Refrigeration System for W 7-X. 3rd IAEA Technical Commitee Meeting on Steady-State Operation of Magnetic Fusion Devices, Greifswald and Arles 2002.

402. *Braams*, B., N. McTaggart, X. Bonnin, A.M. Runov and R. Schneider:* Anisotropic Transport Equations on a Poincaré Grid. 44th Annual Meeting of the Division of Plasma Physics, Orlando,FL 2002. Bulletin of the American Physical Society **47** (9), 82 (2002).

403. *Brakel, R., P. Grigull, K. McCormick, R. Burhenn, Y. Feng, F. Sardei, J. Baldzuhn, H. Ehmler, F. Gadelmeier, L. Giannone, D. Hildebrandt, K. Ida*, R. Jaenicke, J. Kisslinger, T. Klinger, J.-P. Knauer, R. König, G. Kühner, H.P. Laqua, R. Narayanan, D. Naujoks, H. Niedermeyer, E. Pasch, N. Rust, F. Wagner, A. Weller, U. Wenzel, A. Werner and W7-AS Team:* Improved Performance of the W7-AS Stellarator with the New Island Divertor. 19th IAEA Fusion Energy Conference, Lyon 2002.

404. *Brandl*, W., G. Marginean*, M. Heintze*, H. Bubert* and E. Pasch:* Functionalisation of Vapour Grown Carbon Nano-Fibers by Plasma Treatment. 8th International Conference on Plasma Surface Engineering, Garmisch-Partenkirchen 2002.

405. *Braun, F.:* 3 dB Coupler Enhancement Study for the ICRH System at JET (JWO-EH-2.7). Studie, JET, Abingdon 2002.

406. *Brendel, A. and C. Popescu:* Herstellung und Charakterisierung von kupferbeschichteten SiC-Fasern. Plansee AG, Reutte 2002.

407. *Brendel, A. and C. Popescu:* Herstellung und Charakterisierung von SiC-faserverstärkten Kupfermatrix-Verbundwerkstoffen. Deutsches Zentrum für Luft- und Raumfahrt, Köln 2002.

408. *Brill, R.:* Characterization of Hydrogen Permeation Barriers: Filtered Arc Deposited Aluminum Oxide Coatings. 1st HGF Young Scientist Colloquium "Materials for Fusion Devices", Forschungs-zentrum Jülich 2002.

409. *Bruchhausen*, M., R. Burhenn, M. Endler, A. Pospieszczyk* and S. Zoletnik*:* Untersuchung der Struktur von Elektronen-dichtefluktuationen am Stellarator W7-AS mit einem supra-thermischen atomaren Lithiumstrahl. Verhandl. DPG (VI) **37**, 24, P9.3 (2002).

410. *Bruschi*, A., V. Muzzini*, N. Spinicchia*, R. Benocci*, G. Carcano*, S. Cirant*, F. Gandini*, G. Gittini*, V. Mellera*, A. Nardone*; E. Signorelli*, A. Simonetto*, C. Sozzi*, F. Leuterer, F. Monaco, M. Münich and H. Schütz:* Matched Calorimetric Loads for High Power Millimeter-Wave Gyrotrons. 22nd Symposium on Fusion Technology, Helsinki 2002.

411. *Burhenn, R., H. Ehmler, L. Giannone, R. Brakel, P. Grigull, J.-P. Knauer, F. Kunkel, H. Maaßberg, K. McCormick, E. Pasch, A.Weller, W7-AS Team, ECRH Group and NI Group:* Favourable Impurity Transport in the W7-AS Improved Confinement Regime with Regard to Long Pulse Operation. 3rd IAEA Technical Committee Meeting on Steady-State Operation of Magnetic Fusion Devices, Greifswald and Arles 2002.

412. *Chirkov*, A.V., G.G. Denisov*, E. Filipovic*, G. Gantenbein*, F. Hollmann*, W. Kasparek*, S.V. Kuzikov*, K. Ohkubo*, B. Plaum*, R. Wacker* and D. Wagner:* Experimental Results of a Remote Steering Antenna Based on 4-Wall Corrugated Square Waveguide. 6th International Workshop on ECRH Transmission Systems, San Diego,CA 2002.

413. *Cooper*, W.A., M.Yu. Isaev*, M.F. Heyn*, V.N. Kalyuzhnyi*, S.V. Kasilov*, W. Kernbichler*, A.Yu. Kuyanov*, M.I. Mikhailov*, V.V. Nemov*, J. Nührenberg, M.A. Samitov*, V.D. Shafranov*, A.A. Skovoroda*, A.A. Subbotin*, R. Zille and A.V. Zvonkov*:* New Schemes for Confinement of Fusion Products in Stellarators. 19th IAEA Fusion Energy Conference, Lyon 2002.

414. *Coster, D.P., X. Bonnin, B. Braams*, H. Bürbaumer*, E. Kaveeva*, J.-W. Kim, A.S. Kukushkin*, Y. Nishimura, D. Reiter*, V. Rozhansky*, R. Schneider, B.D. Scott, S. Voskoboynikov* and ASDEX Upgrade Team:* Further Developments of the Edge Transport Simulation Package, SOLPS. 19th IAEA Fusion Energy Conference, Lyon 2002.

415. *Coster, D.P., X. Bonnin, G. Corrigan*, R. Dejarnac*, M. Fenstermacher*, W. Fundamenski*, A. Geier, J. Hogan*, A. Kallenbach, A. Kirschner*, K. Krieger, A. Loarte*, G.F. Matthews*, R.A. Pitts*, G. Porter*, R. Pugno, D. Reiser*, D.Reiter*, S.Sipilä*, J. Spence*, P.C. Stangeby*, E. Tsitrone*, D. Tskhakaya*, M. Wischmeier* and Contributors to the EFDA-JET Work Programme:* An Overview of JET Edge Modelling Activities. 15th International Conference on Plasma Surface Interactions in Controlled Fusion Devices, Gifu 2002.

416. *Coster, D.P., X. Bonnin, G. Corrigan*, R. Dejarnac*, W. Fundamenski*, A. Geier, J. Hogan*, A. Kirschner*, K. Krieger, G.F. Matthews*, R.A. Pitts*, R. Pugno, D. Reiser*, D. Reiter*, S. Sipilä*, J. Spence*, P.C. Stangeby*, G. Dammertz*, S. Alberti*, A. Arnold*, E. Borie*, V. Erckmann, G. Gantenbein*, E. Giguet*, R. Heidinger*, J.P. Hogge*, S. Illy*, W. Kasparek*, K. Koppenburg*, M. Kuntze*, H.P. Laqua, G. LeCloarec*, Y. Legoff*, W. Leonhardt*, C. Lievin*, R. Magne*, G. Michel, G. Müller*, G. Neffe*, B. Piosczyk*, M. Schmid*, M. Thumm* and M.Q. Tran*:* Status of the 1 MW, 140 GHz, CW Gyrotron for W7-X. 5th International Workshop on Strong Microwaves in Plasmas, Nizhny Novgorod 2002.

417. *De Juan Pardo, E., M. Balden, U. Fantz, P. Starke and C. García-Rosales*:* Erosion Behaviour of Doped Carbon and Composite Materials due to High Deuterium Fluence. 15th International Conference on Plasma Surface Interactions in Controlled Fusion Devices, Gifu 2002.

418. *De Juan Pardo, E., M. Balden, C. García-Rosales*, E. Oyarzabal, J. Roth and A. Weghorn:* Chemical Erosion by Hydrogen Bombardment: Mitigation by Doping. CIEMAT, Madrid 2002.

419. *De Juan Pardo, E., M. Balden, C. García-Rosales*, J. Roth and A. Weghorn:* Chemical Erosion of Carbon Materials under Hydrogen Bombardment and their Mitigation by Doping. Technische Universität München 2002.

420. *De Juan Pardo, E., M. Balden, C. García-Rosales*, J. Roth and A. Weghorn:* Chemical Erosion Processes of Carbon Materials under Hydrogen Bombardment and their Mitigation by Doping. 1st HGF Young Scientist Colloquium "Materials for Fusion Devices", Forschungszentrum Jülich 2002.

421. *Dose, V.:* Bayesian Data Analysis. Kolloquium, Interdisziplinäres Zentrum für Dynamik komplexer Systeme, Universität Potsdam 2002.

422. *Düchs, D.:* Is Controlled Nuclear Fusion Research Still Desirable and Promising? Eingeladener Vortrag, 1st International Workshop on Plasma Dynamics of the Institute for Studies in Theoretical Physics and Mathematics, Qeshm,Iran 2002.

423. *Düchs, D.:* Status and Open Problems for Fusion Plasmas in Tokamak Devices. Eingeladener Vortrag, 1st International Workshop on Plasma Dynamics of the Institute for Studies in Theoretical Physics and Mathematics, Qeshm,Iran 2002.

424. *Düchs, D.:* Wechselwirkung von Teilchen in Plasmen. Vorlesung, Ruhr-Universität Bochum, WS 2001/2002.

425. *Düchs, D.:* Wellen im Plasma. Vorlesung, Ruhr-Universität Bochum, SS 2002.

426. *Düchs, D.:* Wozu ist die Erforschung von Fusionsplasmen noch gut? Vorlesung, Ruhr-Universität Bochum, WS 2002/2003.

427. *Dux, R.:* Impurity Transport in Tokamaks. Seminar on "New Trends in Plasma Physics", IPP Garching 2002.

428. *Dux, R.:* Plasmaphysik und Fusionsforschung II. Vorlesung, Universität Augsburg, SS 2002.

429. *Dux, R.:* Die Rolle von Verunreinigungen in Plasmen zur kontrollierten Kernfusion. Physikalisches Kolloquium, Universität Würzburg 2002.

430. *Dux, R., C. Giroud*, R. Neu, J. Stober, K.-D. Zastrow*, Contributors to the EFDA-JET Work Programme and ASDEX Upgrade Team:* Accumulation of Impurities in Advanced Scenarios. 15th International Conference on Plasma Surface Interactions in Controlled Fusion Devices, Gifu 2002.

431. *Dux, R., C. Giroud*, K.-D. Zastrow* and Contributors to the EFDA-JET Work Programme:* Impurity Transport in Internal Transport Barrier Discharges on JET. 19th IAEA Fusion Energy Conference, Lyon 2002.

432. *Ehmler, H., J. Baldzuhn, K. McCormick, A. Kreter, T. Klinger und W7-AS Team:* Charge-Exchange Spectroscopy with a High-Energy Li-Beam. German-Polish Conference on Plasma Diagnostics for Fusion and Applications, Greifswald 2002.

433. *Eich, T., A. Herrmann, P. Andrew, A. Loarte*, ASDEX Upgrade Team and Contributors to the EFDA-JET Work Programme:* Divertor Target Load during Type-I ELM in ASDEX Upgrade and JET Measured by IR-Thermography. IEA Workshop on ELMs, Culham Science Centre, Abingdon 2002.

434. *Eich, T., A. Herrmann, P. Andrew, A. Loarte* and Contributors to the EFDA-JET Work Programme:* Power Deposition Measurements in Deuterium and Helium Discharges in JET MKII GB Divertor by IR-Thermography. 15th International Conference on Plasma Surface Interactions in Controlled Fusion Devices, Gifu 2002.

435. *Encheva, A.:* A Magnetic Filter with Variable Field Strength. Coordinating Committee on Neutral Beams, Schloss Ringberg 2002.

436. *Erckmann, V.:* The 10 MW ECRH-System for W7-X. Alberta 2002.

437. *Erckmann, V.:* 20 Years of ECRH at W7-A and W7-AS. IPF-Kolloqium, Universität Stuttgart 2002.

438. *Erckmann, V., U. Gasparino*, H.P. Laqua, H. Maaßberg, N.B. Marushchenko, H. Renner, M. Romé*, W7-AS Team, W. Kasparek* and G. Müller*:* 20 Years of ECRH at W7-A and W7-AS. 5th International Workshop on Strong Microwaves in Plasmas, Nizhny Novgorod 2002.

439. *Erckmann, V., H.P. Laqua, H. Maaßberg, N.B. Marushchenko, M. Romé*, F. Volpe*, W. Kasparek*, G. Müller* and W7-AS Team:* ECRH at W7-AS. 19th IAEA Fusion Energy Conference, Lyon 2002.

440. *Falter, H.:* Planning and Cost Analysis for RF Source on ITER. Ad Hoc Group Meeting on RF Source for ITER, IPP Garching 2002.

441. *Fantz, U., B. Heger, D. Wünderlich, R. Pugno and ASDEX Upgrade Team:* Photon Efficiency (S+D)/XB of Hydrogen Molecules at Low Electron Temperatures. 15th International Conference on Plasma Surface Interactions in Controlled Fusion Devices, Gifu 2002.

442. *Federici*, G., P. Andrew*, P. Barabaschi*, J. Brooks*, R. Doerner*, A. Geier, A. Herrmann, G. Janeschitz*, K. Krieger, A.S. Kukushkin*, A. Loarte*, R. Neu, G. Saibene*, M. Shimada*, G. Strohmayer* and M. Sugihara*:* Key ITER Plasma Edge and Plasma-Material Interaction Issues. 15th International Conference on Plasma Surface Interactions in Controlled Fusion Devices, Gifu 2002.

443. *Feist, J.-H. and W7-X Construction Team:* Status of the Construction of Wendelstein 7-X. 3rd IAEA Technical Committee Meeting on Steady-State Operation of Magnetic Fusion Devices, Greifswald and Arles 2002.

444. *Feng, Y., F. Sardei, P. Grigull, K. McCormick, L. Giannone, J. Kisslinger, D. Reiter*, Y. Igitkhanov and R. Liu:* Modelling of Island Divertor Physics and Comparison to W7-AS Experimental Results. 15th International Conference on Plasma Surface Interactions in Controlled Fusion Devices, Gifu 2002.

445. *Feng, Y., F. Sardei, P. Grigull, K. McCormick, J. Kisslinger, D. Reiter* and Y. Igitkhanov:* Island Divertor Physics and 3D Transport Modeling. 13th International Stellarator Workshop, Canberra 2002

446. *Feng, Y., F. Sardei, P. Grigull, K. McCormick, J. Kisslinger, D. Reiter* and Y. Igitkhanov:* Transport in Island Divertors. Physics, Modelling and Comparison to First Experimental Results. IEA-DED and TEXTOR Workshop, Jülich 2002.

447. *Fink, M., M. Endler and T. Klinger:* Investigation of Fluctuations of the Plasma Potential in W7-AS Using Emissive Probes. German-Polish Conference on Plasma Diagnostics for Fusion and Applications, Greifswald 2002.

448. *Fink, M., M. Endler and T. Klinger:* Untersuchung der Fluktuationen des Plasmapotentials mittels emissiver Sonden. Verhandl. DPG (VI) **37**, 32, P21.5 (2002).

449. *Fischer, R.:* Bayesian Model Comparison. CIPS Fachbeirat, Garching 2002.

450. *Fischer, R.:* Methods for Reliable Error Estimation. 2nd Workshop on Fusion Data Processing, Validation and Analysis, IPP Greifswald 2002.

451. *Fischer, R., A. Dinklage, J.-S. Yoon, E. Pasch, J.-P. Knauer and J. Svensson:* Bayesian Modelling of Fusion Diagnostics. German-Polish Conference on Plasma Diagnostics for Fusion and Applications, Greifswald 2002.

452. *Fischer, R., C.C. Rodriguez* and V. Dose:* Reversible Jump Markov Chain Monte Carlo in Physics and the Role of Priors. 7th Valencia International Meeting on Bayesian Statistics, Tenerife 2002.

453. *Franck, C.M. and T. Klinger:* Ausbreitung von Whistlerwellen in berandeter und unberandeter Plasmageometrie. Verhandl. DPG (VI) **37**, 29, P18.1 (2002).

454. *Franck, C.M., T. Klinger and O. Grulke:* Investigation of the Influence of Different Boundary Conditions on Helicon Discharges. 11th International Conference on Plasma Physics, Sydney 2002.

455. *Franck, C.M., T. Klinger and O. Grulke:* Ion and Electron Whistler Wave Dispersion Experiments. 11th International Conference on Plasma Physics, Sydney 2002.

456. *Franck, C.M., T. Klinger and O. Grulke:* 2D Messung der magnetischen Modenstruktur in einer Helikonentladung. Verhandl. DPG (VI) **37**, 32, P21.8 (2002).

457. *Franzen, P., J. Sielanko*, H.P.L. de Esch*, B. Heinemann, R. Riedl and E. Speth:* In-Line Magnetic Residual Ion Dump for the ITER Neutral Beam System. Coordinating Committee on Neutral Beams Meeting, JET, Abingdon 2002.

458. *Franzen, P., J. Sielanko*, E. Speth, B. Heinemann, R. Riedl and A. Encheva:* Inline Magnetic Residual Ion Dump for ITER Neutral Beam System. 22nd Symposium on Fusion Technology, Helsinki 2002.

459. *Fußmann, G.:* Atom- und Molekülphysik. Vorlesung, Humboldt-Universität Berlin, SS 2002.

460. *Fußmann, G.:* Challenging Problems in Plasma Physics. Festvortrag anlässlich der Verabschiedung von Prof. Wiesemann, Bochum 2002.

461. *Fußmann, G.:* How to Get Pure Plasmas. Kolloquiumsvortrag, Forschungszentrum Jülich 2002.

462. *Fußmann, G.:* Plasmaphysik und Fusionsforschung (Plasmaphysik II). Vorlesung, Humboldt-Universität Berlin, WS 2002/03.

463. *Fußmann, G., W. Bohmeyer, Zh. Kiss'ovski* and B. Koch:* Flow of Magnetized Plasma in a Linear Device. 11th International Conference on Plasma Physics, Sydney 2002.

464. *Gadelmeier, F.:* Untersuchungen zur Targetbelastung im W7-AS. Vortrag, Heisenberg-Zentrum Garching 2002.

465. *Gadelmeier, F., Y. Feng, P. Grigull, K. McCormick and W7-AS Team:* Edge Transport Studies in the Island Divertor of the W7-AS Stellarator. Verhandl. DPG (IV) **37**, 24, P9.2 (2002).

466. *Gadelmeier, F., P. Grigull, K. McCormick, A. Weller, J. Baldzuhn, R. Brakel, R. Burhenn, H. Ehmler, Y. Feng, L. Giannone, D. Hartmann, D. Hildebrandt, R. Jaenicke, J. Kisslinger, T. Klinger, J.-P. Knauer, R. König, G. Kühner, R. Narayanan, D. Naujoks, E. Pasch, F. Sardei, F. Wagner, U. Wenzel, A. Werner and W7-AS Team:* A New Quasi-Stationary Operational Mode in the W7-AS Stellarator. 3rd IAEA Technical Committee Meeting on Steady-State Operation of Magnetic Fusion Devices, Greifswald and Arles 2002.

467. *García-Rosales*, C., N. Ordás*, M. Balden and S. Lindig:* Influence of Carbide Addition on the Porosity of Isotropic Fine Grain Graphite Based on Carbonaceous Mesophase. 6th International Symposium on the Characterization of Porous Solids, Alicante 2002.

468. *Geier, A., K. Krieger, J.D. Elder*, R. Pugno and ASDEX Upgrade Team:* Modeling of Tungsten Transport in the SOL for Sources at the Central Column of ASDEX Upgrade Using DIVIMP. 15th International Conference on Plasma Surface Interactions in Controlled Fusion Devices, Gifu 2002.

469. *Giannone, L., K. McCormick, J. Baldzuhn, R. Brakel, R. Burhenn, H. Ehmler, Y. Feng, P. Grigull, Y. Igitkhanov, J.-P. Knauer, E. Pasch, N. Rust, U. Stroth, F. Wagner, A. Weller and W7-AS Team:* Transport at the Density- and ß-Limit of W7-AS. 9th EU-US Transport Task Force Workshop, Cordoba 2002.

470. *Giruzzi*, G. and H. Zohm:* ECCD Requirements for NTM Stabilization in ITER. Joint Meeting of Large Tokamak Workshop (W49), US/Japan MHD Workshop and ITPA Topical Group on MHD, Naka 2002.

471. *Goodman*, T.P., A. Mück, C. Angioni*, M.A. Henderson*, O. Sauter*, F. Ryter, E. Westerhof*, H. Zohm and ASDEX Upgrade Team:* Control of the Sawtooth Instability by Electron Cyclotron Heating and Current Drive in the TCV and ASDEX Upgrade Tokamaks. 19th IAEA Fusion Energy Conference, Lyon 2002.

472. *Graves*, J.P., C. Angioni*, R.J. Buttery*, T.P. Goodman*, S. Günter, M.A. Henderson*, M. Mantsinen*, M.L. Mayoral*, A. Mück and O. Sauter*:* Sawtooth Control in View of Controlling NTM Seed Islands. 10th European Fusion Physics Workshop, Vaals 2002.

473. *Greuner, H., B. Böswirth and H. Bolt:* IPP High Heat Flux Test Facility. ITER Divertor Meeting, Cadarache 2002.

474. Greu*ner, H., B. Böswirth, J. Boscary, G. Hofmann, B. Mendelevitch, H. Renner and R. Rieck:* Final Design of W7-X Divertor Plasma-Facing Components - Tests and Thermo-mechanical Analysis of Baffle Prototypes. 22nd Symposium on Fusion Technology, Helsinki 2002.

475. *Grigull, P., K. McCormick, J. Baldzuhn, R. Burhenn, R. Brakel, H. Ehmler, Y. Feng, F. Gadelmeier, L. Giannone, D. Hartmann, D. Hildebrandt, M. Hirsch, R. Jaenicke, J. Kisslinger, T.Klinger, J. Knauer, R. König, R. Narayanan, D. Naujoks, H. Niedermeyer, E. Pasch, F. Sardei, F. Wagner, A. Weller and W7-AS Team:* Effects of the New Island Divertor on the Plasma Performance in the W7-AS Stellarator. 11th International Conference on Plasma Physics, Sydney 2002.

476. *Grigull, P., K. McCormick, Y. Feng, A. Werner, R. Brakel, H. Ehmler, F. Gadelmeier, D. Hartmann, D. Hildebrandt, R. Jaenicke, J. Kisslinger, T. Klinger, R. König, R. Narayanan, D. Naujoks, H. Niedermeyer, F. Sardei, F. Wagner, U. Wenzel and W7-AS Team:* Influence of Magnetic Field Configurations on Divertor Plasma Parameters in the W7-AS Stellarator. 15th International Conference on Plasma Surface Interactions in Controlled Fusion Devices, Gifu 2002.

477. *Grigull, P., K. McCormick, H. Renner, S. Masuzaki*, R. König, J. Baldzuhn, R. Burhenn, R. Brakel, H. Ehmler, Y. Feng, F. Gadelmeier, L. Giannone, D. Hartmann, D. Hildebrandt, M. Hirsch, R. Jaenicke, J. Kisslinger, T. Klinger, J.-P. Knauer, R. Narayanan, D. Naujoks, H. Niedermeyer, E. Pasch, F. Sardei, F. Wagner, U. Wenzel, A. Werner and W7-AS Team:* Divertor Operation in Stellarators: Results from W7-AS and Implications for Future Devices. 22nd Symposium on Fusion Technology, Helsinki 2002.

478. *Grigull, P. and W7-AS Team:* First Island Divertor Experiments on the W7-AS Stellarator. Forschungszentrum Jülich 2002.

479. *Grote, H., J. Kisslinger, H. Renner, J. Boscary, H. Greuner, F.W. Hoffmann and B. Mendelevitch:* Neutral Particle Modelling and Particle Exhaust in the Wendelstein 7-X Stellarator. 15th International Conference on Plasma Surface Interactions in Controlled Fusion Devices, Gifu 2002.

480. *Gruber, O.:* Progress in Advanced Scenarios at ASDEX Upgrade. 44th Annual Meeting of the Division of Plasma Physics, Orlando,FL (2002). Bulletin of the American Physical Society **47** (9), 92 (2002).

481. *Gruber, O.:* Report on ITPA Topical Group on MHD, Disruptions & Control. ITPA Coordinating Committee Meeting 2, San Diego,CA 2002.

482. *Gruber, O.:* Report on ITPA Topical Group on MHD, Disruptions & Control. ITPA Coordinating Committee Meeting 3, Garching 2002.

483. *Gruber, O. and ASDEX Upgrade Team:* ASDEX Upgrade Programme and Schedule in 2003. ITPA-IEA Tokamak Coordination Meeting, Boston,MA 2002.

484. *Gruber, O., S. Günter, A. Herrmann, L.D. Horton, P.T. Lang, M. Maraschek, S. Saarelma*, A.C.C. Sips, J. Stober, W. Suttrop, H. Zohm and ASDEX Upgrade Team:* Tolerable ELMs in Conventional and Advanced Scenarios at ASDEX Upgrade. 19th IAEA Fusion Energy Conference, Lyon 2002.

485. *Gruber, O., S. Günter, A. Herrmann, L.D. Horton, P.T. Lang, M. Maraschek, S. Saarelma*, A.C.C. Sips, J. Stober, W. Suttrop, H. Zohm and ASDEX Upgrade Team:* Tolerable ELMs in Conventional and Advanced Scenarios at ASDEX Upgrade. ITPA Topical Group on MHD, Disruptions & Control Meeting 2, Garching 2002.

486. *Gruber, O., G. Pautasso, B. Streibl, U. Seidel, Y. Nakamura and ASDEX Upgrade Team:* Disruption Prediction, Avoidance and Mitigation. ITPA Topical Group on MHD, Diagnostic & Control Meeting 1, Naka 2002.

487. *Gruber, O., A.G. Peeters, F. Ryter, J. Stober, G. Tardini, R. Wolf and ASDEX Upgrade Team:* ITB Results on ASDEX Upgrade and Comparison with ITG/TEM Models. ITPA Topical Group on Transport & ITBs Meeting 2, San Diego,CA 2002.

488. *Gruber, O., A.G. Peeters, A.C.C. Sips, J. Hobirk, W. Treutterer and ASDEX Upgrade Team:* Control of Advanced Scenarios on ASDEX Upgrade. Joint Meeting of Large Tokamak Workshop (W49), US/Japan MHD Workshop and ITPA Topical Group on MHD, Disruptions & Control, Naka 2002.

489. *Gruber, O., A.C.C. Sips, A. Herrmann, J. Hobirk, M. Maraschek, Y.-S. Na, A.G. Peeters, A. Stäbler, J. Stober, H. Zohm and ASDEX Upgrade Team:* Towards Integrated Steady State Advanced Scenarios at ASDEX Upgrade. 3rd IAEA Technical Committee Meeting on Steady-State Fusion Devices, Greifswald and Arles 2002.

490. *Gruber, O., A.C.C. Sips, A. Herrmann, J. Hobirk, Y.-S. Na, A.G. Peeters, J. Stober and ASDEX Upgrade Team:* Integrated Advanced Tokamak Scenario on ASDEX Upgrade. Joint Meeting of Large Tokamak Workshop (W49), US/Japan MHD Workshop and ITPA Topical Group on MHD, Disruptions & Control, Naka 2002.

491. *Gruber, O., A.C.C. Sips, A. Herrmann, J. Hobirk, Y.-S. Na, A.G. Peeters, J. Stober and ASDEX Upgrade Team:* Sustained Advanced H-Mode on ASDEX Upgrade. ITPA Topical Group on Transport & ITBs Meeting 2, San Diego,CA 2002.

492. *Grulke, O.:* Plasma Turbulence. Kolloquium, Arbeitsgruppe "Komplexe Systeme", Universität Marburg 2002.

493. *Grulke, O.:* Wellenexperimente an der Greifswalder Plasmaanlage VINETA. Physikalisches Kolloquium, Universität Greifswald 2002.

494. *Grulke, O., C.M. Franck and T. Klinger:* Excitation and Propagation of Alfvén Waves in a Helicon Plasma. 11th International Conference on Plasma Physics, Sydney 2002.

495. *Grulke, O., C. Schröder and T. Klinger:* Transition from Electrostatic Drift Waves to Drift Alfvén Waves in a Helicon Plasma. International Conference on Plasma Science, Banff 2002.

496. *Günter, S.:* Konventionelle und alternative Konzepte für einen Fusionsreaktor. Kolloquium, Universität Rostock 2002.

497. *Günter, S.:* Mikroskopische und makroskopische Instabilitäten und ihr Einfluss auf das Einschlussverhalten im magnetisierten Plasma. Kolloquium, Universität Bayreuth 2002.

498. *Günter, S.:* Neoclassical Tearing Modes: Beta Limits and Direct Control. 10th European Fusion Physics Workshop, Vaals 2002.

499. *Günter, S.:* Die Rolle von groß- und kleinskaligen Plasma-Insta-bilitäten in Tokamakplasmen. Kolloquium, Universität Greifswald 2002.

500. *Günter, S.:* Turbulenter Transport und makroskopische Instabilitäten in magnetisch eingeschlossenen Plasmen. Kolloquium, Universität Erlangen 2002.

501. *Günter, S.:* Turbulenter Transport und makroskopische Instabilitäten in magnetisch eingeschlossenen Plasmen. Kolloquium, Universität München 2002.

502. *Günter, S., G. Gantenbein*, A. Gude, V. Igochine, M. Maraschek, O. Sauter*, A.C.C. Sips, H. Zohm and ASDEX Upgrade Team:* Neoclassical Tearing Modes on ASDEX Upgrade: Improved Scaling Laws, High Confinement at High β_N and New Stabilization Experiments. 19th IAEA Fusion Energy Conference, Lyon 2002.

503. *Günter, S., A. Gude, M. Maraschek, E. Poli, O. Sauter*, H. Zohm and ASDEX Upgrade Team:* NTM Physics and Extrapolation to ITER Joint Meeting of Large Tokamak Workshop (W49), US/Japan MHD Workshop and ITPA Topical Group on MHD, Naka 2002.

504. *Günter, S., M. Maraschek, H. Zohm and ASDEX Upgrade Team:* NTM Stabilization Requirements. Joint Meeting of Large Tokamak Workshop (W49), US/Japan MHD Workshop and ITPA Topical Group on MHD, Naka 2002.

505. *Günther*, J., B. Heger, U. Fantz and K. Behringer:* Messungen und Rechnungen der H_2-Strahlung (Fulcher-Übergang) in verschiedenen Experimenten. Verhandl. DPG (VI) **37**, 39, P22.22 (2002).

506. *Hagino*, Y, M.Y. Ye, N. Ohno* and S. Takamura*:* Experimental Evaluation of Space-Charge Limited Emission Current from Tungsten Surface in High Density Helium Plasma. 15th International Conference on Plasma Surface Interactions in Controlled Fusion Devices, Gifu 2002.

507. *Hallatschek, K.:* Numerical Study of Zonal Flow Saturation. Symposium on Transport and Structural Formation Combined with US/Japan JIFT Workshop Structural Formation and Drift/MHD Turbulence, Kyushu 2002.

508. *Hallatschek, K. and W. Dorland*:* Passing Particle Pinch Effects in Core ITG, TEM and ETG Turbulence. DPP-APS Meeting, Orlando,FL 2002.

509. *Hallatschek, K., J.L. Terry*, B. LaBombard*, B. Rogers* and S.J. Zweben*:* Nonlocal Simulation of Finite Beta-Effects in L-Mode Edge Plasmas. International Sherwood Fusion Theory Conference, Rochester,NY 2002.

510. *Hamacher, T.:* Bilder einer zukünftigen Energieversorgung. KTG Ortsverband München 2002.

511. *Hamacher, T.:* Biomasse für Augsburg. Workshop "Biomasse für Augsburg", Augsburg 2002.

512. *Hamacher, T.:* Energie für die Zukunft - Stand und Perspektiven der Fusion. Informationskreis Kernenergie, Bonn 2002.

513. *Hamacher, T.:* Energy for India: A Challenge for Sustainable Development, Engineering Ways to Improve the World. Culham 2002.

514. *Hamacher, T.:* Stand und Aussichten der Kernfusion. Treffen des Arbeitskreises "Energie der DPG", Bad Honnef 2002.

515. *Hamacher, T.:* Technik im Mittelalter - zwischen dem heiligen Benedikt und dem heiligen Franz. Studententreff Schackstraße, München 2002.

516. *Hamacher, T., R.P. Shukla* and A.J. Seebregts*:* The Possible Role of Fusion in the Indian Energy System of the Future. 22nd Symposium on Fusion Technology, Helsinki 2002.

517. *Harmeyer, E. and J. Kisslinger:* Improved Support Concept for the Helias Reactor Coil System. 22nd Symposium on Fusion Technology, Helsinki 2002.

518. *Hatzky, R.:* Domain Cloning for the TORB Code on a Clustered Symmetric-Multiprocessor (SMP) Computer. 13th Summer School on Computing Techniques in Physics, Trest 2002.

519. *Hatzky, R.:* Energy Conservation in a Nonlinear Gyrokinetic Particle-in-Cell Code for Ion-Temperature-Gradient-Driven (ITG) Modes Using the Delta f Method. Seminar, CRPP, Lausanne 2002.

520. *Heger, B., U. Fantz and K. Behringer:* Besetzungsmechanismen von molekularem Wasserstoff und Deuterium in Niederdruckplasmen. Verhandl. DPG (VI) **37**, 22, P7.1 (2002).

521. *Heinemann, B.:* Design and Fabrication of the Type 6/2 Source Body. Coordinating Committee on Neutral Beams, Schloss Ringberg 2002.

522. *Heinemann, B.:* Design of Selected Components. Ad Hoc Group Meeting on RF Source for ITER, Garching 2002.

523. *Heintze*, M., V. Brüser*, E. Pasch and W. Brandl*:* Surface Functionalisation of Carbon Nano-Fibers in a Fluidized bed Plasma. 8th International Conference on Plasma Surface Engineering, Garmisch-Partenkirchen 2002.

524. *Heinzel, S. and H. Lederer:* Garching Computer Center of the Max Planck Society. Supercomputer Center, San Diego,CA 2002.

525. *Hennig, C.:* Netzwerkprogrammierung mit Java. Informatica Feminale, Universität Bremen 2002.

526. *Hergenhahn, U.:* Inner Shell Photionization of Small Molecules. Physics Faculty Seminar, University of Windsor 2002.

527. *Hergenhahn, U.:* Die Photoionisation der inneren Schalen kleiner Moleküle. Freie Universität Berlin 2002.

528. *Herrmann, A., T. Eich, S. Jachmich*, M. Laux, P. Andrew*, A. Bergmann, A. Loarte*, G.F. Matthews*, J. Neuhauser, ASDEX Upgrade Team and Contributors to the EFDA-JET Work Programme:* Stationary and Transient Divertor Heat Flux Profiles and Extra-polation to ITER. 15th International Conference on Plasma Surface Interactions in Controlled Fusion Devices, Gifu 2002.

529. *Herrnegger, F., J. Junker*, A. Weller and H. Wobig:* Neutron Field in the Wendelstein 7-X Hall. 22nd Symposium on Fusion Technology, Helsinki 2002.

530. *Hildebrandt, D.:* Das UHV-Labor in Berlin. Veranstaltung anläßlich des 10. Jahrestages der Gründung des Bereiches Plasmadiagnostik, Berlin 2002.

531. *Hildebrandt, D., F. Gadelmeier, P. Grigull, K. McCormick, D. Naujoks, D. Sünder and W7-AS Team:* Thermographic Observation of the Divertor Target Plates in the Stellarators W7-AS and W7-X. 15th International Conference on Plasma Surface Interactions in Controlled Fusion Devices, Gifu 2002.

532. *Hopf, C.:* Erosion von a-C:H: Synergismus Wasserstoff und Ionen. 9. Erfahrungsaustausch "Oberflächentechnologie mit Plasmaprozessen", Mühlleithen 2002.

533. *Hopf, C. and A. von Keudell:* Ion-Induced Effects in Growth and Erosion of a-C:H Films. 4th Specialist Meeting on Amorphous Carbon, Barcelona 2002.

534. *Horvath, K., J. Lingertat and M. Otte:* First Experimental Results from the WEGA Stellarator. German-Polish Conference on Plasma Diagnostics for Fusion and Applications, Greifswald 2002.

535. *Howard*, J., L. Carraro*, M.E. Sattin*, P. Scarin*, M. Valisa*, B. Zaniol*, R. König and J. Chung:* A Coherence-Imaging Approach to Time-Resolved Charge Exchange Recombination Spectroscopy in High Temperature Plasma. 14th Topical Conference on High Temperature Plasma Diagnostics, Madison,WI 2002.

536. *Hubbard*, A., P. Bonoli*, J.W. Hughes*, D. Mossessian*, S. Wukitch*, L.D. Horton, W. Suttrop, F. Meo, R. Neu, J.-M. Noterdaeme, J. Schweinzer and J. Stober:* Edge Threshold and Pedestal Similarity Studies in ALCATOR C-Mod and ASDEX Upgrade. 44th Annual Meeting of the Division of Plasma Physics, Orlando,FL 2002. Bulletin of the American Physical Society **47** (9), 139 (2002).

537. *Hutton*, R., C. Biedermann, R. Radtke, R. Neu and A. Geier.* Tungsten Lines in Hot Plasmas. 11th International Conference on the Physics of Highly Charged Ions, Caen 2002.

538. *Igitkhanov, Y., L. Giannone, P. Grigull, K. McCormick and H. Wobig:* On the High Density Modes of Operation in W 7-AS as a Prototype for HSR Mode of Operation. 9th EU-US Transport Task Force Workshop, Cordoba 2002.

539. *Jacob, W.:* Elementarreaktionen der Plasma-Oberflächen-Wechselwirkung bei der Deposition und Erosion von a-C:H-Schichten. Seminar zur Dünnschichttechnologie, Universität Essen 2002.

540. *Jacob, W., C. Hopf, A. von Keudell, M. Mayer, M. Meier and T. Schwarz-Selinger:* Sticking Coefficients and Surface Loss Probabilities of Hydrocarbon Radicals on Plasma-Facing Surfaces. IAEA Technical Meeting on Atomic and Plasma-Material Interaction Data for Fusion Science and Technology, Jülich 2002.

541. *Jacob, W., C. Hopf, M. Meier, A. von Keudell and T. Schwarz-Selinger:* Review on Laboratory Results: Interaction of Ions, Atomic Hydrogen, and Neutral Hydrocarbon Radicals with C:H Surface. Meeting on Erosion and Deposition and Related Modelling Activities, JET, Culham 2002.

542. *Jaenicke, R.:* Quasistationäre Hochdichteentladungen im Stellarator Wendelstein 7-AS. Verhandl. DPG (VI) **37**, 10, PV.IV (2002).

543. *Jaenicke, R., S. Bäumel, J. Baldzuhn, R. Brakel, R. Burhenn, H. Ehmler, M. Endler, V. Erckmann, Y. Feng, F. Gadelmeier, J. Geiger, L. Giannone, P. Grigull, H.-J. Hartfuß, D. Hartmann, D. Hildebrandt, M. Hirsch, E. Holzhauer, M. Kick, J. Kisslinger, T. Klinger, S. Klose, J.-P. Knauer, R. König, G. Kühner, H. Laqua, H. Maaßberg, K. McCormick, R. Narayanan, H. Niedermeyer, W .Ott, E.Pasch, N. Ruhs, N. Rust, J. Saffert, F. Sardei, F. Schneider, M. Schubert, E. Speth, F. Volpe*, F. Wagner, A. Weller, U. Wenzel, A. Werner and E. Würsching:* Overview on Recent W7-AS Results. 19th IAEA Fusion Energy Conference, Lyon 2002.

544. *Jaenicke, R., A. Weller, J. Geiger, S. Klose, E. Sallander, C. Nührenberg and W7-AS Team:* MHD Stability at Operational Limits on the W7-AS Stellarator. 10th European Fusion Physics Workshop on Operational Limits in Toroidal Devices with Particular Reference to Steady State Operation, Vaals 2002.

545. *Jaksic, N. and J. Simon-Weidner:* Suspension of the W7-X Coils. 22nd Symposium on Fusion Technology, Helsinki 2002.

546. *Jauregi*, E., D. Ganuza*, I. García*, J.M. Del Río*, T. Rummel and F. Füllenbach:* Power Supply of the Control Coils of Wendelstein 7-X Experiment. 22nd Symposium on Fusion Technology, Helsinki 2002.

547. *Jenko, F., W. Dorland*, B.D. Scott and D. Strintzi:* Simulation and Theory of Temperature Gradient Driven Turbulence. Joint Varenna-Lausanne International Workshop, Varenna 2002.

548. *Jenko, J., B.D. Scott, W. Dorland*, A. Kendl and D. Strintzi:* Simulations of Finite β Turbulence in Tokamaks and Stellarators. 19th IAEA Fusion Energy Conference, Lyon 2002.

549. *Joffrin*, E., C.D. Challis*, G.D. Conway, X. Garbet*, A. Gude, S. Günter, N.C. Hawkes*, T.C. Hender*, J. Hobirk, D.F. Howell*, G. Huysmans*, E. Lazzaro*, P. Maget*, M. Maraschek, A.G. Peeters, S.D. Pinches, S. Sharapov*, R. Wolf and Contributors to the EFDA-JET Work Programme:* Internal Transport Barrier Triggering by Rational Magnetic Flux Surfaces in Tokamaks. 19th IAEA Fusion Energy Conference, Lyon 2002.

550. *Kallenbach, A.:* Energieszenarien für das 21. Jahrhundert. Vorlesung, Universität Hannover, WS 2002/2003.

551. *Kallenbach, A., R. Dux, J. Gafert, G. Haas, L.D. Horton, M. Jakobi, B. Kurzan, H.W. Müller, R. Neu, J. Neuhauser, R. Pugno, T. Pütterich, V. Rohde, W. Sandmann, S.-W. Yoon and ASDEX Upgrade Team:* Edge Transport and its Interconnection with Main Chamber Recycling in ASDEX Upgrade. 19th IAEA Fusion Energy Conference, Lyon 2002.

552. *Kasparek*, W., G. Dammertz*, V. Erckmann, G. Gantenbein*, H. Hailer*, F. Hollmann*, L. Jonitz, H.P. Laqua, W. Leonhardt*, G. Michel, M. Schmid*, P.G. Schüller*, K. Schwörer*, R. Wacker* and M. Weißgerber:* The Transmission System for ECRH on the Stellarator W7-X: Design Issues and Tests of Prototype Components. 5th International Workshop on Strong Microwaves in Plasmas, Nizhny Novgorod 2002.

553. *Kaufmann, M.:* Einführung in die Plasmaphysik und Fusionsforschung I. Vorlesung, Universität Bayreuth, WS 2002/03.

554. *Kendl, A.:* Simulation of Drift Wave Turbulence in Stellarators. Joint Theoretical Physics and Plasma Research Laboratory Seminar, Australian National University, Canberra 2002.

555. *Keudell, A. von:* a-C:H Growth Mechanism. Chelsea Conference on Amorphous Semiconductors, Cambridge 2002.

556. *Keudell, A. von:* Elementarprozesse der Plasma-Oberflächen-Wechselwirkung. Kolloquium, IPP Jülich 2002.

557. *Keudell, A. von:* Surface Processes during Thin Film Growth. Plasma Surface Engineering Tutorial, Garmisch-Partenkirchen 2002.

558. *Keudell, A. von:* Surface Processes during Thin Film Growth. Summer School on Low Temperature Plasma Physics, Bad Honnef 2002.

559. *Keudell, A. von and M. Bauer:* Bedeutung von Wachstumsynergismen für die Schichtabscheidung in gepulsten Plasmen. Treffen des BMBF-Forscherverbundes "Analyse und Modellierung der Einwirkung gepulster Plasmen auf Oberflächen", Dresden 2002.

560. *Kim, B.Y.:* Shakedown Analysis of Fiber-Reinforced Metal Matrix Composites (FRMMCs) under Fusion-Relevant Thermo-Mechanical Loading. 1st HGF Young Scientist Colloquium "Materials for Fusion Devices", Forschungszentrum Jülich 2002.

561. *Klages, K.U., A. Wiltner, J. Luthin and C. Linsmeier:* Deuterium Bombardment of Carbon and Carbon Layers on Titanium. 15th International Conference on Plasma Surface Interactions in Controlled Fusion Devices, Gifu 2002.

562. *Kleiber, R.:* Introduction to Stellarator Theory. IPP Summer School, Greifswald 2002.

563. *Klinger, T.:* Entladungsmodellierung. Vorlesung, Universität Greifswald, WS 2002/2003.

564. *Klinger, T.:* Noise at Stability Boundaries in Plasma Discharge Experiments. 3. Dresdner Herbstseminar des Arbeitskreises "Statistische Physik", MPI für Physik komplexer Systeme, Dresden 2002.

565. *Klinger, T.:* Plasmaturbulenz im Experiment. Verhandl. DPG (VI) **37**, 10, PV.I (2002).

566. *Klinger, T.:* Plasmawellen und Plasmainstabilitäten. Vorlesung, Universität Greifswald, SS 2002.

567. *Klinger, T.:* Stochastische Resonanz in der Plasmaphysik. Kolloquiumsvortrag, Universität Bochum 2002.

568. *Klinger, T., C.M. Franck and O. Grulke:* Ion and Electron Whistler Wave Experiments. 44th Annual Meeting of the Division of Plasma Physics, Orlando,FL 2002. Bulletin of the American Physical Society **47** (9), 188 (2002).

569. *Knapp*, W., D. Schleussner* and M. Balden:* Investigations of Well-Defined Ion Bombardments as Reproducible Burn-in Operations for Carbon Nanotube (CNT) Field Emitters. 15th International Vacuum Microelectronics Conference and 48th International Field Emission Symposium, Lyon 2002.

570. *Knauer, J.-P., E. Pasch, G. Kühner and W7-AS Team:* High-Resolution Ruby Laser Thomson Scattering Diagnostic for the W7-AS Stellarator. 14th Topical Conference on High Temperature Plasma Diagnostics, Madison,WI 2002.

571. *Koch, B., W. Bohmeyer and G. Fußmann:* Angular Dependence of the Floating Potential in a Magnetized Plasma. 15th International Conference on Plasma Surface Interactions in Controlled Fusion Devices, Gifu 2002.

572. *Koch, F., H. Maier, M. Balden, D. Levchuk, R. Brill, J. Mazurelle and H. Bolt:* Crystal Structure Characterization of Filtered Arc Deposited Alumina Coatings: Temperature and Bias Voltage. 8th International Conference on Plasma Surface Engineering, Garmisch-Partenkirchen 2002.

573. *Könies, A.:* Investigation of Alfvén Eigenmodes with the Three-Dimensional Kinetic MHD Code CAS3D-K. IAEA Technical Meeting on Theory of Plasma Instabilities, Kloster Seeon 2002.

574. *König, R., K. McCormick, P. Grigull, F. Gadelmeier, R. Narayanan, U. Wenzel, B. Schweer and M. Brix*:* First Experience with Island Divertor Diagnostics on the Wendelstein W7-AS Stellarator. German-Polish Conference on Plasma Diagnostics for Fusion and Applications, Greifswald 2002.

575. *König, R., R. Narayanan, K. McCormick, P. Grigull, F. Gadelmeier, U. Wenzel, B. Schweer and M. Brix*:* Island Divertor Spectroscopy at the Wendelstein W7-AS Stellarator. 14th Topical Conference on High Temperature Plasma Diagnostics, Madison,WI, 2002.

576. *Koslowski*, H.R., C. Perez*, B. Alper*, T. Eich, T.C. Hender*, G. Huysmans*, S. Sharapov*, P. Smeulders*, E. Westerhof* and Contributors to the EFDA-JET Work Programme:* Observation of Pre- and Postcursor Modes of Type-I ELMs on JET. 19th IAEA Fusion Energy Conference, Lyon 2002.

577. *Kraus, W.:* Status of BATMAN. Coordinating Committee on Neutral Beams, Schloss Ringberg 2002.

578. *Kraus, W., P. McNeely, P. Franzen, A. Encheva, M. Bandyopadhyay, B. Heinemann, R. Riedl, E. Speth and R. Wilhelm:* Development of Large RF Driven Negative Ion Sources for Neutral Beam Injection. 22nd Symposium on Fusion Technology, Helsinki 2002.

579. *Krieger, K., X. Gong, J. Roth, M. Balden, D. Hildebrandt, H. Maier, R. Neu, V. Rohde and ASDEX Upgrade Team:* Erosion and Migration of Tungsten Employed at the Main Chamber First Wall of ASDEX Upgrade. 15th International Conference on Plasma Surface Interactions in Controlled Fusion Devices, Gifu 2002.

580. *Krieger, K., H. Maier, M. Balden, S. Lindig, J. Linke* and H. Bolt:* Development of Tungsten Coated First Wall and High Heat Flux Components for Application in ASDEX Upgrade. Japan-US Workshop on High Heat Flux Components and Plasma Surface Interactions in Next Step Fusion Devices, Nagoya 2002.

581. *Kugeler, O.:* Photoelektron - Auger-Elektron Koinzidenzmessungen der N 1s Photoionisation von N_2O. "Science on the Fly" - BESSY-Nutzerseminar, Berlin 2002.

582. *Kus, A.:* The Wendelstein 7-X Project in Greifswald. Polish Association of Deans of Physics Faculties (FORUM) Meeting, University of Poznan 2002.

583. *Lang, P.T.:* Experimental Approach for Active ELM Control in ASDEX Upgrade. IEA Workshop on ELMs, Culham Science Centre, Abingdon 2002.

584. *Laqua, H., H. Niedermeyer and J. Schacht:* Control System of Wendelstein 7-X Experiment. 22nd Symposium on Fusion Technology, Helsinki 2002.

585. *Laqua, H., H. Niedermeyer and J. Schacht:* System Control of Wendelstein 7-X. 3rd IAEA Technical Committee Meeting on Steady-State Operation of Magnetic Fusion Devices, Greifswald and Arles 2002.

586. *Laqua, H.P.:* Fusionsplasmen. Vorlesungsreihe zur Plasmatechnologie, FH Stralsund, WS 2002/2003.

587. *Laqua, H.P.:* Heizung und Stromtrieb mit Elektron-Zyklotron-Wellen an den Wendelstein Stellaratoren. Kolloquium, Forschungszentrum Jülich 2002.

588. *Laqua, H.P.:* Plasma Waves. Vorlesung, Universität Greifswald, SS 2002.

589. *Laqua, H.P., V. Erckmann, H. Maaßberg, F. Volpe* and N.B. Marushchenko:* Electron Bernstein Wave Heating and Current Drive Plasmas at the Wendelstein 7-AS. 14th Joint Russian-German Meeting on ECRH and Gyrotrons, Nizhny Novgorod/Moscow 2002.

590. *Laqua, H.P, V. Erckmann, F. Volpe*, W7-AS Team and ECRH Group:* Electron Bernstein Wave Heating and Current Drive in Overdense Plasmas at the Wendelstein 7-AS-Stellarator. 19th IAEA Fusion Energy Conference, Lyon 2002.

591. *Laqua, H.P. and F. Volpe*:* Temperature Diagnostic Based on Electron Bernstein Wave Emission. German-Polish Conference on Plasma Diagnostics for Fusion and Applications, Greifswald 2002.

592. *Laqua, H.P., W7-AS Team and ECRH Group:* Electron Heat Transport for High Power Electron Cyclotron Heating at the Wendelstein 7-AS Stellarator. 13th International Stellarator Workshop, Canberra 2002.

593. *Laux, M.:* Arcing of B4C-Covered Limiters in TEXTOR. Textor Seminar, Forschungszentrum Jülich 2002.

594. *Laux, M.:* Electrical Probes Applied to the Edge and Divertor Plasmas of Magnetic Fusion Devices. German-Polish Conference on Plasma Diagnostics for Fusion and Applications, Greifswald 2002.

595. *Laux, M., W. Schneider, E. Hantzsche*, B. Jüttner*, H. Kostial*, J. Linke and P. Wienhold*:* Arcing through a Thick B4C-Layer. 20th International Symposium on Discharges and Electrical Insulation in Vacuum, Tours 2002.

596. *Laux, M., W. Schneider, P. Wienhold*, B. Jüttner*, A. Huber*, M. Balden, J. Linke*, H. Kostial*, M. Mayer, M. Rubel*, A. Herrmann, A. Pospieszczyk*, S. Jachmich*, B. Schweer*, D. Hildebrandt, J. Rossignol* and H. Bolt:* Arcing at B_4C-Covered Limiters Exposed to a SOL-Plasma. 15th International Conference on Plasma Surface Interactions in Controlled Fusion Devices, Gifu 2002.

597. *Lechón*, Y., H. Cabal*, R. Sáez*, B. Hallberg*, K. Aquilonius*, T. Schneider*, S. Lepicard*, D. Ward*, T. Hamacher and R. Korhonen*:* External Costs of Material Recycling Strategies for Fusion Power Plants. 22nd Symposium on Fusion Technology, Helsinki 2002.

598. *Lechón*, Y., H. Cabal*, R. Sáez*, B. Hallberg*, K. Aquilonius*, T. Schneider*, S. Lepicard*, D. Ward*, T. Hamacher and R. Korhonen*:* External Costs of Silicon Carbide Fusion Power Plants Compared to Other Advanced Generation Technologies. 22nd Symposium on Fusion Technology, Helsinki 2002.

599. *Lederer, H.:* Bioinformatics Support and Infrastructure at Rechenzentrum Garching. Bioinformatik-Treffen, Tübingen 2002.

600. *Lederer, H.:* Central Bioinformatics Environment for Microbial Genomics and Structure Prediction. RZG Status Report, Bio-informatics Meeting, Bremen 2002.

601. *Lederer, H.:* Erste Erfahrungen mit einem IBM Power4 TeraFlop/s System. ZKI-Tagung, Garching 2002.

602. *Lederer, H.:* Installation and Operation of a Seven Node IBM Regatta System. Centro Scientifico de Calculo Switzero, Manno 2002.

603. *Lederer,. H.:* Status IBM Hochleistungsrechner der MPG. 19. DV-Treffen der Max-Planck-Institute, GWDG, Göttingen 2002.

604. *Lederer, H., M. Panea and S. Heinzel:* Rechenzentrum Garching: High Performance Computing for the Max-Planck-Gesellschaft. Supercomputer Conference, Heidelberg 2002.

605. *Lehto*, S., J. Likonen*, J.P. Coad*, T. Ahlgren*, D.E. Hole*, M. Mayer, H. Maier and J. Kolehmainen*:* Tungsten Coating on JET Divertor Tiles For Erosion/Deposition Studies. 22nd Symposium on Fusion Technology, Helsinki 2002.

606. *Leuterer, F.:* From Laboratory Plasma Wave Experiments to RF-Heating in Fusion Devices. California Institute of Technology, Pasadena,CA 2002.

607. *Leuterer, F., R. Dux, G. Gantenbein*, J. Hobirk, K. Kirov, M. Maraschek, A. Mück, R. Neu, A.G.Peeters, F. Ryter, J. Stober, W. Suttrop, G. Tardini, H. Zohm and ASDEX Upgrade Team:* ECRH Results from ASDEX Upgrade. 14th Joint Russian-German Meeting on ECRH and Gyrotrons, Nizhny Novgorod/Moscow 2002.

608. *Leuterer, F., K. Kirov, F. Monaco, M. Münich, H. Schütz, F. Ryter, D. Wagner, H. Zohm, T. Franke, K. Voigt, M. Thumm*, R. Heidinger*, G. Dammertz*, K. Koppenburg*, W. Kasparek* G. Gantenbein*, H. Hailer*, G. Müller*, A. Bogdashov*, G.G. Denisov*, V. Kurbatov*, A. Kuftin*, A. Litvak*, S. Malygin*, E. Tai* and V. Zapevalov*:* Plans for a New ECRH System at ASDEX Upgrade. 22nd Symposium on Fusion Technology, Helsinki 2002.

609. *Leuterer, F., K. Kirov, G. Pereverzev, F. Ryter and D. Wagner:* Modulated ECRH Power Deposition. 14th Joint Russian-German Meeting on ECRH and Gyrotrons, Nizhny Novgorod/Moscow 2002.

610. *Levchuk, S.:* Development of SiC-Fibre Reinforced Steel. 1st HGF Young Scientist Colloquium "Materials for Fusion Devices", Forschungszentrum Jülich 2002.

611. *Lievin*, C., S. Alberti*, A. Arnold*, E. Borie*, G. Dammertz*, V. Erckmann, G. Gantenbein*, E. Giguet*, R. Heidinger*, J.P. Hogge*, S. Illy*, W. Kasparek*, K. Koppenburg*, M. Kuntze*, H.P. Laqua, G. LeCloarec*, F. Legrand*, W. Leonhardt*, R. Magne*, G. Michel, G. Müller*, G. Neffe*, B. Piosczyk*, M. Schmid*, M. Thumm* and M.Q. Tran*:* Status of the 1 MW, 140 GHz, CW Gyrotron for W7-X. 22nd Symposium on Fusion Technology, Helsinki 2002.

612. *Linsmeier, C.:* Ultra-Thin Carbon Films on Metals: Thermal and Ion-Induced Carbide Formation and Carbon Diffusion. Symposium on Surface Science, St. Christoph 2002.

613. *Linsmeier, C. and M. Balden:* Investigation of Surface Processes for Fusion Devices. MPG Initiative "Material Science at FRM-2", MPI für Metallforschung, Stuttgart 2002.

614. *Loarte*, A., G. Saibene*, R. Sartori*, M. Becoulet*, L.D. Horton, T. Eich, A. Herrmann, M. Laux, G.F. Matthews*, S. Jachmich*, N. Asakura*, A.V. Chankin*, A. Leonard*, G. Porter*, G. Federici*, G. Janeschitz*, M. Shimada* and M. Sugihara*:* ELM Energy and Particle Losses and their Extrapolation to Burning Plasma Experiments. 15th International Conference on Plasma Surface Interactions in Controlled Fusion Devices, Gifu 2002.

615. *Lutsenko*, V.V., Ya.I. Kolesnichenko, A. Weller, A. Werner, H. Wobig, Yu.V. Yakovenko* and O.P. Fesenyuk*:* Peculiarities of Destabilization of Alfvén Modes by Energetic Ions in Stellarators. 19th IAEA Fusion Energy Conference, Lyon 2002.

616. *Maier, H.:* Coatings Development for Plasma-Facing and Barrier Applications. Institute of Advanced Energy, University of Kyoto 2002.

617. *Maier, H.:* Coatings Development for Plasma-Facing and Barrier Applications. NIFS, Toki 2002.

618. *Maier, H. and H. Bolt:* Materials for Fusion Energy Systems. 1st Materials Science Forum on Future Sustainable Technologies, Augsburg 2002.

619. *Mantica*, P., C. Capuano*, X. Garbet*, F. Ryter, A. Thyagaraja*, J. Weiland*, M. De Baar*, G.M.D. Hogeweij*, P. Knight*, E. Min*, G. Tardini and ASDEX Upgrade Team:* Investigation of Heat Pinch Effects in Tokamak Plasmas. 9th EU-US Transport Task Force Workshop, Cordoba 2002.

620. *Marushchenko, N.B., V. Erckmann, H. Laqua, H. Maaßberg, F. Volpe* and W7-AS Team:* Estimations of Electron Bernstein Current Drive Efficiency at the W7-AS Stellarator. 5th International Workshop on Strong Microwaves in Plasmas, Nizhny Novgorod 2002.

621. *Mayer, M.:* Fuel Retention in Plasma Facing Materials. Meeting on Erosion and Deposition and Related Modeling Activities, Culham 2002.

622. *Mayer, M.:* Plasma-Wall-Interaction in Thermonuclear Fusion Devices. Eingeladener Kolloquiumsvortrag, National Tsing Hua University, Hsinchu 2002.

623. *Mayer, M.:* SIMNRA 5.0. Eingeladener Vortrag, IAEA Workshop on Software for Ion Beam Analysis, Wien 2002.

624. *Mayer, M.:* Use of Markers for Determination of Erosion and Re-Deposition in JET. Workshop on Tritium Retention Diagnostics, Culham 2002.

625. *Mayer, M., V. Rohde, A. von Keudell and ASDEX Upgrade Team:* Characterisation of Deposited Hydrocarbon Layers below the Divertor and in the Pumping Ducts of ASDEX Upgrade. 15th International Conference on Plasma Surface Interactions in Controlled Fusion Devices, Gifu 2002.

626. *Mayer, M., P. Wienhold*, D. Hildebrandt and W. Schneider:* Determination of Large Erosion/Deposition Rates by Profilometry of a TEXTOR Limiter. Workshop on Tritium Retention Diagnostics, Culham 2002.

627. *Mayer, M., P. Wienhold*, D. Hildebrandt and W. Schneider:* Erosion and Deposition at the ALT-II Limiter of TEXTOR. 15th International Conference on Plasma Surface Interactions in Controlled Fusion Devices, Gifu 2002.

628. *McCormick, K.:* The Intrinsically Steady-State Solution: The High Density H-Mode on Wendelstein 7-AS. 10th European Fusion Program Workshop on Operational Limits in Toroidal Devices with Particular Reference to Steady State Operation, Vaals 2002.

629. *McCormick, K.:* The New Advanced Operational Regime on the Wendelstein 7-AS Stellarator. 44th Annual Meeting of the Division of Plasma Physics, Orlando,FL 2002. Bulletin of the American Physical Society **47** (9), 20 (2002).

630. *McCormick, K., P. Grigull, J. Baldzuhn, R. Brakel, R. Burhenn, H. Ehmler, Y. Feng, R. Fischer, F. Gadelmeier, L. Giannone, D. Hartmann, D. Hildebrandt, M. Hirsch, R. Jaenicke, J. Kisslinger, T. Klinger, J.-P. Knauer, R. König, G. Kühner, R. Narayanan, D. Naujoks, H. Niedermeyer, E. Pasch, N. Rust, F. Sardei, F .Wagner, A. Weller, U. Wenzel and A. Werner:* Island Divertor Experiments on the Wendelstein 7-AS Stellarator. 15th International Conference on Plasma Surface Interactions in Controlled Fusion Devices, Gifu 2002.

631. *McNeely, P.:* In-situ Work Function and Discovery of an Additional H Production Channel. Coordinating Committee on Neutral Beams, Schloss Ringberg 2002.

632. *McNeely, P.:* Selected Experimental Results of RF Source for ITER. Ad Hoc Group Meeting on RF Source for ITER, Garching 2002.

633. *McNeely, P.:* Studies of the Extraction Region of the Type VI RF Driven Negative Ion Source. Negative Ion Workshop, Saclay 2002.

634. *McNeely, P.:* Studies of the Extraction Region of the Type VI RF Driven Negative Ion Source. Workshop "Inductively Coupled Plasmas", Bochum 2002.

635. *McNeely, P., W. Kraus, P. Franzen, E. Speth, M. Bandyopadhyay, C. Hu, B. Heinemann and R. Riedl:* Investigations on the Effect of Argon on the Production of H^- I on Beams for the Heating of Fusion Plasmas. Verhandl. DPG (VI) **37**, 28, P17.4 (2002).

636. *McTaggart, N.:* Development of a Finite Difference Code for Ergodic Regions. DED Workshop Jülich and IMPRS Greifswald 2002.

637. *Meier, M.:* Adsorption von Methylradikalen auf a-C:H. 9. Erfah-rungsaustausch "Oberflächentechnologie mit Plasmaprozessen", Mühlleithen 2002.

638. *Meier, M.:* Synergistisches Wachstum mit CH_3 und H: Daten, Modell, Bayes'sche Analyse. Mitarbeiterseminar EPIII, Universität Bayreuth 2002.

639. *Meir, S., M. Berger*, U. Fantz and K. Behringer:* Analyse der Korrelation der C_2-Strahlung mit Dichten höherer Kohlenwasserstoffe. Verhandl. DPG (VI) **37**, 23, P7.4 (2002).

640. *Meister, H., J.C. Fuchs, B. Kurzan and ASDEX Upgrade Team:* Erste Ergenisse der erweiterten Z_{eff}-Diagnostik an ASDEX Upgrade. Verhandl. DPG (VI) **37**, 28, P17.2 (2002).

641. *Merkl, D., J. Hobirk, R. Wolf, M. Maraschek, V. Igochine and ASDEX Upgrade Team:* Study of the Radial Electric and Poloidal Magnetic Fields in Fusion Plasmas with the Motional Stark Effect (MSE) in ASDEX Upgrade. Verhandl. DPG (VI) **37**, 28, P17.1 (2002).

642. *Mertens, V. and ASDEX Upgrade Team:* Development of Active Control Systems on ASDEX Upgrade in View of ITER Discharge Scenarii. 22nd Symposium on Fusion Technology, Helsinki 2002.

643. *Meyer-Spasche, R.:* Dynamical Systems and Numerical Analysis. Vorlesung, Universität München, SS 2002.

644. *Meyer-Spasche, R.:* Evolutionsprobleme. Vorlesung, Universität München, WS 2002/03.

645. *Meyer-Spasche, R.:* Secondary Bifurcations in Taylor-Vortex Flows Revisited. Hydrodynamics Day: Nonlinear Apsects of Fluid Dynamics, Center for Dynamics of Complex Systems, Universität Potsdam 2002.

646. *Meyer-Spasche, R.:* Variable-Coefficient Difference Schemes for Nonlinear Evolution Problems. Minisymposium "Numerical Analysis of Problem with Blow-Up Solutions", 5th International Conference on Numerical Methods and Applications, Borovets 2002.

647. *Michel, G.:* Erzeugung und Übertragung von Mikrowellen im MW-Bereich. Kolloquium, Universität Rostock 2002.

648. *Michel, G.:* A Fast and Versatile Interlock System. 14th Joint Russian-German Meeting on ECRH and Gyrotrons, Nizhny Novgorod/Moscow 2002.

649. Mi*chel, G.:* Status of the 10MW, 140GHz, CW ECRH System at W7-X. 14th Joint Russian-German Meeting on ECRH and Gyrotrons, Nizhny Novgorod/Moscow 2002.

650. *Mikhailov*, M.I., W.A. Cooper*, M.F. Heyn*, M.Yu. Isaev*, A.A. Ivanov*, V.N. Kalyuzhnyi*, S.V. Kasilov*, W. Kernbichler*, A.A. Martynov*, S.Yu. Medvedev*, V.V. Nemov*, J. Nührenberg, Yu.Yu. Poshekhonov*, M.A. Samitov*, V.D. Shafranov*, A.A. Skovoroda*, A.A. Subbotin* and R. Zille:* Some Results of Stellarator Optimization. International Conference and School on Plasma Physics and Controlled Fusion, Alushta (Crimea) 2002.

651. *Monier-Garbet*, P., P. Andrew*, M. Becoulet*, M. Beurskens*, Y. Corre*, T. Eich, A. Kallenbach, A. Loarte*, P.J. Lomas*, J. Lönnroth*, G.F. Matthews*, J. Ongena*, V. Parail*, J. Rapp*, G. Saibene*, R. Sartori*, E. Solano*, W. Suttrop and Contributors to the EFDA-JET Work Programme:* Current Physics Understanding of ELMs and Unresolved Issues: Ongoing Work on JET. 10th European Fusion Physics Workshop, Vaals 2002.

652. *Monier-Garbet*, P., P. Dumortier*, T. Eich, J. Hogan*, S. Jachmich*, G. Maddison*, A. Messiaen*, J. Ongena*, V. Parail*, B. Unterberg* and Contributors to the EFDA-JET Work Programme:* Stability Analysis of Argon Seeded ELMy H-Modes in JET. IEA Workshop on ELMs, Culham Science Centre, Abingdon 2002.

653. *Mönnich, T. and T. Rummel:* The Power Supply and the Protection System for the Superconducting Coils in W7-X. 3rd IAEA Technical Committee Meeting on Steady-State Operation of Magnetic Fusion Devices, Greifswald and Arles 2002.

654. *Mönnich, T. and T. Rummel:* Protection System for the Super-conducting Coils in Wendelstein 7-X. 22nd Symposium on Fusion Technology, Helsinki 2002.

655. *Mück, A., T.P. Goodman*, A. Gude, H.R. Koslowski*, F. Ryter, S. Sesnic*, E. Westerhof* and H. Zohm:* The Influence of ECRH/ECCD on the Sawtooth Behaviour of ASDEX Upgrade Discharges. Verhandl. DPG (VI) **37**, 24, P9.1 (2002).

656. *Mukherjee, S., W. Dänner*, M. Balden, J. Simon-Weidner, B. Streibl and R. Uhlemann:* Actively Cooled High-Intensity Heat Shield (from Locked) Design Analysis. 22nd Symposium on Fusion Technology, Helsinki 2002.

657. *Müller, W.-C.:* The Anisotropy of MHD Turbulence. Workshop Turbulence in Astrophysics, Schloss Ringberg 2002.

658. *Müller, W.-C.:* Complex Plasmas: Methods of Numerical Simulation. Ruhr-Universität Bochum 2002.

659. *Müller, W.-C.:* Magnetohydrodynamic Turbulence: Theory, Simulation, Reality. Universität Bayreuth 2002.

660. *Müller, W.-C.:* A New Time-Integration Algorithm for Ideal Magnetohydrodynamics. Conference on Computational Physics, San Diego,CA 2002.

661. *Müller, W.-C.:* Statistical Anisotropy of MHD Turbulence. IAEA Technical Meeting on Theory of Plasma Instabilities, Kloster Seeon 2002.

662. *Müller, W.-C.:* Subgrid Modelling in Magnetohydrodynamic Turbulence. Technische Universität Ilmenau 2002.

663. *Nagel, M. and F. Schauer:* Cooling of the W7-X Super-conducting Coils. 19th International Cryogenic Engineering Conference, Grenoble 2002.

664. *Naujoks, D.:* Computersimulation in der Plasmaphysik. Vorlesung, Humboldt-Universität Berlin, WS 2001/02; WS 2002/03.

665. *Neu, R.:* Magnetic Fusion with High-Z Plasma Facing Components. Seminar on "New Trends in Plasma Physics", IPP Garching 2002.

666. *Neu, R.:* Plasmaphysik und Fusionsforschung. Vorlesung, Universität Tübingen, SS 2002.

667. *Neu, R. and ASDEX Upgrade Team:* New Results of the Tungsten Programme in ASDEX Upgrade. 15th International Conference on Plasma Surface Interactions in Controlled Fusion Devices, Gifu 2002.

668. *Neu, R., K. Behringer, R. Dux, J. Gafert, A. Geier, B. Heger, A. Kallenbach, R. Pugno, T. Pütterich, S.-W. Yoon and ASDEX Upgrade Team:* Data Generation in Fusion Devices: Erosion Yields from Spectroscopy. IAEA Technical Meeting on Atomic and Plasma-Material Interaction Data for Fusion Science and Technology, Forschungszentrum Jülich 2002.

669. *Neu, R., T. Eich, J.C. Fuchs, A. Kallenbach, C. Maggi, V. Rohde, F. Ryter, J. Gafert, O. Gruber, G. Haas, A. Herrmann, M. Kaufmann, M. Laux, V. Mertens, H.W. Müller, J. Neuhauser, T. Pütterich, J. Stober, S.-W. Yoon and ASDEX Upgrade Team:* The ASDEX Upgrade Divertor IIb - a Closed Divertor for Strongly Shaped Plasmas. 19th IAEA Fusion Energy Conference, Lyon 2002.

670. N*eu, R., A. Geier, K. Krieger, H. Maier, R. Pugno, V. Rohde, R. Dux, O. Gruber, A. Kallenbach and ASDEX Upgrade Team:* Tungsten as Plasma Facing Material in ASDEX Upgrade. 1st International Workshop on Innovative Concepts for Plasma-Interactive Components in Fusion Devices, Osaka 2002.

671. *Neuhauser, J. and ASDEX Upgrade Team:* Diagnostic Requirements for Divertor Physics in Toroidal Magnetic Confinement Fusion. German-Polish Conference on Plasma Diagnostics for Fusion and Applications, Greifswald 2002.

672. *Neuner, U. and W7-X Diagnostics Team:* Conceptual Design Status of Wendelstein 7-X. German-Polish Conference on Plasma Diagnostics for Fusion and Applications, Greifswald 2002.

673. *Nishijima*, D., M.Y. Ye, N. Ohno* and S. Takamura*:* Incident Ion Energy Dependence of Bubble Formation on Tungsten Surface with Low Energy and High Flux Helium Plasma Irradiation. 15th International Conference on Plasma Surface Interactions in Controlled Fusion Devices, Gifu 2002.

674. *Nishimura, Y.:* Tokamak Edge Transport Studies by Turbulence and Divertor Codes. PPPL Theory Seminar, Princeton,NJ 2002.

675. *Nishimura, Y., D.P. Coster and B.D. Scott:* Tokamak Edge E_r Studies by Turbulence and Neoclassical Transport Models. 44th Annual Meeting of the Division of Plasma Physics, Orlando,FL (2002). Bulletin of the Americal Physical Society **47** (9), 178 (2002).

676. *Nishimura, Y., D.P. Coster and B.D. Scott:* Tokamak Edge Transport Studies by Turbulence and Divertor Codes. U.S. Transport Task Force Meeting, Annapolis,MD 2002.

677. *Noterdaeme, J.-M.:* Experimental Proposals for 2003 on JET in TF-H. JET, Abingdon 2002.

678. *Noterdaeme, J.-M.:* Full Power Coupling in ELMy H-Mode Plasmas in ASDEX Upgrade. Coordinating Committee on Fast Wave, Brussels 2002.

679. *Noterdaeme, J.-M.:* Heating on JET. 1st International Tokamak Physics Agreement Workshop on Energetic Particles, Heating and Steady State Operation, Naka 2002.

680. *Noterdaeme, J.-M.:* Heating on JET. NIFS, Toki 2002.

681. *Noterdaeme, J.-M.:* The JET Campaign C5 and Outline of the 2003 Experimental Programme. Coordinating Committee on Fast Wave, Brussels 2002.

682. *Noterdaeme, J.-M.:* Nuclear Reactor Theory II. Vorlesung, Interuniversity Graduate Programme in Nuclear Engineering, Belgian Nuclear Higher Education Network, WS 2002/2003.

683. *Noterdaeme, J.-M.:* Possible Contributions by IPP to ITER in the ICRF Area. Coordinating Committee on Fast Wave, Culham 2002.

684. *Noterdaeme, J.-M:* Summary of the 19th IAEA Fusion Energy Conference, Lyon, in the Area of Heating, Current Drive, Rotation and Energetic Particles and of the ITPA Meeting, Cadarache with a View on the JET Programme. JET, Abingdon 2002.

685. *Noterdaeme, J.-M.:* Theorie van de Kernreactor, Puntmodel. Vorlesung, University of Gent, WS 2002/2003.

686. *Noterdaeme, J.-M., R.V. Budny*, A. Cardinali*, C. Castaldo*, R. Cesario*, F. Crisanti*, J. DeGrassie*, D.A. D'Ippolito*, F. Durodié*, A. Ekedahl*, L.C. Ingesson*, E. Joffrin*, D. Hartmann, J.A. Heikkinen*, T. Hellsten*, T.T.C. Jones*, V. Kiptily*, P. Lamalle*, X. Litaudon*, F. Nguyen*, J. Mailloux*, M. Mantsinen*, M.L. Mayoral*, D. Mazon*, F. Meo, I. Monakhov*, J.R. Myra*, J. Pamela*, V. Pericoli*, O. Sauter*, Y. Sarazin*, S. Sharapov*, A.A. Tuccillo*, D. Van Eester* and Contributors to the EFDA-JET Work Programme:* Heating, Current Drive and Energetic Particles Studies on JET in Preparation of ITER Operation. 19th IAEA Fusion Energy Conference, Lyon 2002.

687. *Nührenberg, J.:* Alpha-Particle Confinement in Optimized Stellarators. Kinetic Theory Workshop, Greifswald 2002.

688. *Nührenberg, J.:* Comparison of Quasi-Axisymmetry and Quasi-Isodynamicity at 3 Periods. 13th International Stellarator Workshop, Canberra 2002.

689. *Nührenberg, J.:* Recent Developments in Stellarator Theory. Annual Meeting of the Swedish Research, Unit Gothenburg 2002.

690. *Ogorodnikova, O.V., M. Balden, E. Oyarzabal and J. Roth:* Calculation of Deuterium Retention and Release from Carbon. International Workshop on Hydrogen Isotopes in Fusion Reactor Materials, Tokyo 2002.

691. *Ongena*, J., P. Monier-Garbet*, W. Suttrop, P. Andrew*, M. Becoulet*, R.V. Budny*, Y. Corre*, J.G. Cordey*, P. Dumortier*, T. Eich, L. Garzotti*, D. Hillis*, J. Hogan*, L.C. Ingesson*, S. Jachmich*, E. Joffrin*, P.T. Lang, A. Loarte*, P.J. Lomas*, G. Maddison*, D.C. McDonald*, A. Messiaen*, M.F.F. Nave*, G. Saibene*, R. Sartori*, O. Sauter*, J. Strachan*, B. Unterberg*, M. Valovic*, I. Voitsekhovitch*, M. von Hellermann*, B. Alper*, Yu. Baranov*, M. Beurskens*, G. Bonheure*, J. Brzozowski*, J. Bucalossi*, M. Brix*, M. Charlet*, I. Coffey*, M. DeBaar* , P. De Vries*, C. Giroud*, C. Gowers*, N.C. Hawkes*, G. Jackson*,C. Jupen*, A. Kallenbach, H.R. Koslowski*, K. Lawson*, M. Mantsinen*, G.F. Matthews*, F. Milani*, M. Murakami*, A. Murari*, R. Neu, V. Parail*, S. Podda*, M.E. Puiatti*, J. Rapp*, E. Righi*, F. Sartori*, Y. Sarazin*, A. Stäbler, M. Stamp*, G. Telesca*, M. Valisa*, B. Weyssow*, K.-D. Zastrow* and Contributors to the EFDA-JET Work Programme:* Towards the Realization on JET of an Integrated H-Mode Scenario for ITER. 19th IAEA Fusion Energy Conference, Lyon 2002.

692. *Ordás*, N., E. Oyarzabal, C. García-Rosales*, J. Echeberria*, M. Balden and S. Lindig:* Mejora de las Propiedades Termomecánicas de Trafito Isótropo, Elaborado a Partir de Mesofase Carbonosa, Mediante la Adición de Carburos. VII Congreso Nacional de Materiales, Madrid 2002.

693. *Oyarzabal, E., M. Balden, E. de Juan Pardo, K. Durocher*, J. Roth and C. García-Rosales*:* Deuterium Retention by Implantation in Carbide-Doped Graphites. 15th International Conference on Plasma Surface Interactions in Controlled Fusion Devices, Gifu 2002.

694. *Pasch, E. and J. Ehlbeck*:* Detailed Temperature Measurements of a Microwave Excited Plasma Jet by Using Coherent Anti-Stokes Raman Scattering (CARS). German-Polish Conference on Plasma Diagnostics for Fusion and Applications, Greifswald 2002.

695. *Pautasso, G., S. Egorov, K.-H. Finken*, O. Gruber, A. Herrmann, J.C. Fuchs, M. Maraschek, G. Neu, Y. Nakamura, V. Rohde, A. Savtchkov*, S. Schweizer, U. Seidel, B. Streibl, C. Tichmann and ASDEX Upgrade Team:* Disruption Studies on ASDEX Upgrade. 19th IAEA Fusion Energy Conference, Lyon 2002.

696. *Pautasso, G., B. Streibl, U. Seidel, Y. Nakamura and ASDEX Upgrade Team:* ASDEX Upgrade - Disruption Studies. Large Tokamak Workshop (W49), US/Japan MHD Workshop and ITPA on MHD, Naka 2002.

697. *Peeters, A.G., F. Ryter and G. Tardini:* Current Understanding of Heat Transport in Fusion Plasma. Verhandl. DPG (VI) **37**, 20, P II (2002).

698. *Peeters, A.G., A.C.C. Sips, E. Quigley, O. Gruber, V. Igochine, P.J. McCarthy, F. Ryter, R. Wolf and ASDEX Upgrade Team:* Internal Transport Barriers in ASDEX Upgrade. 19th IAEA Fusion Energy Conference, Lyon 2002.

699. *Pinches, S.D.:* RWMs as a Beta Limit in Tokamaks: Experimental Results and Proposals. 10th European Fusion Physics Workshop, Vaals 2002.

700. *Pitcher*, C.S., X. Bonnin, C.J. Boswell*, B. LaBombard*, B. Lipschultz*, R. Schneider and J.L. Terry*:* Large Scale Poloidal Circulation in the Scrape-off-Layer of Alcator C-Mod. 15th International Conference on Plasma Surface Interactions in Controlled Fusion Devices, Gifu 2002.

701. *Pitts*, R.A., P. Andrew*, Y. Andrew*, B. Becoulet*, I. Coffey*, D.P. Coster, D.C. McDonald*, T. Eich, K. Erents*, M. Fenstermacher*, W. Fundamenski*, J. Gafert, G. Haas, A. Herrmann, C. Hidalgo*, D. Hillis*, A. Huber*, L.C. Ingesson*, S. Jachmich*, A. Kallenbach, A. Korotkov*, K. Lawson*, P.J. Lomas*, T. Loarer*, A. Loarte*, G.F. Matthews*, G. McCracken*, A. Meigs*, P. Mertens*, M.G. O'Mullane*, V. Philipps*, G. Porter*, A. Pospieszczyk*, J. Rapp*, D. Reiter*, V. Riccardo*, G. Saibene*, R. Sartori*, M. Stamp*, E. Tsitrone*, M. Wischmeier* and Contributors to the EFDA-JET Work Programme:* Comparing Scrape-off Layer and Divertor Physics in JET Pure He and D Discharges. 15th International Conference on Plasma Surface Interactions in Controlled Fusion Devices, Gifu 2002.

702. *Poli, E., A.G. Peeters, A. Bergmann, S. Günter and S.D. Pinches:* Monte Carlo δf Simulation of the Current Driving the Neoclassical Tearing Mode. IAEA Technical Meeting on Theory of Plasma Instabilities, Kloster Seeon 2002.

703. *Poli, E., A.G. Peeters, A. Bergmann, S. Günter and S.D. Pinches:* Monte Carlo δf Simulation of the Current Driving the Neoclassical Tearing Mode. Kolloquium, CEA Cadarache 2002.

704. *Poli, E., A.G. Peeters, A. Bergmann, S. Günter and S.D. Pinches:* Neoclassical Tearing Mode Simulations. Kinetic Theory Workshop, Greifswald 2002.

705. *Popescu, C.:* Processing and Microstructure of Cu-SiC Metal-Matrix Composites. 1st HGF Young Scientist Colloquium "Materials for Fusion Devices", Forschungszentrum Jülich 2002.

706. *Popescu, C., A. Brendel and G. Matern:* Processing and Microstructure of Cu-SiC Metal-Matrix Composites. Technische Universität München 2002.

707. *Pospieszczyk*, A., B. Schweer*, V. Philipps*, A. Huber*, G. Sergienko*, U. Samm*, H. Reimer*, M. Freisinger*, M. Rubel*, A. Hermann*, S. Kötterl, H. Renner and H. Bolt:* B_4C-Limiter Experiments at TEXTOR. 15th International Conference on Plasma Surface Interactions in Controlled Fusion Devices, Gifu 2002.

708. *Pütterich, T., R. Dux, J. Gafert, R. Pugno, K. Behringer and ASDEX Upgrade Team:* Untersuchungen des Kohlenstoffzuflusses von den Schutzlimitern in ASDEX Upgrade. Verhandl. DPG (VI) **37**, 42, P.23.10 (2002).

709. *Radtke, R.:* Spektroskopische Untersuchungen von hochgeladenen Ionen mit EBIT. Kolloquium, Institut für Plasmaforschung, Universität Stuttgart 2002.

710. *Radtke, R., C. Biedermann and P. Bachmann:* Sawtooth-Like X-Ray Emission Observed in EBIT. 11th International Conference on the Physics of Highly Charged Ions, Caen 2002.

711. *Rapp*, J., D.C. McDonald*, T. Eich, W. Fundamenski*, M. von Hellermann*, L.C. Ingesson*, S. Jachmich*, A. Loarte*, G.F. Matthews*, V. Philipps*, G. Saibene*, R. Sartori* and Contributors to the EFDA-JET Work Programme:* Strongly Radiating Type-III ELMy H-Mode: An Operating Scenario for ITER. IEA Workshop on ELMs, Culham Science Centre, Abingdon 2002.

712. *Rapp*, J., P. Monier-Garbet*, P. Andrew*, P. Dumortier*, T. Eich, W. Fundamenski*, M. von Hellermann*, J. Hogan*, L.C. Ingesson*, S. Jachmich*, H.R. Koslowski*, A. Loarte*, G. Maddison*, G.F. Matthews*, D.C. McDonald*, A. Messiaen*, J. Ongena*, V. Parail*, V. Philipps*, G. Saibene*, R. Sartori*, B. Unterberg* and Contributors to the EFDA-JET Work Programme:* Reduction of Divertor Heat Load in JET ELMy H-Modes Using Impurity Seeding Techniques. 19th IAEA Fusion Energy Conference, Lyon 2002.

713. *Raupp, G., R. Cole*, K. Behler, M. Fitzek*, P. Heimann, A. Lohs, K. Lüddecke*, G. Neu, J. Schacht, W. Treutterer, D. Zasche, T. Zehetbauer, M. Zilker and ASDEX Upgrade Team:* A Universal Time System for ASDEX Upgrade. 22nd Symposium on Fusion Technology, Helsinki 2002.

714. *Reetz, J., P. Heimann, S. Heinzel, C. Hennig, H. Kroiss, G. Kühner, H. Kühntopf, J. Maier and M. Zilker:* Bilddatenerfassung am W7-X-Experiment. Gemeinsames Kolloquium IWF Universität Rostock und IPP Greifswald, Universität Rostock 2002.

715. *Reich, J., W. Gardebrecht, B. Hein, B. Missal, F. Starke and K.-U. Seidler:* Manufacture of Cryostat Components for Wendelstein 7-X. 22nd Symposium on Fusion Technology, Helsinki 2002.

716. *Reich, M., P.T. Lang, V. Mertens, H.W. Müller, J. Neuhauser, K.F. Renk* and ASDEX Upgrade Team:* First Approach for a HFS-Pellet Penetration Scaling at ASDEX Upgrade. Verhandl. DPG (VI) **37**, 36, P 22.1 (2002).

717. *Renner, H., J. Boscary, H. Greuner, H. Grote, D. Hildebrandt, J. Kisslinger, R. Schneider and D. Sharma:* Divertor Concept for the Wendelstein 7-X Stellarator: Theoretical Studies of the Boundary and Engineering. 19th IAEA Fusion Energy Conference, Lyon 2002.

718. *Renner, H., J. Boscary, H. Grote, R. Schneider, D. Sharma, J. Kisslinger and E. Strumberger:* Theoretical Basis for the Design of the Divertor for the Stellarator Wendelstein 7-X. 3rd IAEA Technical Committee Meeting on Steady-State Operation of Magnetic Fusion Devices, Greifswald and Arles 2002.

719. *Reusch, R., B. Koch, H. Beyer*, P. Kornejew and W. Bohmeyer:* He-I Recombination into the Metastable 2^3S State in the Vicinity of a Material Surface. Verhandl. DPG (VI) **37**, 42, P23.12 (2002).

720. *Richter, S.:* Das WZU-Projekt "Nachhaltige Energieversorgung für die Stadt Augsburg". Institut für Physik, Augsburg 2002.

721. *Riemann, J., M. Borchardt, R. Schneider, X. Bonnin, A. Mutzke, T. Rognlien* and M. Umansky*:* Hierarchy Tests of Edge Transport Models (BoRiS, UEDGE). 15th International Conference on Plasma Surface Interactions in Controlled Fusion Devices, Gifu 2002

722. *Rißе, K., T. Rummel, L. Wegener, R. Holzthüm, N. Jaksic, F. Kerl and J. Sapper:* Fabrication of the Superconducting Coils for Wendelstein 7-X. 3rd IAEA Technical Committee Meeting on Steady-State Operation of Magnetic Fusion Devices, Greifswald and Arles 2002.

723. *Rißе, K., T. Rummel, L. Wegener, R. Holzthüm, N. Jaksic, F. Kerl and J. Sapper:* Fabrication of the Superconducting Coils for Wendelstein 7-X. 22nd Symposium on Fusion Technology, Helsinki 2002.

724. *Rohde, V., M. Mayer and ASDEX Upgrade Team:* Characterisation and Formation of a-C:D Layers below the Divertor of ASDEX Upgrade. International Workshop on Hydrogen Isotopes in Fusion Reactor Materials, Tokyo 2002.

725. *Rohde, V., M. Mayer and ASDEX Upgrade Team:* On the Formation of a-C:D Layers and Parasitic Plasmas Underneath the Roof Baffle of the ASDEX Upgrade Divertor. 15th International Conference on Plasma Surface Interactions in Controlled Fusion Devices, Gifu 2002.

726. *Rohde, V., R. Neu, R. Dux, A. Geier, R. Pugno, X. Gong, A. Kallenbach, K. Krieger, H. Maier, H.W. Müller, W. Schneider and ASDEX Upgrade Team:* Operation of ASDEX Upgrade with Tungsten Coated Walls. 19th IAEA Fusion Energy Conference, Lyon 2002.

727. *Rohde, V., R. Neu, A. Geier, H. Maier, K. Krieger, R. Pugno and ASDEX Upgrade Team:* Wolfram als Wandmaterial im Tokamak ASDEX Upgrade. Verhandl. DPG (VI) **37**, 22, P6.1 (2002).

728. Ros*signol*, J. and H. Bolt:* Arcing at B4C-Covered Limiters Exposed to a SOL-Plasma. 15th International Conference on Plasma Surface Interactions in Controlled Fusion Devices, Gifu 2002.

729. *Roth, J.:* Erosion Behaviour and Location of Sources and Sinks. EFDA Task Force on Plasma-Wall Interaction, Augsburg 2002.

730. *Roth, J.:* Plasma-Wall Interaction at IPP Garching. University of California, San Diego,CA 2002.

731. *Roth, J.:* Plasma-Wall Interaction Studies at IPP Garching on Tritium Inventory in Future Fusion Devices. IPP Hefei 2002.

732. *Roth, J., O.V. Ogorodnikova and M. Mayer:* Deuterium Retention in W in Dependance of Surface Conditions. Workshop on Tritium in Fusion Devices, IAEA Vienna 2002.

733. *Rozhansky*,V., E. Kaveeva*, S. Voskoboynikov*, A. Beckheit*, D.P. Coster, X. Bonnin and R. Schneider:* Impact of *E x B* Drifts on the Distribution of Impurities in the Tokamak Plasma Edge. 15th International Conference on Plasma Surface Interactions in Controlled Fusion Devices, Gifu 2002.

734. *Rubel*, M., V. Philipps*, T. Tanabe*, P. Wienhold*, M. Freisinger*, W. Jacob, J. Linke*, J. von Seggern* and E. Wessel*:* Thick Co-Deposits and Dust in Controlled Fusion Devices with Carbon Walls: Fuel Inventory and Growth Rate of Co-Deposited Layers. International Workshop on Hydrogen Isotopes in Fusion Reactor Materials, Tokyo 2002.

735. *Rummel, T., F. Füllenbach and T. Mönnich:* Power Supplies for the Wendelstein 7-X Stellarator. 22nd Symposium on Fusion Technology, Helsinki 2002.

736. *Runov, A.M., S.V. Kasilov*, D. Reiter*, N. McTaggart, X. Bonnin and R. Schneider:* Transport in Complex Magnetic Geometries: 3-Dimensional Modelling of Ergodic Edge Plasmas in Fusion Experiments. 15th International Conference on Plasma Surface Interactions in Controlled Fusion Devices, Gifu 2002.

737. *Runov, A.M., S.V. Kasilov*, D. Reiter* and W7-X Theory Group:* 3D Monte-Carlo Code E3D: Stellarator Edge Modelling. IEA-DED and IEA-TEXTOR Workshop, Jülich 2002.

738. *Ryter, F. and ASDEX Upgrade Team:* New Power Threshold Data from ASDEX Upgrade. 3rd International Tokamak Physics Agreement Workshop of Confinement Database and Modelling Topical Group, Cadarache 2002.

739. *Ryter, F. and ASDEX Upgrade Team:* Pedestal and Temperature Profile Behaviour in ASDEX Upgrade. 3rd International Tokamak Physics Agreement Workshop of Confinement Database and Modelling Topical Group, Cadarache 2002.

740. *Ryter, F., R. Dux, J. Hobirk, K. Kirov, F. Leuterer, R. Neu, A.G. Peeters, G. Pereverzev, J. Stober, W. Suttrop, G. Tardini and ASDEX Upgrade Team:* A Selection of Experiments with ECH in ASDEX Upgrade. Seminar, Centre de Recherche en Physique des Plasmas, Lausanne 2002.

741. *Ryter, F., F. Leuterer, F. Imbeaux*, P. Mantica*, A.G. Peeters, G. Pereverzev, J. Stober, W. Suttrop, G. Tardini and ASDEX Upgrade Team:* Untersuchung des Elektronenwärmetransports an Fusions-plasmen im Tokamak ASDEX Upgrade. Physikalisches Kolloquium, Universität Kiel 2002.

742. *Ryter, F., W. Suttrop, H.-U. Fahrbach, K. Kirov, F. Leuterer, A.G. Peeters, G. Pereverzev, G. Tardini and ASDEX Upgrade Team:* Diagnosing Electron Heat Transport in ASDEX Upgrade with ECH Power Modulation. 11th International Conference of Plasma Physics, Sydney 2002.

743. *Ryter, F., G. Tardini, F. De Luca*, H.-U. Fahrbach, F. Imbeaux*, A. Jacchia*, K. Kirov, F. Leuterer, P. Mantica*, A.G. Peeters, G. Pereverzev, W. Suttrop and ASDEX Upgrade Team:* Electron Heat Transport in ASDEX Upgrade: Experiment and Modelling. 19th IAEA Fusion Energy Conference, Lyon 2002.

744. *Ryter, F. and Threshold Data Base Group*:* Status of the International Global Database for the H-Mode Power Threshold. 2nd International Tokamak Physics Agreement Workshop of Confinement Database and Modelling Topical Group, Princeton,NJ 2002.

745. *Sallander, E.:* Effects of Toroidal Net Currents on the Stability in W7-AS. MHD Seminar, Garching 2002.

746. *Sallander, E., S. Klose, S. Mohr and A. Weller:* X-Ray Diagnostics on the Wendelstein-7 Stellarators. German-Polish Conference on Plasma Diagnostics for Fusion and Applications, Greifswald 2002.

747. *Sardei, F.:* Magnetohydrodynamik. Vorlesung, Universität der Bundeswehr München, FT 2002.

748. *Sardei, F.:* Rechneranwendungen in der Fluiddynamik. Vorlesung, Universität der Bundeswehr München, WT 2001/2002.

749. *Schauer, F.:* Der Aufbau des Fusionsexperiments Wendelstein 7-X. Physikalisches Kolloquium, Technische Universität Graz und Karl-Franzens Universität Graz 2002.

750. *Schauer, F., H. Bau, Y. Bozhko, R. Brockmann, M. Nagel, M. Pietsch and S. Raatz:* Cryotechnology for Wendelstein 7-X. 22nd Symposium on Fusion Technology, Helsinki 2002.

751. *Schild*, T., L. Genini*, M. Jacquemet*, A. Hölting, T. Rummel and L. Wegener:* W7-X Demo Coil Cryogenic Tests in the CEA/Saclay Test Facility. Applied Superconductivity Conference, Houston,TX 2002.

752. *Schneider, R.:* Computational Physics. Universität Greifswald, WS 2002.

753. *Schneider, R.:* Edge Physics in Fusion Plasmas. Universität Greifswald, WS 2001/2002.

754. *Schneider, R.:* Die Plasmarandschicht in Fusionsplasmen - ein Beispiel für ein Vielskalenproblem. Kolloquium, Universität Kiel 2002.

755. *Schneider, R.:* Quantencomputer - Methoden und Algorithmen. Universität Greifswald, SS 2002.

756. *Schneider, R., X. Bonnin, N. McTaggart, A.M. Runov, M. Borchardt, J. Riemann, A. Mutzke, K. Matyash, H. Leyh, M. Warrier, A. Pulss, D.P. Coster, W. Eckstein, R. Dohmen, T. Rognlien* and M. Umansky*:* Comprehensive Suite of Codes for Plasma-Edge Modelling. Conference on Computational Physics, San Diego,CA 2002. Bulletin of American Physical Society **47** (9), 33 (2002).

757. *Schröder, C., O. Grulke and T. Klinger:* Untersuchungen von Driftwellen in einer Helikonentladung. Verhandl. DPG (VI) **37**, 33, P21.14 (2002).

758. *Schröder, D., W. Bohmeyer, U. Wenzel and B. Koch:* Comparison of Electron Temperature Measurements Applying Langmuir Probes and Passive Spectroscopy. Verhandl. DPG (VI) **37**, 38, P22.15 (2002).

759. *Schubert, M.:* Fast Swept Langmuir Probes and Heat Transport in Wendelstein 7-AS. International Max Planck Research School "Bounded Plasmas", Universität Greifswald 2002.

760. *Schwarz-Selinger, T., M. Bauer, C. Hopf, M. Meier, W. Jacob and A. von Keudell:* Quantifizierte Teilchenstrahlexperimente niederenergetischer Ionen und thermischer Radikale zur Identifizierung mikroskopischer Wachstums- und Erosionsmechanismen. Verhandl. DPG (VI) **37**, 512, SYPO-II (2002).

761. *Schweinzer, J.:* Plasmaphysik I. Vorlesung, Universität Ulm, WS 2002/03.

762. *Sihler, C., M. Huart, C.-P. Käsemann, B. Streibl and ASDEX Upgrade Team:* Operational Experience with Reactive Power Control Methods Optimized for Tokamak Power Supplies. 22nd Symposium on Fusion Technology, Helsinki 2002.

763. *Sihler, C., M. Huart, F. Stobbe, B. Streibl, W. Treutterer and A. Joswig:* Excitation of Torsional Oscillations in Generator Shaft Methods. 22nd Symposium on Fusion Technology, Helsinki 2002.

764. *Simon-Weidner, J. and N. Jaksic:* Buckling Analysis of the Complete W7-X Plasma Vessel. Poster J-25, 22nd Symposium on Fusion Technology, Helsinki 2002.

765. *Sips, A.C.C.:* H-Mode Discharge Control at ASDEX Upgrade. 10th European Fusion Physics Workshop, Vaals 2002.

766. *Sips, A.C.C.:* Physics of ITB's: Recent Results from Experiments. 9th EU-US Transport Task Force Workshop, Cordoba 2002.

767. *Solano*, E., P. Andrew*, F. Villone*, G. Calabro*, A. Loarte*, G.F. Matthews*, M. De Baar*, M. Beurskens*, T. Eich, N.C. Hawkes*, J. Conboy*, F. Sartori*, M. Stamp*, A. Kallenbach and Contributors to the EFDA-JET Work Programme:* ELMs, Plasma Current Loss and Movement of Strike Points. 44th Annual Meeting of the Division of Plasma Physics, Orlando,FL (2002). Bulletin of the American Physical Society **47** (9), 326 (2002).

768. *Sorge, S. and R. Hatzky:* Calculation of ITG Driven Modes in Pinch Configurations via Gyrokinetic Simulation of the Plasma Ions and Electrons. IAEA Technical Meeting on Theory of Plasma Instabilities, Kloster Seeon 2002.

769. *Speth, E.:* Proposal for the Development of an RF Source for ITER NBI. Coordinating Committee on Neutral Beams, Schloss Ringberg 2002.

770. *Speth, E., M. Bandyopadhyay, A. Encheva, P. Franzen, B. Heinemann, C. Hu, W. Kraus, P. McNeely, R. Riedl, A. Tanga and R. Wilhelm:* Progress on the Development of a D-RF Source for ITER NBI. Coordinating Committee on Neutral Beams Meeting, JET, Abingdon 2002.

771. *Spring, A., R. Brakel and H. Niedermeyer:* Wall Conditioning for Wendelstein 7-X by Glow Discharge. 22nd Symposium on Fusion Technology, Helsinki 2002.

772. *Stache, K., F. Kerl, J. Sapper, B. Sombach and L. Wegener:* The Superconducting Busbar System of Wendelstein 7-X. 22nd Symposium on Fusion Technology, Helsinki 2002.

773. *Stark, A., C.M. Franck, O. Grulke and T. Klinger:* Beobachtung ionenakustischer Wellen in verschiedenen Entladungen. Verhandl. DPG (VI) **37**, 33, P21.13 (2002).

774. *Starke, P., U. Fantz and K. Behringer:* Elektronendichte und Energieverteilungsfunktion in planar induktiv gekoppelten HF-Plasmen. Verhandl. DPG (VI) **37**, 23, P7.3 (2002).

775. *Starke, P., S. Meir, M. Balden, U. Fantz and K. Behringer:* Chemische Erosion dotierter Kohlenstoff-Materialien in Niederdruckplasmen. Verhandl. DPG (VI) **37**, 42, P23.9 (2002).

776. *Stober, J., R. Dux, O. Gruber, L.D. Horton, P.T. Lang, R. Lorenzini*, C. Maggi, F. Meo, R. Neu, J.-M. Noterdaeme, A.G. Peeters, G. Pereverzev, F. Ryter, A.C.C. Sips, A. Stäbler, H. Zohm and ASDEX Upgrade Team:* Dependence of Particle Transport on Heating Profiles in ASDEX Upgrade. 19th IAEA Fusion Energy Conference, Lyon 2002.

777. *Streibl, B., N. Berger, U. Brendel, T. Härtl, V. Rohde and G. Schall:* Hydrogen Frosting Scenarios with the ASDEX Upgrade In-Vessel Cryo Pump. 22nd Symposium on Fusion Technology, Helsinki 2002.

778. *Suttrop, W., L.D. Horton, A. Hubbard*, D.C. McDonald*, R. Barnsley*, M. Beurskens*, P. Bonoli*, J.M. Chareau*, J.G. Cordey*, J.W. Hughes*, P.J. Lomas*, G. Maddison*, A. Meigs*, F. Meo, D. Mossessian*, R. Neu, J.-M. Noterdaeme, V. Parail*, F. Ryter, J. Schweinzer, M. Stamp*, J. Strachan*, J. Stober, S. Wukitch*, ASDEX Upgrade Team, ALCATOR C-Mod Team and Contributors to the EFDA-JET Work Programme:* Parameter Similarity Studies in JET, ASDEX Upgrade and ALCATOR C-Mod. 19th IAEA Fusion Energy Conference, Lyon 2002.

779. *Svensson, J., M. von Hellermann* and R. König:* High Precision Measurement of Fuel Density Profiles in Nuclear Fusion Plasmas. International Conference on Artificial Neural Networks, Madrid 2002.

780. *Tanga, A.:* Diagnostic Studies for a Negative Ion Source. Coordinating Committee on Neutral Beams Meeting, JET, Abingdon 2002.

781. *Tasso, H. and G.N. Throumoulopoulos*:* A Possible Dynamical Stabilization of the Wall Mode. IAEA Technical Meeting on Theory of Plasma Instabilities, Kloster Seeon 2002.

782. *Tasso, H. and G.N. Throumoulopoulos*:* Two-Step Control of Wall Mode and the Monodromy Matrix. 44th Annual Meeting of the Division of Plasma Physics, Orlando,FL 2002. Bulletin of the American Physical Society **47** (9), 118 (2002).

783. *Thomsen, H.:* A Dynamics Investigation into Edge Plasma Turbulence. Promotionskolloquium, Universität Greifswald 2002.

784. *Thomsen, H., F. Gadelmeier, M. Hirsch, R. König, J. Lingertat and K. McCormick:* Transport due to Edge Localized Modes in the Wendelstein 7-AS Stellarator. 9th EU-US Transport Task Force Workshop, Cordoba 2002.

785. *Thomsen, H., T. Klinger and M. Endler:* Active Probing Experiments in Wendelstein 7-AS. Verhandl. DPG (VI) **37**, 24, P9.4 (2002).

786. *Thomsen, H. and R. König:* Characterization of Fast Phenomena in the Plasma Boundary of the Wendelstein 7-AS Stellarator by Means of Visible Imaging. 5th Workshop on the Role of Electric Fields in Plasma Confinement and Exhaust, Montreux 2002.

787. *Throumoulopoulos*, G.N. and H. Tasso:* On Axisymmetric Resistive Equilibria with Flow Free of Pfirsch-Schlüter Diffusion. 44th Annual Meeting of the Division of Plasma Physics, Orlando,FL 2002. Bulletin of the American Physical Society **47** (9), 254 (2002).

788. *Toi*, K., S. Ohdachi*, S. Yamamoto*, N. Nakajima*, S. Sakakibara*, K.Y. Watanabe*, S. Inagaki*, Y. Nagayama*, Y. Narushima*, H. Yamada*, K. Narihara*, S. Morita*, T. Akiyama*, N. Ashikawa*, X. Ding*, M. Emoto*, H. Funaba*, M. Goto*, K. Ida*, H. Idei*, T. Ido*, K. Ikeda*, S. Imagawa*, M. Isobe*, K. Itoh*, O. Kaneko*, K. Kawahata*, T. Kobuchi*, A. Komori*, S. Kubo*, A. Kumazawa*, J. Li*, Y. Liang*, S. Masuzaki*, T. Mito*, J. Miyazawa*, T. Morisaki*, S. Murakami, S. Muto*, T. Mutoh*, K. Nagaoka*, Y. Nakamura, H. Nakanishi*, K. Nishimura*, A. Nishizawa*, N. Noda*, T. Notake*, K. Ohkubo*, I. Ohtake*, N. Ohyabu*, Y. Oka*, S. Okamura*, T. Ozaki*, B.J. Peterson*, A. Sagara*, T. Saida*, K. Saito*, R. Sakamoto*, M. Sasao*, K. Sato*, T. Sato*, T. Satow*, T. Seki*, T. Shimozuma*, M. Shoji*, S. Sudo*, M.Y. Tanaka*, N. Tamura*, K. Tanaka*, K. Tsumori*, T. Uda*, T. Watari*, A. Weller, Y. Xu*, M. Yamada*, M. Yokoyama*, S. Yoshimura*, Y. Yoshimura*, K. Yamazaki*, K. Matsuoka*, O. Motojima*, Y. Hamada* and M. Fujiwara*:* MHD Instabilities and Their Effects on Plasma Confinement in the Large Helical Device Plasmas. 19th IAEA Fusion Energy Conference, Lyon 2002.

789. *Toussaint, U. von:* ECE Analysis with Bayesian Probability Theory. 2nd Workshop on Fusion Data Processing, Greifswald 2002.

790. *Treutterer, W., K. Behler, R. Cole*, J. Hobirk, M. Jakobi, A. Lohs, K. Lüddecke*, G. Neu, G. Raupp, W. Suttrop, D. Zasche, T. Zehetbauer, M. Zilker and ASDEX Upgrade Team:* The New ASDEX Upgrade Real-Time Control and Data Acquisition System. 22nd Symposium on Fusion Technology, Helsinki 2002.

791. *Tsitrone*, E., M. Wischmeier* and Contributors to the EFDA-JET Work Programme:* An Overview of JET Edge Modelling Activities. 15th International Conference on Plasma Surface Inter-actions in Controlled Fusion Devices, Gifu 2002.

792. *Villard*, L., S.J. Allfrey*, A. Bottino*, M. Brunetti*, G.L. Falchetto*, V. Grandgirard*, R. Hatzky, J. Nührenberg, A.G. Peeters, O. Sauter*, S. Sorge and J. Vaclavik*:* Full Radius Linear and Nonlinear Gyrokinetic Simulations for Tokamaks and Stellarators: Zonal Flows, Applied *E x B* Flows, Trapped Electrons and Finite Beta. 19th IAEA Fusion Energy Conference, Lyon 2002.

793. *Volpe*, F., H.P. Laqua and W7-AS Team:* Electron Bernstein Emission Diagnostic of Electron Temperature Profiles at W7-AS Stellarator. German-Polish Conference on Plasma Diagnostics for Fusion and Applications, Greifswald 2002.

794. *Wagner, D., K. Kirov, F. Leuterer, F. Monaco, M. Münich, H. Schütz, F. Ryter, R. Wilhelm, H. Zohm, T. Franke, K. Voigt, M. Weißgerber, M. Thumm*, R. Heidinger*, G. Dammertz*, K. Koppenburg*, W. Kasparek*, G. Gantenbein*, H. Hailer*, G. Müller*, A. Bogdashov*, G.G. Denisov*, V. Kurbatov*, A. Kuftin*, A. Litvak*, S. Malygin*, E. Tai* and V. Zapevalov*:* Plans for the New ECRH System of ASDEX Upgrade. 14th Joint Russian-German Meeting on ECRH and Gyrotrons, Nizhny Novgorod/Moscow 2002.

795. *Wagner, D., F. Leuterer, K. Kirov, F. Monaco, M. Münich, H. Schütz, F. Ryter, R. Wilhelm, H. Zohm, T. Franke, K. Voigt, M. Weißgerber, M. Thumm*, R. Heidinger*, G. Dammertz*, K. Koppenburg*, W. Kasparek*, G. Gantenbein*, H. Hailer*, G. Müller*, A. Bogdashov*, G.G. Denisov*, V. Kurbatov*, A. Kuftin*, A. Litvak*, S. Malygin*, E. Tai* and V. Zapevalov*:* A New ECRH System for ASDEX Upgrade. 6th International Workshop on ECRH Transmission Systems, San Diego,CA 2002.

796. *Wagner, D., F. Leuterer and M. Münich:* A Tuneable Double Disk Window. 14th Joint Russian-German Meeting on ECRH and Gyrotrons, Nizhny Novgorod/Moscow 2002.

797. *Wagner, F.:* Development of the Wendelstein Stellarator Line. Board of Councilors Meeting, Tokyo 2002.

798. *Wagner, F.:* Development of the Wendelstein Stellarator Line. EU-Veranstaltung, Brüssel 2002.

799. *Wagner, F.:* Development of the Wendelstein Stellarator Line. 13th International Stellarator Workshop, Canberra 2002.

800. *Wagner, F.:* Die Entwicklung der Wendelstein Stellarator Linie. Kolloquium, Forschungszentrum Jülich 2002.

801. *Wagner, F.:* Kernfusion als nachhaltige Energiequelle - eine Kopie der Sonne? Kolloquium, Dechema Frankfurt 2002.

802. Wagner, F.: Major Results from Wendelstein 7-AS. Opening Ceremony of the HL-2A, Chengdu 2002.

803. *Wagner, F.:* Über das Sternenfeuer. Salon Szczecinski Stettin 2002.

804. *Wagner, F.:* The Wendelstein-7-X Project in Greifswald. Technische Universität Stettin 2002.

805. *Wagner, F., R. Burhenn, F. Gadelmeier, J. Geiger, M. Hirsch, H.P. Laqua, A. Weller, A. Werner, S. Bäumel, J. Baldzuhn, R. Brakel, A. Dinklage, P. Grigull, M. Endler, V. Erckmann, H. Ehmler, Y. Feng, R. Fischer, F. Gadelmeier, L. Giannone, H.-J. Hartfuß, D. Hildebrandt, E. Holzhauer, Y. Igitkhanov, R. Jaenicke, M. Kick, A. Kislyakov*, A. Kreter, J. Kisslinger, T. Klinger, S. Klose, J.-P. Knauer, R. König, G. Kühner, H. Maaßberg, K. McCormick, R. Narayanan, D. Naujoks, H. Niedermeyer, C. Nührenberg, E. Pasch, N. Rust, E. Sallander, F. Sardei, U. Wenzel, H. Wobig, E. Würsching, M. Zarnstorff*, S. Zoletnik* and W7-AS Team:* Major Results from Wendelstein 7-AS Stellarator. 44th Annual Meeting of the Division of Plasma Physics, Orlando,FL 2002. Bulletin of the American Physical Society **47** (9), 91 (2002).

806. *Wagner, F., R. Burhenn, F. Gadelmeier, J. Geiger, M. Hirsch, H.P. Laqua, A. Weller, A. Werner, S. Bäumel, J. Baldzuhn, R. Brakel, A. Dinklage, P. Grigull, M. Endler, V. Erckmann, H. Ehmler, Y. Feng, R. Fischer, L. Giannone, H.-J. Hartfuß, D. Hildebrandt, E. Holzhauer, Y. Igitkhanov, R. Jaenicke, M. Kick, A. Kislyakov*, A. Kreter, J. Kisslinger, T. Klinger, S. Klose, J.-P. Knauer, R. König, G. Kühner, H. Maaßberg, K. McCormick, R. Narayanan, D. Naujoks, H. Niedermeyer, C. Nührenberg, E. Pasch, N. Rust, E. Sallander, F. Sardei, U. Wenzel, H. Wobig, E. Würsching, M. Zarnstorff*, S. Zoletnik* and W7-AS Team:* Major Results from Wendelstein 7-AS Stellarator. 19th IAEA Fusion Energy Conference, Lyon 2002.

807. *Wanner, M.:* Status of Construction of the Wendelstein 7-X Stellarator. German-Polish Conference on Plasma Diagnostics for Fusion and Applications, Greifswald 2002.

808. *Wanner, M. and the W7-X Construction Team:* Status of Wendelstein 7-X Construction. 19th IAEA Fusion Energy Conference, Lyon 2002.

809. *Wegener, L., A. Benndorf, T. Bräuer, K. Liesenberg*, H. Schneider and K. Stache:* The Assembly of W7-X - an Overview. 22nd Symposium on Fusion Technology, Helsinki 2002.

810. *Weidl, I.:* Erste Erfahrungen mit IBM Power4 Systemen. AIX Arbeitskreis, Heidelberg 2002.

811. *Weller, A.:* Experiments Close to the Beta-Limit in W7-AS. 1st IPP MHD Seminar, Heisenberg-Zentrum Garching 2002.

812. *Weller, A., J. Geiger, M. Zarnstorff*, E. Sallander, S. Klose, A. Werner, J. Baldzuhn, R. Brakel, R. Burhenn, H. Ehmler, F. Gadelmeier, L. Giannone, P. Grigull, D. Hartmann, R. Jaenicke, J.-P. Knauer, H.P. Laqua, C. Nührenberg, E. Pasch, N. Rust, E. Speth, D.A. Spong*, F. Wagner, U. Wenzel, W7-AS Team and NBI Group:* Investigation of the β-Limit in the W7-AS Stellarator. 19th IAEA Fusion Energy Conference, Lyon 2002.

813. *Wenzel, U., K. McCormick, R. Narayanan, P. Grigull and R. König:* A New Plasma Condensation Phenomenon in the W7-AS Island Divertor. 15th International Conference on Plasma Surface Interactions in Controlled Fusion Devices, Gifu 2002.

814. *Werner, A., D.S. Darrow* R. Kuduk* and A. Weller:* Invited Talk on Fast Ion Loss Diagnostic for Wendelstein 7-X. German-Polish Conference on Plasma Diagnostics for Fusion and Applications, Greifswald 2002.

815. *Werner, A., D.S. Darrow* R. Kuduk* and A. Weller:* Invited Talk on Fast Ion Loss Diagnostic for Wendelstein 7-X. Institute of Physics, Mme. Curie-Sklodowska University, Lublin 2002.

816. *Werner, A., D.S. Darrow* R. Kuduk* and A. Weller:* Invited Talk on Fast Ion Loss Diagnostic for Wendelstein 7-X. PPPL, Princeton,NJ 2002.

817. *Werner, A., S. Klose, E. Sallander, A. Weller and W7-AS Team:* Interaction of Energetic Ions with Alfvén Eigenmodes in Optimised Stellarators. 44th Annual Meeting of the Division of Plasma Physics, Orlando,FL 2002. Bulletin of the American Physical Society **47** (9), 253 (2002).

818. *Werner, A., A.Weller, D.S. Darrow* and W7-AS Team:* Fast Ion Losses in Wendelstein 7-AS. 13th International Stellarator Workshop, Canberra 2002.

819. *Wesner, F., F. Braun, D.A. Hartmann and J. Wendorf:* ICRF Heating for Wendelstein 7-X. 22nd Symposium on Fusion Technology, Helsinki 2002.

820. *White*, R., C.D. Beidler, S.V. Kasilov*, W. Kernbichler*, H. Maaßberg, D.R. Mikkelsen*, V.V. Nemov*, M. Schmidt, V. Tribaldos* and A. Wakasa*:* Bootstrap Current Simulation for W7-AS and W7-X. International Sherwood Fusion Theory Conference, Rochester,NY 2002.

821. *Wienhold*, P., V. Philipps*, A. Kirschner*, A. Huber*, J. von Seggern*, H.G. Esser*, D. Hildebrandt, M. Mayer, M. Rubel* and W. Schneider:* Short and Long Range Transport of Material Eroded from the Wall Components in Fusion Devices. 15th International Conference on Plasma Surface Interactions in Controlled Fusion Devices, Gifu 2002.

822. *Wilhelm. R.:* H^- Source Physics and Modelling of RF Source for ITER. Ad Hoc Group Meeting on RF Source for ITER, Garching 2002.

823. *Wilhelm, R.:* Hochleistungsquelle für negative Wasserstoffionen: Entwicklung einer H^-Quelle für ITER. Kolloquium, IPP Berlin 2002.

824. *Wilhelm, R.:* Hochleistungsquellen für negative Ionen. Kolloquiumsvortrag, IPF Stuttgart 2002.

825. *Wilhelm, R.:* Plasmaphysik I. Vorlesung, Technische Universität München, WS 2001/2002.

826. *Wilhelm, R.:* Plasmaphysik II. Vorlesung, Technische Universität München, SS 2002.

827. *Wilke, C., H. Kersten*, R. Steffen, H. Brandenburg, M. Endler, M. Geigl*, O. Grulke, F. Jansen*, B. Krames*, M. Quaas*, A. Richter, J. Röpcke*, A. Sonnenfeld*, G. Stockhausen*, D. Uhrlandt*, V. Vartolomei*, A. Wesemann* and R. Wiese*:* Physik-Praktikum für Mediziner. Universität Greifswald, WS 2001/2002.

Lectures

828. *Wobig, H., T. Andreeva, C.D. Beidler, E. Harmeyer, F. Herrnegger, Y. Igitkhanov, J. Kisslinger, Ya.I. Kolesnichenko, V.V. Lutsenko*, V.S. Marchenko*, C. Nührenberg, I.N. Sidorenko, Y. Turkin, A. Wieczorek* and Yu.V. Yakovenko*:* Recent Developments in Helias Reactor Studies. 19th IAEA Fusion Energy Conference, Lyon 2002.

829. *Wright*, J.C., P. Bonoli*, S. Wukitch*, M. Porkolab*, E. D'Azevedo* and M. Brambilla:* Simulations of ICRF Mode Conversion in Alcator C-Mod and ASDEX-U with a Fully Converged Spectral Code. 44th Annual Meeting of the Division of Plasma Physics, Orlando,FL 2002. Bulletin of the American Physical Society **47** (9), 140 (2002).

830. Wünderlich*, D., U. Fantz and K. Behringer: Anwendungen eines Stoß-Strahlungs-Modells zur Diagnostik von Wasserstoff-plasmen. Verhandl. DPG (VI) **37**, 39, P.22.21 (2002).

831. *Ye, M.Y., H. Kanehara*, S. Fukuta*, N. Ohno* and S. Takamura*:* Bubble Formation on Tungsten Surface under Low Energy and High Flux Hydrogen Plasma Irradiation in NAGDIS-I. 15th International Conference on Plasma Surface Interactions in Controlled Fusion Devices, Gifu 2002.

832. *Yoon, S.-W., A. Kallenbach, R. Dux, J.-W. Kim, T. Pütterich, R. Pugno, I. Nunes* and ASDEX Upgrade Team:* Determination of Edge Transport Coefficients of Plasma and Carbon Impurities in ASDEX Upgrade with the B 2.5 Package. 9th EU-US Transport Task Force Meeting, Cordoba 2002.

833. *You, J.-H.:* Long-Fiber-Reinforced Metal Matrix Composites for Fusion Components. MPI für Eisenforschung, Düsseldorf 2002.

834. *Zarnstorff*, M., A. Weller, E. Fredrickson, G. Fu*, J. Geiger, S. Klose and W7-AS Team:* Stability of High Beta Plasmas in W7AS. 44th Annual Meeting of the Division of Plasma Physics, Orlando,FL 2002. Bulletin of the American Physical Society **47** (9), 78 (2002).

835. *Zohm, H.:* Einschluß- und Stabilitätsuntersuchungen mit ECRH am Tokamak ASDEX Upgrade. Kolloquium, Forschungszentrum Karlsruhe 2002.

836. *Zohm, H.:* Magnetohydrodynamics (MHD): Plasma Physics on the Road to a Fusion Reactor. Kolloquium, Universität Karlsruhe 2002.

837. *Zohm, H.:* Magnetohydrodynamische Beschreibung heißer Plasmen. Vorlesung, Universität München, SS 2002.

838. *Zohm, H.:* Transport and Stability Studies in the ASDEX Upgrade Tokamak. University of Wisconsin, Wisconsin,WI 2002.

839. *Zohm, H. and ASDEX Upgrade Team:* Overview of ASDEX Upgrade Results. 19th IAEA Fusion Energy Conference, Lyon 2002.

840. *Zohm, H., G. Gantenbein*, A. Keller, F. Leuterer, M. Maraschek, A. Mück, R. Neu, F. Ryter, J. Stober, W. Suttrop and ASDEX Upgrade Team:* Confinement and Stability Studies with ECRH in ASDEX Upgrade. 5th Conference on Strong Microwaves in Plasmas, Nizhny Novgorod 2002.

Laboratory Reports

IPP 1/329
Bosch, H.-S. (Ed.): ASDEX Upgrade Results, Publications and Conference Contributions Period 3/01 to 12/01.

IPP II/4
Bosch, H.-S. (Ed.): ASDEX Upgrade Results, Publications and Conference Contributions Period 3/01 to 12/01.

IPP III/270
Andreeva, T.: Vacuum Magnetic Configurations of Wendelstein 7-X

IPP III/271
Kolesnichenko, Ya.: Alfvén Eigenmodes in Helias Configurations. (Part II)

IPP 4/280
Kirov, K., F. Leuterer, G. Pereverzev, F. Ryter, W. Suttrop and ASDEX Upgrade Team: Electron Cyclotron Resonance Heating in ASDEX Upgrade: Calculation and Experimental Authentication of the Power Deposition Profile.

IPP 5/98
Pereverzev, G. and P.N. Yushmanov:* ASTRA Automated System for Transport Analysis in a Tokamak.

IPP 5/99
Khutoretsky, A., H.-U. Fahrbach, O. Kardaun, J. Stober, Yu.N. Dnestrovskij* and W. Herrmann:* Recovery of Ion Temperature Profiles from the Analysis of Energy-Resolved Neutral-Flux Measurements.

IPP 5/100
Bosch, H.-S. (Ed.): ASDEX Upgrade Results, Publications and Conference Contributions Period 3/01 to 12/01.

IPP 5/100
Strumberger, E., P. Merkel, E. Schwarz and C. Tichmann: MFBE_2001: Computation of Magnetic Fields of Ideal MHD Equilibria.
http://www.ipp.mpg.de/netreports/ipp-report_5_100.pdf.

IPP 5/101
Igochine, V.: Investigation of MHD Instabilities in Conventional and Advanced Tokamak Scenarios on ASDEX Upgrade.

IPP 9/131
Beikler, R.: Untersuchung der Oberflächensegregation geordneter Legierungen mittels Ionenstreuung am Beispiel CuAu(100) = Investigation of the Surface Segregation of Ordered Alloys Using Ion Scattering Exemplified with CuAu(100).

IPP 9/132
Eckstein, W.: Calculated Sputtering, Reflection and Range Values.

IPP 9/133
Meier, M.: Elementary Mechanisms during Interaction of Methyl Radicals and Hydrogen Atoms with the Surface of Amorphous Hydrocarbon Films.

IPP 10/20
Sergeev, V.Yu., B.V. Kuteev*, O.A. Bakhareva*, A.Y. Kostrukov*, V.G. Skokov*, M.P. Petrov*, A. Kislyakov*, R. Burhenn and M. Kick:* Conceptual Design of Pellet Charge eXchange (PCX) Diagnostics for Stellarator W7-X.

IPP 10/21
Fantz, U.: Atomic Molecular Emission Spectroscopy in Low Temperature Plasmas Containing Hydrogen and Deuterium.

IPP 10/22
Bosch, H.-S. (Ed.): ASDEX Upgrade Results, Publications and Conference Contributions Period 3/01 to 12/01.

IPP 15/1
Thomsen, H.: A Dynamics Investigation into Edge Plasma Turbulence.

IPP 15/2
Bäumel, S.: Zweidimensionale Charakterisierung von Elektronen-Temperaturfluktationen an W7 AS.

Author Index

Teams

ASDEX Upgrade Team:
C.Angioni, C.Atanasiu*, M.Balden,W.Becker, G.Becker, K.Behler, K.Behringer, A.Bergmann, R.Bilato, K.Borrass, M.Brambilla, F.Braun, A.Buhler, A.Carlson, G.Conway, D.P.Coster, R.Drube, R.Dux, S.Egorov*, T.Eich, K.Engelhardt, H.-U.Fahrbach, U.Fantz, H.Faugel, M.Foley*, P.Franzen, J.C.Fuchs, J.Gafert, G.Gantenbein*, O.Gehre, A.Geier, J.Gernhardt, L.Gianonne, O.Gruber, A.Gude, S.Günter, G.Haas, D.Hartmann, B.Heger, B.Heinemann, A.Herrmann, J.Hobirk, H.Hohenöcker, L.D.Horton, M.Huart, V.Igochine, D.Jacobi, M.Jakobi, F.Jenko, A.Kallenbach, O.Kardaun, M.Kaufmann, A.Keller, A.Kendl, M.Kick, J.-W.Kim, K.Kirov, S.Klenge, R.Kochergov, H.Kollotzek, W.Kraus, K.Krieger, T.Kurki-Suonio*, B.Kurzan, P.T.Lang, P.Lauber, M.Laux, F.Leuterer, A.Lohs, A.Lorenz, C.Maggi, H.Maier, K.Mank, A.Manini, M.-E.Manso*, M.Maraschek, K.-F.Mast, H.Mayer, P.McCarthy*, D.Meisel, H.Meister, F.Meo, P.Merkel, R.Merkel, D.Merkl, V.Mertens, F.Monaco, A.Mück, H.W.Müller, M.Münich, H.Murmann, Y.-S.Na, G.Neu, R.Neu, J.Neuhauser, D.Nishijima, Y.Nishimura,J.-M.Noterdaeme, I.Nunes*, M.Pacco-Düchs, G.Pautasso, A.G.Peeters, G.Pereverzev, S.D.Pinches, E.Posthumus-Wolfrum, T.Pütterich, R.Pugno, E.Quigley*, G.Raupp, T.Ribeiro*, R.Riedl, S.Riondato, V.Rohde, J.Roth, F.Ryter, S.Saarelma*, F.Salzedas*, W.Sandmann, H.-B.Schilling, J.Schirmer, W.Schneider, G.Schramm, J.Schweinzer, S.Schweizer, B.D.Scott, U.Seidel, F.Serra*, S.Sesnic*, C.Sihler, A.Silva*, A.C.C.Sips, E.Speth, A.Stäbler, K.-H.Steuer, J.Stober, B.Streibl, D.Strintzi, E.Strumberger, W.Suttrop, A.Tanga, G.Tardini, C.Tichmann, W.Treutterer, M.Troppmann, H.Urano, P.Varela*, D.Wagner, F.Wesner, R.Wolf, E.Würsching, M.Y.Ye, S.-W.Yoon, Q.Yu, D.Zasche, T..Zehetbauer, H.-P.Zehrfeld, M.Zilker, H.Zohm.

ECRH Group (AUG):
F.Leuterer, K.Kirov, F.Monaco, M.Münich, F.Ryter, H.Schütz, D.Wagner.

ICRH Group:
W.Becker, V.Bobkov, D.Birus, F.Braun, H.Faugel, D.Hartmann, F.Meo, J.-M.Noterdaeme, J.Wendorf, F.Wesner, E.Würsching.

ITER International Team:
R.Aymar, A.Costley, G.Janeschitz, Y.Murakami, V.Mukhovatov, A.Polevoi, M.Shimada, Y.Shimomura, M.Sugihara, O.Zolotukhin

ITPA Database and Modelling Group:
T.Aniel*, G.Bateman*, G.Becker, M.Bell*, G.Bracco*, R.Budny*, C.Bush*, T.Carlstrom*, A.Chudnovskij*, J.Connor*, J.Cordey*, A.Coté*, J.DeBoo*, A.Dnestrovskij*, Yu.Dnestrovskij*, T.Fukuda*, M.Greenwald*, Y.Gribov*, G.Hammett*, T.Hatae*, T.Hoang*, L.Horton, W.Houlberg*, A.Hubbard*, Y.Kamada*, O.Kardaun, S.Kaye*, S.Konovalov*, A.Kritz*, A.Kukushkin*, A.Kus, S.Lebedev*, V.Leonov*, Y.Martin*, Y.Miura*, J.Ongena*, T.Onjun*, T.Osborne*, G.Pacher*, A.Pankin*, V.Parail*, G.Pereverzev, F.W.Perkins*, C.Roach*, F.Ryter, R.Sartori*, K.Shinohara*, J.Snipes*, A.Stäbler, J.Stober, L.Sugiyama*, W.Suttrop, A.Sykes*, T.Takizuka*, K.Thomsen*, K.Tsuzuki*, H.Urano*, M.Valovic*, I.Voitsekhovich*, M.Walsh*, M.Wakatani*, J.Weiland*.

NI Group:
M.Bandyopadhyay, A.Entscheva, H.Falter, P.Franzen, B.Heinemann, D.Holtum, C.Hu, M.Kick, W.Kraus, P.McNeely, S.Obermayer, F.Probst, R.Riedl, P.Rong, N.Rust, W.Schärich, R.Schroeder, E.Speth, A.Stäbler, R.Süß, A.Tanga.

NI Team (W7-AS):
F.Probst, R.Riedl, N.Rust, W.Schärich, E.Speth, R.Süß.

Threshold Database Group:
T.N.Carlstrom*, J.G.Cordey*, J.C.DeBoo*, T.Fukuda*, M.Greenwald*, Y.Kamada*, O.Kardaun, S.M.Kaye*, S.Lebedev*, Y.Miura*, Y.Martin*, E.Righi*, F.Ryter, J.A.Snipes*, J.Stober, T.Takizuka*, K.Thomsen*, K.Tsuchiya*, M.Valovic*.

W7-AS Team:
T.Andreeva, S.Bäumel, J.Baldzuhn, C.Beidler, T.Bindemann, R.Brakel, H.Braune, R.Burhenn, J.Chung, A.Dinklage, A.Dodhy, H.Ehmler, M.Endler, V.Erckmann, Y.Feng, M.Fink, C.Franck, F.Gadelmeier, J.Geiger, L.Giannone, P.Grigull, O.Grulke, E.Harmeyer, H.-J.Hartfuss, D.Hartmann, F.Herrnegger, M.Hirsch, E.Holzhauer*, K.Horvath, Yu.L.Igitkhanov, R.Jaenicke, F.Karger, W.Kasparek*, M.Kick, J.Kisslinger, T.Klinger, S.Klose, J.Knauer, R.König, G.Kühner, A.Kus, H.Laqua, K.D.Lee, J.Lingertat, R.Liu, H.Maaßberg, S.Marsen, N.B.Marushchenko, K.McCormick, G.Michel, G.Müller*, R.Narayanan, U.Neuner, M.Otte, M.G.Pacco-Düchs, E.Pasch, A.Pasternak, E.Polunovsky*, A. Reichert, N.Ruhs, J.Saffert, E.Sallander, J.Sallander, F.Sardei, F.Schneider, M.Schmidt, C.Schröder, M.Schubert, A.Stark, J.Svensson, H.Thomsen, Y.Turkin, F.Volpe, F.Wagner, A.Weller, A.Werner, H.Wobig, E.Würsching, D.Zhang, D.Zimmermann.

W7-X Construction Division Engineering Team:
Y.Bozhko, J.Boscary, T.Bräuer, J.-H.Feist, W.Gardebrecht, H.Grote, B.Hein, H.Laqua, J.Ludvik, M.Nagel, H.Niedermeyer, J.Reich, H.Renner, K.Rieße, T.Rummel, J.Schacht, F.Schauer, H.Schneider, D.Sharma, S.Y.Shim, A.Spring, K.Stache, M.Wanner, L.Wegener.

W7-X Construction Division Technical Team:
H.Bau, A.Benndorf, A.Berg, H.-J.Bramow, R.Brockmann, A.Brückner, M.Czerwinski, H.Dutz, M.Fricke, F.Füllenbach, G.Gliege, M.Gottschewsky, S.Heinrich, A.Hölting, U.Kamionka, T.Kluck, E.Köster, C.Kopplin, U.Krybus, F.Kunkel, K.Lang, H.Lentz, B.Missal, T.Mönnich, I.Müller, F.Nankemann, A.Opitz, M.Pietsch, S.Pingel, S.Raatz, R.Rieck, U.Schultz, M.Schweitzer, K.-U.Seidler, F.Starke, H.Viebke, O.Volzke, A.Vorköper, A.Wölk.

Organisational structure of Max-Planck-Institut für Plasmaphysik

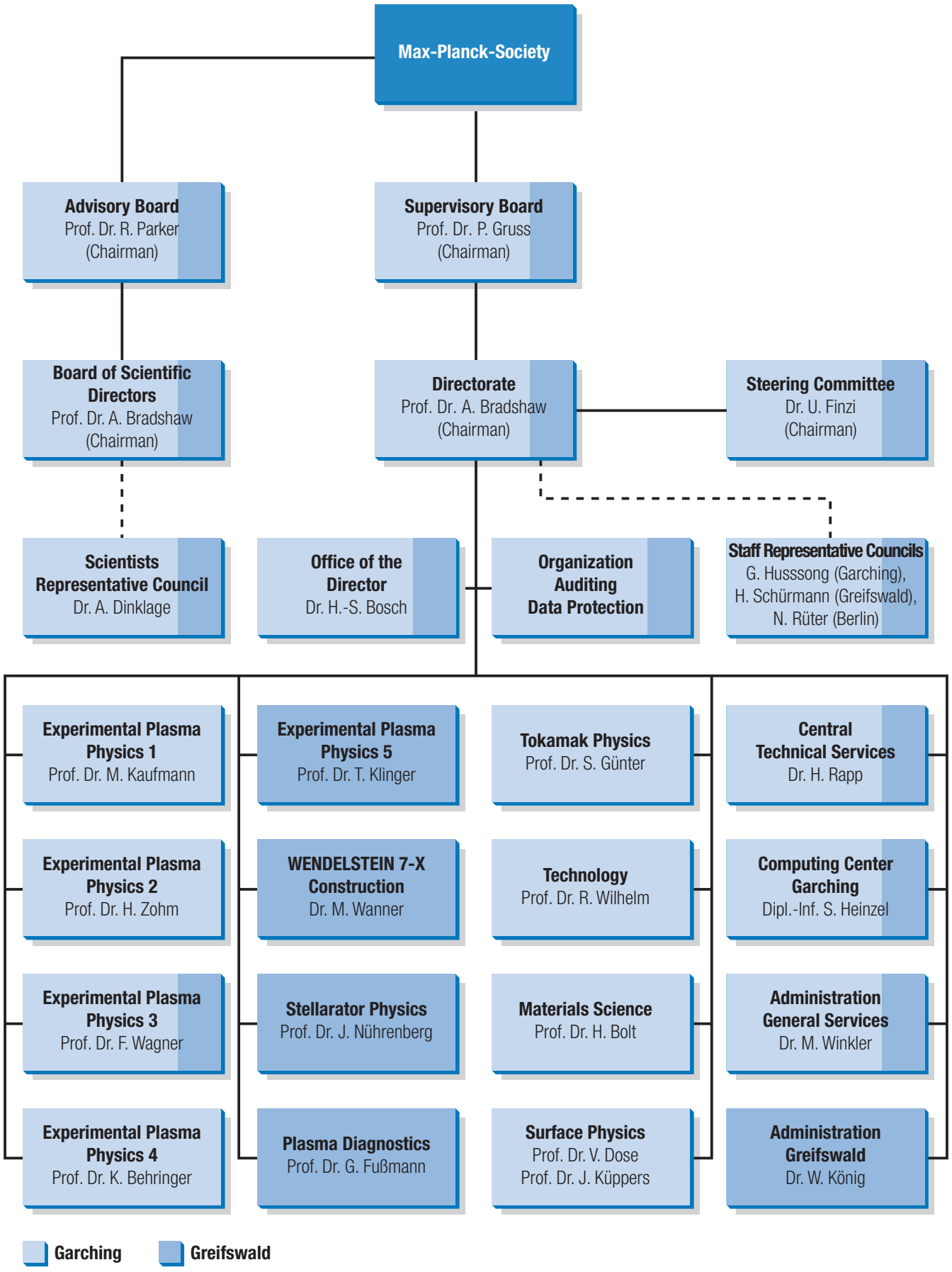

Scientific division of IPP

Experimental Plasma Physics Division 1

Director: Prof. Michael Kaufmann

ASDEX Upgrade (Divertor Tokamak)
- operation of ASDEX Upgrade
- investigation of ITER plasma boundary in a reactor-relevant divertor
- advanced tokamak studies
- investigation of energy transport, MHD stability, beta limit, density limit and disruptions

JET collaboration
- participation in experiments on JET under EFDA
- operation of special discharge scenarios at JET
- comparative studies together with ASDEX Upgrade

Experimental Plasma Physics Division 2

Director: Prof. Hartmut Zohm

ASDEX Upgrade
- Analysis and control of MHD instabilities

Diagnostics
- Control and data acquisition

ITER
- Coordination of ITER related activities at IPP

JET
- Contributions to task forces S1, S2 and M

Experimental Plasma Physics Division 3

Director: Prof. Friedrich Wagner

WENDELSTEIN 7-AS (Advanced Stellarator)
- stellarator with improved magnetic characteristics
- Experiment-orientated stellarator Theory
- interpretation of stellarator experiments
- Stellarator power plant system studies
- development of the HELIAS power plant concept
- Preparation of the WENDELSTEIN 7-X diagnostics
- Preparation of ECRH for WENDELSTEIN 7-X
- Development of Greifswald site

Experimental Plasma Physics Division 4

Director: Prof. Kurt Behringer

Experimental and theoretical investigations of plasma boundary and divertor physics, impurity transport, chemical impurity production and plasma radiation in ASDEX Upgrade and WENDELSTEIN 7-AS

- spectroscopic diagnostics on ASDEX Upgrade
- spectroscopic diagnostics on WENDELSTEIN 7-AS laboratory experiments at the University of Augsburg, Experimental Plasma Physics

Experimental Plasma Physics Division 5

Director: Prof. Thomas Klinger

dynamical behaviour of stellarator plasmas physics of the plasma edge and divertor region stellarator magnetohydrodynamics data acquisition and control

WENDELSTEIN 7-AS
- development and optimization of diagnostics

WENDELSTEIN 7-X
- preparation of the experiment program

VINETA
- basic behaviour of plasmas waves and plasma instabilities

INTERNATIONAL MAX-PLANCK RESEARCH SCHOOL "BOUNDED PLASMAS"
- training of PhD students

Stellarator Theory Division

Director: Prof. Jürgen Nührenberg

General stellarator theory
- Further development of the stellarator concept and computational as well as analytical methods to investigate equilibrium, stability and transport problems in three-dimensional toroidal configurations.

Plasma edge physics
- Theoretical work on 3D plasma edge physics

Scientific division of IPP

Plasma Diagnostics Division

Director: Prof. Gerd Fussmann

Edge plasma physics
- experimental and theoretical work relating to fusion devices

Plasma generator PSI-II
- basic plasma physics
- plasma interaction with solid surfaces
- development and testing of plasma diagnostics

Electron Beam Ion Trap (EBIT)
- production of highly charged ions
- X-ray spectroscopy and atomic physics measurements

UHV laboratory, arc physics, ITER collaboration

Materials Research Division

Director: Prof. Harald Bolt

- Characterisation of fusion relevant properties of plasma facing materials; development and qualification of plasma facing materials for present fusion devices, esp. ASDEX Upgrade and WENDELSTEIN 7-X
- Design and development of materials for plasma facing components in fusion reactors

Surface Physics Division

Directors: Prof. Volker Dose, Prof. Jürgen Küppers

Surface physics
- atomistic characterisation of surfaces

Plasma-wall interactions
- interactions of atoms, ions and electrons with solid surfaces
- wall fluxes in the boundary layer of plasma devices
- limiter and wall analyses

Low temperature plasma physics
- preparation and characterisation of thin-film coatings for plasma devices and plasma diagnostics

Data analysis*
- application of Bayesian techniques to experimental data

* Part of Centre for Interdisciplinary Plasma Science

WENDELSTEIN 7-X Construction

Director: Dr. Manfred Wanner

WENDELSTEIN 7-X Construction
- engineering, construction and installation of the W 7-X device

incl. system control, plasma heating, in-vessel components, and auxiliary systems
- project control and quality management

Technology Division

Director: Prof. Rolf Wilhelm

Neutral injection
- development, constuction and operation of the injection systems for ASDEX Upgrade and WENDELSTEIN 7-X
- development of RF-driven negative ion sources for ITER

Electron cyclotron resonance heating
- construction and operation of an ECRH system for ASDEX Upgrade

Ion cyclotron resonance heating
- development, construction and operation of ICRH systems for ASDEX Upgrade and WENDELSTEIN 7-X

Tokamak Physics

Director: Prof. Sibylle Günter

Theoretical support for the tokamak activities of IPP as well as study of fundamental plasma physics in toroidal magnetic confinement devices:

- plasma edge physics
- nonlinear plasma dynamics and turbulence
- heat and particle transport in tokamaks
- large scale instabilities in tokamaks including MHD and kinetic effects
- wave propagation and absorption in inhomogeneous plasmas

How to reach IPP in Garching

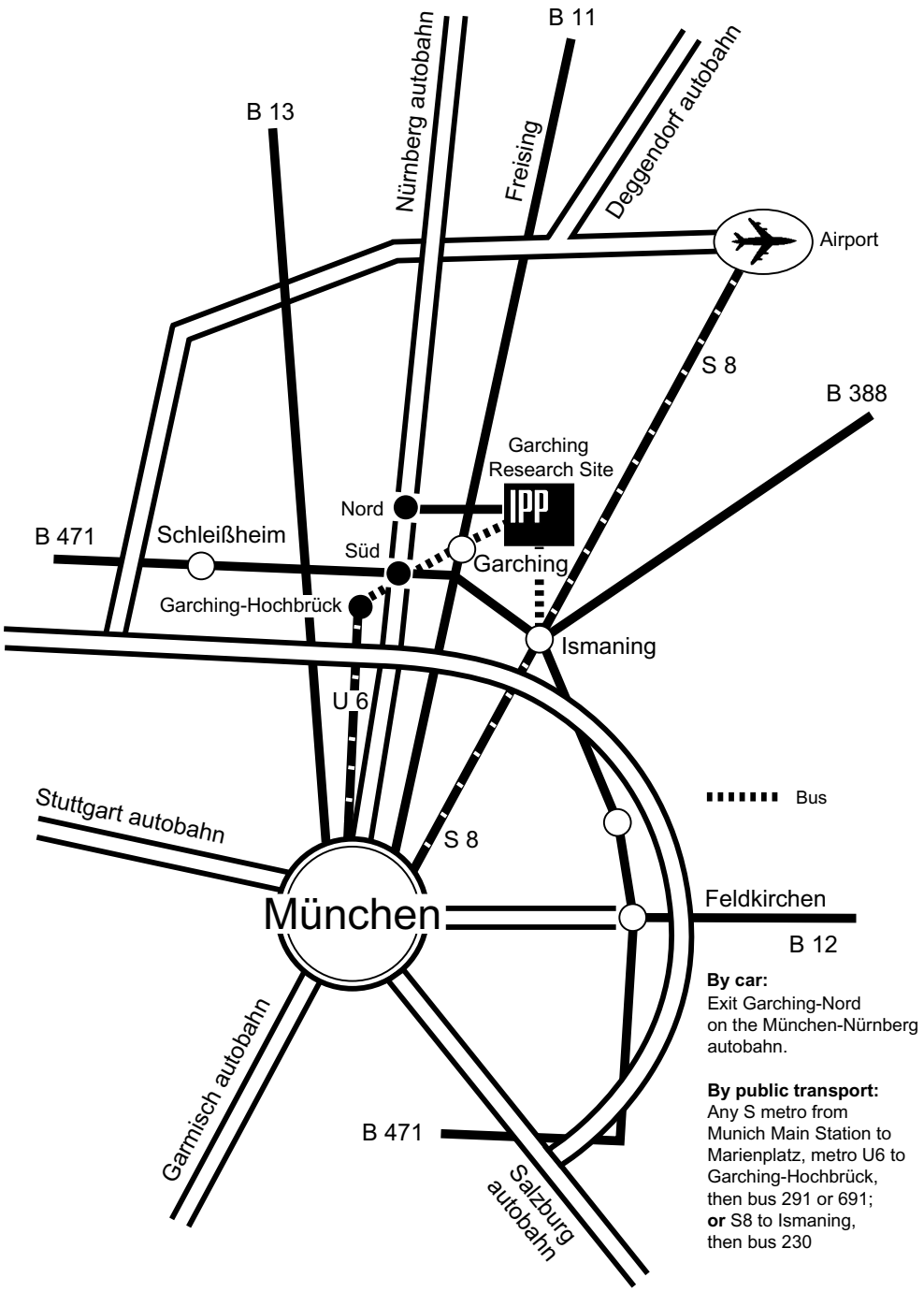

By car:
Exit Garching-Nord
on the München-Nürnberg
autobahn.

By public transport:
Any S metro from
Munich Main Station to
Marienplatz, metro U6 to
Garching-Hochbrück,
then bus 291 or 691;
or S8 to Ismaning,
then bus 230

How to reach Greifswald Branch Institute of IPP

Greifswald Branch Institute of
Max-Planck-Institut für Plasmaphysik
Wendelsteinstraße 1
D-17491 Greifswald

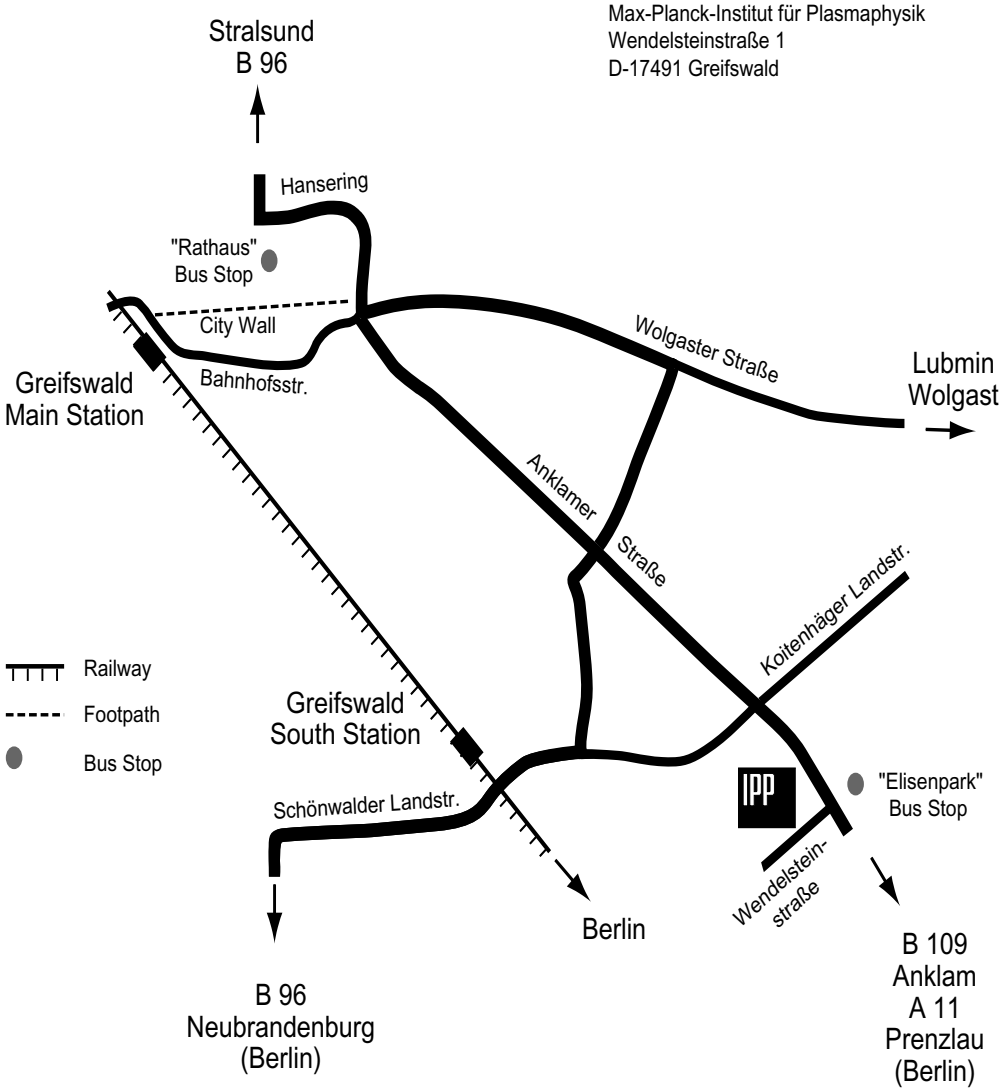

By air:
Via Berlin: from Berlin Tegel Airport by bus No. X9 to Zoologischer Garten, by train to Greifswald
Via Hamburg: from the airport to Main Railway Station, by train to Greifswald.

By car:
Via Berlin, Neubrandenburg to Greifswald **or** via Hamburg, Lübeck, Stralsund to Greifswald,
in Greifswald follow the signs "Max-Planck-Institut".

By bus:
From Greifswald Railway Station walking distance of 10 minutes to the "Rathaus" (Town Hall).
Then from "Rathaus's" stop by bus No. 2 or 3 to the "Elisenpark's" stop.